

DESIGN, SYNTHESIS AND BIOLOGICAL EVALUATION OF NEW AGENTS
TARGETING ESTROGEN RECEPTOR-ALPHA AND -BETA

by

Jelena M. Janjic

PharmD, Belgrade University, Yugoslavia, 1998

Submitted to the Graduate Faculty of

School of Pharmacy in partial fulfillment

of the requirements for the degree of

Doctor of Philosophy

University of Pittsburgh

2005

UNIVERSITY OF PITTSBURGH
FACULTY OF DEPARTMENT OF PHARMACUETICAL SCIENCES

This dissertation was presented

by

Jelena M. Janjic

It was defended on

December 8th, 2005

and approved by

Billy W. Day, PhD
Dissertation Co-Director

Peter Wipf, PhD
Dissertation Co-Director

Wen Xie, MD PhD

Mark Nichols, PhD

Michael Mokotoff, PhD

*To my husband Bratislav
for his endless love, support and encouragement.*

DESIGN, SYNTHESIS AND BIOLOGICAL EVALUATION OF NEW AGENTS
TARGETING ER-ALPHA AND ER-BETA

Jelena M. Janjic, PhD

University of Pittsburgh, 2005

The two known estrogen receptors, ER α and ER β , are the products of different genes on separate chromosomes. Of these, ER α has been the most extensively studied, and its expression in breast cancer determines the ER $^{+}$ phenotype. ER β , on the other hand, was discovered only recently and its role in breast cancer pathology remains unclear. ER β inhibits E2-induced proliferation of T47D breast cancer cells in addition to decreasing the expression of cell cycle related genes. Clinical studies have shown a positive correlation between ER β expression with disease-free survival and overall survival in breast cancer patients. ER β activation with a selective ER β agonist could antagonize the stimulating activity of the ER α in breast cancer cells, and such an ER β agonist could help overcome acquired resistance. Therefore, this work began a search for such agents.

A one-pot hydrozirconation-transmetallation-alimine addition sequence that leads to allylic amides, homoallylic amides and *C*-cyclopropylalkylamides was significantly accelerated by microwave technology and used for library preparation. The conventional methodology provided a first generation discovery library. A potentially antiestrogenic compound was identified in a transcriptional screening assay from this library, *C*-cyclopropylalkylamide **26a** (*O*-

ethyl-*N*-{2-[(1*S**,2*R**)-2-{(*R**)[(diphenylphosphino)amino](phenyl)methyl}cyclopropyl]-ethyl}-*N*-[(4-methylphenyl)sulfonyl]carbamate; a.k.a. CK1-183).

Following up on these findings and with the goal to expand the scope of the synthesis methodology, a second generation library of allylic amides and *C*-cyclopropylalkylamides was prepared. The new library was screened in a fluorescence polarization based homogenous *in vitro* assay at ER α , and hits were further evaluated in cell-based assays. Three new *C*-cyclopropylalkylamides, **37c**, **37a** and **39c**, were identified with improved potency over the lead agent **26a** against 17 β -estradiol (E2) stimulated MCF-7 cells.

This second generation library was screened against both ERs. The screening results served to build an SAR model of allylic amides and *C*-cyclopropylalkylamides at ER α and ER β .

A hit from the ER β screen, *C*-cyclopropylalkylamide **37d** (*N*-(*R**)-(((1*R**,2*R**)-2-butylcyclopropyl)-(4-(phenyl)phenyl)methyl)benzamide), contained a biphenyl core and served as a starting point for the design and synthesis of a third generation of *C*-cyclopropylalkylamide ER targeting agents.

Biphenyl *C*-cyclopropylalkylamides represent novel structural scaffolds for design and synthesis of ER α and ER β targeting agents and a novel avenue for selective estrogen receptor modulator (SERM) development.

TABLE OF CONTENTS

1. INTRODUCTION	1
1.1. Estrogen Receptors in Breast Cancer.....	2
1.1.1. Estrogen Receptor Mechanism of Action.....	2
1.1.2. Estrogen Receptor Alpha	5
1.1.3. Estrogen Receptor Beta.....	7
1.1.4. Structural versus Functional Difference Between ER Subtypes.....	7
1.2. Selective Estrogen Receptor Modulators (SERMs).....	8
1.2.1. Tamoxifen and Raloxifene as Model SERMs	9
1.2.2. Molecular Basis for SERM Tissue Selectivity	10
1.3. Estrogen Receptor Subtype Selective Agents.....	11
1.3.1. Pharmacophore Models for ER Subtype Selectivity	12
1.3.2. Estrogen Receptor Beta Selective Agents – SAR and Applications.....	13
1.4. Synthetic Methods for Allylic Amides, Homoallylic Amides and C-Cyclopropylalkyl Amides	16
1.4.1. Conventional Synthetic Methods and Discovery Library Synthesis	16
1.4.2. Microwave Chemistry.....	22
1.4.3. Synthesis of the Second Generation Library of Allylic Amides and C-Cyclopropylalkylamides Using Microwave	24
2. RESULTS AND DISCUSSION	27
2.1. New ER Targeting Agents from the Discovery Library of Allylic Amides, Homoallylic Amides and C-Cyclopropylalkylamides.....	27
2.1.1. Discovery Library Screening at ER α	27
2.1.2. C-Cyclopropylalkylamide 26a (CK1-183) as a New ER α Partial Antagonist.....	31
2.1.2.1. C-Cyclopropylalkylamide 26a (CK1-183) Inhibits Transcriptional Activity of ER α	31
2.1.2.2. C-Cyclopropylalkylamide 26a (CK1-183) Inhibits E2 Stimulated Proliferation of MCF-7 Cells.....	32
2.1.2.3. C-Cyclopropylalkylamide 26a (CK1-183) is a Modest Competitor on ER α	33
2.1.2.4. C-Cyclopropylalkylamide 26a (CK1-183) Has No Effect on ER α Negative Breast Cancer Cells.....	34
2.1.3. Synthetic Efforts Based on C-Cyclopropylalkylamide 26a (CK1-183) as a Lead.....	36
2.1.4. SAR of C-Cyclopropylalkylamides from Discovery Library.....	39
2.1.4.1. SAR from Cell-Based Assays.....	39
2.1.4.2. Docking studies.....	41
2.1.5. Microwave Supported Synthesis.....	45
2.1.5.1. Hydrozirconation – Transmetallation – Aldimine Addition.....	47
2.1.6. Biological Evaluation of the Second Generation Library.....	50
2.1.6.1. Design of the Second Generation Library	50
2.1.6.2. Second Generation Library Tests <i>in vitro</i> and in Cells.....	52

2.1.6.3.	Screening of the Second Generation Library on ER β	57
2.1.7.	SAR of the Second Generation Library on ER α and ER β	64
2.2.	Biphenyl C-Cyclopropylalkylamide Analogues of 37d (CC1-243)	69
2.2.1.	Synthesis of Biphenyl C-Cyclopropylalkylamides	71
2.2.2.	Evaluation of Biphenyl C-Cyclopropylalkylamides for <i>in vitro</i> Binding to the ER α and ER β	76
2.2.3.	Docking studies	79
2.2.4.	Biphenyl C-cyclopropylalkylamides Tested on Breast Cancer Cells	81
2.2.5.	SAR of Biphenyl C-Cyclopropylalkylamides on ER α and ER β	83
3.	CONCLUSIONS	86
4.	FUTURE DIRECTIONS	90
4.1.	Role of ER β in Breast Cancer	90
4.2.	Hypothesized Model for Targeting ER β in SERM Resistant Cancer	90
5.	EXPERIMENTAL SECTION	94
5.1.	Chemistry	94
5.1.1.	General Experimental Procedures	94
5.2.	Biology	129
5.2.1.	Plasmids and Transient Transfection Assays	129
5.2.2.	Luciferase Assay	129
5.2.3.	Antagonism	130
5.2.4.	Antiproliferative Assays	130
5.2.5.	ER Competitor Assays	131
5.2.6.	Docking in CAChe	133
6.	Appendix	135
7.	References	168

LIST OF TABLES

Table 1. Structures of the 67-member discovery library	18
Table 2. Fifty percent inhibitory concentrations of compounds examined for E2-induced luciferase activity and MCF-7 cell proliferation, and for E2-independent MDA-MB231 cell proliferation.....	35
Table 3. Hydrozirconation in toluene in the microwave – flash heat mode.	46
Table 4. Hydrozirconation and aldimine addition in a microwave – flash heat mode.	48
Table 5. Hits from the testing of the second generation library in MCF-7 cells	55
Table 6. Activities of <i>C</i> -cyclopropylalkylamides from the second generation library in fluorescence polarization displacement-based screen assays at ER α and ER β	59
Table 7. Biphenyl <i>C</i> -cyclopropylalkylamides tested in displacement assays on ERs.....	78

LIST OF FIGURES

Figure 1. Model ligands for ERs.....	1
Figure 2. Transcriptional regulation of ER target genes.....	3
Figure 3. Structural domains of the human ER α and ER β	4
Figure 4. Representative subtype selective agents.....	12
Figure 5. ER β selective ligands.....	14
Figure 6. Screen of the discovery library for ER α agonists at classical ERE.....	28
Figure 7. Structures of lead <i>C</i> -cyclopropylalkylamide 26a (CK1-183) and control agents (40 , 41 and 42).	29
Figure 8. Test for potential ER α antagonism in the transcriptional assay.....	30
Figure 9. <i>C</i> -Cyclopropylalkylamide 26a (CK1-183) inhibits E2 induced transcriptional activation of ER α	31
Figure 10. <i>C</i> -Cyclopropylalkylamide 26a (CK1-183) inhibits E2 induced MCF-7 proliferation.....	32
Figure 11. <i>C</i> -Cyclopropylalkylamide 26a (CK1-183) tested in ER α competition assay.....	34
Figure 12. Analogues of <i>C</i> -cyclopropylalkylamide 26a (CK1-183) biologically tested.....	37
Figure 13. Lead compound 26a (CK1-183) and control compounds 40 and 41 , tested for inhibition of E2 induced transcriptional activation of ER α at classical ERE.....	39
Figure 14. Raloxifene docked into ER α -LBD using BioMedCACHe.....	42
Figure 15. <i>C</i> -Cyclopropylalkylamide 26a (CK1-183) docked into the ER α -LBD raloxifene binding pocket using BioMedCACHe.....	43
Figure 16. Results of screening the second generation library with the ER α fluorescence polarization based displacement assay (Panvera).....	52
Figure 17. Hits from Screening the Second Generation Library at the ER α	53
Figure 18. Inhibition of E2-induced proliferation of MCF-7 cells.....	55
Figure 19. Results of screening the second generation library in the ER β competitor assay (Panvera).....	58
Figure 20. Preliminary SAR presented on compound 37d (CC1-243) from ER screens of the second generation library.....	65
Figure 21. Structures of biologically tested biphenyl <i>C</i> -cyclopropylalkylamides (37d , 69a , 70b-d , 71 , 72) and control oxime (13).	74
Figure 22. Biphenyl <i>C</i> -cyclopropylalkylamides tested in a displacement assay on ER α	77
Figure 23. Biphenyl <i>C</i> -cyclopropylalkylamides tested in a displacement assay on ER β	77
Figure 24. Biphenyl oxime 13 docked into the GEN binding pocket of ER β -LBD (BioMedCACHe).....	80
Figure 25. Biphenyl <i>C</i> -cyclopropylalkylamine 72 docked into GEN binding pocket of ER β -LBD (BioMedCACHe).....	81
Figure 26. Biphenyl <i>C</i> -cyclopropylalkylamides tested for inhibition of E2 stimulated growth of breast cancer cells.....	82
Figure 27. Hypothesized ideal SERM that targets both ERs.....	92

LIST OF SCHEMES

Scheme 1. Synthesis of the discovery library of <i>C</i> -cyclopropylalkylamides (26), allylic amides (27) and homoallylic amides (28).....	17
Scheme 2. Second generation library microwave supported synthesis.....	25
Scheme 3. <i>C</i> -Cyclopropylalkylamide analogue synthesis.....	36
Scheme 4. Allylic amide synthesis in a microwave.....	49
Scheme 5. Synthesis of biphenyl oxime 13	70
Scheme 6. Synthesis of phosphinoyl protected biphenyl <i>C</i> -cyclopropylalkylamide precursors...	71
Scheme 7. CC1-243 analogues derived from a common precursor.....	72
Scheme 8. Synthesis of the lead structure 37d (CC1-243).....	73

LIST OF ABBREVIATIONS

AFs	activation functions
β -Gal	beta-galactosidase
CBD	coactivator-binding domain
CMX	cytomegalovirus expression vector
DBD	DNA-binding domain
DMAP	4-dimethylaminopyridine
DMEM	Dulbecco's Modified Eagle Medium
DMSO	dimethylsulfoxide
DOTAP	(<i>N</i> -[1-(2,3-dioleoyloxy)]- <i>N,N,N</i> -trimethylammonium propane methylsulfate
ER	estrogen receptor
EREs	estrogen response elements
ERE-tk-LUC	construct of estrogen receptor, tyrosine kinase promoter and luciferase gene
HPLC	high performance liquid chromatography
HSP	heat shock protein
LBD	ligand-binding domain
LUC	luciferase reporter gene
MAPK	mitogen-activated protein kinase
NTD	N-terminal domain
SAR	structure-activity relationship
SERMs	selective estrogen receptor modulators

TBAF	tetrabutylammonium fluoride
TBDPSCI	<i>tert</i> -butyldiphenylsilyl chloride
THF	tetrahydrofuran
tk	tyrosine kinase promoter
TLC	thin layer chromatography
wt	wild-type

PREFACE

The author would like to thank Prof. Billy Day for opening an amazing world of medicinal chemistry and drug discovery to her. I will never forget his words of encouragement and his belief in me even at times I had doubts. “You can do it!” was Prof. Day’s style. I can only say he sets the tone of the professor and a mentor I hope to be. I would also like to thank Prof. Day for introducing me to Prof. Wipf. Working in Prof. Wipf’s laboratory taught me not only chemistry but also gave me the tools to think, analyze and understand better scientific problems in biology. Prof. Wipf was an enormous source of both encouragement and challenge. Working in the Day and Wipf groups at the same time was the most unique experience of my life. I would like to thank both of my advisors for their joint support during my PhD work through both chemistry and biology.

I would also like to thank Prof. Michael Mokotoff for introducing me to peptide chemistry and giving me hands-on synthetic experience at the very beginning of my PhD work. Prof. Mokotoff was a constant source of inspiration. He kindly encouraged and supported my passion for teaching.

This work would be so much less of a fun experience if it were not for my friends. I would like to thank Drs. Corey Stephenson and Christopher Kendall, former Wipf group members, for their endless support and help in the beginning year of my work in synthetic chemistry. I would especially like to thank Dr. Michael Rishel for his help and encouragement in the world of chemistry, for passionate scientific discussions and his support. I would like to thank Dr. Raghavan Balachandran – Balu – for his help with cell culture and valuable scientific discussions. Balu was my friend in biology I could always rely on. Without Dr. Ying Mu from Prof. Xie’s group and his help at the beginning of my PhD work, no discovery I made would

have been possible. I would like to thank Miranda Sarachine, from the Day group for being my help, motivation and inspiration during the final year of my PhD work. Miranda's hard work, enthusiasm and curiosity were my inspiration to do more.

At the end, I would like to thank my husband Bratislav Janjic, a researcher from the Hillman Cancer Center at the University of Pittsburgh. Bratislav was my first research mentor and teacher in early 2000 when I only began to understand the beauty of science. Through numerous scientific discussions he supported me in discovering new things and encouraged me to think as an independent researcher. I want to mention here that my going back to school and getting a PhD was his idea. His devotion and love helped me discover the kind of a scientist I would like to be. My PhD thesis is therefore entirely dedicated to Bratislav.

1. INTRODUCTION

Breast cancer is one of the leading causes of death in women in the USA. According to the National Cancer Institute, the cumulative risk of an average woman in the United States to develop breast cancer in her lifetime is 1 in 8.^{1,2} Estrogens such as 17 β -estradiol (E2, **1**; Figure 1) are known to be both initiators and promoters of carcinogenesis. Depleting secretion of estrogens via ovariectomy (surgical-, chemical- or radiation-induced) has been the most effective treatment of hormone-responsive breast cancer. Estrogens act as mitogens in breast cancer via the estrogen receptor (ER). Antiestrogens primarily function through competing with endogenous estrogens for binding to the ER and thus preventing the estrogens' action in breast cancer.

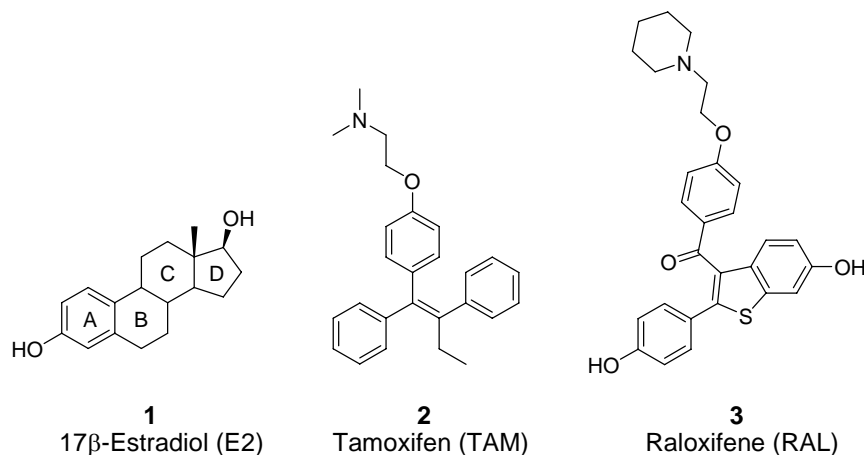


Figure 1. Model ligands for ERs.

The most prescribed antiestrogen therapeutic agent for treating breast cancer is tamoxifen (Nolvadex®) (TAM, **2**; Figure 1). For the last 20 years, tamoxifen has been the therapy of

choice for all stages of ER positive breast cancer and in 1998 FDA approved it as chemoprevention agent in women at high risk of developing breast cancer.^{3,4}

1.1. Estrogen Receptors in Breast Cancer

The steroid hormone E2 (**1**) is a key regulator of growth, differentiation, and function of male and female reproductive tissues, mammary gland, and the skeletal, cardiovascular and nervous systems. The predominant biological effects of E2 are mediated through two distinct intracellular receptors, ER α and ER β . Although ER signaling is required for normal mammary gland development, it has been hypothesized that aberrant signaling could lead to abnormal cellular proliferation and survival, potentially participating in the development and progression of breast cancer.⁵ There is direct evidence that estrogen has mitogenic effects in breast cancer. Estrogen directly increases the number of cells transiting the cell cycle in cell culture. This effect is blocked by known antiestrogens.⁶ ER α expression in breast cancer determines the ER positive (ER+) phenotype. However, the role of ER β in breast cancer pathology remains unclear.

1.1.1. Estrogen Receptor Mechanism of Action

ER α and ER β are type I nuclear receptors and transcriptional factors. Both receptors belong to the family of nuclear hormone receptors and have similar functional domains: an N-terminal domain (NTD), a central DNA-binding domain (DBD) and a C-terminal, ligand-binding domain (LBD).^{2,7} The DBD mediates interaction with target genes. In the absence of a ligand, ER

monomers are associated with a heat shock protein (HSP90). Upon ligand binding, the HSP90 and ER dissociate. Concomitantly, ERs undergo a conformational change, resulting in recruitment of a large coactivator complex. Depending on the conformation of the ligand-bound ER and the precise composition of this coactivator complex, the ER is then free to bind to specific estrogen response elements (EREs) in the genome, resulting in the regulation of specific genes (Figure 2).

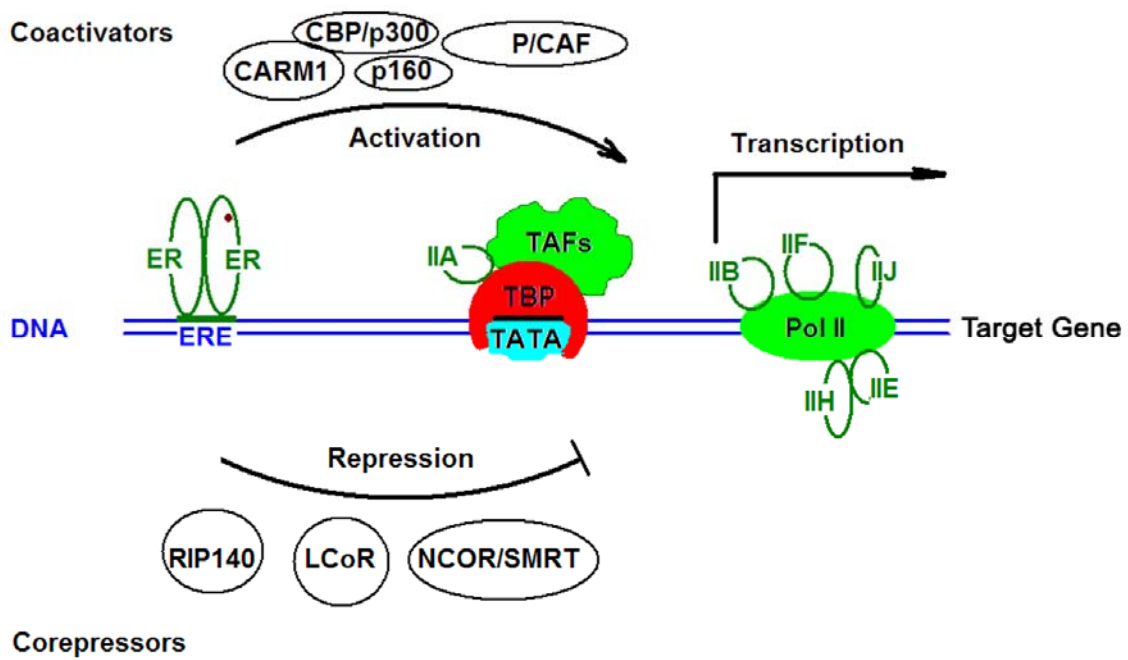


Figure 2. Transcriptional regulation of ER target genes.

The N-termini of both ER α and ER β are targets for phosphorylation by the mitogen-activated protein kinase (MAPK) pathway.² The LBD and NTD contain two separate activation functions (AFs) (Figure 3). The LBD activation function (AF-2) contacts NR boxes within the coactivator p160 molecule, and the NTD activation function (AF-1) binds to the p160 C-terminus and CBP/p300. Depending on cellular and promoter context, coactivator binding exclusively to AF-

1 leads to either partial activation or no activation of the ER.⁸ N-Terminal domains of both receptors interact with the coactivator GRIP-1, but the ER β does so much more weakly than the ER α . In contrast to ER α , ER β appears to have diminished AF-1 activity while, at the same time, it possesses a fully functional AF-2.⁸ This interaction is necessary for transcriptional activity of both receptors.

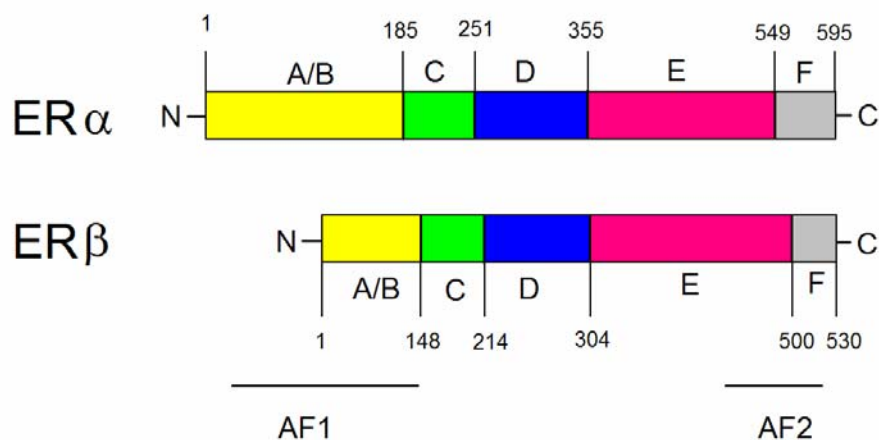


Figure 3. Structural domains of the human ER α and ER β .⁸

The coactivator complexes enhance the transcription by chromatin remodeling.² Full activation generally requires that coactivators bind simultaneously to both AF-1 and AF-2.⁸ The 70-80 amino acid long DBD forms two zinc binding motifs that are involved in target gene promoter recognition, ERE binding and ER dimerization. Side chains of four amino acids on the recognition helix (called the p-box) of each monomer make direct and indirect hydrogen bonds to ERE nucleotides.²

The most studied drug discovery target on the ER is the LBD. This domain is multifunctional. The LBD mediates ligand binding, receptor dimerization, interaction with chaperone and

coregulator proteins, nuclear translocation and transcription activation.⁹ The AF2 in the LBD constitutes the ligand-dependent activation function. Upon agonist binding to LBD, helix 12 (H12) of the ER dramatically changes its position in space and closes the ligand binding cavity, a structural change that is crucial for AF2 recruitment of coactivators. Helices 1, 2, 3, 4 and 5 form a shallow hydrophobic pocket that can recognize the LxxLL motif (NR-box) on coactivator proteins. Thus, it is named the coactivator-binding domain (CBD) and is necessary for transcriptional activity of ERs. Coactivators bind to the AF2 surface via the amino acid motif LxxLL in which the leucine residues dock into the hydrophobic cleft. Binding specificity is aided by oppositely charged amino acids at either end of the ER hydrophobic cleft that form a charge clamp with the LxxLL peptide backbone.⁶ Coactivators then participate in the chromatin remodeling and recruitment of basal transcription factors leading to activation of target gene transcription and downstream stimulatory effects of the ER ligand interaction. The role of each ER receptor in breast cancer pathology and their drug targeting are discussed in more detail in the following sections.

1.1.2. Estrogen Receptor Alpha

Only a small percentage of the cells in the normal breast express ER α (15-17%), and these are not the same normal breast cells as those that are proliferating. Expression of this receptor was found to be much higher in invasive breast cancer and ductal carcinoma *in situ* (30–75%).⁵ The presence of ER α in breast cancer tissue is usually correlated with better prognosis and is the key determining factor for indicating endocrine therapy.^{2,10} ER-mediated estrogen signaling is

known to involve cross-talk with other signaling pathways, such as MAPK and growth factors. The biological effects of E2 through the ER α are mediated through four distinct but interconnected pathways: (1) **classical ligand-dependent**, leading to an up- or down-regulation of target gene transcription and subsequent tissue responses; (2) **ligand-independent**, through interaction with kinase pathways activated by growth factors that lead to phosphorylation of ER; (3) **ERE-independent**, ligand-ER complexes alter transcription of genes containing alternative response elements such as AP-1; and (4) **cell-surface (nongenomic) signaling**, activation of a membrane-associated form of ER linked to intracellular signal transduction pathways that generate rapid tissue responses.¹¹

The classical ligand-dependent pathway of ER α is the most studied and has been used to develop clinically-used antiestrogens for breast cancer treatment. As stated above, there are two activation domains in the ER α , AF-1 and AF-2 that act synergistically to recruit various coactivator proteins to the DNA/ER complex. Depending on the cellular and promoter context, coactivator binding exclusively to AF-1 leads to either partial activation or no activation of ER α . However, the full activation generally requires that coactivators bind simultaneously to both AF-1 and AF-2.⁸ It was recently proposed that ER α corepressors play an important role in breast cancer pathophysiology by controlling the magnitude of the estrogen response, mediating antiestrogen inhibition of ER α , repressing DNA-bound ER α in the absence of the ligand, and conferring active repression of ER α -downregulated genes.¹²

1.1.3. Estrogen Receptor Beta

ER β was discovered only recently,¹³ whereas the first description of ER α came 50 years ago. ER β mechanisms in breast cancer pathology remain unclear. Ström *et al.*¹⁴ have recently shown that ER β inhibits E2-induced proliferation of T47D breast cancer cells, in addition to decreasing the expression of cell cycle related genes. Clinical studies have shown a positive correlation between ER β expression with disease-free survival and overall survival in breast cancer patients.¹⁵ Furthermore, ER β expression has been inversely correlated with HER2 expression.¹⁶ It has been shown that ER β is the more abundant ER in the normal breast, and examination of the ductal epithelium of ER β $-/-$ mice suggests that it is a prodifferentiative factor.⁸ Overall, the role of ER β is currently suggested to be antiproliferative in breast cancer.

1.1.4. Structural versus Functional Difference Between ER Subtypes

ER α and ER β share great homology in their DBD (97%), but only 56% homology in their LBDs.¹⁷ Only 20-25 residues are in close contact with bound ligands and that region is almost identical in the two receptors. Studies using point mutations and chimeric constructs identified two key differing residues: Leu384 in ER α vs. Met336 in ER β , and Met421 in ER α vs. Ile373 in ER β .¹⁷ However, subtype-specific ligands¹⁷ have recently been developed to assist in our understanding of the biology and interactions of these receptors. The subtype-specific ligands will be discussed in greater detail later in the text.

The X-ray crystallographically determined structure of ER β -LBD bound by the isoflavone genistein (GEN, **6**) and the natural ligand E2 shows that ER β Met336 lies above the ligand and delineates part of the pre-formed pocket on the β -face of the cavity. ER β Ile 373 lies on the α face, right below the D ring of E2. Therefore, Pike *et al.*³⁸ suggested that the change of the weakly polar methionine from the α - to the β -face of the cavity enables ER β to accommodate more polar substituents at the distal end of the cavity. It has also been suggested that ER β is easier to antagonize than ER α because the agonist position of H12 in ER β is more unstable than in ER α .³⁸ This feature is important for selective ER β agonist design, and could explain why most of the ER β -selective agents are generally more rigid and smaller in size than those that are selective for ER α .

1.2. Selective Estrogen Receptor Modulators (SERMs)

TAM **2** was prepared in the early 1960's as a potential antifertility agent. It was not until the early 1970s that TAM was suggested as an antiestrogenic agent for the treatment of breast cancer. The term "selective estrogen receptor modulators" (SERMs) came into the scientific literature after the finding that TAM exerts mixed effects in humans in that it is antiestrogenic in the breast but estrogenic in the uterus and bone.

1.2.1. Tamoxifen and Raloxifene as Model SERMs

The ligand binding cavity in ER α is completely partitioned from the external environment and occupies a relatively large portion of the LBD's hydrophobic core. When a typical agonist such as the hormone E2 binds the ER α , it interacts with the binding cavity through a combination of specific hydrogen bonds and hydrophobic interactions. The phenolic hydroxyl of the A-ring of E2 situates between H3 and H6 and makes direct hydrogen bonds to the carboxylate of ER α Glu353, the guanidinium group of ER α Arg394, and a highly ordered water molecule. The 17 β hydroxyl of the D-ring makes a single hydrogen bond with ER α His524 in H11. The remainder of the molecule participates in a number of hydrophobic contacts.¹⁸ The antagonist raloxifene (RAL, **3**) binds to the same site and its phenolic moieties form hydrogen bonds with ER α Glu353, ER α Arg394 and ER α Glu353. In addition, its nitrogen in the piperidine ring forms a hydrogen bond with the carboxyl group of ER α Asp351, resulting in the displacement of H12 and the protrusion of the 11A side chain of raloxifene from the pocket between H3 and H11. This helix H12 displacement is found to be a general feature of both steroidal and non-steroidal antiestrogens that possess a bulky side-chain substituent.¹⁸ At the molecular level there is a clear difference between the binding modes of an agonist and an antagonist. However, the molecular interaction on its own fails to fully explain the complexity of the selective ER modulator pharmacology. TAM (**2**) and RAL (**3**) were originally considered antagonists, and are in certain species, but they truly represent model SERMs in humans. They are agonists in some tissues (bone, liver, and the cardiovascular system), antagonists in other tissues (brain and breast), and mixed agonists/antagonists in the uterus, with TAM having greater uterine-stimulatory activity than RAL.¹⁹

1.2.2. Molecular Basis for SERM Tissue Selectivity

Whether a compound will act as an agonist or antagonist or as a mixed agonist/antagonist in the target tissue depends upon its structure, the conformational change in the receptor LBD upon ligand binding, the promoters of the target genes and the coregulator proteins present in the cells comprising the tissue.¹⁹ Hall *et al.*²⁰ have shown that the sequence of the ERE in the promoter of the target gene influences the structure of the ER and coregulator recruitment. Coregulator proteins, on the other hand, actively stabilize the ER-ligand complex. Different classes of coactivator proteins combine with ER bound by estrogen agonists of different structure to elicit varying degrees of receptor stabilization, and antagonists and coactivator binding inhibitors disfavor the costabilized conformation.²¹

In the development of new antiestrogens for breast cancer, it is crucial to understand the diverse mechanisms of antagonism at ERs. Active antagonists, when complexed with ER, can cause the ER to bind to DNA and recruit corepressors so that the complex is transcriptionally inactive. Passive antagonists cause the ligand-bound ER to simply not bind to DNA because of several possible reasons: the HSP90 does not dissociate; dimer formation is inhibited; and/or translocation to the nucleus is prevented. There are also direct and indirect antagonists. When H12 is sterically pushed by the ligand side chain (most antagonists that have a bulky side chain exert their action in this way), coactivator recruitment is blocked, resulting in transcriptional inactivation. In the case of indirect antagonists, the ligand-induced conformational change results in a situation where H12 is not pulled into agonist conformation or the hydrophobic cleft for

coactivator binding is distorted.⁸ The endpoint of antagonist binding is, regardless of the exact mechanism, inhibition of transcription of ER-regulated genes.

1.3. Estrogen Receptor Subtype Selective Agents

Several groups have developed subtype selective ligands for the ERs (reviewed in Ref. 22), which allow study of the pharmacology of ERs. Here, only a few selective agents, those used in the present work as control agents in biological assays and/or guides for the design of new ER targeting agents, will be discussed. The Katzenellenbogen group has developed a compound called propylpyrazole-triol (PPT, **5**; Figure 4), a triarylpyrazole that was found to be an approximately 1000-fold selective agonist at ER α over ER β .²³ They also developed a 100-fold selective ER β agonist, diarylpropionitrile (DPN, **4**; Figure 4).²⁴ These two compounds have served as tools to uncover structural differences between the ligand binding pockets of the two receptors.¹⁷ *Ab initio* quantum chemical calculations of the interaction between a phenyl ring and the respective side chains of ER β Met336 and ER α Leu384 suggest that the side chain of ER β Met336 has a greater potential for interaction with the aromatic ring than the side chain of ER α Leu384.²⁵ It was also suggested that GEN's 5-OH group has a repulsive interaction with ER α Met421 in ER α , which does not occur with the side chain of ER β Ile373.³⁹ Based on these findings, it is not a surprise that GEN (**6**) has been commonly used as a lead structure for the design of ER β selective agents (Figure 5) and that it has guided the design and synthesis of numerous subtype selective agents.

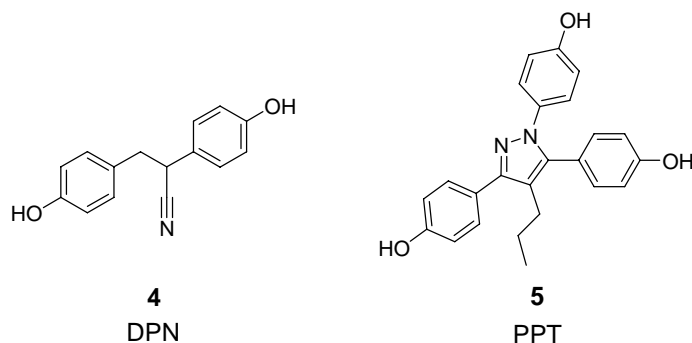


Figure 4. Representative subtype selective agents.^{23,24}

ER subtype selectivity as a medicinal chemistry problem was attractive at first in order to design chemical tools to assist in the study of the complex biology of each receptor, and potentially their interplay. However, subtype selective agents do have important clinical implications. One of the recent successful examples is ERB-041 (7; Figure 5), developed by the Wyeth Corp.³³ ERB-041 is an orally available ER β -selective agonist that has shown dramatic beneficial effects in rodent preclinical models for inflammatory bowel disease.²⁶ Other positive attributes of ERB-041 are that it is not uterotrophic, does not prevent bone loss nor weight gain after ovariectomy, is not mammatrophic and does not inhibit ovulation.²⁶

1.3.1. Pharmacophore Models for ER Subtype Selectivity

Katzenellenbogen's group³² developed a pharmacophore model for ER β -selective agents by taking into an account the smaller size of the ER β binding cavity, and the key differing residues ER α Met421 and ER α Leu384 vs. ER β Ile373 and ER β Met336. They began with their original pharmacophore model for ER targeting agents²⁷ and modified it accordingly. The size of the

ligand was reduced by removal of the third, typically aryl, substituent on the core. One of the two phenol rings was fused to a heterocycle to reduce the size further. They imposed other rules, including one stating that the introduced substituents should interact favorably with ER β Ile373, or ER β Met336 and/or unfavorably with ER α Met421 and ER α Leu384.³² Their pharmacophore model fits relatively well with the structures of selective ER β ligands developed by others (compounds **6**, **7** and **10**,²⁸ **9** and **12**,²⁹ **8** and **13**,³⁰ **11**,³¹ **15**,³² **5** and **14**,³³ **17**,³⁴ **18**,³⁵ **19**³⁶) shown in Figure 5. Interestingly, a virtual screening approach utilizing direct receptor-based molecular docking and indirect ligand-based pharmacophore mining approaches, focusing the search for plant-based ER β -selective ligands, gave phytoestrogens structurally similar to genistein as hits with over 100-fold selectivity for ER β . Also, it was evident that ligands relatively larger in size were preferably selective for ER α .³⁷

1.3.2. Estrogen Receptor Beta Selective Agents – SAR and Applications

The phytoestrogen GEN was one of the first agents discovered to be selective (30-40 fold) for ER β . GEN has been cocrystallized with ER β LBD and from the crystal structure only a few features indicate that its interaction with ER β might be more favorable than its interaction with ER α .³⁸ It has been suggested that the stabilizing the van der Waals interaction of the isoflavone ring with the side chain of ER β Met336 contributes to genistein's selectivity.³⁸ *Ab initio* quantum chemical calculations of the interaction between a phenyl ring and the respective side chains of ER β Met336 and ER α Leu384 suggest that the side chain of ER β Met336 has a greater potential for interaction with the aromatic ring than does the side chain of ER α Leu384.³⁹

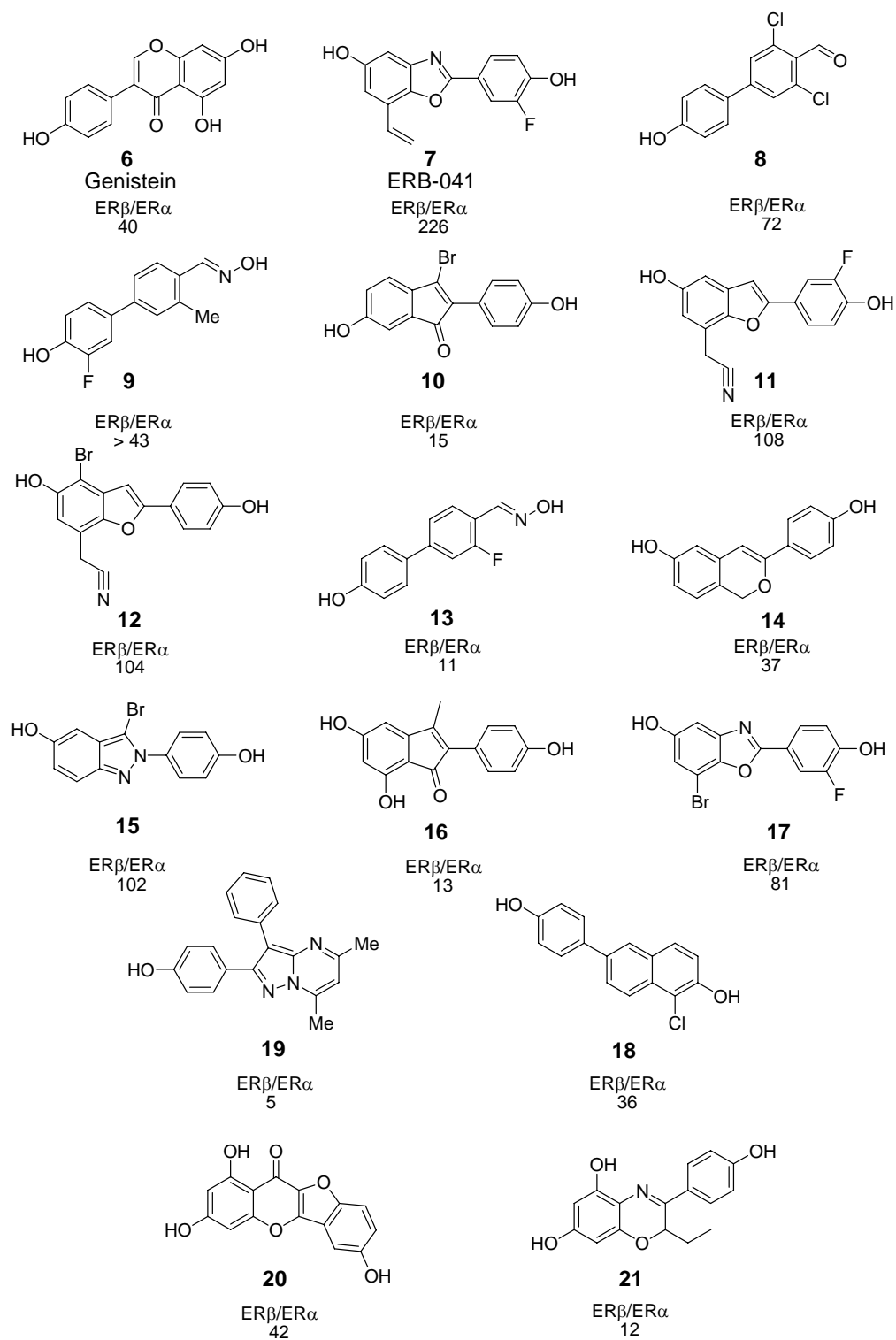


Figure 5. ER β selective ligands.²⁵⁻³³

Selectivity for ER β over ER α in binding assays is presented as the number below each structure. Data is taken from literature references 25-33.

It was also suggested that the 5-OH group on GEN has repulsive interactions with the side chain of ER α Met421, interactions not present in with the side chain of ER β Ile373.³⁹ Based on these findings, it is not a surprise that GEN was commonly used as a lead structure for the design of ER β selective agents. Figure 5 shows a select but structurally diverse set of compounds that are selective to various degrees for ER β in order to illustrate the more general SAR of these agents. Biphenyl-containing compounds **9** and **13** were recently developed by Wyeth Corp. research groups.²⁸ The phenolic A ring from estradiol was preserved to guarantee the binding affinity of these agents, and an oxime was used to mimic the D ring of estradiol.

Varying the substitution on the biphenyl core gave various levels of selectivity: biphenyl hydroxime **13** was only 11-fold selective, but by introducing a methyl group and changing the position of the fluorine substituent to give biphenyl oxime **9**, selectivity was improved to >43-fold. The majority of ER β selective ligands have two phenolic groups separated by ~9-12 Å, and distance and positioning of OH groups can increase or decrease selectivity. High selectivity and high binding potency agents (*e.g.*, compounds **7**, **11**, **12** and **15**) have two phenol rings connected through a five-membered heterocyclic ring (oxazole, pyrazole, furan), with the distance between the OH groups averaging 11.5Å. The structure of the heterocycle seems not to affect the potency or selectivity as long as the ligand size and distance between OH groups remains constant. Less selective agents usually have a larger distance between the OH groups.⁴⁰ Vinyl, cyano and halogen substituents, in the majority of cases, are more selective for ER β by either promoting the favorable soft-soft interaction with ER β Met336 or by inducing unfavorable interactions with ER α Met421 (reviewed in Ref. 22).

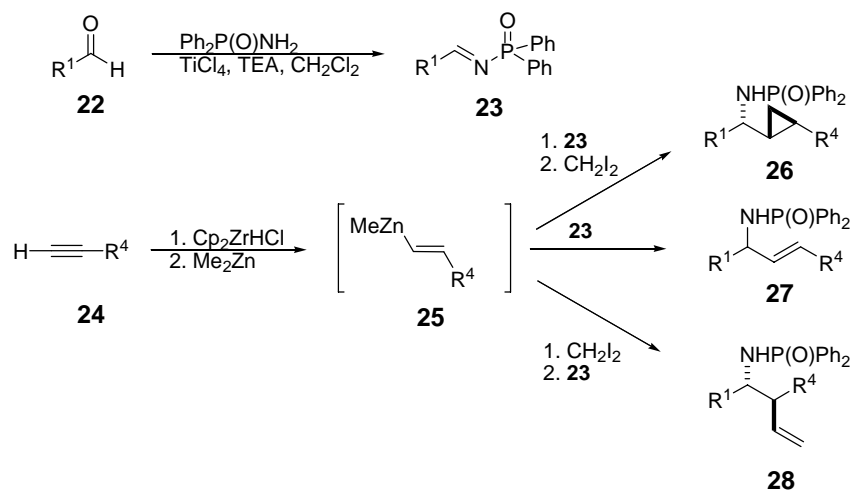
The role that ER β selective agents could play in breast cancer pharmacotherapy is yet to be determined. A proposed model for possible advantages of these agents towards targeting SERM-resistant cancer is discussed later in section 4.2. Synthetic and screening efforts in the present work were oriented towards discovering new scaffolds for ER targeting agents and for designing agents with features that potentially could target both ER α and ER β .

1.4. Synthetic Methods for Allylic Amides, Homoallylic Amides and C-Cyclopropylalkyl Amides

1.4.1. Conventional Synthetic Methods and Discovery Library Synthesis

Wipf *et al.*^{41,42,43} recently reported a new method for the synthesis of homoallylic amides, allylic amides and C-cyclopropylalkylamides. The methodology provided a 67-member discovery library (Table 1). The library members were prepared using a novel three-component aldimine addition reaction. By controlling the solvent and order of addition of the reagents, C-cyclopropylalkylamides (**26**), allylic amides (**27**) or homoallylic amides (**28**) can be prepared from readily available starting materials, aldehydes (**22**) and alkynes (**24**). The general synthesis is presented in **Error! Reference source not found.** The synthetic sequence begins with the hydrozirconation⁴⁴ of alkynes (**24**) with the Schwartz reagent (Cp₂ZrHCl), followed by *in situ* Zr-Zn transmetalation.⁴⁵ The resulting alkenylzinc species (**25**) readily adds to *N*-diphenylphosphinoylimines (**23**)⁴⁶ to provide the allylic amides (**27**). Addition of diiodomethane

(CH₂I₂) to the reaction mixture, once all *N*-diphenylphosphinoylimines (**23**) are consumed, affords *C*-cyclopropylamides (**26**) through a Simmons-Smith type cyclopropanation.⁴⁷

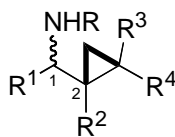


Scheme 1. Synthesis of the discovery library of *C*-cyclopropylalkylamides (**26**), allylic amides (**27**) and homoallylic amides (**28**).

Simply by changing the order of addition of reagents and solvents, diversity was introduced into cyclopropane (**26**) and alkene (**27**, **28**) scaffolds.

In contrast, addition of CH₂I₂ and *N*-diphenylphosphinoylimines (**23**) simultaneously to the alkenylzinc (**4**) afforded exclusively the homoallylic amides (**28**).⁴² The obtained 67-member discovery library was screened in transcriptional cell based assays for agonism and antagonism at ER α .⁴⁸ The discovery library screening data and detailed biological evaluation of the lead structure, part of the present work, are presented and discussed in detail in the Results section (2.1). Furthermore, the synthetic methods were tested under microwave conditions, and this new methodology will also be described.

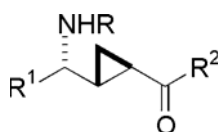
Table 1. Structures of the 67-member discovery library



C-Cyclopropylalkylamides*	C ₁ -C ₂	R	R ¹	R ²	R ³	R ⁴
26a (CK1183)	anti	P(O)Ph ₂	Ph	H	H	CH ₂ CH ₂ N(Ts)CO ₂ Et
26b	anti	P(O)Ph ₂	3-OMe-Ph	H	H	C ₄ H ₉
26c	anti	P(O)Ph ₂	2-OMe-Ph	H	H	C ₄ H ₉
26d	anti	P(O)Ph ₂	4-Cl-Ph	H	H	C ₄ H ₉
26e	anti	P(O)Ph ₂	Ph	H	H	CH ₂ CH ₂ OH
26f	anti	P(O)Ph ₂	Ph	H	H	CH ₂ CH ₂ CO ₂ Si(ⁱ Pr) ₃
26g	anti	P(O)Ph ₂	Ph	H	H	CO ₂ Me
26h	anti	P(O)Ph ₂	Ph	H	H	CH=CH ₂
26i	anti	P(O)Ph ₂	Ph	H	H	CH ₂ CH ₂ OSi(^t Bu)Ph ₂
26j	anti	P(O)Ph ₂	Ph	H	H	C ₄ H ₉
26k	syn	P(O)Ph ₂	Ph	H	H	C ₄ H ₉
26l	anti	P(O)Ph ₂	PhCC	H	H	C ₄ H ₉
26m	anti	CO ₂ CH ₂ Ph	Ph	H	H	CO ₂ Me
26n	anti	CO ₂ CH ₂ Ph	Ph	H	H	C(O)NH ⁱ Pr
26o	syn	CO ₂ CH ₂ Ph	Ph	H	Me	C(O)NH ⁱ Pr
26p	syn	P(O)Ph ₂	Ph	H	Me	C ₄ H ₉
26q	anti	P(O)Ph ₂	Ph	Et	H	Et
26r	anti	P(O)Ph ₂	Ph	Me	H	CH=CH ₂

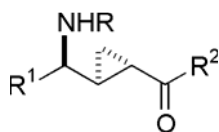
26s	anti	Ts	Ph	H	H	C ₄ H ₉
26t	syn	Ts	Ph	H	H	C ₄ H ₉
26u	anti	CO ₂ CH ₂ Ph	Ph	Me	H	C(O)NH ⁱ Pr
26v	anti	Ts	PhCH ₂ CH ₂	H	H	C ₄ H ₉
26w	anti	C(O)Ph	Ph	H	H	C ₄ H ₉
26x	anti	C(O)Ph-4-NO ₂	Ph	H	H	C ₄ H ₉

* Diastereomerically pure



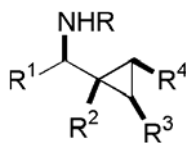
C-Cyclopropylalkylamino acids*	R	R ¹	R ²
26-1a	CO ₂ CH ₂ Ph	Ph	(S)-NHCH(Me)Ph
26-1b	CO ₂ CH ₂ Ph	Ph	NHPh-4-Br
26-1c	CO ₂ CH ₂ Ph	Ph	l-Ph-OMe
26-1d	C(O)Ph-4-Br	Ph	OMe

* Enantiomerically pure

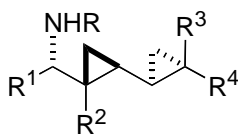


C-Cyclopropylalkylamino acids*	R	R ¹	R ²
26-2a	CO ₂ CH ₂ Ph	Ph	l-Ph-OMe

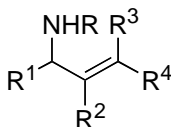
* Enantiomerically pure



C-Cyclopropylalkylamides	R	R ¹	R ²	R ³	R ⁴
26-3a	P(O)Ph ₂	Ph	H	Me	C ₄ H ₉
26-3b	C(O)Ph-3,5-diNO ₂	Ph	H	Me	C ₄ H ₉
26-3c	C(O)Ph	Ph	H	Me	C ₄ H ₉
26-3d	P(O)Ph ₂	Ph	Me	H	H

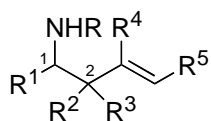


C-Cyclopropylalkylamides	R	R ¹	R ²	R ³	R ⁴
26-4a	C(O)Ph-3,5-(NO ₂) ₂	Ph-4-CO ₂ Me	H	Me	C ₆ H ₁₃
26-4b	P(O)Ph ₂	Ph	H	Me	CH ₂ CH ₂ OH
26-4c	P(O)Ph ₂	Ph-4-CO ₂ Me	H	Me	C ₆ H ₁₃



Allylic amides	R	R ¹	R ²	R ³	R ⁴
27a	P(O)Ph ₂	Ph	H	H	CH ₂ CH ₂ N(Ts)CO ₂ Et
27b	P(O)Ph ₂	(<i>E</i>)-PhCH=C(CH ₃)	H	H	C ₄ H ₉
27c	P(O)Ph ₂	Ph	H	H	C ₄ H ₉
27d	P(O)Ph ₂	Ph	H	H	CH ₂ CH ₂ OSi(<i>t</i> Bu)Ph ₂
27e	P(O)Ph ₂	Ph	H	H	CH ₂ CH ₂ CO ₂ Si(<i>i</i> Pr) ₃
27f	P(O)Ph ₂	(<i>E</i>)-PhCH=CH	H	H	C ₄ H ₉

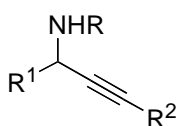
27g	P(O)Ph ₂	4-CO ₂ Me-Ph	H	H	C ₄ H ₉
27h	P(O)Ph ₂	3-OMe-Ph	H	H	C ₄ H ₉
27i	P(O)Ph ₂	2-OMe-Ph	H	H	C ₄ H ₉
27j	P(O)Ph ₂	4-NO ₂ -Ph	H	H	C ₄ H ₉
27k	P(O)Ph ₂	3-NO ₂ -Ph	H	H	C ₄ H ₉
27l	P(O)Ph ₂	4-Cl-Ph	H	H	C ₄ H ₉
27m	P(O)Ph ₂	PhCC	H	H	C ₄ H ₉
27n	Ts	Ph	H	H	C ₄ H ₉
27o	Ts	PhCH ₂ CH ₂	H	H	C ₄ H ₉
27p	P(O)Ph ₂	Ph	H	Me	C ₄ H ₉
27q	P(O)Ph ₂	Ph	Me	H	H
27r	P(O)Ph ₂	Ph	Et	H	Et
27s	P(O)Ph ₂	4-CO ₂ Me-Ph	Si(CH ₃) ₃	H	(<i>E</i>)-CH=CHC ₆ H ₁₃
27a1	P(O)Ph ₂	Ph	H	H	CH ₂ CH ₂ N(Ts)CO ₂ Et



Homoallylic amides*	C1-C2	R	R ¹	R ²	R ³	R ⁴	R ⁵
28a	anti	P(O)Ph ₂	Ph	CH ₂ CH ₂ OSi(^t Bu)Ph ₂	H	H	H
28b		P(O)Ph ₂	Ph	Me	Me	H	Me
28c	anti	P(O)Ph ₂	4-CO ₂ Me-Ph	CH ₂ CH ₂ OSi(^t Bu)Ph ₂	H	H	H
28d	syn	P(O)Ph ₂	4-OMe-Ph	C ₄ H ₉	H	H	H
28e	syn	P(O)Ph ₂	Ph	C ₄ H ₉	H	H	H

28f	syn	Ts	Ph	C ₄ H ₉	H	H	H
28g	syn	Ts	Ph	CH ₂ CH ₂ OSi(^t Bu)Ph ₂	H	H	H
28h	syn	P(O)Ph ₂	Ph	Et	H	Et	H
28i	anti	P(O)Ph ₂	Ph	Et	H	Et	H
28j		P(O)Ph ₂	Ph	H	H	Me	H
28k	syn	3,5-(NO ₂) ₂ -PhC(O)	Ph	C ₄ H ₉	H	H	H

* Diastereomerically pure



Propargylic amides	R	R ¹	R ²
28-1a	P(O)Ph ₂	Ph	C ₄ H ₉

1.4.2. Microwave Chemistry

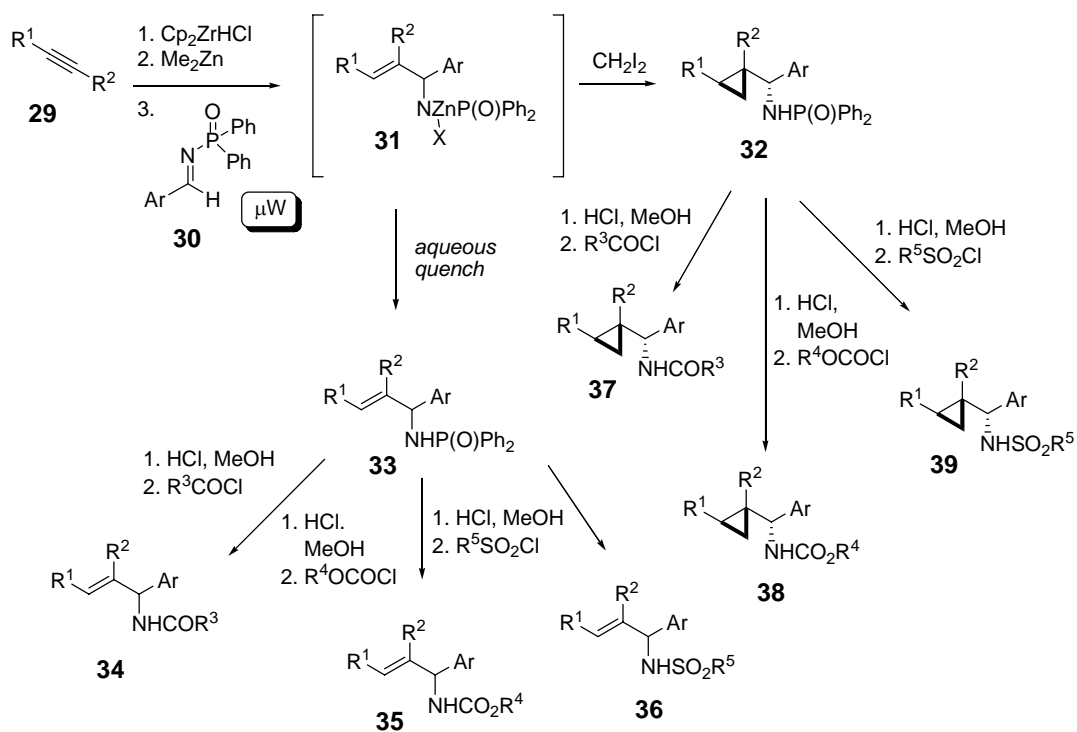
Microwaves have been used for heating food since the late 1950's. However, their use for heating and accelerating reactions in synthetic organic chemistry came about at a much later date, 1986.⁴⁹ In the late 1980's and early 1990's, domestic microwaves were used for microwave-assisted organic synthesis (MAOS). This approach met with many problems with temperature and pressure control that resulted in poor reproducibility. However, it became increasingly evident that microwave presented advantages over conventional heating.⁵⁰ Microwave irradiation is electromagnetic irradiation in the frequency range of 0.3 to 300 GHz. All domestic microwaves and all microwave reactors for chemical synthesis operate at a frequency of 2.45 GHz (which corresponds to a wavelength of 12.24 cm) to avoid interference

with telecommunication and cellular phone frequencies. The energy of the microwave photon in this frequency region (0.0016 eV) is too low to break chemical bonds and is also lower than the energy of Brownian motion. Therefore, microwaves cannot induce chemical reactions.⁵⁰ Microwave-supported synthesis takes advantage of highly efficient dielectric heating. Microwave heating is highly dependent on the ability of the irradiated material to absorb microwave energy and convert it to heat. The conduction of heat is different than in conventional heating. Simply put, microwave heating can be visualized as heating from “inside out” and conventional heating from “outside in”. Modern microwave reactors provide a homogenous distribution of the microwaves through the reaction vessel and therefore a very high efficiency of microwave heating is achieved. These features of microwave heating generally result in an increased reaction rate and fewer byproducts for many synthetic organic reactions, in particular those that use solvents and/or reactants that have a high dielectric constant. In some cases, it is enough that reactive intermediates have a sufficient dipole moment, increasing the ability of the entire reaction mixture to absorb microwave energy and thus increase the reaction rate. Many reactions that take hours, even days with conventional heating may proceed in only min. in a microwave. Reasons behind this increased rate lie in the superheating that microwaves produce in a closed vessel, with an increased pressure ($PV = nRT$). Incorporation of a microwave system significantly accelerated the hydrozirconation–transmetallation–aldimine addition sequence and served as a more efficient platform for library synthesis, as described below (section 1.4.3). The development of key protocols for these microwave based syntheses is discussed in the results (section 2.1.5.1).

1.4.3. Synthesis of the Second Generation Library of Allylic Amides and C-Cyclopropylalkylamides Using Microwave

Extensions of the recently reported microwave methodology⁵¹ were used in library syntheses. The University of Pittsburgh Center for Chemical Methodologies & Library Development (CMLD, <http://ccc.chem.pitt.edu/UPCMLD/index.html>) prepared a 20-membered library of allylic and C-cyclopropylalkylamides from three alkynes and seven phosphinoylimines using microwave acceleration followed by serial chromatographic purification. Subsequent functionalization of this library with ten different acyl chlorides, seven carbamoyl chlorides, and nine sulfonyl chlorides resulted in the synthesis of a 100-membered focused library of allylic and C-cyclopropylalkylamides for this second generation library. All microwave reactions in the library were performed on a Personal Chemistry Emrys Optimizer. Experimental details of the second generation library synthesis are reported elsewhere,⁵² Scheme 2. The design of the second generation library is discussed in detail in section 2.1.6.1.

In brief, the library synthesis involved the following steps. Diverse alkynes, internal and terminal, unfunctionalized or with various functionalities, were submitted to hydrozirconation reaction conditions in a microwave. In a typical case, a suspension of the Schwartz reagent in toluene was treated with alkyne at 100 °C, 300W for 1 minute and provided a clear yellow solution of alkenyl zirconocene. The mixture was then cooled to -78 °C, and treated with a solution of dimethylzinc.



Scheme 2. Second generation library microwave supported synthesis.

After warming to $0\text{ }^\circ\text{C}$, the resulting zinc intermediate was treated with the aldimine in a microwave at $100\text{ }^\circ\text{C}$, 150W for 2 min. The desired phosphinoyl-protected allylic amide was obtained after aqueous quench. After removal of the amine protecting group under acidic conditions, the free amine salts were further functionalized by *N*-acylation, *N*-carbamoylation, and *N*-sulfonation, providing allylic amide second generation library members.⁵² Without purification, the crude phosphinoyl allylic amides were submitted to Simmons-Smith type cyclopropanation conditions in the presence of diiodomethane at $60\text{ }^\circ\text{C}$, 300W for 30 min. in the microwave. The deprotection and further functionalization were performed the same way as for allylic amides, providing *C*-cyclopropylalkylamide library members.⁵²

Seventy allylic amides and *C*-cyclopropylalkylamides with purities exceeding 85% (as determined by C-18 reverse-phase HPLC with monitoring at 220 nm) were tested for their effects on ER α ⁵² and ER β (Table 6, section 2.1.7). The novel ER targeting agents identified from these screens, their biological evaluation and their SAR are discussed in greater detail in section 2.1.6.

2. RESULTS AND DISCUSSION

2.1. New ER Targeting Agents from the Discovery Library of Allylic Amides, Homoallylic Amides and C-Cyclopropylalkylamides

Antiestrogens primarily function by competing with endogenous estrogens for binding to the ER. In the case of SERMs, binding to the ER can produce estrogenic and antiestrogenic responses depending on tissue type and the specific chemical structure of the compound. SERM resistance is one of the major problems in current hormonal therapy of breast cancers. Therefore, there is a growing need for the design and synthesis of structurally novel antiestrogens in the hope to overcome these problems. Many of the discovery library (Table 1, section 1.4.1) components contained a combination of a di- or triaryl ring system with a central electron-rich (*e.g.*, olefin) moiety. This is a structural feature common for some estrogens and many antiestrogens. The initial goal was to find novel structural scaffolds with antiestrogenic properties and no stimulatory effects on ER α .

2.1.1. Discovery Library Screening at ER α

The purpose of the initial screen of the discovery library was to determine if library members held potential for agonism or antagonism of ER α at a classical ERE. All library members were tested for ligand-dependent transcriptional activity of ER α using a transient transfection assay.^{53,54} ER naïve HEK293 cells were co-transfected with three plasmids containing genes for

CMV promoter-driven ER α , the reporter ERE-tk-Luc, and standard CMV- β -galactosidase (β -Gal) for transfection efficiency control using DOTAP liposomes as the transfection reagent. In this system, ER α and β -Gal are constitutively expressed, and compounds that cause the ER α to adopt an agonist-bound conformation cause binding of the receptor to the ERE and transcription of luciferase, providing a readout of ligand-dependent ER α transcriptional activation that can be standardized against β -Gal expression. Library members and TAM were screened at 10 μ M. E2 (10 nM) was used as the positive control. Figure 6 shows the compound-induced fold induction

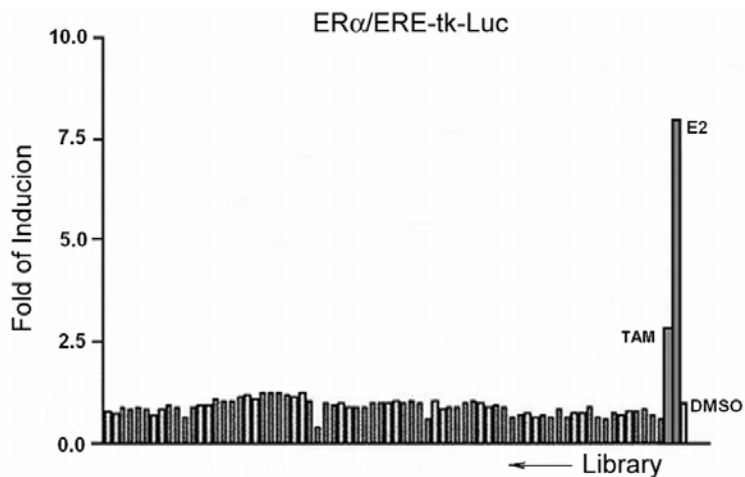


Figure 6. Screen of the discovery library for ER α agonists at classical ERE.

ER naïve HEK293 cells were transfected with CMV promoter-driven human ER α , an ERE-tk-Luc reporter and a CMV- β -gal transfection control using DOTAP liposomes. E2 and TAM were used as positive controls. Library compounds and TAM were tested at 10 μ M and E2 at 10 nM. Data represents fold of induction (mean \pm SD, N=3). This screen in search for agonists was optimized and performed by Dr. Ying Mu.⁴⁸

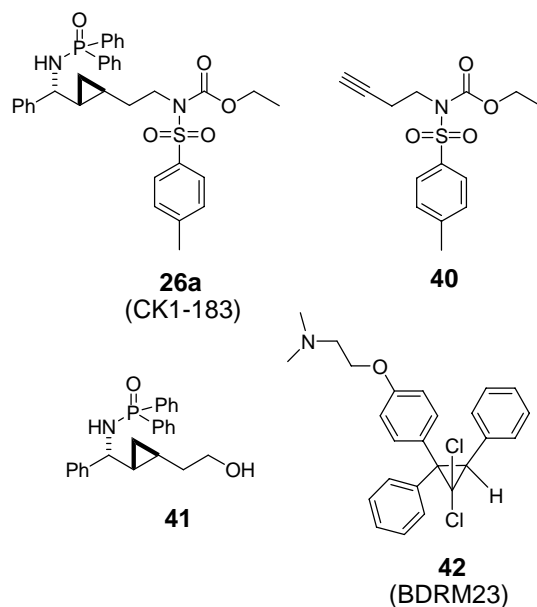


Figure 7. Structures of lead C-cyclopropylalkylamide 26a (CK1-183) and control agents (40, 41 and 42).

of luciferase activity compared to the activity in cells treated only with vehicle (DMSO, 0.1%). As expected, TAM showed modest estrogenic activity in this assay. In contrast, none of the library compounds promoted ER transcription.

To search for ER α antagonists, the same experimental setup was used, but the compounds were tested for antagonism of E2-induced luciferase transcription. From the 67-member discovery library, thirteen compounds, structurally representative of all three subgroups (three homoallylic amides, three allylic amides and seven C-cyclopropylalkylamides), were tested as potential antagonists. The transiently transfected HEK293 cells were co-incubated with E2 (10 nM) and with the candidate antagonists at both 10 μ M and 1 μ M concentrations. (*Z*)-1,1-Dichloro-2,3-diphenyl-2-[4-[2-(dimethylamino)ethoxy]phenyl]cyclopropane **42** (BDRM23)⁵⁵ and TAM (Figure 7), known ER α antagonists, were used at 10 μ M and 1 μ M as positive controls (Figure 6). The synthetic precursor alkyne **40** (1 and 10 μ M) was used as a negative control.

Two compounds, the allylic amide **27b**, (*E*)-*N*-[1-(1-Methyl-2-phenylvinyl)hept-2-enyl]-*P,P*-diphenylphosphinamide, (Table 1) and the *C*-cyclopropylalkylamide **26a** (CK1-183), *O*-ethyl-*N*-{2-[(1*S**,2*R**)-2-[(*R**)-[(diphenylphosphinoyl)amino](phenyl)methyl]cyclopropyl]ethyl}-*N*-[(4-methylphenyl)sulfonyl]carbamate (Figure 7), significantly inhibited E2-induced transcription at the ERE at 1 and 10 μ M (Figure 8).

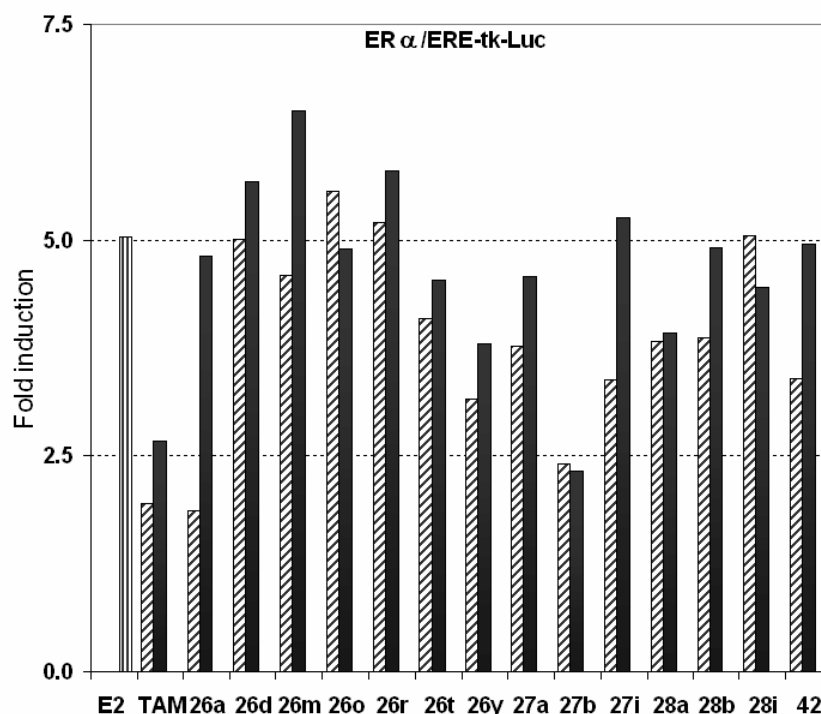


Figure 8. Test for potential ER α antagonism in the transcriptional assay.

Library compounds, seven *C*-cyclopropylalkylamides (**26a** (CK1-183), **26d**, **26m**, **26o**, **26r**, **26t**, **26y**), three allylic amides (**27a**, **27b**, **27i**), three homoallylic amides (**28a**, **28b**, **28i**), and TAM and **42** were tested at 10 μ M (hatched bars) and 1 μ M (black bars) in the presence of E2 at 10 nM. Data represents fold of induction (mean \pm SD, N=3) and stimulation control E2 (N=9).

Preliminary tests for inhibition of E2-induced proliferation of MCF-7 cells showed compound **27b** to be inactive at the concentrations used (Table 2), whereas *C*-cyclopropylalkylamide **26a** (CK1-183), the second-most active antagonist in the transcriptional screen, inhibited MCF-7 cell

proliferation in these initial tests. Therefore, **26a** (CK1-183) was evaluated in more detail for antagonistic activity in cell-based and protein-ligand displacement assays.

2.1.2. C-Cyclopropylalkylamide **26a** (CK1-183) as a New ER α Partial Antagonist

2.1.2.1. C-Cyclopropylalkylamide **26a** (CK1-183) Inhibits Transcriptional Activity of ER α

The C-cyclopropylalkylamide **26a** (CK1-183) was further examined for concentration-dependent inhibition of the E2-induced transcriptional activation of ER α . Transfected HEK293 cells were stimulated with E2 (1 nM) in the presence of a range of concentrations (3.2 nM - 50 μ M) of compound **26a** (CK1-183) or TAM (Table 2).

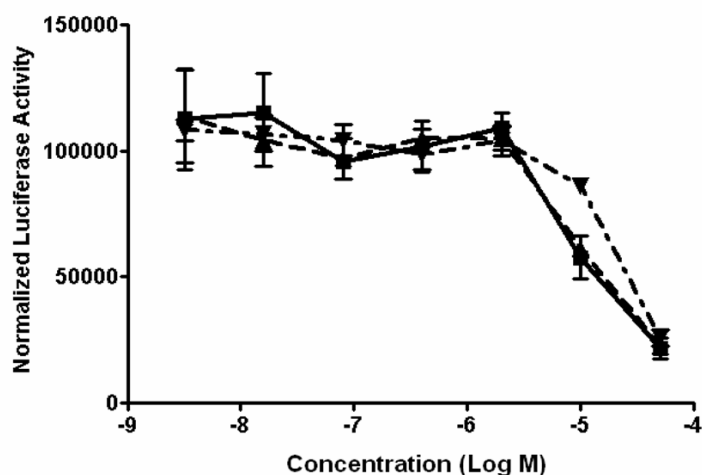


Figure 9. C-Cyclopropylalkylamide **26a** (CK1-183) inhibits E2 induced transcriptional activation of ER α .

The separated enantiomers, **26a** (CK1-183-*ent1*) (▲) and **26a** (CK1-183-*ent2*) (▼), and the racemate (■) of C-cyclopropylalkylamide **26a** (CK1-183) show indistinguishable activities. Data represents normalized luciferase counts to β -Gal read out used as an internal standard (means \pm SD, N = 3).

IC₅₀ values were estimated from concentration-dependence curves that best fit the data obtained as an average from at least two transfections done in triplicate (Figure 9).

Compound **26a** (CK1-183) antagonized the effects of E2 in a concentration-dependent manner, yielding an IC₅₀ of 11 ± 2 μM. In this assay, TAM gave an IC₅₀ of 4.9 ± 2.0 μM. Compound **26a** (CK1-183) failed to induce transcription at ERE as compared to TAM and E2 (Figure 6). These findings indicated that **26a** (CK1-183) is likely to be a full or partial antagonist.

2.1.2.2. C-Cyclopropylalkylamide 26a (CK1-183) Inhibits E2 Stimulated Proliferation of MCF-7 Cells

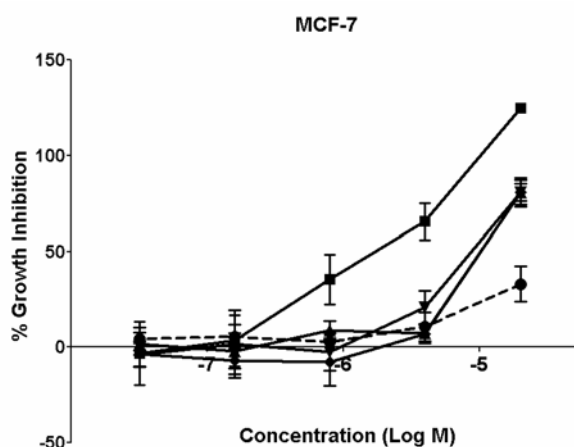


Figure 10. C-Cyclopropylalkylamide 26a (CK1-183) inhibits E2 induced MCF-7 proliferation.

Compound **26a** (CK1-183) (▲) and its enantiomers, **26a-ent1** (▼) and **26a-ent2** (◆) inhibit E2 (1 nM) induced proliferation of MCF-7 cells in a concentration dependent manner (Figure 10). TAM (■) and alkyne **8** (●), the synthetic precursor for **26a** (CK1-183) (Figure 7), were used as positive and negative controls, respectively. Data represents percent growth inhibition (mean ±SD, N=4).

Compound **26a** (CK1-183) was further evaluated for antiestrogenic action in an E2-stimulated MCF-7 cell proliferation assay. It inhibited the E2 stimulated growth of MCF-7 cells in a concentration-dependent manner.

2.1.2.3. C-Cyclopropylalkylamide 26a (CK1-183) is a Modest Competitor on ER α

Compound **26a** (CK1-183) was tested for its ability to displace a fluorescent E2 derivative from the ER α . Recombinant human ER α was complexed with fluorescently labeled estradiol (ES2) and then treated with test agents. After 2 h, the fluorescence polarization was measured. ES2 bound to ER α protein gave high fluorescence polarization. In this assay, the presence of a displacing ligand causes a decrease in the fluorescence polarization. Concentration dependence curves were constructed and IC₅₀s were calculated from the best-fit curves for the controls E2 (5 ± 4 nM) and TAM (28 ± 20 nM). Although compound **26a** (CK1-183) showed a concentration-dependent displacement of ES2 in this *in vitro* assay, its IC₅₀ value was above the highest concentration tested ($> 10 \mu$ M), leading to the conclusion that **26a** (CK1-183) is at best a modest E2 competitor at the ER α (Figure 11).

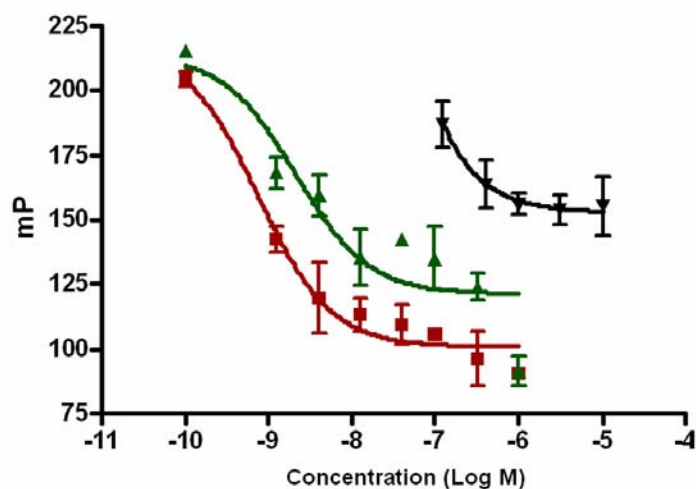


Figure 11. C-Cyclopropylalkylamide 26a (CK1-183) tested in ER α competition assay

Compound **26a** (CK1-183) (\blacktriangledown) ($IC_{50} > 10\mu M$) shows low potency in an *in vitro* ER α competition assay (Panvera) as compared to E2 (\blacksquare) ($IC_{50} 5 \pm 4$ nM) and TAM (\blacktriangle) ($IC_{50} 28 \pm 20$ nM). Data (mP) represents fluorescence polarization (mean \pm SD, N=3), $mP = 1000 \times (S - G \times P) / (S + G \times P)$, where S and P are the background-subtracted intensity measurements for the parallel and perpendicular components, and G is a constant of the instrument. The one site competition method in GraphPad Prism 4 software was used for constructing dose-response curves and calculating IC_{50} s.

2.1.2.4. C-Cyclopropylalkylamide 26a (CK1-183) Has No Effect on ER α Negative Breast Cancer Cells

The unusual structure of **26a** (CK1-183) as compared to a variety of known antiestrogens stimulated further evaluation of the specificity of **26a** (CK1-183) in ER-negative MDA-MB231 human breast cancer cells. The growth inhibitory properties of **26a** (CK1-183) were ER-dependent, as it had no effect on the proliferation of MDA-MB231 cells. C-Cyclopropylalkylamide **26a** (CK1-183) did not demonstrate any antiproliferative effects on these

cells even at high micromolar concentrations (Table 2). Colchicine was used as a positive control.⁴⁸

Table 2. Fifty percent inhibitory concentrations of compounds examined for E2-induced luciferase activity and MCF-7 cell proliferation, and for E2-independent MDA-MB231 cell proliferation.

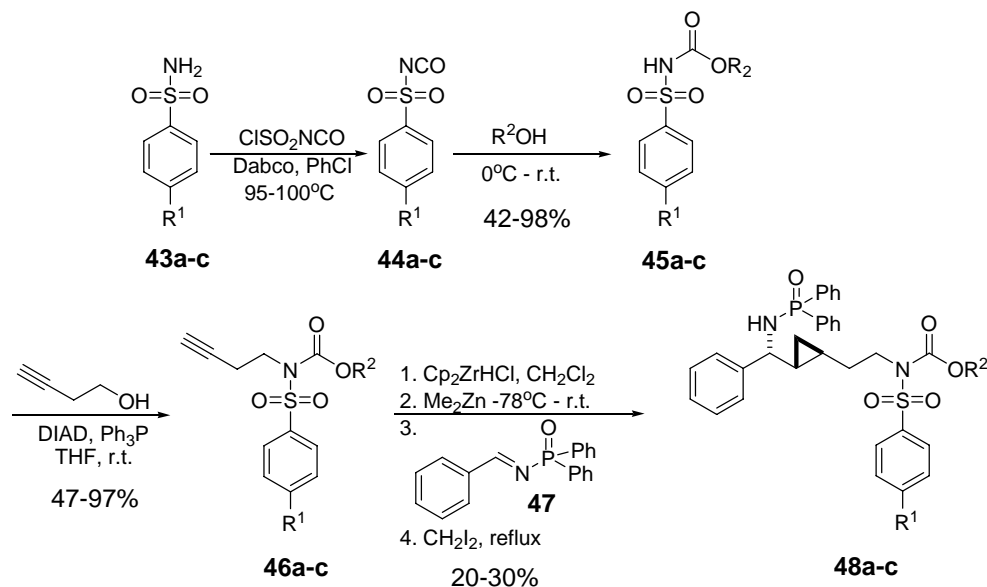
Compound	ER α /ERE-tk-Luc IC ₅₀ (μ M)	MCF-7 GI ₅₀ (μ M)	MDA-MB231 GI ₅₀ (μ M) ^e
TAM	4.9 \pm 2.0 ^a	3.9 \pm 2.3 ^b	>50 ^e
Colchicine	-	-	0.082 \pm 0.009 ^e
26a	11 \pm 2 ^a	12 \pm 4 ^c	>50 ^e
26a-ent1	13 \pm 4 ^a	8.8 \pm 2.1 ^b	>50 ^e
26a-ent2	23 \pm 7 ^a	13 \pm 0 ^b	>50 ^e
27a	-	15 \pm 0 ^d	-
27b	-	>20 ^d	-
28a	-	13 \pm 0 ^d	-
28b	-	16 \pm 1 ^d	-
40	-	>20 ^d	-
42	-	12 \pm 0 ^d	-

Values given are means + SD. The range of concentrations used was 3.2 nM - 50 μ M. ^aN = 6. ^bN = 8. ^cN=20. ^dN = 4. ^eN = 8.

In conclusion, a new structural class of ER α modulating agent was identified from a library screen of 67 homoallylic amides, allylic amides, and C-cyclopropylalkylamides (this is the discovery library described in section 1.4.1). Constructs containing CMV promoter-driven ER α and the estrogen-regulated element of the *Xenopus* vitellogenin A2 gene inserted into the tk-

luciferase plasmid were transiently transfected into mammalian cells. ER α antagonists were identified by their ability to antagonize 17 β -estradiol (E2)-induced transcription in transfected cells. One compound, *C*-cyclopropylalkylamide **26a** (CK1183),^{42,48} was shown to inhibit E2-induced proliferation of ER-positive MCF-7 human breast cancer cell lines while having no effect on ER-negative MDA-MB231 human breast cancer cells. This compound served as a lead for a second generation library (described in section 1.4.3) synthesis towards new ER targeting agents.⁵² Preliminary SAR around *C*-cyclopropylalkylamide **26a** (CK1-183) as a lead is discussed in the next section.

2.1.3. Synthetic Efforts Based on *C*-Cyclopropylalkylamide **26a** (CK1-183) as a Lead



Scheme 3. *C*-Cyclopropylalkylamide analogue synthesis.

R¹=H, R²=*t*Bu (**45a**, **46a**, **48a**); R¹=Me, R²=*t*Bu (**45b**, **46b**, **48b**); R¹=Cl, R²=Et (**45c**, **46c**, **48c**)

In order to better understand the structure-activity relationships within the first generation discovery library, the synthesis of a number of analogues based on systematic modification of the sulfonylcarbamate moiety of **26a** (CK1-183) was undertaken (Scheme 3). Synthetic protocols for the synthesis of *C*-cyclopropylalkylamides were developed previously in the Wipf group and will be discussed in detail in the experimental section.

Briefly, sulfonylisocyanates **44a-c** (**44a** R¹=H, **44b** R¹=Me, **44c** R¹=Cl), commercially available or easily obtained from corresponding sulfonamides **43a-c**, were converted to sulfonylcarbamates **45a-c** in moderate to high yields (42-98%). The Mitsunobu protocol^{56,57} gave the highly functionalized alkynes **46a-c** in moderate to high yields (47-97%), which were submitted to one pot hydrozirconation–transmetallation–aldimine (**47**) addition–cyclopropanation give *C*-cyclopropylalkylamides **48a-c** (Scheme 3). Synthesis of the library of analogues of **26a** (CK1-183) proved to be problematic. Alkyne precursors that were highly functionalized (**46a-c**) provided poor yields (20-30%) of *C*-cyclopropylalkylamides **48a-c**. Unfortunately, only three analogues were obtained in purity (> 90%) sufficient for testing in biological assays (Figure 12).

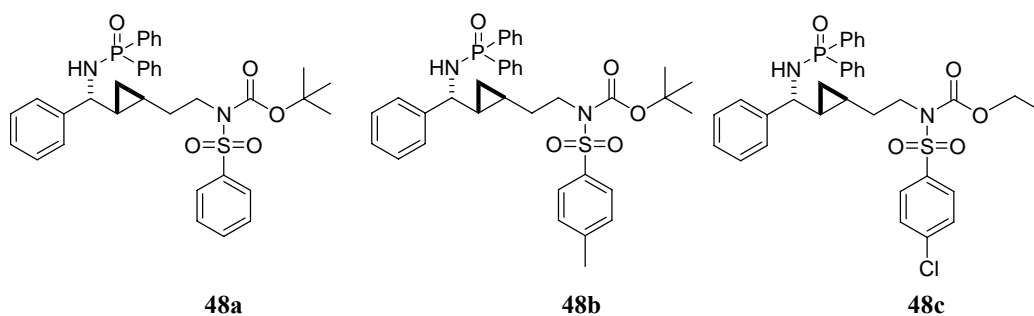


Figure 12. Analogues of *C*-cyclopropylalkylamide **26a (CK1-183) biologically tested.**

New methodology was needed for more efficient focused library syntheses. In addition, more elaborate changes in the lead structure were necessary to increase the chances of obtaining new compounds with improved cell potency.

The newly developed microwave-supported methodology for the synthesis of allylic amides and *C*-cyclopropylalkylamides will be discussed in more detail in section 2.1.5.

2.1.4. SAR of C-Cyclopropylalkylamides from Discovery Library

2.1.4.1. SAR from Cell-Based Assays

To investigate the importance of the sulfonylcarbamate moiety of **26a** (CK1-183), a synthetic precursor of this compound, alkyne **40** (Figure 7), and C-cyclopropylalkylamide **41** were tested in the MCF-7 antiproliferative assay and the transcriptional assays. Alkyne **40** was tested in order to evaluate any biological activity arising from the sulfonylcarbamate portion of **26a** (CK1-183), and compound **41** to test the contribution from the bulky lipophilic phosphinoyl group. Interest in the effect of the sulfonylcarbamate moiety of these compounds was stimulated by a recent report on ER targeting agents that contain sulfonamide moieties⁵⁸ and the results of an antagonist screen (Figure 8) where structural analogues of **26a** (CK1-183) lacking the sulfonylcarbamate had no antagonistic activity.

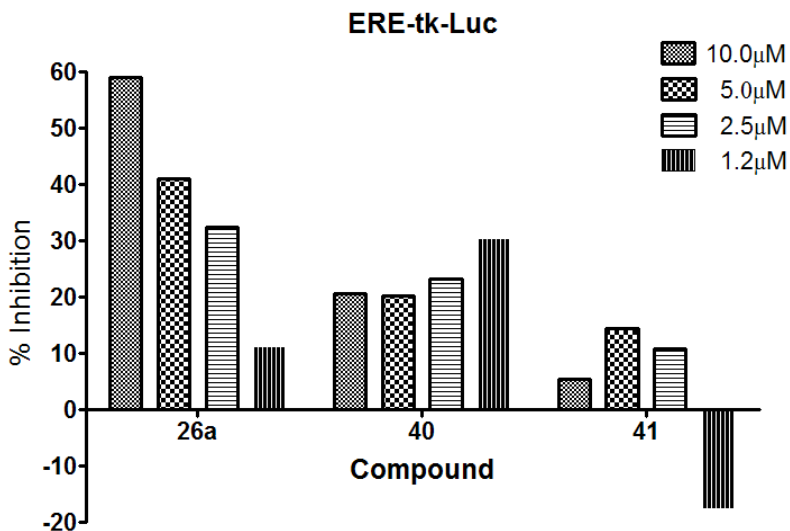


Figure 13. Lead compound **26a** (CK1-183) and control compounds **40** and **41**, tested for inhibition of E2 induced transcriptional activation of ER α at classical ERE.

Data represents the % inhibition calculated from the means of normalized luciferase counts (N=3). Luciferase counts were normalized by β -Gal counts used as an internal standard and cotransfected with the receptor and the reporter.

Alkyne **40** demonstrated poor-to-moderate MCF-7 growth inhibition (Figure 7) and almost no activity in the transcriptional assay (Figure 13). Compound **41**, representing the phosphinoyl bulky lipophilic portion of **26a** (CK1-183), showed similar low activity in altering the growth of MCF-7 cells and no inhibitory activity on E2-induced transcriptional activation of the ER α at a classical ERE (Figure 13). These findings suggested that the **26a** (CK1-183) structure as a whole was necessary for biological activity.

Molecular docking studies of **26a** (CK1-183) using the CAChe suite of algorithms with a model of the ER α LBD were performed. Docking studies (for details, see section 2.1.4.2) using the model of the LBD when bound by raloxifene indicated that the sulfonylcarbamate portion of the molecule binds deep inside the ligand binding pocket of the ER α -LBD while the phosphinoyl group lies outside the pocket.

In order to test the importance of the sulfonylcarbamate moiety, three structurally close analogues of **26a** (**48a-c**) were synthesized (Figure 12). It was expected that small modifications in sulfonylcarbamate portion of **26a** (CK1-183) would induce changes in the antagonistic activity. The introduced changes did not significantly affect the MCF-7 antiproliferative activity, yielding IC₅₀ values of 14.7 μ M (**48a**), 20.2 μ M (**48b**) and 17.8 μ M (**48c**). These results indicated that the proposed model with the sulfonylcarbamate portion binding deep inside the ligand binding pocket was not sufficient to explain the antagonistic activity of **26a** (CK1-183) and its close analogues (**48a**, **48b** and **48c**). Attention was then directed towards the phosphinoyl

group and its positioning as a cap to the binding pocket (Figure 15), interfering with helix 12 movement as discussed in section 2.1.4.2.

Since biological activity is often due to a single enantiomer in a racemate, the enantiomers of **26a** (CK1-183) (**26a-ent1** and **26a-ent2**) were separated by chiral HPLC and tested in parallel with racemic **26a** (CK1-183) in the transcriptional assay. Interestingly, no difference was observed between the activities of the enantiomers of **26a** (CK1-183), both being equipotent to the racemate (Figure 9). The activities of the enantiomers and the racemate were also compared in the MCF-7 antiproliferative assay (Figure 10). Again, the enantiomers and the racemate of **26a** (CK1-183) were not statistically different in their inhibition of E2-induced growth of this ER-positive cell line.

2.1.4.2. Docking studies

Molecular docking studies using the CAChe suite of algorithms with a model of the ER α LBD were conducted to compare the binding mode of both enantiomers of **26a** (CK1-183), as well as raloxifene (Figure 14). The crystal structure of human ER α -LBD in complex with RAL (1ERR)³⁸ was downloaded from the Protein Data Bank web page. RAL was used as a standard to test the docking system used. RAL was redocked into the pocket in the 1ERR crystal structure by holding the residues of the protein fixed and allowing the ligand to be flexible. The orientation and hydrogen bonding of the redocked complex were close to that in the crystal structure (Figure 14). The lead structure **26a** (CK1-183) was superimposed on RAL in the ER

binding pocket, the model of RAL was removed, and the model of **26a** (CK1-183) was docked into the pocket by holding the protein rigid and the ligand flexible. Docking studies indicated that the phosphinoyl group of **26a** (CK1-183) may serve as a cap to the binding pocket (Figure 15), interfering with helix 12 movement, while the remainder of the structure of **26a** (CK1-183) binds deeper into the raloxifene binding cleft and may interact with residues at helices H3 (A350, D351), H6 (W383, R394) and H11 (L525, L536), suggesting a partial or full antagonist binding mode. The docking energy (a.k.a. score) was -74.4 kcal/mole (Figure 15), comparable to the score obtained for RAL, -104.4 kcal/mole (Figure 14).

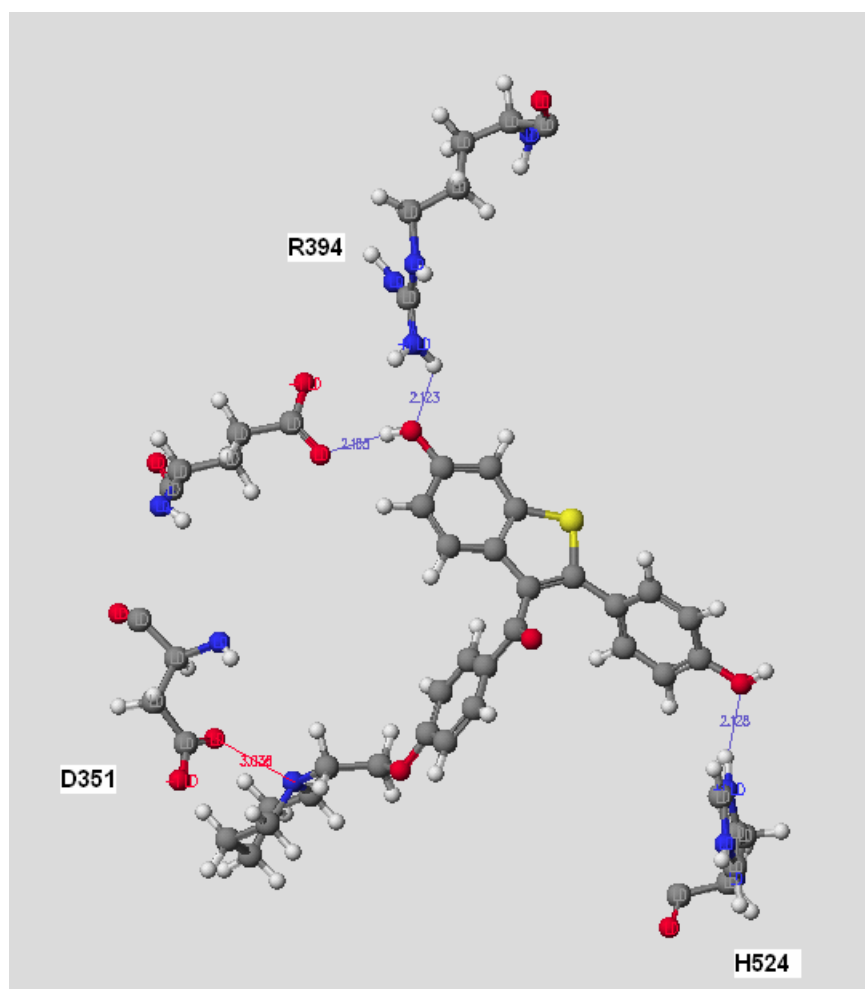


Figure 14. Raloxifene docked into ER α -LBD using BioMedCACHe.

The scores and the orientation in the pocket indicate the possible interaction of **26a** (CK1-183) being at best comparable to that of RAL. The observation that the phosphinoyl system lies essentially outside of the ligand binding pocket in the molecular docking exercises helps to explain the absence of enantiomer specificity for this compound. Taken together, the modeling and the results of the biological evaluation of the individual enantiomers of **26a** (CK1-183) and its close analogues (**48a**, **48b** and **48c**) indicated that the interaction of this compound with the ER ligand binding pocket is likely to be governed solely by hydrophobic interactions.

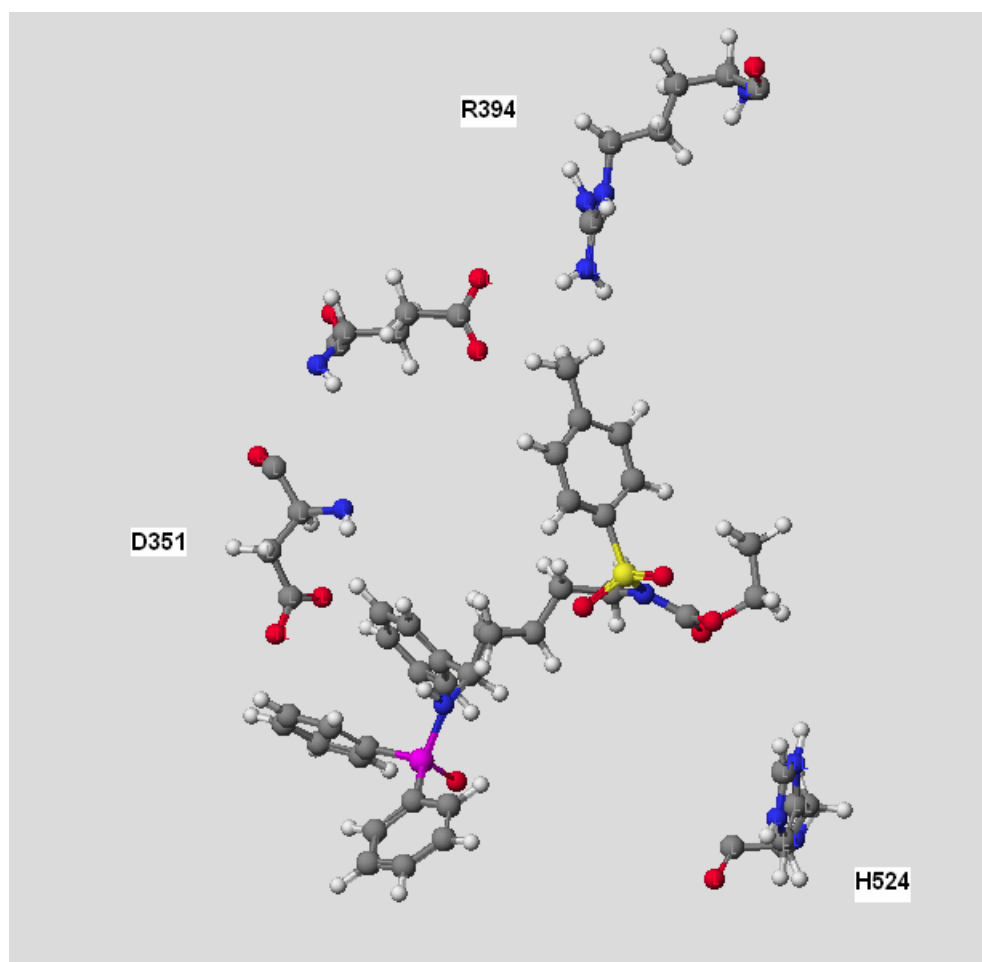


Figure 15. *C*-Cyclopropylalkylamide **26a** (CK1-183) docked into the ER α -LBD raloxifene binding pocket using BioMedCACHe.

Therefore, it is understandable that the results obtained in the MCF-7 cells, were quite similar regardless of the changes to the sulfonylcarbamate moiety or the different spatial orientation of the enantiomers.

Overall, the unusual structure of **26a** (CK1-183), its ability to antagonize E2 in the cell-based assays and its modest ability to displace E2 in the binding pocket suggested new avenues for SERM design.

The lead structure **26a** (CK1-183) suffered from a lack of drug-like properties, high ClogP (7.6) and high molecular weight (616.7) as opposed to a preferable ClogP value < 5 and a molecular weight < 500, found in most drugs and drug like molecules.⁵⁹ A lack of drug-likeness of **26a** (CK1-183) and results presented above in the biological assays and molecular docking studies indicated that the following steps were necessary in order to optimize the potency of this compound: (1) remove the large and hydrophobic phosphinoyl group and introduce smaller and more functionalized aromatic substituents on the nitrogen; (2) replace the sulfonylcarbamate with smaller size moieties in order to test whether this portion of the molecule is crucial for biological activity; and (3) introduce substituents that would promote hydrogen bonding with key residues in the pocket. These concepts were addressed in the second generation library design. It was important to elaborate further on the replacement of the sulfonyl carbamate and the phosphinoyl group that initially appeared to be necessary for the action of **26a** (CK1-183) in cells. When small changes were introduced, such as changing the acyl substituent and changing the *para* substitution on the phenyl ring of the sulfonylcarbamate, the MCF-7 activity failed to improve.

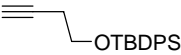
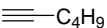
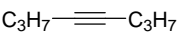
A second generation library⁵² of allylic amides and C-cyclopropylalkyl amides was designed to explore the chemical space around **26a** (CK1-183) and identify new ER agents with improved cell potency (see Introduction 1.4.3.). Biological evaluation of the second generation library and its SAR are discussed in detail in upcoming sections (2.1.6, 2.1.7).

2.1.5. Microwave Supported Synthesis

Initial synthesis of the library of analogues of **26a** (CK1-183) proved to be problematic and provided only three analogues in relatively poor yields (20-30%), discussed in section 2.1.3. This result initiated a search for alternative and more efficient synthetic protocols. In consideration of the polarity and dipole moments of the reactants in the one-pot sequence of hydrozirconation-transmetallation-alimine addition, it was proposed that microwave heating could improve the reaction times and yields. Therefore, the hydrozirconation and alimine addition steps were tested in a microwave reactor.

Microwave heating has been increasingly used in organometallic chemistry. Heck and Sonogashira couplings are a few of the Pd(0)-catalyzed reactions that have been performed under microwave conditions with high yields and high selectivity.⁵⁰ Palladium chemistry is the most explored microwave-accelerated reaction involving metals. Zirconium chemistry was yet to be explored in the microwave.

Table 3. Hydrozirconation in toluene in the microwave – flash heat mode.

Entry	Alkyne	Tmax (°C)	Power (W)	Conversion
1		150	300	>99%
2	49	100	300	>99%
3		100	150	>99%
4		80	300	~ 50%
<hr/>				
5		100	30	>99%
6	50	80	75	>99%
7		80	50	90%
8		80	30	~ 90%
<hr/>				
9		150	300	>99%
10		100	300	>99%
<hr/>				

*For a detailed explanation of the microwave conditions, see text.

The original protocol for the “one-pot” hydrozirconation-transmetallation-alimine addition⁴¹ entailed a solvent switch from dichloromethane to toluene following the hydrozirconation step. The reason for this switch was that the hydrozirconation was much faster in dichloromethane and THF than in toluene. To simplify this procedure, the efficiency of the hydrozirconation in toluene in a microwave was tested. The reaction mixture was heated in the microwave reactor in “flash heat mode”. This procedure entails fast heating the reaction mixture to high temperature followed by almost immediate cooling. Under these conditions, the reaction mixture stays at high temperature less than one minute. This allows the reaction to proceed and it is believed that the fast and immediate cooling prevents side reactions from taking place. Under these conditions,

the hydrozirconation of the alkynes tested proceeded with greater than 99% conversion as determined by GC-FID (Table 3). The total reaction time required for full conversion was 1-2 min in the “flash heat mode”.⁵¹ The next step of this “one pot” protocol was the transmetallation of the hydrozirconation products with dimethylzinc at $-78\text{ }^{\circ}\text{C}$. After the transmetallation was completed, an aldimine was added and the aldimine addition reaction was optimized in the microwave. Initially, the aldimine addition was tested at lower temperatures ($60\text{ }^{\circ}\text{C}$) for 15–30 min.. This protocol gave similar or lower yields to those provided by the conventional heating and the reaction products were less pure. The optimized protocol involved fast heating at higher temperatures followed by fast cooling. Representative examples shown in Table 4 are discussed in detail in the next section.

2.1.5.1. Hydrozirconation – Transmetallation – Aldimine Addition

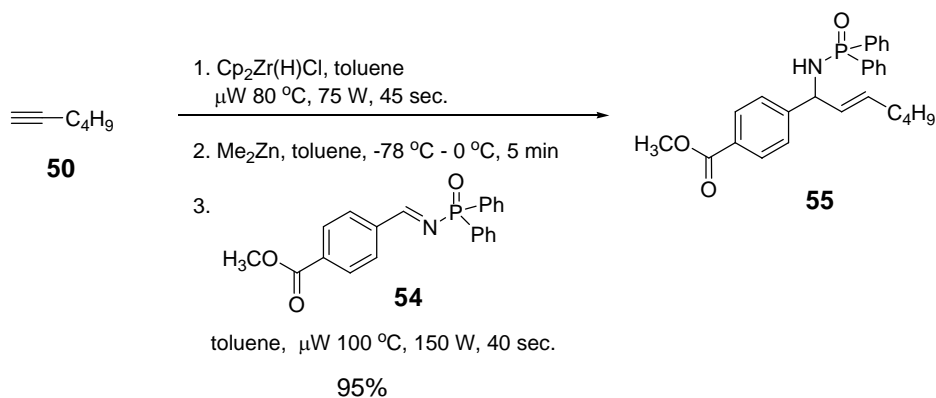
Further improvement in the synthesis of allylic amides was observed when the aldimine addition was carried out using the microwave’s flash heating mode (Scheme 4).⁵¹ This methodology proved to be highly efficient and time saving. The methodology worked well for internal alkynes and terminal alkynes.⁵¹ Representative examples of this process are provided in Table 4. Electron withdrawing groups on the phenyl ring of the aldimine as in **54** provided the highest yields with both terminal and symmetric internal alkynes (Table 4, entries 1, 4, 6 and 8).

Electronically less activated aldimines showed decreased addition efficiencies in the microwave, resulting in lower yield (*e.g.* entry 2) when terminal alkynes were used. However, the aldimine addition improved when internal alkynes were used (entries 3 and 5).

Table 4. Hydrozirconation and aldimine addition in a microwave – flash heat mode.

Entry	Alkyne	Aldimine	Allylic amide	Microwave	Conventional
1	$\equiv\text{C}_4\text{H}_9$ 50	 54	 55	95%	84%
2	50	 47	 56	43%	76%
3	$\text{C}_2\text{H}_5\equiv\text{C}_2\text{H}_5$ 52	47	 57	78%	72%
4	52	54	 58	74%	N/A
5	$\text{C}_3\text{H}_7\equiv\text{C}_3\text{H}_7$ 51	47	 59	62%	N/A
6	51	54	 60	74%	N/A
7	 49	47	 61	64%	73%
8	 53	54	 62	80%	N/A

* The examples for the conventional method were published previously.⁴¹



Scheme 4. Allylic amide synthesis in a microwave.

The conventional method for the hydrozirconation–transmetalation–aldimine addition required an inert atmosphere (dry nitrogen or argon gas). The microwave protocol under closed vessel conditions proceeded without any need for an inert atmosphere. This finding is in accord with published results for microwave-assisted reactions of transition metals.⁵⁰ It is believed that the rate increase by the more efficient heating allows the desired reaction to proceed at a rate much faster than oxygen- and moisture-initiated side reactions.

This was the first reported example of hydrozirconation and aldimine addition reactions performed in the microwave.⁵¹ An extension of this methodology was used to prepare a second generation library of allylic and *C*-cyclopropylalkylamides (second generation library) as described in the introduction (1.4.3).

2.1.6. Biological Evaluation of the Second Generation Library

2.1.6.1. Design of the Second Generation Library

The second generation library (Scheme 2, Table 6) was designed and synthesized based on *C*-cyclopropylalkylamide **26a** (CK1-183) as a lead structure in order to explore in greater detail SAR on both receptors. The goal was to increase cell potency in this series against breast cancer cells. The starting activity of the lead structure **26a** (CK1-183) in the high micromolar range and the failure to improve on its activity with initially explored changes on the sulfonamide (see section 2.1.4.1) suggested more radical changes were needed. The unusual structure of **26a** (CK1-183) as compared to the well defined pharmacophore model for ER targeting agents²⁷ provided an opportunity to explore novel scaffolds for ER targeting agents. Interest in the effect of the sulfonylcarbamate moiety of these compounds was stimulated by a recent report on ER targeting agents containing sulfonamide moieties.⁵⁸ The first three analogues (**48a**, **48b** and **48c**) of **26a** (CK1-183) (Figure 12) with changes in the sulfonamide failed to improve or change the activity as compared to the lead. Therefore, the sulfonamide was conserved but its positioning was varied in the design of the second generation library. Some derivatives (compounds **36a-36m** and **39a-39c**, Table 6) were synthesized with alternate substituents on the arylsulfonamide. It was anticipated that the sulfonamide, a common moiety in many drugs, would improve upon the drug like properties of the new agents. The phenyl ring on **26a** (CK1-183) was decorated with the following substituents: chloro, trifluoromethyl and methyl acetyl (see Table 6). These substituents were introduced to increase solubility and/or promote binding to the ER ligand binding pocket via either hydrogen bonding (methyl acetyl and trifluoromethyl) or favorable

hydrophobic or soft-soft interactions (chloro). The series also included agents with the biphenyl core that were designed to promote interactions with the ER β .

In order to clarify the role of the cyclopropane ring in this series, the majority of the cyclopropane-containing library members had a matched counterpart that contained a double bond instead of the cyclopropane ring, with the rest of the structure remaining quite similar (see Table 6). For the sake of ease of library synthesis and the fact that alkyne precursors containing the sulfonamide gave analogues with no improvement over **26a (CK1-183)**, the alkyne precursors in the second generation library synthesis were restricted to simple terminal alkynes (1-hexyne) and internal alkynes (3-hexyne, 4-octyne). The cyclohexylmethyl alkyne precursor was used to introduce bulk to the molecule and test the notion that the size of ER targeting agents can be important in designing selective agents (for discussion, see section 1.3). In this series, the main feature of a majority of ER targeting agents, the phenolic OH group, necessary for the hydrogen bonding with key residues on both ERs, was not introduced for two reasons. First, the initial microwave-supported synthetic scheme,⁵² designed with a limited number of steps, could not support the additional steps needed for the introduction of protected OH groups. Second, the initial lead structure did not contain a hydroxyl group and was hypothesized to act on ER transcription and breast cancer cell proliferation through novel mechanisms,⁴⁸ leading the SAR explorations toward new structural changes as compared to classical pharmacophore models. It was an open possibility that **26a (CK1-183)** could act on an alternative site, such as coregulator binding domain. However, to be able to test this hypothesis, a compound or with a lower IC₅₀ value was needed. The second generation library design had two goals: (1) to explore the novel structural scaffolds for targeting ERs; and (2) to increase the cell potency of the lead structure.

2.1.6.2. Second Generation Library Tests *in vitro* and in Cells

Seventy high-purity (>85% by HPLC using UV monitoring at 210 nm) library members (presented in Table 6) were screened for their ability to compete with fluorescently labeled 17 β -estradiol for binding to human ER α . The MCF-7 proliferation assay was used for the reevaluation of hits from the second generation library in the ER α competitor assay (Table 5).

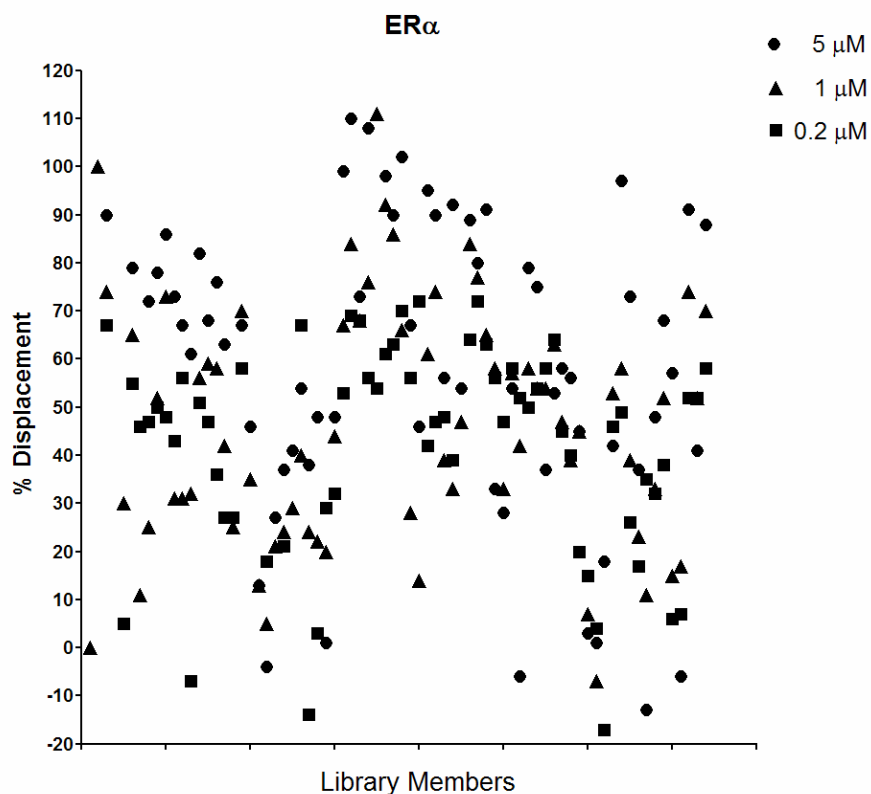


Figure 16. Results of screening the second generation library with the ER α fluorescence polarization based displacement assay (Panvera).

When fluorescently labeled E2 was complexed with recombinant ER α , slow tumbling of the labeled E2 resulted in high fluorescent polarization. In the presence of a test compound, the labeled E2 was displaced and the polarization value decreased. Displacement % was calculated from the obtained difference in fluorescence polarization value and plotted for each compound in three tested concentrations (0.2, 1 and 5 μ M). Data represents the means \pm SD (N=2).

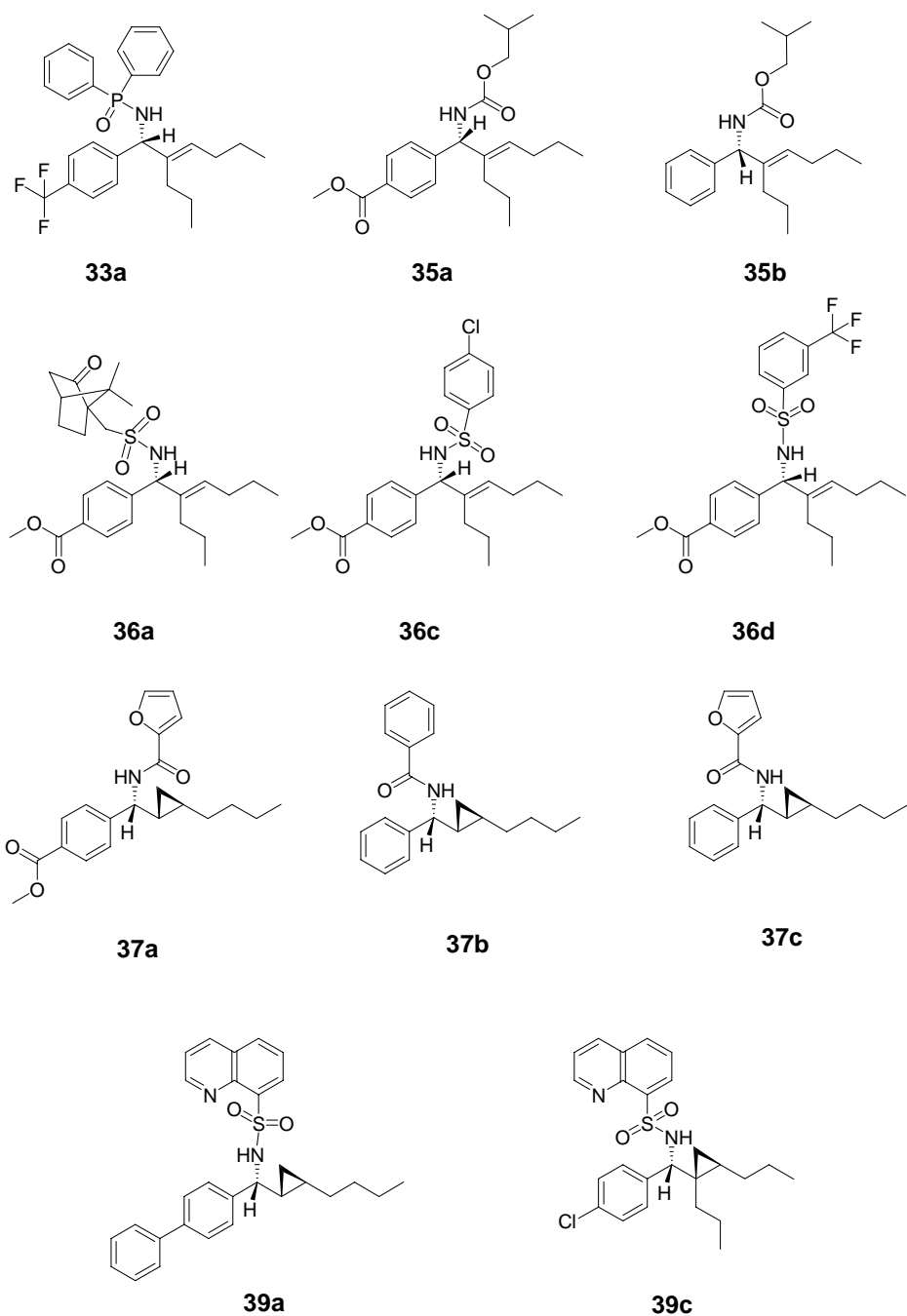


Figure 17. Hits from Screening the Second Generation Library at the ER α .

Compounds that showed >50% displacement and concentration dependence were identified as hits. The order of appearance of data points in Figure 15 corresponds to the library members and

the structural information listed in Table 6. The data represents the percent of displacement (%I), calculated based on the following formula:

$$\% I = ((mP_0 - mP)/(mP_0 - mP_{100})) \times 100$$

where mP_0 is the mP value for 0% competition as referred to high polarization of fluorescently labeled estradiol complexed to $ER\alpha$ (ER/ES2 complex); mP_{100} is the mP value for 100% competition, as referred to the low polarization in the presence of E2 (1 μ M); and mP is the fluorescence polarization observed in the presence of test compounds. The fluorescence polarization (mP) values are calculated using the following formula:

$$mP = mP = 1000 \times (S - G \times P) / (S + G \times P)$$

where S and P are the background-subtracted fluorescence intensity measurements for the parallel and perpendicular components, and G is a constant of the instrument.

The MCF-7 proliferation assay was used for the reevaluation of those agents that were identified from $ER\alpha$ competitor assay. The second generation allylic amide and C-cyclopropylalkylamide library *in vitro* screening at $ER\alpha$ gave 11 hits (Figure 17).

Out of these hits, three compounds (**37a**, **37c** and **39a**; Figure 17) showed improvement in cell potency over the original lead structure **26a (CK1-183)** (GI_{50} : $12.0 \pm 4.0 \mu$ M) as tested in MCF-7 cells, identified from the discovery library with GI_{50} values below 10 μ M (Table 5 and Figure 17). In addition to these three compounds, compound **35b** showed a low micromolar value for

GI₅₀ value in MCF-7 cells, but in a counterassay showed inhibitory effect on the growth of the MDA-MB231 ER negative cell line, and therefore was excluded from further study.

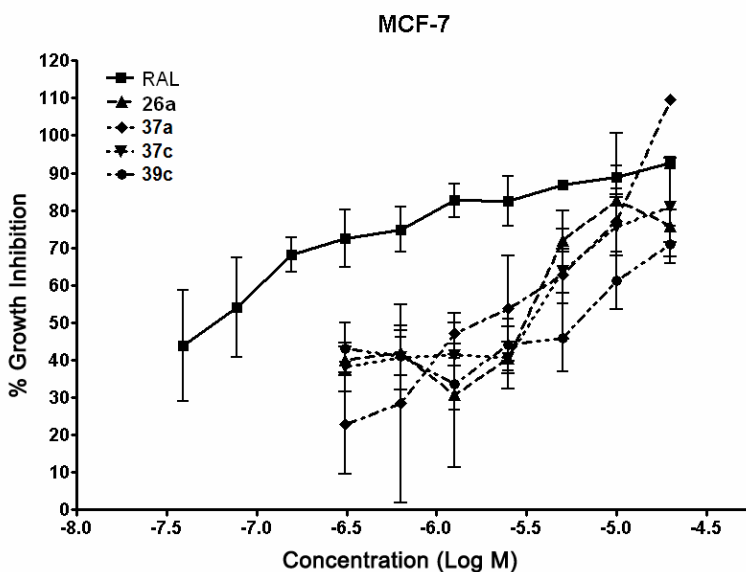


Figure 18. Inhibition of E2-induced proliferation of MCF-7 cells.

Data represents percent growth inhibition (%GI) versus concentration (Log M) of each agent (mean± SD, N = 4). MCF-7 cells were stimulated with E2 (10 nM) and treated with decreasing concentrations of test compounds for six days. Cell density was evaluated by a colorimetric MTS assay and data represents percent growth inhibition (%GI). Shown are means ± SD (N = 4).

Table 5. Hits from the testing of the second generation library in MCF-7 cells

Compound	ERα ^a			MCF-7 ^b
	% displacement at 0.2, 1 and 5 μM			GI ₅₀ (μM)
RAL	67	74	90	0.6 ± 0.0
33a	55	65	79	13.0 ± 9.3
35a	53	67	99	32.5 ± 1.0

35b	69	84	110	3.5 ± 0.5
36a	56	76	108	ND
36c	61	92	98	ND
36d	63	86	90	ND
37a	64	84	89	3.7 ± 2.8
37b	72	77	80	12.5 ± 2.0
37c	63	65	91	2.7 ± 0.8
39a	52	74	91	> 50.0
39c	58	70	88	5.7 ± 2.0

^aData represents % of displacement from fluorescent polarization assay for test compounds at each test concentration. Shown are the means ± SD (N = 2); ^bMCF-7 cells were stimulated with E2 (10 nM) and treated with decreasing concentrations of test compounds (50 μM – 3.2 nM) for six days. At day seven, the cell density was evaluated by a colorimetric MTS assay and data represents percent growth inhibition (%GI). Shown are means ± SD (N = 4).

The structures of the three new *C*-cyclopropylalkylamides **37a**, **37c** and **39c** are markedly different from the initial lead **26a** (CK1-183). The cyclopropane ring and a phenyl ring were present in all lead structures. Surprisingly, *C*-cyclopropylalkylamides **37a**, **37c** and **39c** have neither the phosphinoyl group nor the sulfonylcarbamate moiety present in the lead compound **26a** (CK1-183). However, the cyclopropane ring was present and appeared to be important for activity in cells. The hits from fluorescence polarization-based displacement assay on ERα when retested in MCF-7 cells, and those compounds that contained a cyclopropane (**37a**, **37c** and **39c**) showed significant activity (Table 5). With the exception of compound **35b**, other members

that contained a double bond instead of a cyclopropane were markedly less active, for example compound **35a** (Table 5). The 1,1-dichloro-2,2,3-triarylcyclopropanes (DTACs) were developed by Day *et al.* as pure antiestrogens lacking the uterotrophic effect of tamoxifen,⁵⁵ and the dichlorocyclopropyl analogue of tamoxifen, (*Z*)-1,1-dichloro-2,3-diphenyl-2-[4-[2-(dimethylamino)ethoxy]phenyl]cyclopropane (**42**)⁵⁵ was used as a control antiestrogen in the cell based assays. It appears that neither the double bond nor the cyclopropane moiety in the second generation library were critical for the activity in fluorescence polarization-based assays. Based on the limited data available the exact role of the cyclopropane ring remains unclear.

2.1.6.3. Screening of the Second Generation Library on ER β

Seventy high-purity second generation library members (>85% by HPLC at 210nm UV) listed in Table 6 were screened for their ability to compete with fluorescently labeled 17 β -estradiol for binding to human ER β under the same conditions as on ER α (see experimental section 5.2.5).

The results clearly showed that the ER α is much more tolerant to diverse substitutions in this series than is the ER β (see Figure 16 and Figure 19). Therefore, the criteria for hits at the ER α and ER β were adjusted accordingly. In the screen on the ER α , compounds that gave $\geq 50\%$ displacement at the lowest concentration tested (0.2 μM) and showed concentration dependence over all three concentrations tested (0.2, 1 and 5 μM) were considered hits and were further evaluated in cells (Figure 17).

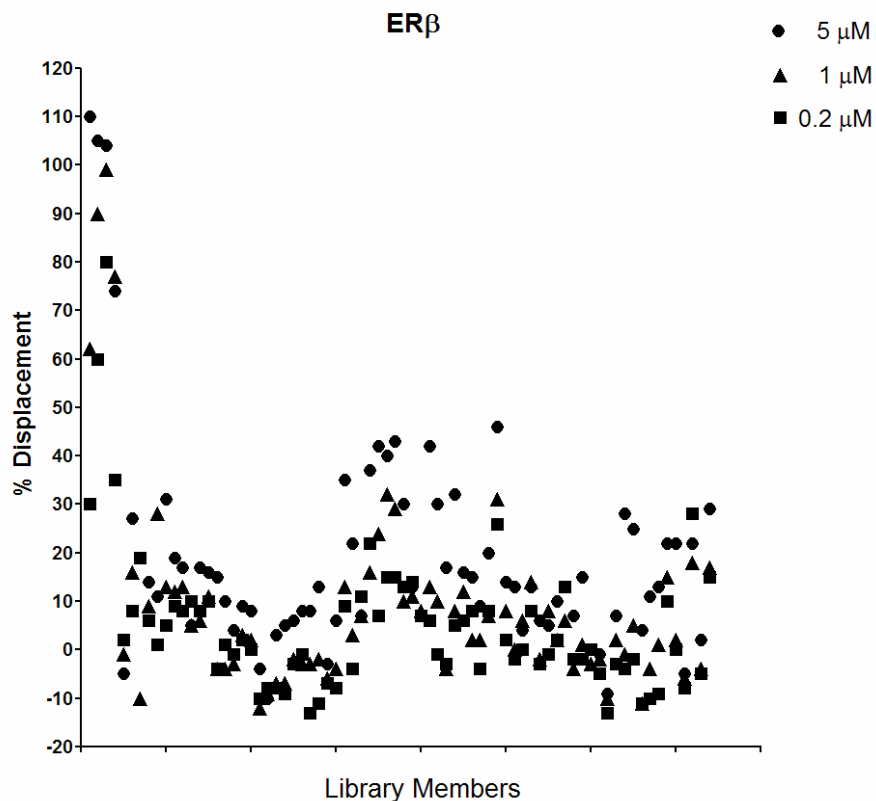


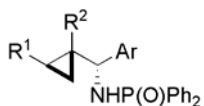
Figure 19. Results of screening the second generation library in the ER β competitor assay (Panvera).

When fluorescently labeled E2 was complexed with ER, slow tubling of the labeled E2 resulted in high fluorescent polarization. In the presence of a test compound, the labeled E2 was displaced and the polarization value decreased. Displacement % was calculated from the obtained difference in fluorescence polarization value and plotted for each compound in three tested concentrations (0.2, 1 and 5 μ M). Data represents the means \pm SD (N=2).

When the second generation library was screened for ER β displacement, the efficiency of displacement was significantly lower for the entire series, and only those compounds that gave close to 50% displacement were considered as hits. As a result, only one compound, biphenyl *C*-cyclopropylalkylamide **37d** (CC1-243), fulfilled these criteria and was further evaluated.

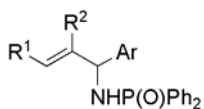
For the purpose of clearer representation, the screening data on both estrogen receptors for all tested second generation library members, with included structures and substitution patterns, is presented in Table 6.

Table 6. Activities of C-cyclopropylalkylamides from the second generation library in fluorescence polarization displacement-based screen assays at ER α and ER β .



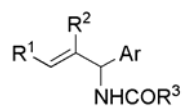
32a

	R ¹	R ²	Ar	ER α			ER β		
				% displacement at 0.2, 1 and 5 μ M			% displacement at 0.2, 1 and 5 μ M		
32a	<i>n</i> -C ₃ H ₇	<i>n</i> -C ₃ H ₇	<i>p</i> -ClC ₆ H ₄	5	30	-44	2	-1	-5



33a-c

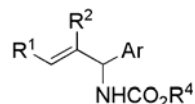
	R ¹	R ²	Ar	ER α			ER β		
				% displacement at 0.2, 1 and 5 μ M			% displacement at 0.2, 1 and 5 μ M		
33a	<i>n</i> -C ₃ H ₇	<i>n</i> -C ₃ H ₇	<i>p</i> -CF ₃ C ₆ H ₄	55	65	79	8	16	27
33b	<i>n</i> -C ₃ H ₇	<i>n</i> -C ₃ H ₇	<i>p</i> -PhC ₆ H ₄	46	11	-77	19	-10	-25
33c	<i>n</i> -C ₃ H ₇	<i>n</i> -C ₃ H ₇	Ph	47	25	72	6	9	14



34a-w

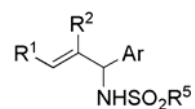
	R ¹	R ²	Ar	R ³	ER α			ER β		
					% displacement at 0.2, 1 and 5 μ M			% displacement at 0.2, 1 and 5 μ M		
34a	<i>n</i> -C ₃ H ₇	<i>n</i> -C ₃ H ₇	(<i>p</i> -CO ₂ Me)C ₆ H ₄	Ph	0	52	78	1	28	11
34b	<i>n</i> -C ₃ H ₇	<i>n</i> -C ₃ H ₇	(<i>p</i> -CO ₂ Me)C ₆ H ₄	2-thiophene	48	73	86	5	13	31
34c	<i>n</i> -C ₃ H ₇	<i>n</i> -C ₃ H ₇	<i>p</i> -CF ₃ C ₆ H ₄	2-thiophene	43	31	73	9	12	19
34d	<i>n</i> -C ₃ H ₇	<i>n</i> -C ₃ H ₇	<i>p</i> -CF ₃ C ₆ H ₄	CH ₂ CH ₂ Ph	56	31	67	8	13	17
34e	<i>n</i> -C ₃ H ₇	<i>n</i> -C ₃ H ₇	<i>p</i> -CF ₃ C ₆ H ₄	<i>p</i> -CF ₃ C ₆ H ₄	-7	32	61	10	5	5
34f	<i>n</i> -C ₃ H ₇	<i>n</i> -C ₃ H ₇	Ph	Ph	51	56	82	8	6	17
34g	<i>n</i> -C ₃ H ₇	<i>n</i> -C ₃ H ₇	Ph	<i>p</i> -CF ₃ C ₆ H ₄	47	59	68	10	11	16
34h	<i>n</i> -C ₃ H ₇	<i>n</i> -C ₃ H ₇	(<i>p</i> -CO ₂ Me)C ₆ H ₄	2-furanyl	36	58	76	-4	-4	15
34i	<i>n</i> -C ₃ H ₇	<i>n</i> -C ₃ H ₇	(<i>p</i> -CO ₂ Me)C ₆ H ₄	<i>t</i> -Bu	27	42	63	1	-4	10
34kj	<i>n</i> -C ₃ H ₇	<i>n</i> -C ₃ H ₇	(<i>p</i> -CO ₂ Me)C ₆ H ₄	<i>p</i> -PhC ₆ H ₄	27	25	27	-1	-3	4
34k	H	<i>n</i> -C ₄ H ₉	Ph	Ph	58	70	67	2	3	9
34l	H	<i>n</i> -C ₄ H ₉	Ph	CH ₂ CH ₂ Ph	-33	35	46	0	2	8
34m	H	<i>n</i> -C ₄ H ₉	Ph	^t Bu	-67	13	13	-10	-12	-4
34n	H	<i>n</i> -C ₄ H ₉	Ph	Ph-Ph	18	5	-4	-8	-9	-10
34o	H	<i>n</i> -C ₄ H ₉	Ph	<i>p</i> -CF ₃ C ₆ H ₄	-61	21	27	-8	-7	3
34p	H	<i>n</i> -C ₄ H ₉	Ph	(<i>p</i> -CO ₂ Me)C ₆ H ₄	21	24	37	-9	-7	5
34r	H	<i>n</i> -C ₄ H ₉	Ph	2-furanyl	-111	29	41	-3	-2	6
34s	H	<i>n</i> -C ₄ H ₉	Ph	2-thiophene	67	40	54	-1	-3	8

34t	<i>n</i> -C ₃ H ₇	<i>n</i> -C ₃ H ₇	(<i>p</i> -CO ₂ Me)C ₆ H ₄	(<i>p</i> -CO ₂ Me)C ₆ H ₄	-14	24	38	-13	-3	8
34u	<i>n</i> -C ₃ H ₇	<i>n</i> -C ₃ H ₇	(<i>p</i> -CO ₂ Me)C ₆ H ₄	CH ₂ Ph	3	22	48	-11	-2	13
34v	<i>c</i> -C ₆ H ₁₁	Me	<i>p</i> -PhC ₆ H ₄	<i>p</i> -CF ₃ C ₆ H ₄	29	20	1	-7	-6	-3
34w	<i>c</i> -C ₆ H ₁₁	Me	<i>p</i> -PhC ₆ H ₄	3-pyridyl	32	44	48	-8	-4	6



35a-c

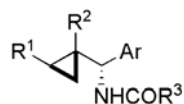
	R ¹	R ²	Ar	R ⁴	ER α			ER β		
					% displacement at 0.2, 1 and 5 μ M			% displacement at 0.2, 1 and 5 μ M		
35a	<i>n</i> -C ₃ H ₇	<i>n</i> -C ₃ H ₇	(<i>p</i> -CO ₂ Me)C ₆ H ₄	^t Bu	53	67	99	9	13	35
35b	<i>n</i> -C ₃ H ₇	<i>n</i> -C ₃ H ₇	Ph	CH ₂ CH(CH ₃) ₂	69	84	110	-4	3	22
35c	H	<i>n</i> -C ₄ H ₉	Ph	<i>o</i> -ClC ₆ H ₄	68	68	73	11	7	7



36a-m

	R ¹	R ²	Ar	R ⁵	ER α			ER β		
					% displacement at 0.2, 1 and 5 μ M			% displacement at 0.2, 1 and 5 μ M		
36a	<i>n</i> -C ₃ H ₇	<i>n</i> -C ₃ H ₇	(<i>p</i> -CO ₂ Me)C ₆ H ₄	<i>rac</i> - camphorsulfonyl	56	76	108	22	16	37
36b	<i>n</i> -C ₃ H ₇	<i>n</i> -C ₃ H ₇	(<i>p</i> -CO ₂ Me)C ₆ H ₄	8-quinoline	54	111	54	7	24	42
36c	<i>n</i> -C ₃ H ₇	<i>n</i> -C ₃ H ₇	(<i>p</i> -CO ₂ Me)C ₆ H ₄	<i>o</i> -ClC ₆ H ₄	61	92	98	15	32	40

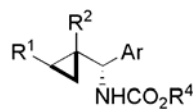
36d	<i>n</i> -C ₃ H ₇	<i>n</i> -C ₃ H ₇	(<i>p</i> -CO ₂ Me)C ₆ H ₄	<i>p</i> -CF ₃ C ₆ H ₄	63	86	90	15	29	43
36e	<i>n</i> -C ₃ H ₇	<i>n</i> -C ₃ H ₇	<i>p</i> -CF ₃ C ₆ H ₄	Ph	70	66	102	13	10	30
36f	<i>n</i> -C ₃ H ₇	<i>n</i> -C ₃ H ₇	<i>p</i> -PhC ₆ H ₄	8-quinolinyl	56	28	67	14	11	13
36g	<i>n</i> -C ₃ H ₇	<i>n</i> -C ₃ H ₇	<i>p</i> -PhC ₆ H ₄	<i>p</i> -CF ₃ C ₆ H ₄	72	14	46	7	8	7
36h	<i>n</i> -C ₃ H ₇	<i>n</i> -C ₃ H ₇	Ph	<i>p</i> -ClC ₆ H ₄	42	61	95	6	13	42
36i	<i>n</i> -C ₃ H ₇	<i>n</i> -C ₃ H ₇	Ph	<i>p</i> -CF ₃ C ₆ H ₄	47	74	90	-1	10	30
36j	<i>n</i> -C ₃ H ₇	<i>n</i> -C ₃ H ₇	Ph	Me	48	39	56	-3	-4	17
36l	<i>n</i> -C ₃ H ₇	<i>n</i> -C ₃ H ₇	(<i>p</i> -CO ₂ Me)C ₆ H ₄	2-thiophene	39	33	92	5	8	32
36m	<i>n</i> -C ₃ H ₇	<i>n</i> -C ₃ H ₇	(<i>p</i> -CO ₂ Me)C ₆ H ₄	<i>p</i> -PhC ₆ H ₄	-69	47	54	6	12	16



37a-y

	R ¹	R ²	Ar	R ³	ER α			ER β		
					% displacement at 0.2, 1 and 5 μ M			% displacement at 0.2, 1 and 5 μ M		
37a	<i>n</i> -C ₄ H ₉	H	(<i>p</i> -CO ₂ Me)C ₆ H ₄	2-furanyl	64	84	89	8	2	15
37b	<i>n</i> -C ₄ H ₉	H	Ph	Ph	72	77	80	-4	2	9
37c	<i>n</i> -C ₄ H ₉	H	Ph	2-furanyl	63	65	91	8	7	20
37d	<i>n</i> -C ₄ H ₉	H	<i>p</i> -PhC ₆ H ₄	Ph	56	58	33	26	31	46
37e	<i>n</i> -C ₄ H ₉	H	<i>p</i> -PhC ₆ H ₄	CH ₂ Ph	47	33	28	2	8	14
37f	<i>n</i> -C ₄ H ₉	H	<i>p</i> -PhC ₆ H ₄	2-furanyl	58	57	54	-2	0	13
37g	<i>n</i> -C ₄ H ₉	H	<i>p</i> -PhC ₆ H ₄	<i>p</i> -PhC ₆ H ₄	52	42	-6	0	6	4
37h	<i>n</i> -C ₄ H ₉	H	<i>p</i> -CF ₃ C ₆ H ₄	2-thiophene	50	58	79	8	14	13

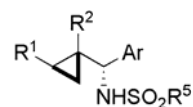
37i	<i>n</i> -C ₄ H ₉	H	(<i>p</i> -CO ₂ Me)C ₆ H ₄	Ph	54	54	75	-3	-2	6
37j	<i>n</i> -C ₄ H ₉	H	<i>p</i> -PhC ₆ H ₄	2-thiophene	58	54	37	-1	8	5
37k	<i>n</i> -C ₄ H ₉	H	<i>p</i> -PhC ₆ H ₄	3-pyridyl	64	63	53	2	2	10
37l	<i>n</i> -C ₄ H ₉	H	<i>p</i> -CF ₃ C ₆ H ₄	Ph	45	47	58	13	6	13
37m	<i>n</i> -C ₄ H ₉	H	<i>p</i> -CF ₃ C ₆ H ₄	^t Bu	40	39	56	-2	-4	7
37n	<i>n</i> -C ₄ H ₉	H	(<i>p</i> -CO ₂ Me)C ₆ H ₄	<i>p</i> -CF ₃ C ₆ H ₄	20	45	45	-2	1	15
37o	<i>c</i> -C ₆ H ₁₁	Me	<i>p</i> -PhC ₆ H ₄	2-thiophene	15	7	3	0	-3	0
37p	<i>c</i> -C ₆ H ₁₁	Me	<i>p</i> -PhC ₆ H ₄	Ph	4	-7	1	-5	-2	-1
37q	<i>c</i> -C ₆ H ₁₁	Me	<i>p</i> -PhC ₆ H ₄	CH ₂ Ph	-17	-22	18	-13	-10	-9
37r	<i>c</i> -C ₆ H ₁₁	Me	(<i>p</i> -CO ₂ Me)C ₆ H ₄	Ph	46	53	42	-3	2	7
37s	<i>c</i> -C ₆ H ₁₁	Me	(<i>p</i> -CO ₂ Me)C ₆ H ₄	2-furanyl	49	58	97	-4	-1	28
37t	<i>n</i> -C ₃ H ₇	<i>n</i> -C ₃ H ₇	<i>p</i> -ClC ₆ H ₄	2-furanyl	26	39	73	-2	5	25
37u	<i>c</i> -C ₆ H ₁₁	Me	<i>p</i> -ClC ₆ H ₄	^t Bu	17	23	37	-11	-11	4
37v	<i>c</i> -C ₆ H ₁₁	Me	<i>p</i> -ClC ₆ H ₄	<i>p</i> -PhC ₆ H ₄	35	11	-13	-10	-4	11
37w	<i>n</i> -C ₄ H ₉	H	<i>o</i> -CF ₃ C ₆ H ₄	Ph	32	33	48	-9	1	13
37x	<i>n</i> -C ₄ H ₉	H	<i>o</i> -CF ₃ C ₆ H ₄	2-thiophene	38	52	68	10	15	22
37y	<i>n</i> -C ₄ H ₉	H	<i>o</i> -CF ₃ C ₆ H ₄	2-furanyl	6	15	57	0	2	22



38a

	R ¹	R ²	Ar	R ⁴	ER α	ER β
					% displacement at 0.2, 1 and 5 μ M	% displacement at 0.2, 1 and 5 μ M

38a	<i>n</i> -C ₃ H ₇	<i>n</i> -C ₃ H ₇	<i>p</i> -PhC ₆ H ₄	CH ₂ Ph	7	17	-6	-8	-6	-5
------------	---	---	---	--------------------	---	----	----	----	----	----



39a-c

	R ¹	R ²	Ar	R ⁵	ER α			ER β		
					% displacement at 0.2, 1 and 5 μ M			% displacement at 0.2, 1 and 5 μ M		
39a	<i>n</i> -C ₄ H ₉	H	<i>p</i> -PhC ₆ H ₄	8-quinolinyl	52	74	91	28	18	22
39b	<i>c</i> -C ₆ H ₁₁	Me	<i>p</i> -PhC ₆ H ₄	8-quinolinyl	52	52	41	-5	-4	2
39c	<i>n</i> -C ₃ H ₇	<i>n</i> -C ₃ H ₇	<i>p</i> -PhC ₆ H ₄	8-quinolinyl	58	70	88	15	17	29

2.1.7. SAR of the Second Generation Library on ER α and ER β

Evaluation of the screening data gave preliminary SAR for the second generation library on both receptors. Compound **37d** showed the highest displacement efficiency in the ER β screen and it did not satisfy the criteria for being a hit on the ER α (see Table 6). However, the highest displacement value on ER β did not pass 50% for any tested agent. Therefore, it was rather difficult to choose hits that had potential for further development to target ER β based only on the screening results. Instead, the selection criteria were modified to include known structural features that were shown earlier to promote ER β binding.³⁶ Screening results on ER α were used as co-selection criteria.

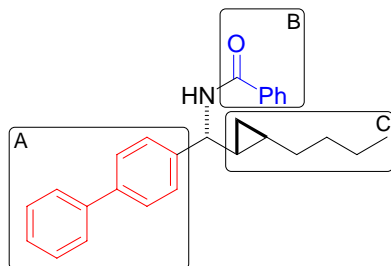


Figure 20. Preliminary SAR presented on compound 37d (CC1-243) from ER screens of the second generation library.

The biphenyl core (site A) was shown to be beneficial for the selective targeting of ER β .³⁶ Young *et al.* used GEN as a lead structure in the search for new ER β selective ligands. The phenolic group in GEN was acting as an A ring mimic in estradiol and was preserved as the key pharmacophore element. Young *et al.* chose the biphenyl core in order to simplify the chromenone moiety in GEN.³⁶ In addition, the biphenyl was a synthetically easily accessible core through Suzuki couplings and a large number of substituted phenyl precursors was readily available. 4'-Hydroxy-biphenyl-carbaldehyde oxime derivatives were synthesized with varied substituents.³⁶ It was shown that placing fluorine and/or chlorine on the biphenyl core, while keeping the phenol OH group, provided selective agents for ER β , with more than 10 fold (compound **13**), and up to 40-fold in some cases (compound **9**), increased binding affinity for the receptor (Figure 5).

The biphenyl core was present in the following second generation library members, allylic amides (**33b**, **34v**, **34w**, **36f**, **36g** and **36m**) and C-cyclopropylalkylamides (**37d**, **37e**, **37f**, **37g**, **37i**, **37j**, **37k**, **37o**, **37p**, **39a**, **39b** and **39c**) (Table 6). Biphenyl C-cyclopropylalkylamide **37d** (CC1-243) was selected as the lead since it was the most efficient agent as measured by the percent of displacement of E2 at ER β (Table 6) and also failed to meet the hit criteria on ER α .

Figure 20 illustrates sites on **37d** used in the SAR discussions. Based on the screening data on both receptors, the initial SAR model is discussed below.

Only one biphenyl core-containing library member **39a** satisfied the criteria for hit selection in the screen on ER α (Table 6). However, this compound failed to inhibit estradiol-stimulated growth of MCF-7 cells ($GI_{50} > 50 \mu\text{M}$; Table 5). Replacement of the biphenyl with smaller a substituted aryl ring, *p*-chlorophenyl in **39c**, preserved the displacement activity on ER α and the cell based activity was recovered ($GI_{50} = 5.7 \pm 2.0 \mu\text{M}$, Table 5). This result indicated the biphenyl core was less tolerated on ER α if combined with larger substituents on the nitrogen (**39a**). Therefore the possibilities were opened for the search for ER β selective agents from this series. In addition, based on the screening results, when the biphenyl present in **37d** was replaced with a phenyl ring while the remaining structure was kept constant (**37b**), the activity at ER β dropped to insignificant levels (<10% displacement) while the activity on ER α slightly improved (Table 6). Changes in site B (Figure 20) also led to similar detrimental consequences in displacement efficiency on ER β . A phenylamide was the best tolerated moiety for activity at the ER β (**37b**), while other rings were much better tolerated by the ER α . When the simple phenylamide on compound **37d** was replaced by a biphenylamide moiety (compound **37g**), a complete loss of activity at the ER β resulted. It was concluded that only one biphenyl core was necessary and that increasing the size of the ligand is detrimental for the activity on ER β . When the size of the alkyl chain (site C) was increased to cyclohexyl (compound **37p**) while keeping the rest of the molecule **37d** unchanged, the activity at both receptors was lost. Therefore, site C was kept unchanged in the further synthetic elaborations.

Sites A and B were chosen for further elaboration. The synthesis was guided around the biphenyl core and the amide linkage. The earlier results of discovery library screening suggested that a cyclopropane ring is important for the cell based activity. The screening data on both receptors gave some indication that this was still holding true. When the activity of biphenyl-C-cyclopropylalkylamide **37d** was compared to that of compounds with the biphenyl core and lacking the cyclopropane ring (**36f**, **36g** and **36m**), the activity on both receptors was reduced (Table 6). However, these comparisons were not sufficient to give a final determining conclusion, simply for the lack of pure analogue of **37d** where only the cyclopropane ring was replaced by a double bond. The most significant indication for the importance of the cyclopropane ring lies in the finding that majority of active library members on both receptors did contain a cyclopropane ring.

In conclusion, the second generation library was tested in biochemical assays *in vitro* and in human breast cancer cells with the goal of finding ER α antagonists with improved properties over the lead structure **26a** (CK1-183) identified from the first generation library (section 2.1). The library was also tested in the hopes of finding new scaffolds for ER β targeting agents. The second generation library was screened at ER α and ER β using a fluorescence polarization-based homogenous displacement assay (adapted from kits purchased from Panvera).⁶⁰ The collected displacement data was used to develop an SAR model (2.1.7) that served towards the design and synthesis of agents with further improved activity and modest selectivity for ER β (see section 2.2.2 for details).

The second generation library gave three new ER targeting agents (**37a**, **37c** and **39c**) with cell activity in the lower micromolar range, supporting the hypothesis that *C*-cyclopropylalkylamides are novel ER targeting scaffolds. However, the second generation library failed to give compounds with potencies in the submicromolar range both *in vitro* and in cells. The library was designed with the lack of the classical ER pharmacophore – a phenolic ring – that would drive the agent into the pocket and form crucial hydrogen bonds as does the estradiol A ring with Glu ER α 353/ER β Glu305 and ER α Arg394/ER β Arg346. This lack of classical pharmacophore features was addressed in the follow up, limited size series of biphenyl *C*-cyclopropylalkylamide analogues.

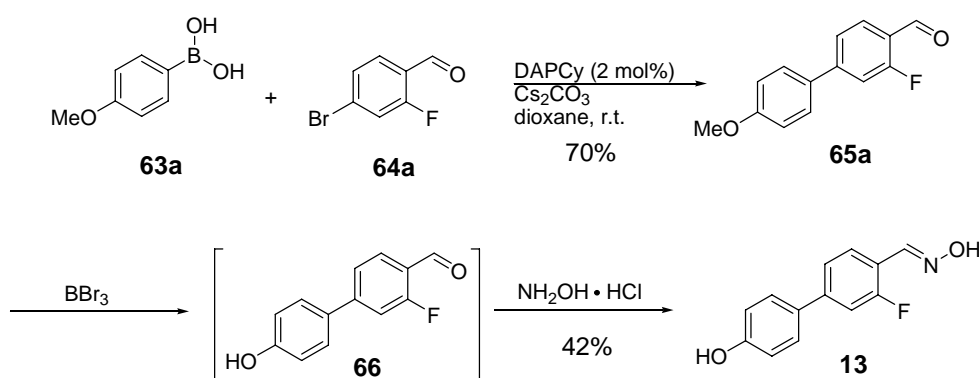
2.2. Biphenyl *C*-Cyclopropylalkylamide Analogues of **37d** (CC1-243)

Based on the initial SAR from the fluorescence polarization based screening on ER α and ER β and the published SAR of biphenyl agents selective for ER β ³⁶, six analogues of compound **37d** (CC1-243) were designed and synthesized (**69a**, **70b-d**, **71** and **72**; Figure 21). Attempts were made to improve the *in vitro* and cellular potency, and preferably selectively target ER β .

The biphenyl core was supplied with a key phenolic 4'-OH group to promote hydrogen bonding with ER β Glu305 (ER α Glu353) and ER β Arg346 (ER α Arg394). A fluorine substituent was chosen based on published SAR for known biphenyl agents³⁶ because this one substituent was able to provide the selectivity over a non-substituted biphenyl 11-fold (compound **13**, Figure 5). Although, additional substitutions did provide higher selectivity,³⁶ at this stage of the biphenyl-*C*-cyclopropylalkylamide design, fluorine was considered enough to support the proof of principle and test the importance of the biphenyl core in the *C*-cyclopropylalkylamide series. The alkyl chain was kept simple and small in order not to compromise already existing activity on ER β (see detailed SAR discussions in section 2.1.7). The phenylamide was changed into a smaller acetylamide or simply removed. These changes were designed to further decrease the size of the *C*-cyclopropylalkylamide ligand and therefore, hopefully, improve selectivity for ER β .

Six analogues of biphenyl *C*-cyclopropylalkylamide **37d** (CC1-243) were synthesized (Figure 21), and tested in a fluorescence polarization-based assays on both ERs as well as for inhibition

of E2-induced proliferation of MCF-7 breast cancer cells. The final goal of the design was to develop a dual agent, agonist on ER β and antagonist (or inactive) on ER α . Preliminary synthetic efforts and biological evaluation are presented, and the rationale behind the dual agent design and its potential use are discussed in the future directions section. Analogues **69a**, **70b-d**, **71** and **72** were therefore synthesized and tested. The synthesis and biological evaluation of these third generation C-cyclopropylalkylamides are presented in the following sections.

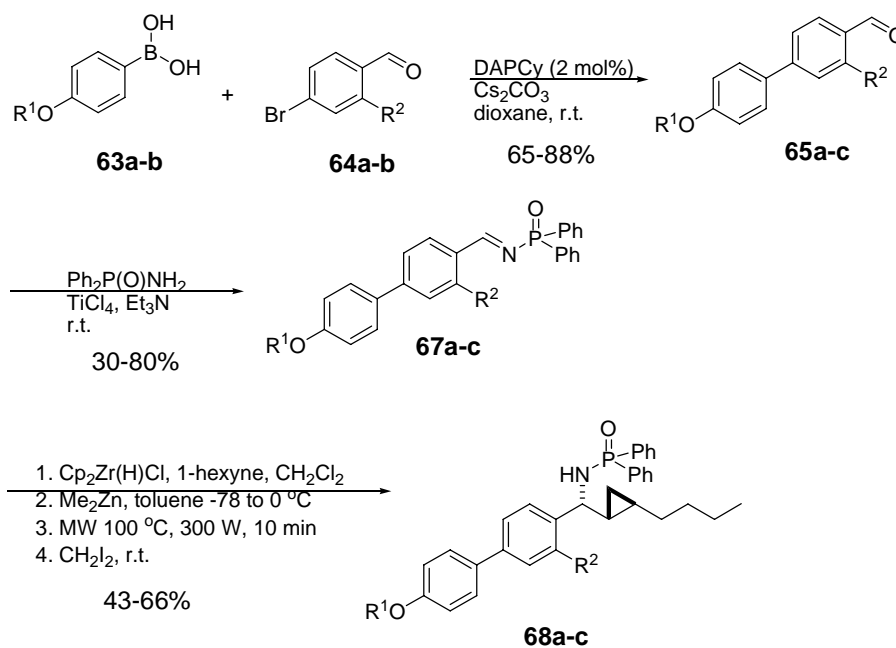


Scheme 5. Synthesis of biphenyl oxime 13.

2-Fluoro-4'-hydroxybiphenyl-4-carbaldehyde oxime (**13**)³⁶ was synthesized to serve as a positive control and as a representative compound containing the biphenyl core known to target ERs. The originally reported synthetic approach³⁶ for this compound was modified, resulting in an improved yield (42%). The palladium catalyst *trans*-(Cy₂NH)₂Pd-(OAc)₂ (DAPCy) was recently developed by Boykin *et al.*⁶¹ for Suzuki couplings⁶² in dioxane at room temperature. The catalyst⁶³ was easily prepared as yellow crystals from palladium (II) acetate and dicyclohexylamine in dioxane at room temperature. As reported, the catalyst was stable at room temperature and under no protection from air for up to four months. Suzuki coupling using DAPCy gave the desired biphenyl aldehyde **65a** in 70% yield. The aryl methyl ether was

removed by a standard procedure using BBr_3 at low temperature and the resulting deprotected aldehyde, after simple basic aqueous work up, was submitted to the next step without further purification. Oxime **13** was formed in 42% yield over two steps by treating the aldehyde **66** with hydroxyloxime hydrochloride³⁶ in methanol at room temperature (Scheme 5).

2.2.1. Synthesis of Biphenyl C-Cyclopropylalkylamides

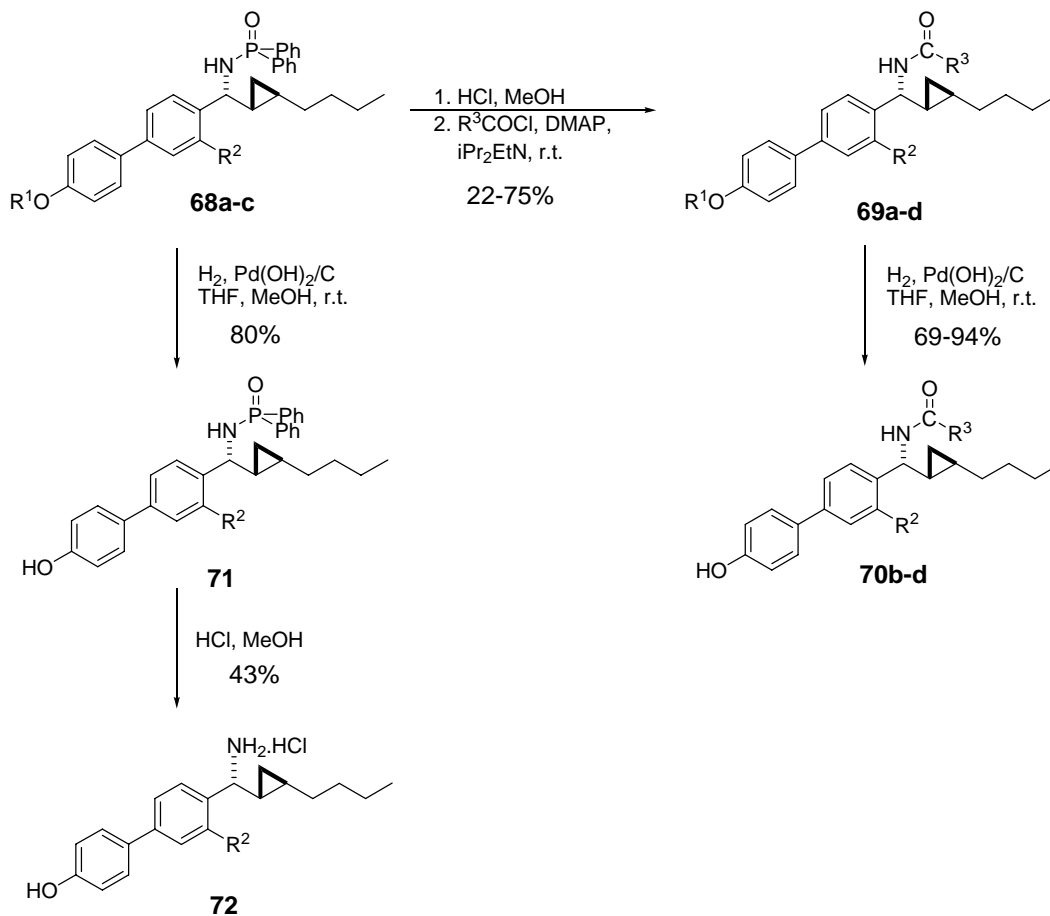


Scheme 6. Synthesis of phosphinoyl protected biphenyl C-cyclopropylalkylamide precursors.

$\text{R}^1=\text{Me}$ (**63a**), $\text{R}^1=\text{OBn}$ (**63b**); $\text{R}^2=\text{F}$ (**64a**), $\text{R}^2=\text{H}$ (**64b**); $\text{R}^1=\text{Me}$, $\text{R}^2=\text{F}$ (**65a**, **67a**, **68a**); $\text{R}^1=\text{Bn}$, $\text{R}^2=\text{F}$ (**65b**, **67b**, **68b**); $\text{R}^1=\text{Bn}$, $\text{R}^2=\text{H}$ (**65c**, **67c**, **68c**).

Suzuki coupling of commercially available benzyl- or methyl-protected 4-hydroxybenzeneboronic acid (**63a**) to 4-bromobenzaldehyde (**64a**) using the DAPCy catalyst developed by Boykin^{61,63} provided biphenyl aldehydes in good to excellent yields (65-88%).

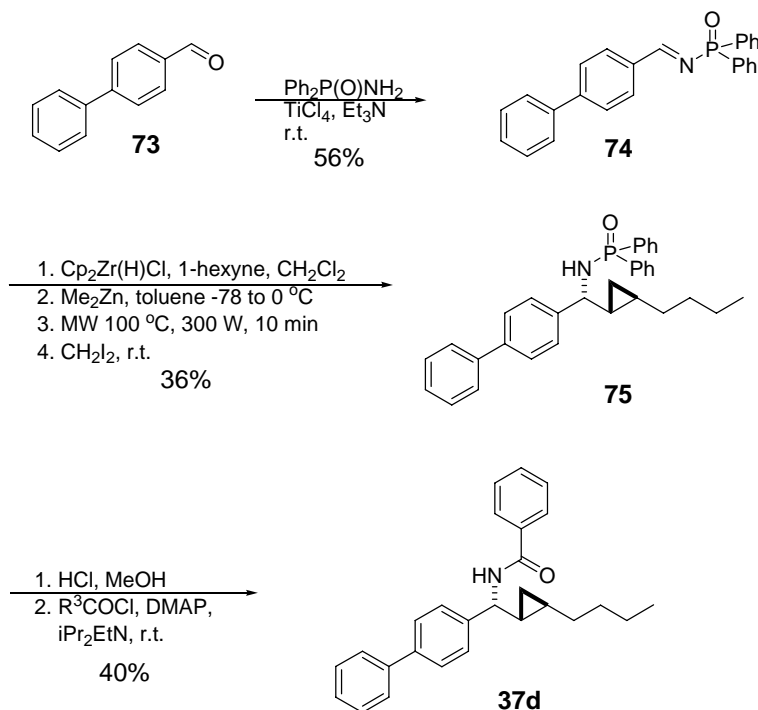
Imine formation using titanium (IV) chloride as the Lewis acid catalyst initially gave phosphinoylimine **67a** in poor to moderate yields (30-47%).⁵² Changing the work up to a fast filtration over a pad of silica gel and washing with ethyl acetate significantly improved the yields (80%) of the phosphinoylimines **67b-c**.⁶⁴



Scheme 7. CC1-243 analogues derived from a common precursor.

One-pot hydrozirconation-transmetallation-alimine addition in dichloromethane in the microwave (100 °C, 300 W, 10 min) immediately followed by cyclopropanation in the presence of excess of diiodomethane at room temperature (16-20 h) gave the phosphinoyl-protected biphenyl C-cyclopropylalkylamides **68a-c** in moderate yields (43-66%), (Scheme 6). Acidic deprotection followed by acylation gave the final product **69a** (61%) or benzyl-protected

compounds **69b-d** (22-75%). Benzyl ethers were easily removed by hydrogenolysis under 1 atm of H₂ in the presence of palladium hydroxide on carbon (Scheme 7).



Scheme 8. Synthesis of the lead structure 37d (CC1-243).

The synthetic schemes (Scheme 7 and Figure 21) presented above allowed for diversification in two ways. Substituents on the biphenyl core were attainable by changing the substitution on aryl boronic acid and aryl bromide coupling partners. The amide linkage also allowed for diversification by changing the acylation coupling partner, as done previously in the synthesis of the second generation library. After the acidic deprotection step, the amine salt could be coupled without further purification in the presence of DMAP with diverse acyl chlorides, carbamoyl chlorides and sulfonyl chlorides.⁵²

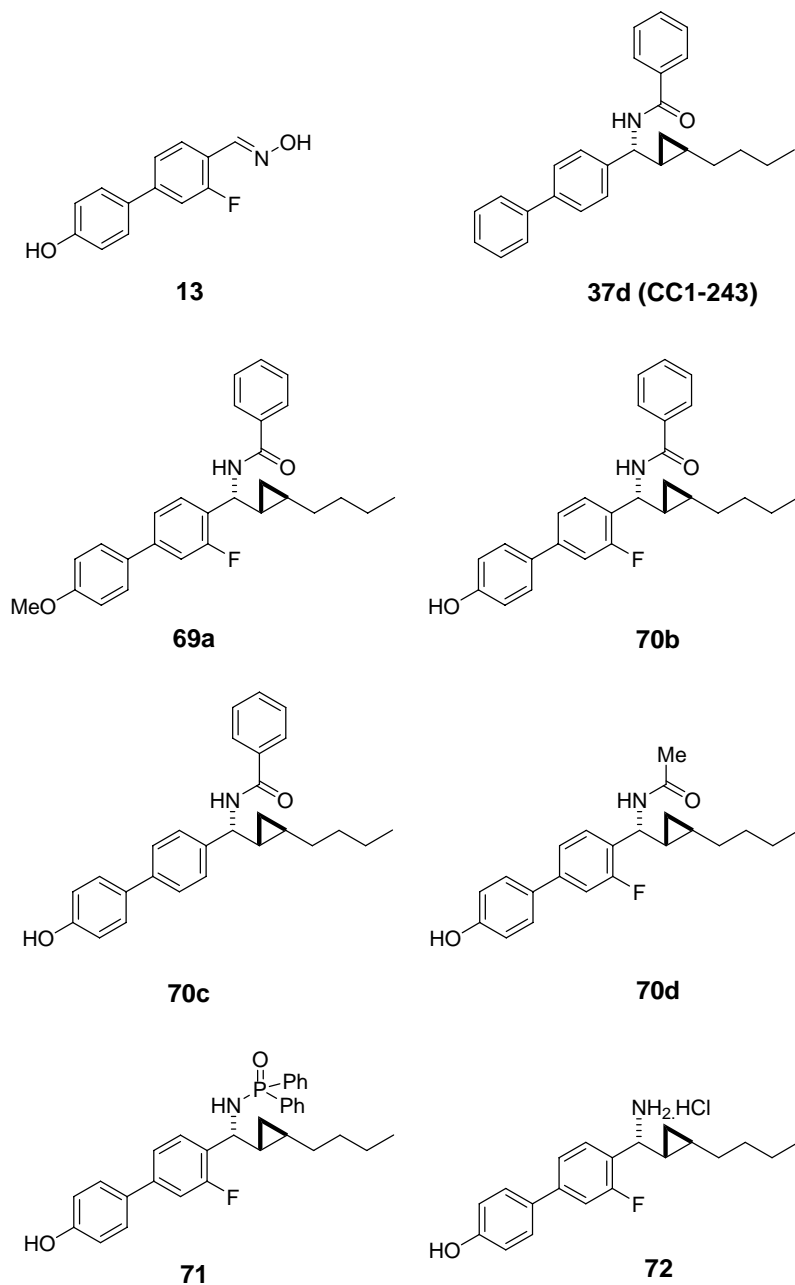


Figure 21. Structures of biologically tested biphenyl C-cyclopropylalkylamides (37d, 69a, 70b-d, 71, 72) and control oxime (13).

In this initial exploration around lead structure **37d** (CC1-243), only six analogues were made, one at a time. For deprotection and acylation steps, reactions were performed in parallel using a Bradley Greenhouse and purified individually by column chromatography. The lead compound

37d (CC1-243) was resynthesized following the literature procedure with small modifications,⁵² Scheme 8. The cyclopropanation step that provides the phosphinoyl-protected biphenyl *C*-cyclopropylalkylamide **75** was performed in the presence of a large excess of diiodomethane (10 eq) and the reaction mixture was kept at room temperature overnight to give the product in 36% yield. Deprotection and acylation gave the final product **37d** in 40% yield. Biological evaluation of the biphenyl *C*-cyclopropylalkylamides, shown in Figure 21, as ER targeting agents and preliminary SAR is discussed in greater detail below.

2.2.2. Evaluation of Biphenyl C-Cyclopropylalkylamides for *in vitro* Binding to the ER α and ER β

Biphenyl C-cyclopropylalkylamide **37d** (CC1-243), the hit found in the second generation library screen on ER β ligand displacement assays (2.1.6.3), was only modestly active at the ERs, with the highest concentration tested (25 μ M) giving only 50% displacement of fluorescent estradiol on both proteins (data not shown). This was attributed to the lack of a key phenolic OH to orient the ligand into the binding pocket of the ERs, necessary for key hydrogen bonding with ER β Glu 305 (ER α Glu353) and ER β Arg346 (ER α Arg394), the compound's high ClogP value (7.6) and its poor water solubility. Six analogues were synthesized to improve on its activity. Aryl substituents, such as 4'-OH, 4'-OMe and 2-fluoro groups of the biphenyl core, were introduced and the amine substituent was changed from phenyl to smaller or larger groups or left unprotected (Figure 21). The biological evaluation of these analogues is discussed below in detail.

Biphenyl C-cyclopropylalkylamides (**69a**, **70b-d**, **71**, **72**) and the control compound 3-fluoro-4'-hydroxybiphenyl-4-carbaldehyde oxime (**13**) were tested in a commercial assay (Panvera) adapted to 384-well plate format for their ability to displace a fluorescent E2 derivative (ES2) complexed with ER α (Figure 22) and ER β (Figure 23). The recombinant human ERs were incubated with ES2 and then treated with test agents. After 1-2 h, the fluorescence polarization was measured. ES2 bound to ER protein gave a high fluorescence polarization. In this assay, the presence of a displacing ligand causes a decrease in the fluorescence polarization.

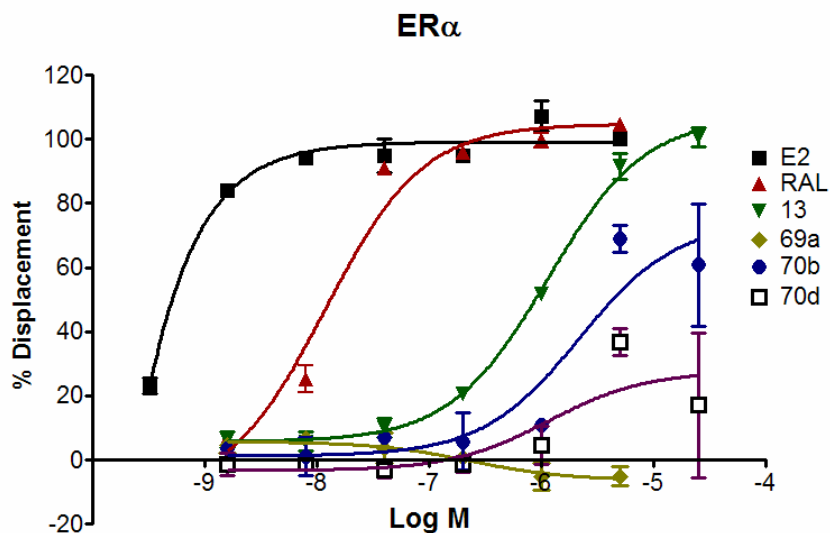


Figure 22. Biphenyl *C*-cyclopropylalkylamides tested in a displacement assay on ER α .

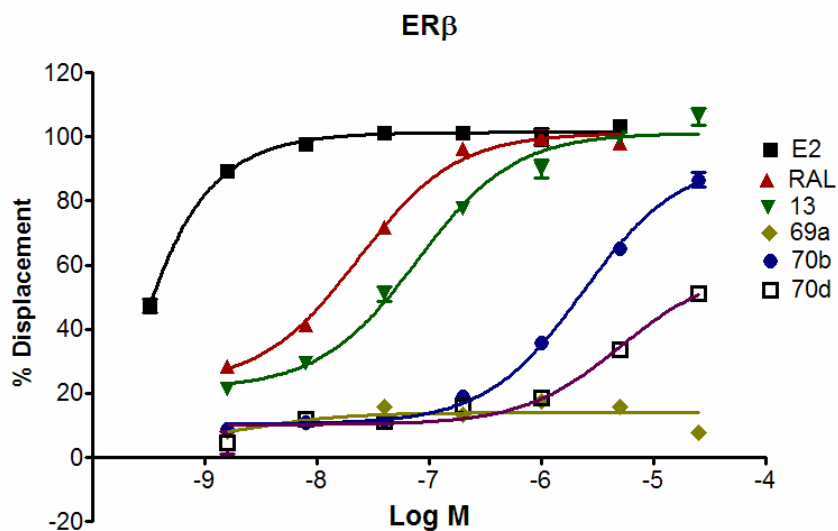


Figure 23. Biphenyl *C*-cyclopropylalkylamides tested in a displacement assay on ER β .

The displacement assays were performed with ligands present in the concentration range of 1.6 nM – 25 μ M.

Concentration-dependence curves on both receptors were constructed from the one site competition best-fit curves using Graph Pad Prism 4 software. The data is presented as mean % displacement \pm SD, (N=2).

The data shown in Figure 22 and Figure 23 is representative of experiments run in duplicate, from a minimum of two separate experiments. The data is presented as percent displacement (%I) \pm SD. The estimated one site competition IC₅₀ values are presented in Table 7. E2, RAL and GEN were used as standards in each run. The known biphenyl oxime **13** was used as a positive control and gave comparable IC₅₀ values to those found previously in radioactive ligand binding assays.³⁶

Table 7. Biphenyl C-cyclopropylalkylamides tested in displacement assays on ERs.

Compound	ERα IC₅₀ (nM)	ERβ IC₅₀ (nM)	ERβ/ ERα
E2	1.0	1.0	1
RAL	13.1	12.5	1
GEN	403	13	31
13	888.1	43.5	20
69a	>25000	>25000	NA
70b	4300	2200	2
70c	>25000	>25000	NA
70d	>25000	22700	NA
71	>25000	>25000	NA
72	>25000	6700	>4

The displacement assays were performed with test compounds present in the concentration range of 1.6 nM – 25 μ M and controls (E2, RAL and GEN) present in the range 0.16 nM – 5 μ M. Concentration-dependence curves on both receptors were constructed and IC₅₀ values were calculated from the one site competition best-fit curves using Graph Pad Prism 4 software. The selectivity ratios were calculated by dividing the IC₅₀ value on ER α by the IC₅₀ value on ER β .

2.2.3. Docking studies

Docking studies using the CAChe suite of algorithms were performed with a molecular model of the ER β LBD obtained from X-ray crystallographic coordinates and were conducted to compare the binding mode of biphenyl *C*-cyclopropylalkylamide **72**, with biphenyl oxime **13**. The coordinates for the binding pocket from structural studies of human ER β -LBD in complex with GEN (1QKM)⁶⁵ were downloaded from the Protein Data Bank. GEN was used first as a standard to validate the docking system. GEN was redocked into the pocket by holding the residues of the protein fixed and allowing the ligand to be flexible. The orientation and hydrogen bonding were close to that in the crystal structure (data not shown). The biphenyl oxime structure **13**³⁶ was superimposed on that of GEN in the ER β -LBD binding pocket, the model of GEN was removed, and oxime **13** was then docked into the pocket by holding the protein rigid and the ligand flexible. Figure 24 shows the binding energy (-46.7 kcal/mole) for this interaction. The ligand adopted similar orientation to that of GEN in the pocket. The phenolic OH of **13** formed a hydrogen bond with Glu474 and the oxime OH formed a hydrogen bond with His475, the same residues with which GEN forms hydrogen bonds (Figure 24).

An analogue of compound **37d** (CC1-243), the free amine **72**, was superimposed on the model of docked biphenyl oxime **13** and then after removal of the oxime ligand the model of the ligand was docked under the same conditions outlined above. Interestingly, the alkyl chain of **72** slid deep into the back wall of the pocket and formed favorable hydrophobic interactions with the side chain of Met336 (Figure 25).

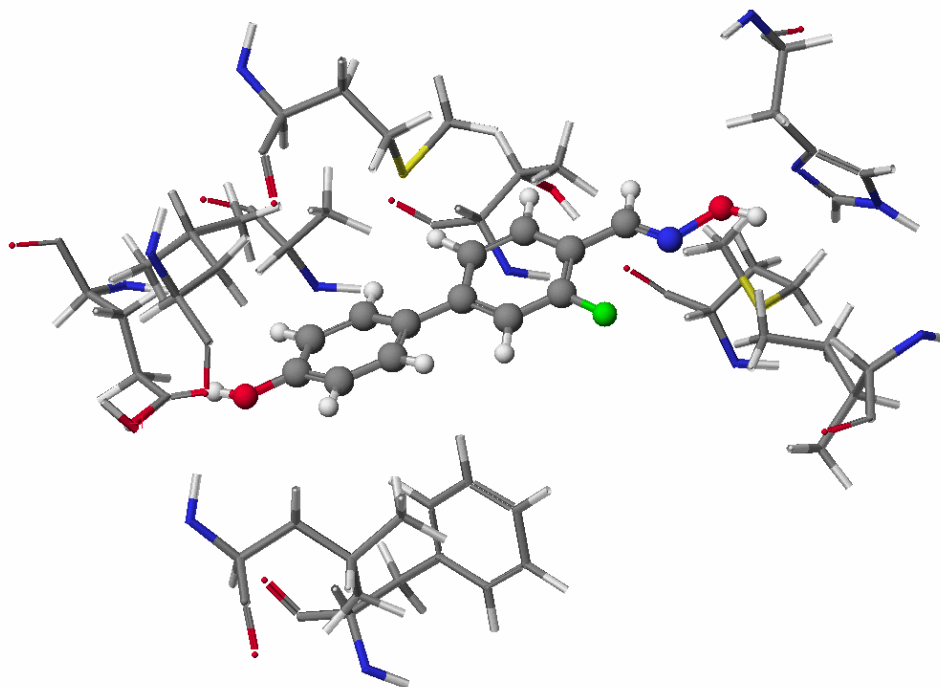


Figure 24. Biphenyl oxime 13 docked into the GEN binding pocket of ER β -LBD (BioMedCACHe).

This finding indicated the possibility that compound **72** might be selective for ER β . The docking exercise also showed compound **72** orients in the GEN pocket in the same way as the tested oxime, including a hydrogen bond with Glu475. However, the prediction did not hold true as the behavior of compound **72** in the displacement assays was poor. It was anticipated that removal of the bulky phenyl ring on the amide would promote more favorable binding to both receptors. This assumption was confirmed in the molecular docking exercises. In the displacement assays, however, compound **72** did not interact with ER α to displace the fluorescently labeled estradiol, even at the highest concentrations used ($>2 \mu\text{M}$). Compound **72** showed competitive activity on ER β ($6.7 \mu\text{M}$). This was a disappointing result considering the activity of this compound in

MCF-7 cells, discussed in the next section. The encouraging finding was the selectivity for ER β in this assay, even though it was at best very modest.

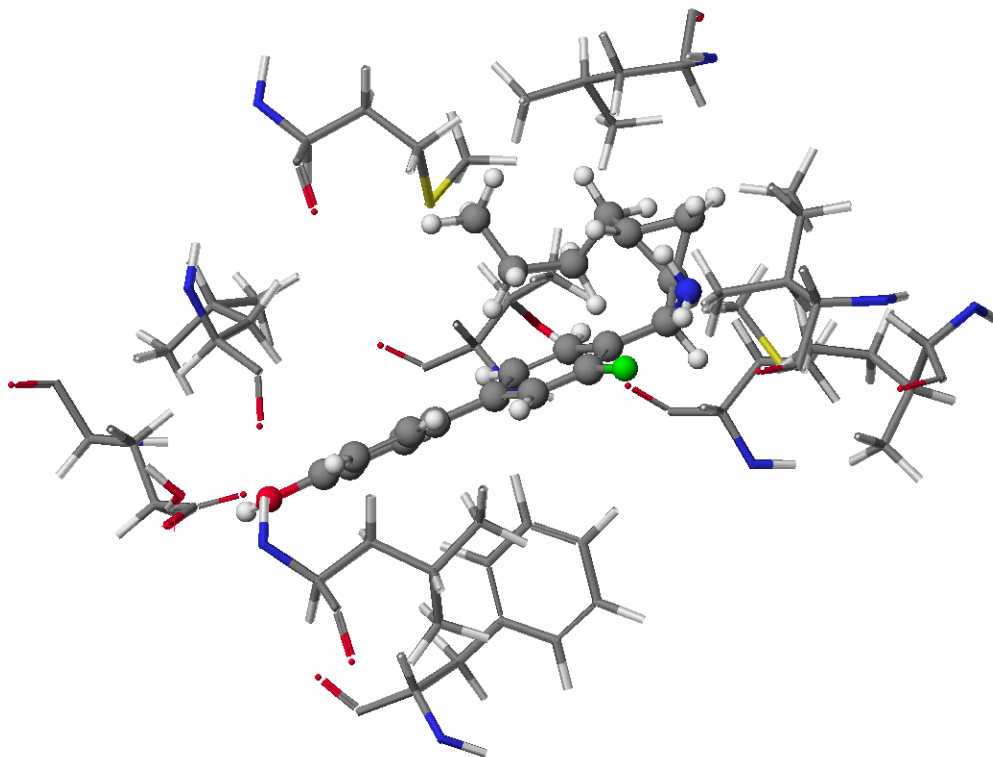


Figure 25. Biphenyl *C*-cyclopropylalkylamine 72 docked into GEN binding pocket of ER β -LBD (BioMedCACHe).

2.2.4. Biphenyl *C*-cyclopropylalkylamides Tested on Breast Cancer Cells

A new model for simultaneous targeting both ERs in breast cancer is proposed and discussed in detail in section 4.2. The above described biphenyl *C*-cyclopropylalkylamides were tested for inhibition of estradiol-induced proliferation of MCF-7 human breast cancer cells in order to identify potential antiestrogens. Three analogues of compound **37d** (CC1-243) were shown to inhibit E2 induced proliferation of MCF-7 cells. Data presented in Figure 26⁶⁶ are means \pm SD

(N = 4). Statistical Graph Pad 4 software was used to estimate GI₅₀ values from non-linear best curve fit ($p=0.9 > 0.05$): **RAL** (65.4 nM), **13** (20.9 μ M), **70b** (500 nM), **70c** (13.5 μ M) and **72** (400 nM) and. The MCF-7 cell based evaluation was performed by Miranda Sarachine.

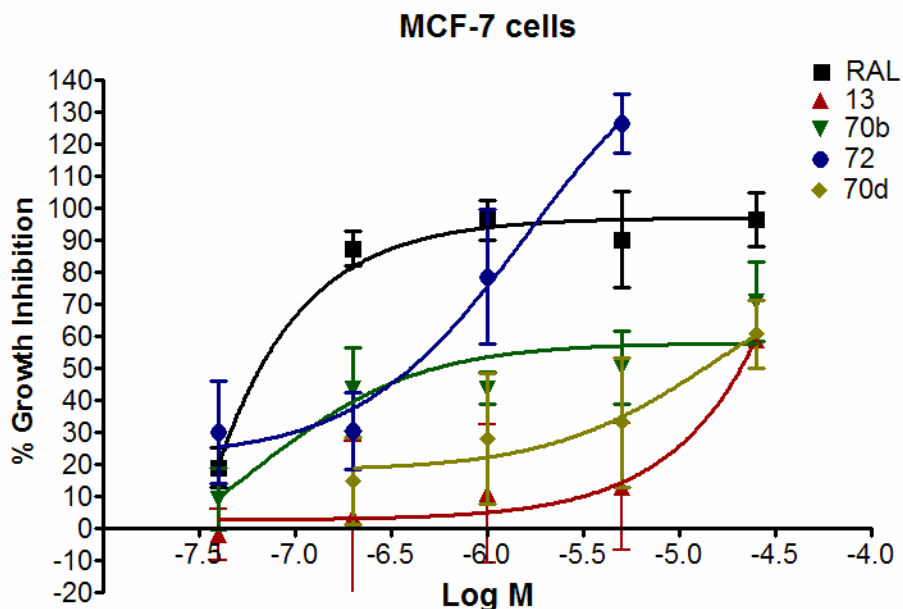


Figure 26. Biphenyl *C*-cyclopropylalkylamides tested for inhibition of E2 stimulated growth of breast cancer cells.⁶⁶

RAL was used as a positive control. The MCF-7 antiproliferative assay is usually the first-used cell-based test in search for ER α antagonists. The biphenyl oxime **13** had a high GI₅₀ value (20.9 μ M), not a surprise considering that this compound was designed as an agonist for both receptors.³⁶ The desired compound should compete with estradiol at ER β with good selectivity and yet act as an antagonist, or be inactive, on ER α . However, the MCF-7 antiproliferative assay is an indirect measure of ER α antagonism and was used here only as a first cell-based test of these agents. Surprisingly, two compounds, **70b** and **72** showed GI₅₀ values in the submicromolar range, inhibiting estradiol-induced MCF-7 proliferation. However, this is not

sufficient evidence to declare these compounds as antiestrogens. Compound **70b** was found to interact with both receptors *in vitro* in the fluorescence polarization-based displacement assay (Table 7). However, the IC₅₀ values of this compound were significantly higher in the fluorescence polarization assay as compared to its GI₅₀ determined in MCF-7 cells, indicating that the compound likely exerted its cell growth-inhibitory actions by a mechanism that did not involve the ER α . In addition, the second-most active analogue in MCF-7 cells, compound **72**, showed no interaction with ER α in the fluorescence polarization-based assay and only a modest interaction with ER β .

2.2.5. SAR of Biphenyl C-Cyclopropylalkylamides on ER α and ER β

The biphenyl core³⁶ has recently been extensively explored for the selective targeting of ER β . Biphenyl oxime **13** was used as a model agent. In the fluorescence polarization-based displacement assays, this compound showed 20-fold selectivity for ER β . The attempt was made to develop agents that would selectively target ER β as agonists and at the same time act as antagonists on ER α . It was disappointing to find that the biphenyl C-cyclopropylalkylamides synthesized had modest to poor activity in the ER displacement assays. One compound, **70b**, had low micromolar activity, which was achieved by simple modification of the original hit CC1-234 through introduction of one phenol group and one aryl fluorine. When the phenol was masked as a methyl ether (compound **69a**), the activity at both receptors was lost, indicating that the phenolic OH was critical for ER binding. When the benzamide in **70b** was replaced by the bulky and lipophilic phosphinoyl group, the activity was also lost, showing that the size was

important. It was suspected that by changing the benzamide to an acetamide (compound **70d**), activity at both ERs in the displacement assays would be improved simply by the decreased size of the agent. Unfortunately, the change from benzamide to acetamide resulted in complete loss of activity on both receptors, yielding a compound with IC₅₀ values of >25 μM (Table 7).

From the published literature on agents that have been found to be selective for ERβ, it can be noted that the most potent and most selective agents are small in size and have low ClogP values (2-4.5 on average). In an effort to further decrease the size and the ClogP value of our analogues, the amide on the biphenyl *C*-cyclopropylalkylamide was replaced by a free primary amine and analogue **72** was synthesized. It was anticipated that this compound would have good potency at the ERβ and show selectivity. This compound did not interact with ERα in such a way that was measurable by the competition with fluorescently labeled estradiol, and it competed with labeled estradiol on the ERβ only modestly with an IC₅₀ of 6.7 μM. However, this compound showed significant inhibitory activity against MCF-7 cell growth. This inhibitory activity of **72** is likely derived from either an active metabolite of the aliphatic primary amine, or from activation through alternative pathways that would lead to cell growth inhibition without binding to the ERs. It is possible that this agent could bind to the ER, but in a way that would not interfere with the interaction of labeled estradiol. It might also interact with the coactivator binding domain of the ER, resulting in the inhibition of MCF-7 cell growth by preventing the transcriptional activation of ERα through interference with coactivator recruitment. The fluorescence polarization-based displacement assay used is unable to detect this kind of possible interaction of test agents with the ERs. A recent report suggests that bi- and terphenyls can provide a backbone that mimics a peptide alpha helix and inhibit the interaction of ERs with

coregulators.⁶⁷ This report proposed their use to block coactivator recruitment and therefore inhibit breast cancer cell proliferation. In this vein, future studies could explore the agents presented here for their ability to target the coregulator binding domain. The fact that introduction of the OH to the biphenyl core did not result in significant improvement of the biological activity, as well as the presence of an aliphatic alkyl chain on the compounds, could support the notion that the coregulator binding site is an alternative target for the binding of these agents. This hypothetical mechanism of action can be tested in future explorations of the biological activity of this series. Briefly, one possible *in vitro* test for the coregulator binding agents on ERs is proposed in the future directions section.

3. CONCLUSIONS

The work presented here resulted in the identification of new scaffolds from libraries of allylic amides, *C*-cyclopropylalkylamides and homoallylic amides for targeting ERs. Cell-based screening for agonists and antagonist in transcriptional activation assays of the ER α at a classical ERE identified one new antagonist, *C*-cyclopropylalkylamide **26a** (CK1-183).⁴⁸ *C*-Cyclopropylalkylamide **3a** was characterized as an antagonist on ER α when it was found to inhibit E2-induced ERE-tk-Luc transcription ($IC_{50} = 11 \pm 2 \mu\text{M}$) and MCF-7 ($GI_{50} = 12 \pm 4 \mu\text{M}$) cell proliferation in a concentration-dependent manner (Figure 9 and Figure 10, respectively). To further confirm this finding, antiproliferative activity of **26a** (CK1-183) against the ER-negative MDA-MB231 human breast cell line was examined, **26a** (CK1-183) was found to be inactive ($GI_{50} > 50 \mu\text{M}$, Table 2). However, this compound was able to displace fluorescently labeled estradiol at ER α to modest extent. Furthermore, biological activities of the individual enantiomers of compound **26a** (CK1-183) were not statistically different (Figure 9 and Figure 10).⁴⁸ Molecular docking studies using the CAChe suite of algorithms indicated that the phosphinoyl group of **26a** (CK1-183) capped the binding pocket and probably in that way interfered with helix 12 movement, while the remainder of **26a** (CK1-183)'s, sulfonyl-carbamate moiety bound deeper into the raloxifene binding cleft and interacted with residues at helices H3, H6 and H11, suggesting a partial or full antagonist binding mode.

Overall, the unusual structure of **26a** (CK1-183), its ability to antagonize E2 in the cell-based assays, and its modest ability to displace E2 in the binding pocket suggested new avenues for

SERM design. *C*-cyclopropylalkylamide **26a** (CK1-183) served as the lead structure for further synthetic efforts. An initial set of modifications targeted the *N*-acyl segment of **26a** (CK1-183), but these changes led to no improvement in the antiproliferative activity in MCF-7 cells. This was a disappointing result, but it did show that changes in the phosphinoyl group protected portion of the molecule were necessary for two reasons: (a) to increase drug like properties and (b) to explore in greater detail SAR around the *C*-cyclopropylalkylamide core.

A second generation library of allylic amides and *C*-cyclopropylalkylamides was designed as a focused library around **26a** (CK1-183) as a lead structure to explore the SAR.⁵² Initial goal of this library synthesis was to find more potent ER α antagonists in breast cancer cells. However, the library was tested at both receptors and it was interesting to find hits on both ERs. Initial screening on ER α identified three compounds **37c**, **37a** and **39c** that had somewhat improved activities in MCF-7 cells as compared to lead structure **26a** (CK1-183) (Figure 17). The GI₅₀ values of the hits were in low micromolar range, see section 2.2.4. It was very important to find a key finding was that that these new compounds had significantly smaller aromatic portions compared to the large phosphinoyl group of **26a** (CK1-183), and the sulfonamide group was present only in one of them (**39c**). In addition, all three contained a simple alkyl chain on the cyclopropane ring. Most importantly, all compounds that showed significant activity at ER α from the second generation library were *C*-cyclopropylalkylamides, whereas analogues with a double bond instead of the cyclopropane showed no activity in breast cancer cells. The cyclopropane ring appeared to be important for interaction with both ERs.

When the second generation library was screened in fluorescence polarization displacement assay on ER β , biphenyl *C*-cyclopropylalkylamide **37d** was identified as a hit. This compound was also interesting due to the fact it contained the biphenyl core, explored previously by the Wyeth research group and found to be important for ER β selectivity.^{35,36} Six analogues of compound **37d** were synthesized and tested in displacement assays and for inhibition of E2 induced proliferation of breast cancer cells. The most promising compound in this limited size series was **70b**. Biphenyl *C*-cyclopropylalkylamide **70b** showed two fold selectivity for ER β in displacement assays, but with IC₅₀ values on both receptors were in the low micromolar range (Table 7). Surprisingly, this compound showed submicromolar activity in inhibiting estradiol induced MCF-7 cell proliferation. This finding suggested alternative mechanisms for how this compound might act as an antiestrogen and further studies are needed. An even larger surprise were the assay results of compound **72**. This compound was an analogue of **70b** that lacked the phenylamide and contained instead a free amine. When docked into the GEN binding pocket of ER β , compound **72** showed interaction with key amino acids through hydrogen bonding. The alkyl chain on the cyclopropane was oriented deeper into the pocket and showed promising hydrophobic interactions with Met336. These findings from modeling studies were suggesting higher potency and selectivity of this compound over the lead **37d**. Disappointingly, compound **72** did not show any activity in the displacement assay on ER α , and very modest activity on ER β . However, in MCF-7 cells this compound was most active inhibitor of cell proliferation of all libraries compounds tested in this work. The IC₅₀ value of **72** at 400nM in MCF-7 cells suggested was very encouraging finding; however, a plethora of alternative mechanisms than direct antagonism on ER α is possible, some of which are discussed in section 4.

In summary, a new class of antiestrogens was discovered. The selectivity of novel SERMs and the selectivity of these compounds for ER subtypes was investigated and addressed. The goal was to improve the potency and subtype selectivity by using the uniqueness of *C*-cyclopropylalkylamides as ER targeting agents. Novel biphenyl structures for targeting ERs were discovered, opening new avenues for SERM design and targeting both estrogen receptors.

4. FUTURE DIRECTIONS

4.1. Role of ER β in Breast Cancer

The relationship between tamoxifen resistance and ER β expression and function is not clear. However, a limited size study in breast cancer patients' samples suggests that low levels of ER β expression predict tamoxifen resistance.⁶⁸ In a more detailed clinical study, ER β and coregulator expression were correlated with tamoxifen resistance.⁶⁹ These studies point out that ER β may play a significant role in breast cancer. Whether that role could be targeted for SERM design with improved pharmacological profile over tamoxifen remains an open question.

4.2. Hypothesized Model for Targeting ER β in SERM Resistant Cancer

Clinically, tamoxifen has been used as a therapy of choice not only for its effectiveness in stopping breast cancer proliferation and increasing survival of patients, but for its relatively mild side effects compared to other chemotherapy. The major problem with tamoxifen use in breast cancer therapy is the development of resistance. When tamoxifen therapy is continued beyond five years, tamoxifen becomes more likely to promote a clonal selection of metastatic breast cancer resistant to tamoxifen. De novo resistance is usually attributed to the loss or absence of estrogen receptor.¹ Acquired resistance develops in approximately 50% of ER+ patients that initially respond to tamoxifen therapy and leads to disease progression and death. In acquired

tamoxifen resistance two different but closely related phenotypes are known: tamoxifen unresponsiveness and tamoxifen stimulation of breast cancer proliferation. In many instances when aromatase inhibitors are given as secondary endocrine therapy after tamoxifen failure, patients respond well. This is not a surprise since acquired tamoxifen resistance usually is not attributable to estrogen receptor loss and patients are still considered ER+. As an antiestrogen, tamoxifen can affect the negative feedback in the pituitary-ovarian axis and that can result in increased circulatory levels of estrogens and compromise tamoxifen effectiveness.⁷⁰ This mechanism in resistance development can be applied to all antiestrogens, but what makes tamoxifen specifically interesting is its switch in pharmacological action from an antagonist at the ER α to an agonist on a cellular level. It has been shown that MCF-7 breast cancer cells, upon prolonged treatment with tamoxifen are likely to begin to proliferate.⁷¹ This *in vitro* finding correlates with the clinical data and presents MCF-7 tamoxifen resistant cells as a good model to study acquired tamoxifen resistance. The mechanism of a tamoxifen antagonist – agonist switch in breast cancer is not clear. Breast cancer cells T47D that are dependent on estradiol for proliferation continued to grow in the presence of tamoxifen when PKA was activated. It has been proposed that phosphorylation of Ser305 on ER α by protein kinase A (PKA) induced Tamoxifen to switch from an antagonist to agonist. It was found that this phosphorylation in the hinge region prevents bound tamoxifen to perturb ER α and alter coactivator recruitment, therefore allowing tamoxifen to bind as an agonist and lead to ER α -dependent transactivation.⁷² Additional mechanisms were proposed to lead to tamoxifen resistance. Osborne *et al.*⁷³ have shown that in patients with breast tumors HER2/neu positive and high levels of AIB1 (amplified in breast cancer 1) protein correlate with a poor outcome of tamoxifen therapy. They proposed using AIB1 and HER2/neu expression as potential markers to

predict tamoxifen therapy efficacy. Osborne *et al.* also proposed that high expression levels of AIB1 would promote tamoxifen agonism. Whether AIB1 is upregulated in tamoxifen-stimulated tumors is not known. Furthermore, AIB1 activation through phosphorylation could be another possible pathway that increases the AIB1 stimulation of ER α transcriptional activation.

It is evident that there are several mechanisms that could lead to ER α transcriptional activation in the presence of an antagonist, such as tamoxifen, in SERM resistant cells. The proposed model suggests taking advantage of ER β inhibitory action on ER α , and also that ER β targeting with an agonist is not stimulatory in breast cancer cells. The model is shown in

Figure 27. ER β agonistic/ER α antagonistic agents are envisioned as being able to activate ER β , leading to indirect inhibition of ER α and at the same time antagonize ER α . The result would be double inactivation of ER α transcriptional activation and inhibition of tamoxifen-stimulated breast cancer progression.

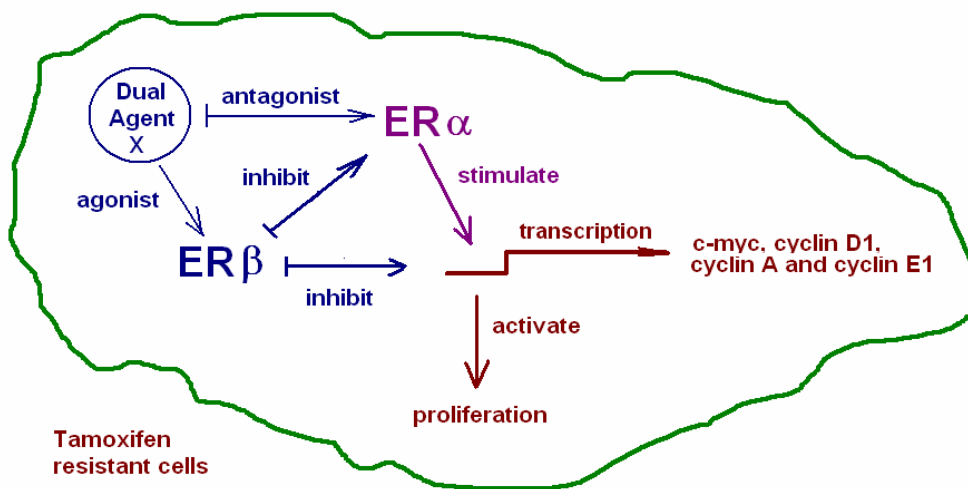


Figure 27. Hypothesized ideal SERM that targets both ERs.

Agents with these highly advantageous properties are currently not available. In addition, screening *in vitro* test for the desired type of agents is not available and its design is briefly discussed bellow.

I propose here an assay that would at the same time test agents for displacement on both ERs and coregulator binding interference. The assay would entail dual color fluorescence polarization. Fluorescence polarization (FP) assays can be used to directly measure the interaction between a protein (not labeled) and a labeled ligand or peptide. The literature gives a precedent for using dual color fluorescence polarization in genotyping assays.⁷⁴ To the best of my knowledge, dual color fluorescence polarization has not been used for testing nuclear receptor-targeting agents. In the new assay, simultaneously recombinant human ER α or ER β would employ fluorescently labeled estradiol (E2-FITC, green) and a labeled coactivator peptide (LXXLL-Rhodamine, red). In a recent study, the coactivator-derived peptide ⁶⁸⁵EKHKILERLLKDS⁶⁹⁷ was shown to be recruited by agonist-bound ER α , ER β and TR,⁷⁵ making it a good candidate for the dual color FP assay. In the assay, FP will be measured in the green and red channels. When agonist is added, the expected result is low green polarization (displaced E2-FITC) and high red polarization (receptor-recruited peptide); when antagonist is added, low polarization will occur in both channels (displacement of E2 and no peptide recruitment); when a coregulator domain binding competitor is added, high polarization in the green (no displacement of E2) channel and low polarization in the red (displacement of the labeled coregulator peptide) channel will occur. The assay and the agents as described above are believed to open a new avenue for SERM discovery and design.

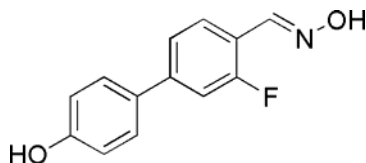
5. EXPERIMENTAL SECTION

5.1. Chemistry

5.1.1. General Experimental Procedures

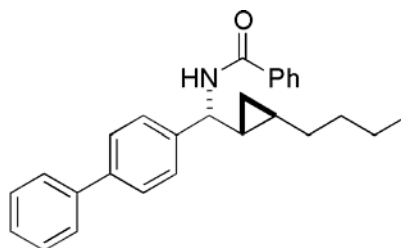
All reactions were performed in flame dried round bottom flasks under a nitrogen atmosphere unless indicated otherwise. Microwave irradiation was performed in microwave vessels (10 mL tubes) in either a CEM Discoverer or an Emrys Optimizer (Biotage) microwave reactor as indicated. Solvents were dried by distillation: CH₂Cl₂ and Et₃N were distilled over CaH₂; THF was distilled over sodium benzophenone ketyl; toluene was purified by filtration through activated alumina; EtOAc and hexanes were distilled prior use. Anhydrous ether and dioxane were purchased from Aldrich Chemical Co. and used without further purification. 1-Hexyne, 3-butyn-1-ol, 3-hexyne, 3-octyne, 4-benzyloxybenzeneboronic acid, 4-bromo-2-fluorobenzaldehyde, 4-bromobenzaldehyde, 4-chlorobenzenesulfonylamide, 4-methoxybenzeneboronic acid, 4-methylbenzenesulfonylisocyanate, BBr₃ (1 M solution in hexanes), benzaldehyde, benzenesulfonylisocyanate, biphenyl-4-carbaldehyde, chlorosulfonylisocyanate, Cp₂ZrCl₂, Dabco®, dicyclohexylamine, diisopropyl azodicarboxylate (DIAD), diphenylphosphine chloride, diiodomethane, isopropanol, Me₂Zn (2 M in toluene), methyl 4-formylbenzoate, palladium (II) acetate, TBAF, TBDPSCl, *tert*-butanol, TiCl₄ and triphenylphosphine were purchased from Aldrich, Acros, TCI or Lancaster Synthesis. Reactions were monitored by TLC analysis (EM Science pre-coated silica gel 60 F254 plates, 250 μm

thickness) and visualized with a 254 nm UV light, by staining with PAA solution (2.5 mL of *p*-anisaldehyde, 2 mL of AcOH, and 3.5 mL of conc. H₂SO₄ in 100 mL of 19:1 EtOH/H₂O) and/or staining with Vaughn's reagent (4.8 g of (NH₄)₆Mo₇O₂₄•4 H₂O and 0.2 g of Ce(SO₄)₂ in 100 mL of 3.5 N H₂SO₄). All crude products were purified by flash chromatography on SiO₂ (Merck, pore size 60 Å, particle size 200-400 mesh, for column chromatography) unless indicated otherwise. Chromatography columns were packed dry and equilibrated with the appropriate solvent system as noted. Melting points were determined using Laboratory Devices Mel-Temp II and Fisher-Jones Melting Point apparatus. Infrared spectra were determined on a Nicolet Avatar 360 FT-IR spectrometer. ¹H and ¹³C NMR spectra were obtained on Bruker Avance 300 and Varian Mercury 400 instruments at 300 and 75 MHz or 400 and 100 MHz, respectively, in CDCl₃ unless otherwise noted. Chemical shifts were reported in parts per million (ppm) using the residual solvent signal as an internal standard.⁷⁶ ¹H NMR spectra are tabulated as follows: chemical shift, multiplicity (s = singlet, d = doublet, t = triplet, q = quartet, qn = quintet, m = multiplet, b = broad), number of protons and coupling constant(s). ¹³C NMR spectra were acquired using a proton decoupled pulse sequence with a pulse sequence delay of 3 sec. Low resolution and high resolution mass spectra (MS and HRMS, respectively) were obtained in positive ion mode by electron ionization (EI), electrospray ionization (ESI), or by matrix-assisted laser desorption ionization (MALDI) using either α-cyano-4-hydroxycinnamic acid or a germanium-doped polysilicate (NanoHorizons, Inc.) matrix with either a Micromass Autospec double focusing instrument or an Applied Biosystems 4700 MALDI-TOF/TOF-MS.



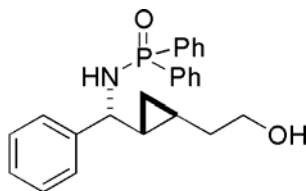
13

2-Fluoro-4'-hydroxybiphenyl-4-carbaldehyde oxime (13)³⁶ was prepared according to the literature procedure³⁶ from the corresponding aldehyde (**65a**) with some modifications. 3-Fluoro-4'-methoxybiphenyl-4-carbaldehyde **65a** (0.05 g, 0.20 mmol) was dissolved in freshly distilled CH₂Cl₂ (5 mL) under a nitrogen atmosphere, cooled to -78 °C and treated dropwise with BBr₃ (1M in hexanes, 0.5 mL, 0.3 mmol). The reaction mixture was left to stir at -78 °C for 2h, warmed to r.t., and stirred for an additional 3h. The mixture was poured into an ice-cold 1 M solution of NaHCO₃ (10 mL) and, while at 0°C, diluted with EtOAc (50 mL). The solution was acidified at 0°C by dropwise treatment with conc. HCl. The organic phase was separated, dried over Na₂SO₄, filtered and concentrated in vacuo. The obtained aldehyde (**66**) was submitted to next step without further purification. The residue was dissolved in absolute MeOH (2.5 mL). Hydroxylamine (0.4 mmol), pyridine (0.4 mmol) and 5Å molecular sieves (0.25 g) were added and the reaction heated to reflux in a sealed tube for 6 h. The solvent was removed under high vacuo, and the residue dissolved in EtOAc, filtered and concentrated. Purification by preparative TLC (1:1 EtOAc/hexanes) afforded **13** (20 mg, 42%) as a colorless solid: ¹H NMR (300MHz, DMSO-*d*₆) δ 11.51 (s, 1 H), 9.68 (s, 1 H), 8.18 (s, 1 H), 7.72 (t, 1 H, *J* = 7.7 Hz), 7.55 (d, 2 H, *J* = 8.6 Hz), 7.46 (m, 2 H), 6.82 (d, 2 H, *J* = 8.6 Hz). The data matched the previously reported.³⁶



37d

N-(*R*^{*})-(((1*R*^{*},2*R*^{*})-2-Butylcyclopropyl)-(4-(phenyl)phenyl)methyl)benzamide (**37d**)⁵² (12 mg, 31%) was obtained from **75** following the literature procedure⁵² as a colorless solid: m.p. 176.0-178.0 °C (EtOAc/hexanes); IR (KBr) 3303, 2955, 2923, 2855, 1631, 1527, 1489, 1076, 761, 694 cm⁻¹; ¹H NMR (300MHz, CDCl₃) δ 7.82 (d, 2 H, *J* = 6.9 Hz), 7.58 (d, 4H, *J* = 6.9 Hz), 7.50 (d, 4H, *J* = 9.2 Hz), 7.44 (t, 1 H, *J* = 6.1 Hz), 7.34 (t, 1 H, *J* = 7.2 Hz), 6.54 (d, 2 H, *J* = 7.8 Hz), 4.71 (t, 1 H, *J* = 8.3 Hz), 1.44 – 1.28 (m, 5H), 1.22 (t, 1 H, *J* = 7.0 Hz), 1.07 – 0.98 (m, 2 H), 0.86 (t, 3 H, *J* = 7.0 Hz), 0.66 (dt, 1 H, *J* = 8.3, 4.7 Hz), 0.50 (dt, 1 H, *J* = 7.9, 4.1 Hz); ¹³C NMR (75MHz, CDCl₃) δ 166.9, 141.3, 141.1, 140.5, 134.9, 131.8, 129.0, 128.9, 127.54, 127.47, 127.4, 127.3, 127.2, 57.3, 33.7, 32.2, 24.6, 22.7, 18.2, 14.3, 11.7; MS (APCI) 384 ([M+H]⁺, 100), 263 (30); MS (EI) 383 (M⁺, 17), 105 (100), 77 (24); HRMS (EI) calcd for C₂₇H₂₉NO 383.2249 found 383.2244.

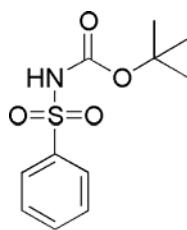


41

N-(*R*^{*})-(((1*R*^{*},2*S*^{*})-2-(2-Hydroxyethyl)cyclopropyl)(phenyl)methyl)-*P,P*-

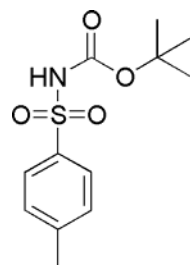
diphenylphosphinamide (41) (135 mg, 87%) was prepared as described previously.⁷⁷ ¹H NMR (300MHz, CDCl₃) δ 7.90-7.79 (m, 4 H), 7.52-7.47 (m, 2 H), 7.45 – 7.38 (m, 4 H), 7.35 (app d, 2 H, *J* = 9.0 Hz), 7.32 – 7.29 (m, 2 H), 4.68 (bs, 1 H), 3.86-3.73 (m, 3 H), 3.59-3.54 (m, 1 H),

2.18-2.08 (m, 1 H), 1.71 (bs, 1 H), 1.06-0.98 (m, 1 H), 0.90 – 0.85 (m, 1 H), 0.82 – 0.71 (m, 1 H), 0.38 (dt, 1 H, $J = 9.6, 4.8$ Hz), 0.33 (dt, 1 H, $J = 8.4, 5.4$ Hz).



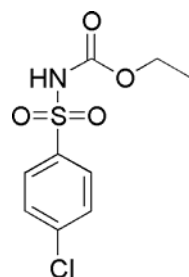
45a

***O*-tert-Butyl-*N*-phenylsulfonylcarbamate (45a).** **General Procedure A:** A previously reported method⁴² was used with some modifications. Dry THF (20 mL) and *tert*-butanol (2.1 mL, 22 mmol) were mixed in a round bottom flask (50 mL) under an N₂ atmosphere and cooled to 0 °C. Benzenesulfonylisocyanate (2.0 g, 1.5 mL, 10 mmol) was added via syringe dropwise while stirring at 0 °C. Stirring was continued until the reaction mixture reached r.t., approximately 1 h. The solvent was removed in vacuo to afford **45a** as colorless oil that, after crystallization from hexanes, gave a colorless solid (2.8 g, 98%). m.p. 119-120 °C (hexanes/EtOAc); IR (KBr) 3242, 3000, 2981, 2934, 1721, 1476, 1344, 1249, 1145, 1089, 918, 826, 737, 583; ¹H NMR (300MHz) δ 8.02 (d, 2 H, $J = 7.7$ Hz), 7.65 (t, 1 H, $J = 6.3$ Hz), 7.57 (d, 2 H, $J = 7.8$ Hz), 7.28 (s, 1 H), 1.38 (s, 9 H); ¹³C NMR δ 144.7, 129.6, 129.4, 128.1, 126.4, 84.0, 27.8; MS (EI) 242 (M⁺-15, 10), 202 (9), 141 (35), 137 (21), 94 (39), 77 (74), 57 (100); HRMS (EI) calcd for C₁₀H₁₂NO₄S⁺ (M-CH₃)⁺ 242.0482, found 242.0482.



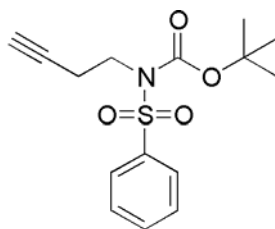
45b

***O*-tert-Butyl-*N*-phenylsulfonylcarbamate (45b).** General method A was used with minor modifications. Dry THF (20 mL) and *tert*-butanol (1.9 mL, 20 mmol) were mixed in a round bottom flask (50 mL) under an N₂ atmosphere and cooled to 0 °C. 4-methylbenzenesulfonylisocyanate (2.0 g, 1.5 mL, 10 mmol) was added dropwise via syringe while stirring at 0 °C. Stirring was continued until the temperature reached r.t. (1 h). The solvent was removed by vacuo to afford **45b** as colorless oil that, after crystallization from EtOAc/hexanes, gave a colorless solid (2.4 g, 88%). m.p. 104-105 °C (hexanes/EtOAc); IR (KBr) 3358, 3262, 3001, 2979, 2930, 1750, 1597, 1477, 1186, 918, 835, 818, 740, 579; ¹H NMR (300MHz) δ 7.88 (d, 2 H, *J* = 7.8 Hz), 7.32 (d, 2 H, *J* = 8.3 Hz), 2.44 (s, 3 H), 2.17 (s, 1 H), 1.37 (s, 9 H); ¹³C NMR δ 144.7, 129.6, 129.4, 128.1, 126.4, 84.0, 27.8, 21.6; MS (EI) 256 (M⁺-15, 7), 216 (34), 212 (67), 197 (34), 155 (39), 108 (51), 91 (100)65 (42), 57 (87); HRMS (EI) calcd for C₁₁H₁₄NO₄S⁺ (M-CH₃)⁺ 256.0638, found 256.0628.



45c

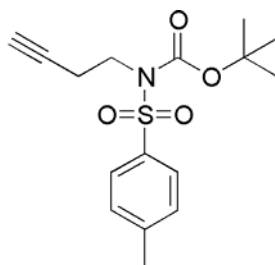
***O*-Ethyl-*N*-(4-chlorophenyl)sulfonylcarbamate (45c).** 4-Chlorobenzenesulfonylisocyanate was prepared in situ using a literature procedure.⁷⁸ In brief, 4-Chlorobenzenesulfonylamide (2.0 g, 10 mmol) was suspended in dry chlorobenzene (15 mL) in a round bottom flask (50 mL) equipped with a condenser, Dabco® (0.05 g, 0.50 mmol) was added and the reaction mixture was vigorously stirred for 10 min. at r.t. Chlorosulfonylisocyanate (1.6 g, 11 mmol) was added and the mixture was heated to 100 °C for 2.5 h. The reaction mixture was cooled to 0 °C and absolute EtOH was added in excess via syringe while stirring at 0 °C. The mixture was left to stir for 30 min. while warming up to r.t. The solvent was removed by vacuo and the residue redissolved and purified by flash chromatography on SiO₂ (gradient of 4:1 to 7:3 hexanes/EtOAc) to afford **45c** (1.2 g, 42%) as a colorless solid: m.p. 85-86 °C (hexanes/EtOAc); IR (KBr) 3225, 3097, 2989, 2909, 1752, 1586, 1445, 1353, 1233, 1161, 1085, 917, 839, 819, 773, 619 cm⁻¹; ¹H NMR (300MHz) δ 7.99 (d, 2 H, *J* = 8.5 Hz), 7.52 (d, 2 H, *J* = 8.5 Hz), 4.15 (quartet, 2 H, *J* = 7.1 Hz), 1.22 (t, 3 H, *J* = 7.1 Hz). ¹³C NMR δ 150.4, 140.9, 136.9, 130.0, 129.5, 63.5, 14.2; MS (EI) 263 (M⁺, 19), 199 (42), 175 (47), 128 (100), 111 (87), 75 (66); HRMS (EI) calcd for C₉H₁₀ClNO₄S 263.0019, found 263.0018.



46a

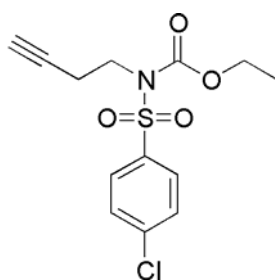
***O*-tert-Butyl-*N*-but-3-ynyl-*N*-phenylsulfonylcarbamate (46a). General Procedure B,**

Mitsunobu Reaction: A literature procedure^{56,57} was used with some modifications. *O*-tert-butyl-benzenesulfonylcarbamate **45a** (2.5 g, 10 mmol) and triphenylphosphine (2.5 g, 10 mmol), were dissolved in dry THF (20 mL) in a round bottom flask under an N₂ atmosphere, treated with 3-butyn-1-ol (0.5 mL, 6.7 mmol) and cooled to 0 °C (ice bath). While stirring at 0 °C, diisopropyl azodicarboxylate (DIAD) (1.9 mL, 10 mmol) was added dropwise. The reaction mixture was warmed to r.t. and stirring was continued for 2 h. The solvent was removed by vacuo and the residue redissolved and purified by flash chromatography on SiO₂ (9:1 hexanes/EtOAc) to afford **46a** (1.8 g, 62%) as a colorless solid: m.p. 51.0-53.0 °C (hexanes/EtOAc); IR (KBr) 3288, 3062, 3002, 2983, 2940, 2920, 1724, 1452, 1294, 1089, 968, 844, 746, 658 cm⁻¹; ¹H NMR (300MHz) δ 7.90 (d, 2 H, *J* = 7.3 Hz), 7.57 (t, 2 H, *J* = 7.2 Hz), 7.50 (t, 2 H, *J* = 7.7 Hz), 4.00 (t, 2 H, *J* = 7.3 Hz), 2.65 (td, 2 H, *J* = 5.2, 2.5, Hz), 2.01 (t, 1 H, *J* = 2.5 Hz), 1.30(s, 9H); ¹³C NMR (75MHz) δ 150.7, 140.2, 133.4, 128.8, 127.8, 84.8, 80.4, 70.6, 45.2, 27.8, 20.1; MS (EI) 253 (17), 170 (70), 141 (44), 94 (17), 77 (51), 57 (100); HRMS (EI) calcd for C₁₁H₁₁NO₄S 253.0409 (M-C₄H₈)⁺, found 253.0412.



46b

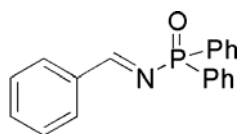
***O*-tert-Butyl-*N*-but-3-ynyl-*N*-(4-methylphenyl)sulfonylcarbamate (46b):** According to the general procedure B, *O*-tert-Butyl-4-methylbenzenesulfonylcarbamate **45b** (2.2 g, 8.1 mmol), triphenylphosphine (2.1 g, 8.1 mmol), 3-butyne-1-ol (0.4 mL, 5.4 mmol) and DIAD (1.6 mL, 8.1 mmol), afforded **46b** (1.2 g, 47%) as a colorless solid: m.p. 72.0-73.5 °C (hexanes/EtOAc); IR (KBr) 3297, 2983, 1726, 1357, 1275, 1169, 722, 651, 577 cm⁻¹; ¹H NMR (300MHz) δ 7.78 (d, 2 H, *J* = 8.3 Hz), 7.30 (d, 2 H, *J* = 8.1 Hz), 4.01 (t, 2 H, *J* = 4.6 Hz), 2.65 (t, d, 2 H, *J* = 4.9, 2.6 Hz), 2.44 (s, 3 H), 2.02 (t, 1 H, 2.7 Hz), 1.34 (s, 9H); ¹³C NMR (75MHz) δ 150.9, 144.2, 137.3, 129.4, 128.0, 84.7, 80.6, 70.6, 45.3, 28.0, 21.7, 20.1; MS (EI) 267 (9), 203 (25), 184 (74), 155 (69), 108 (23), 91 (74), 65 (28), 57 (100); HRMS (EI) calcd for C₁₂H₁₃NO₄S (M-C₄H₈)⁺ 267.0565, found 267.0571.



46c

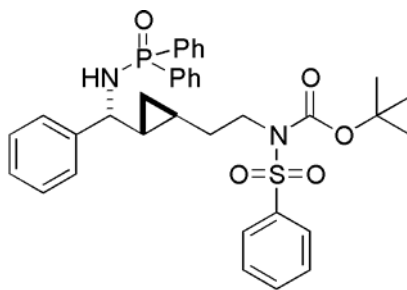
***O*-Ethyl-*N*-but-3-ynyl-*N*-(4-chlorophenyl)sulfonylcarbamate (46c):** According to the general procedure B, *O*-ethyl-4-chlorobenzenesulfonylcarbamate **45c** (1.3 g, 4.9 mmol), triphenylphosphine (1.3 g, 4.9 mmol), 3-butyne-1-ol (0.25 mL, 3.3 mmol) and DIAD (1.0 mL, 4.9

mmol), afforded **46c** (97 %) as a colorless solid: m.p. 58.0-60.0 °C (hexanes/EtOAc); IR (KBr) 3299, 3099, 2983, 2910, 1736, 1585, 1478, 1281, 1173, 1012, 970, 824, 765, 659 cm⁻¹; ¹H NMR (300MHz) δ 7.92 (d, 2 H, *J* = 8.7 Hz), 7.49 (d, 2 H, *J* = 8.7 Hz), 4.16 (q, 2 H, *J* = 7.1 Hz), 4.02 (t, 2 H, *J* = 7.2 Hz), 2.66 (td, 2 H, *J* = 4.9, 2.6, Hz), 2.02 (t, 1 H, *J* = 2.6 Hz), 1.21 (t, 3 H, *J* = 7.1 Hz); ¹³C NMR (75MHz) δ 152.0, 140.5, 138.0, 130.1, 129.2, 80.1, 70.9, 63.9, 45.5, 20.1, 14.2; MS (EI) (*M*⁺, 315), 315 (21), 276 (21), 204 (58), 11 (87), 75(30); HRMS (EI) calcd for C₁₃H₁₄ClNO₄S 315.0332, found 315.0339.



47

Diphenylphosphinylimino-methyl-benzene (47). **General Procedure C, imine synthesis:** A literature procedure⁴³ was used with some modifications. In brief, TiCl₄ (0.61 mL, 5.5 mmol) in a round bottom flask (100 mL) was diluted in freshly distilled CH₂Cl₂ (30 mL) under an argon atmosphere. The solution was cooled to 0 °C and benzaldehyde (0.9 g, 8.7 mmol) was added neat, followed by Et₃N (3.9 mL, 28 mmol). Stirring was continued at 0 °C for 5 min. Diphenylphosphinamide (2.0 g, 9.2 mmol), prepared using literature procedure^{52,79} was added as a solid and the mixture was stirred at 0 °C for 15 min. The mixture was warmed to r.t. and stirring was continued for 2 h. The reaction mixture was poured into dry diethyl ether (200 mL) and stirred for 15 min at r.t. The resulting solution was filtered through a pad of Florisil/Celite (4:1) and the filtrate concentrated by vacuo. The residue was chromatographed over deactivated SiO₂ (9:1 EtOAc/hexane containing 1% v/v Et₃N) to afford **54** (1.1 g, 32%) as a colorless solid



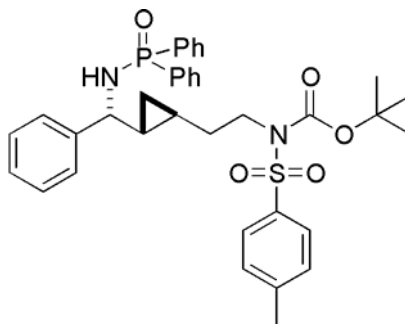
48a

***O*-Ethyl-*N*-2-((1*R**,2*R**)-2-((*R**)-((diphenylphosphoryl)amino)(phenyl)methyl)-**

cyclopropyl]-*tert*-butyl-*N*-phenylsulfonylcarbamate (48a**). **General Procedure D:** A**

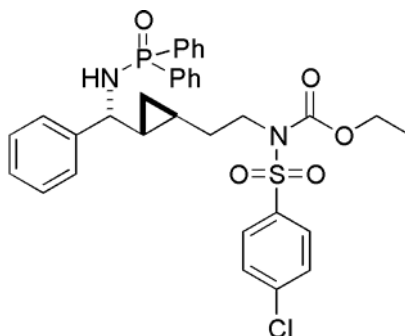
literature procedure⁴² for structurally similar compounds was used with some modifications. In brief, Cp₂ZrHCl (0.3 g, 1.2 mmol) was suspended in dichloromethane (freshly distilled, 2 mL) and immediately treated with alkyne **46a** (0.4 g, 1.2 mmol), added as a solid. The reaction mixture was stirred vigorously for 2 min. at r.t. and cooled to -78 °C and treated with Me₂Zn, 2M solution in toluene (0.6 mL, 1.2 mmol) and warmed up over 5 min. to 0 °C. Aldimine **47** (0.1 g, 1.2 mmol) was added as a solid, and the reaction vessel was transferred to an oil bath and heated at reflux for 4 h. Reaction was quenched with NH₄Cl aqueous solution, diluted with EtOAc and separated organic layer filtered through a pad of Florisil/Celite (4:1), dried over MgSO₄ and concentrated in vacuo. The resulting residue was purified by flash chromatography (EtOAc/hexanes 9:1, 1% Et₃N) to afford **48a** (25 mg, 10%) as a colorless solid: m.p. 166.0-168.0 °C (EtOAc/hexanes); IR (KBr) 3189, 3060, 2980, 2930, 1727, 1439, 1356, 1291, 1154, 1089, 724, 699, 581 cm⁻¹; ¹H NMR (300MHz, (CD₃)₂CO) δ 7.93 – 7.91 (m, 5 H), 7.79 – 7.72 (m, 4 H), 7.47 – 7.41 (m, 6 H), 7.35 – 7.30 (m, 4 H), 7.27 (app d, 1 H, *J* = 7.8 Hz), 5.17 (t, 1 H, *J* = 10.2 Hz), 3.92 (tdt, 1 H, *J* = 15.9, 9.6, 5.7 Hz), 3.55 (app q, 1 H, *J* = 8.7 Hz), 1.71 – 1.57 (m, 2 H), 1.27 (s, 9 H), 1.23 – 1.08 (m, 2 H), 0.96 – 0.93 (m, 1 H), 0.53 (dt, 1 H, *J* = 9.3, 4.8Hz), 0.33 (dt, 1 H, *J* = 8.4, 5.0Hz); ¹³C NMR (100 MHz, CDCl₃) δ 150.9, 140.6, 133.2, 132.6, 132.5, 132.1,

132.05, 132.01, 131.8, 128.8, 128.7, 128.6, 128.5, 128.4, 127.8, 127.3, 127.0, 84.3, 58.8, 47.0, 34.3, 28.0, 26.7, 16.3, 10.6; HRMS (MALDI) calcd for C₃₅H₄₀N₂O₅PS 631.2396 [M+H]⁺, found 631.2256.



48b

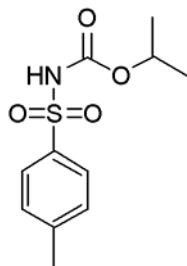
***O*-Ethyl-*N*-2-((1*R**,2*R**)-2-((*R**)-((diphenylphosphoryl)amino)(phenyl)methyl)-cyclopropyl]-*tert*-butyl-*N*-(4methylphenyl)sulfonylcarbamate (48b).** According to the general procedure D, Cp₂ZrHCl (0.3 g, 1.0 mmol), alkyne **46b** (0.3 g, 1.0 mmol), aldimine **47** (0.1 g, 0.3 mmol) and Me₂Zn (2 M in toluene, 0.5 mL, 1.0 mmol) afforded **48b** (19 mg, 9%) as a colorless solid: m.p. 78.0-79.0 °C (EtOAc/hexanes); IR (KBr) 3192, 3060, 2980, 2928, 1727, 1438, 1355, 1155, 724, 700, 578 cm⁻¹; ¹H NMR (300MHz, (CD₃)₂CO) δ 7.93 – 7.87 (m, 2 H), 7.80 – 7.72 (m, 4H), 7.47 – 7.40 (m, 8H), 7.35 – 7.22 (m, 6H), 3.92 (tdt, 1 H, *J* = 15.9, 9.6, 5.7 Hz), 3.55 (app q, 1 H, *J* = 9.3 Hz), 2.41 (s, 3 H), 1.66 – 1.55 (m, 2 H), 1.27 (s, 9H), 1.25 – 1.11 (m, 2 H), 0.94 – 0.88 (m, 1 H), 0.51 (dt, 1 H, *J* = 8.2, 4.1Hz), 0.31 (dt, 1 H, *J* = 8.1, 3.9Hz); ¹³C NMR (100 MHz, CDCl₃) δ 151.1, 144.2, 137.5, 132.7, 132.6, 132.2, 132.1, 132.08, 131.9, 129.4, 128.8, 128.7, 128.6, 128.5, 128.0, 127.4, 127.1, 84.2, 66.1, 58.8, 47.1, 34.4, 28.1, 26.7, 21.8, 16.4, 15.5, 10.6; HRMS (MALDI) calcd for C₃₆H₄₂N₂O₅PS 645.2552 [M+H]⁺, found 645.3829.



48c

***O*-Ethyl-*N*-2-((1*R**,2*R**)-2-((*R**)-((diphenylphosphoryl)amino)(phenyl)methyl)-**

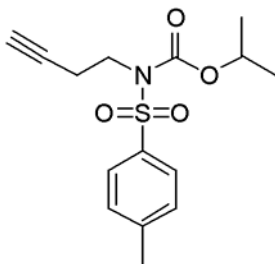
cyclopropyl)-ethyl-*N*-(4-chlorophenyl)sulfonylcarbamate (48c). According to the general procedure D, with some modifications (CH₂I₂ was added and the reaction mixture was stirred at r.t. for additional 2.5h), Cp₂ZrHCl (0.3 g, 1.0 mmol), alkyne **46c** (0.4 g, 1.0 mmol), aldimine **47** (0.1 g, 0.3 mmol), Me₂Zn (2 M in toluene, 0.5 mL, 1.0 mmol) and CH₂I₂ (0.1 mL, 1.7 mmol) afforded **48c** (46 mg, 23%) as a colorless solid: m.p. 125.0-126.0 °C (EtOAc/hexanes); IR (KBr) 3342, 3188, 3059, 2991, 1733, 1439, 1371, 1275, 1180, 1090, 1014, 759, 699, 572, 539 cm⁻¹; ¹H NMR (300MHz, CDCl₃) δ 7.94 – 7.88 (m, 2 H), 7.85 (d, 2 H, *J* = 8.7 Hz), 7.51 – 7.41 (m, 7H), 7.36 – 7.23 (m, 7H), 3.92 (q, 2 H, *J* = 7.2 Hz), 3.88 (t, 1 H, *J* = 7.5 Hz), 3.73 (t, 1 H, *J* = 7.5 Hz), 2.51 (broad s, 1 H), 1.81 – 1.68 (m, 1 H), 1.56 – 1.46 (m, 1 H), 0.80 – 0.75 (m, 1 H), 0.42 (dt, 1 H, *J* = 9.6, 4.8Hz), 0.35 (dt, 1 H, *J* = 8.4, 5.1 Hz); ¹³C NMR (75MHz, CDCl₃) δ 152.0, 142.8, 140.0, 138.0, 132.4, 132.3, 131.9, 131.8, 129.7, 128.9, 128.6, 128.4, 128.4, 128.2, 127.2, 126.7, 63.4, 59.0, 47.2, 34.1, 26.6, 16.3, 14.0, 10.5; MS (API-ES) 637 ([M+H]⁺, 100); MS (EI) 636 (M⁺, 35), 306 (73), 201 (100), 156 (35); HRMS (EI) calcd for C₃₃H₃₄ClN₂O₅PS 636.1615 found 636.1655.



53-1

Sulfonylcarbamate Synthesis. *O*-Isopropyl-*N*-(4-methylphenyl)sulfonylcarbamate (53-1).

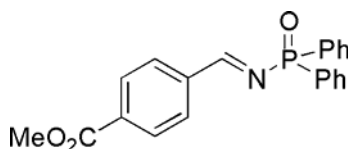
According to the general procedure A, methylbenzenesulfonylisocyanate (1.9 g, 1.5 mL, 10 mmol) and isopropanol (1.5 mL, 20 mmol) afforded **53-1** as colorless oil that, after crystallization from hexanes, gave a colorless solid (2.8 g, quant.): m.p. 76.0-78.0 °C (hexanes/EtOAc); IR (KBr) 3271, 2984, 1747, 1597, 1437, 1340, 1238, 1167, 1091, 892, 817, 660 cm⁻¹; ¹H NMR (300MHz) δ 7.92 (d, 2 H, *J* = 8.3 Hz), 7.77 (s, 1 H), 7.33 (d, 2 H, *J* = 8.2 Hz), 4.87 (septet, 1 H, *J* = 6.33 Hz), 2.44 (s, 3 H), 1.19 (d, 6H, *J* = 6.3 Hz); ¹³C NMR δ 150.2, 145.1, 135.8, 129.6, 128.5, 71.6, 21.8; MS (EI) 257 (M⁺, 23), 242 (20), 230 (52), 215 (19), 193 (24), 155 (47), 108 (100), 91 (90); HRMS (EI) calcd for C₁₁H₁₅NO₄S 257.0722, found 257.0734.



53

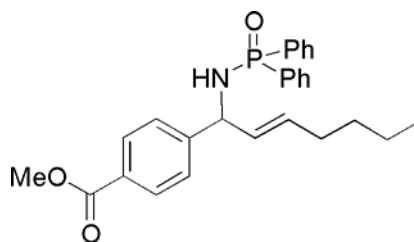
***O*-Isopropyl-*N*-but-3-ynyl-*N*-(4-methylphenyl)sulfonylcarbamate (53):** According to the general procedure B, *O*-Isopropyl-4-methylbenzenesulfonylcarbamate **53-1** (2.6 g, 10.0 mmol), triphenylphosphine (2.6 g, 10 mmol), 3-butyn-1-ol (0.5 mL, 6.7 mmol) and DIAD (1.6 mL, 10 mmol), afforded **53** (1.5 g, 72%) as a colorless solid: m.p. 71.6-73.4 °C (hexanes/EtOAc); IR

(KBr) 3308, 2988, 2934, 1731, 1597, 1357, 1170, 1089, 1102, 899, 811, 735 cm^{-1} ; ^1H NMR (300MHz) δ 7.83 (d, 2 H, $J = 8.3$ Hz), 7.30 (d, 2 H, $J = 8.4$ Hz), 4.89 (septet, 1 H, $J = 6.3$ Hz), 4.01 (t, 2 H, $J = 7.3$ Hz), 2.65 (td, 2 H, $J = 7.6, 2.7$ Hz), 2.43 (s, 3 H), 2.02 (t, 1 H, 2.6 Hz), 1.15 (d, 6 H, $J = 6.3$ Hz); ^{13}C NMR (75MHz) δ 151.9, 144.8, 137.2, 129.6, 129.3, 128.6, 80.6, 72.3, 70.8, 45.5, 21.9, 21.6, 20.3, 16.4; MS (EI) 309 (M^+ , 27), 287 (12), 270 (34), 245 (28), 206 (37), 184 (100), 155 (74), 91 (46); HRMS (EI) calcd for $\text{C}_{15}\text{H}_{19}\text{NO}_4\text{S}$ 309.1035, found 309.1041.



54

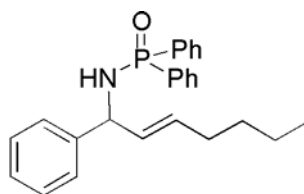
Methyl 4-[(diphenylphosphinylimino)methyl]benzoate (54). According to the general procedure C, methyl 4-formylbenzoate (1.4 g, 8.7 mmol), diphenylphosphinamide (2.0 g, 9.2 mmol), TiCl_4 (0.6 mL, 5.5 mmol) and Et_3N (3.9 mL, 28 mmol), afforded **54** (1.1 g, 32%) as a colorless solid. ^1H NMR (300MHz) δ 9.37 (d, 1 H, $J = 30$ Hz), 8.16 (d, 2 H, $J = 6.0$ Hz), 8.06 (d, 2 H, $J = 6.0$ Hz), 7.98-7.89 (m, 4H), 7.53-7.26 (m, 6H), 3.91 (s, 3 H).



55

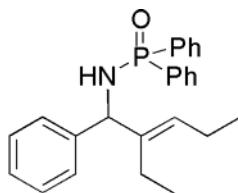
(E)-Methyl 4-(1-((diphenylphosphinoyl)amino)hept-2-enyl)benzoate (55).⁵¹ **Aldimine Addition in a Microwave. General Procedure E:** According to the general procedure E, A suspension of Cp_2ZrHCl (0.1 g, 0.4 mmol) in dry toluene (1.6 mL) was treated with 1-hexyne (0.05 mL, 0.4 mmol) and the mixture was heated in the CEM Discoverer microwave in flash heat

mode (80 °C, 75 W) for 40 sec. The mixture was cooled to -78 °C, treated with Me₂Zn (2 M in toluene, 0.2 mL, 0.4 mmol), warmed to 0 °C and aldimine **54** (0.1 g, 0.3 mmol) was added. The mixture was heated in the microwave in flash heat mode (100 °C, 150 W) for 40 sec. then cooled to r.t. The reaction was quenched by addition of 1M NH₄Cl (0.5 mL) with vigorous stirring, then diluted with EtOAc (50 mL) and 1M NaHCO₃ (1 mL). The organic layer was collected and the aqueous layer was extracted with EtOAc (2 x 50 mL). The combined organic extracts were washed with H₂O (2 x 10 mL) and a saturated aqueous NaCl solution (brine) (2 x 10 mL), dried (MgSO₄, 2 g), filtered and concentrated by vacuo. The residue was chromatographed over deactivated SiO₂ (9:1 EtOAc/hexane containing 1% v/v Et₃N) to afford **55** (110 mg, 95%) as a colorless solid: ¹H NMR (300MHz, CDCl₃) δ 7.99-7.93 (m, 2 H), 7.81 – 7.80 (m, 2 H), 7.46 – 7.22 (m, 10H), 5.65 (dd, 1 H, *J* = 15.3, 6.1), 5.40 (dt, 1 H, *J* = 15.5, 6.6 Hz), 4.85 (td, 1 H, *J* = 9.3, 6.0 Hz), 3.92 (s, 3 H), 3.29 (td, 1 H, *J* = 8.8, 5.6 Hz), 2.08 – 1.98 (m, 2 H), 1.30 – 1.26 (m, 4H), 0.87 (t, 3 H, *J* = 6.9 Hz).



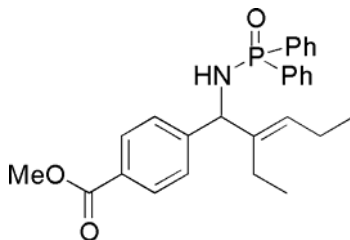
56

(E)-N-(1-Phenylhept-2-enyl)-P,P-diphenylphosphinamide (56).⁵¹ According to the general procedure E, Cp₂ZrHCl (0.2 g, 0.8 mmol), 1-hexyne (0.1 mL, 0.8 mmol), aldimine **47** (0.2 g, 0.5 mmol) and Me₂Zn (2 M in toluene, 0.4 mL, 0.8 mmol) afforded **56** (84 mg, 43%) as a colorless solid: ¹H NMR (300MHz, CDCl₃) δ 7.95 (m, 2 H), 7.84 (m, 2 H), 7.48-7.26 (m, 11 H), 5.64 (dd, 1 H, *J* = 9.1, 6.2 Hz), 5.53 (dd, 1 H, *J* = 15.4, 6.0), 4.81 (td, 1 H, *J* = 9.4, 6.2 Hz), 3.27 – 3.24 (m, 1 H), 1.99 – 1.95 (m, 2 H), 1.31 – 1.24 (m, 4H), 0.90 – 0.85 (m, 3 H).



57

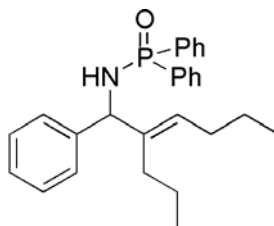
(E)-N-(2-Ethyl-1-phenylpent-2-enyl)-P,P-diphenylphosphinamide (57). According to the general procedure E, Cp_2ZrHCl (0.10 g, 0.4 mmol), 3-hexyne (0.05 mL, 0.4 mmol), aldimine **47** (0.08 g, 0.25 mmol) and Me_2Zn (2 M in toluene, 0.2 mL, 0.4 mmol) afforded **57** (75 mg, 77%) as a colorless solid: NMR (300MHz, CDCl_3) δ 7.95-7.85 (m, 4 H), 7.45-7.29 (m, 11 H), 5.53 (t, 1 H, $J = 14.3$ Hz), 4.73 (t, 1 H, $J = 10.7$ Hz), 3.24 (td, 1 H, $J = 10.0, 6.1$ Hz), 2.16-2.04 (m, 3 H), 1.78 – 1.68 (m, 1 H), 1.63 (s, 1 H), 1.03 (t, 3 H, $J = 7.5$ Hz), 0.70 (t, 3 H, $J = 7.6$ Hz).



58

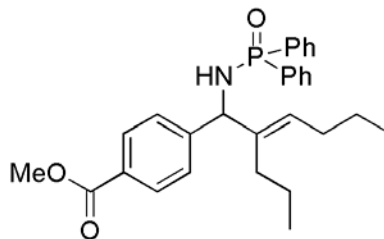
(E)-Methyl 4-(1-diphenylphosphinoylamino-2-ethylbut-2-enyl)benzoate (58)⁵¹. According to the general procedure E, Cp_2ZrHCl (0.2 g, 0.8 mmol), 3-hexyne (0.13 mL, 0.9 mmol), aldimine **54** (0.19 g, 0.5 mmol) and Me_2Zn (2 M in toluene, 0.4 mL, 0.8 mmol) afforded **58** (188 mg, 74%) as a colorless solid: m.p. 91.9-92.3 °C (EtOAc/hexanes); IR (KBr) 3181, 2957, 2930, 2869, 1722, 1610, 1436, 1281, 1185, 1107, 1123, 1019 cm^{-1} ; ^1H NMR (300MHz, CDCl_3) δ 7.97-7.77 (m, 6 H), 7.50-7.35 (m, 8 H), 5.50 (t, 1 H, $J = 7.2$ Hz), 4.76 (t, 1 H, $J = 10.6$ Hz), 3.90 (s, 3 H), 3.28 (dd, 1 H, $J = 10.3, 6.3$ Hz), 2.14-2.02 (m, 3 H), 1.74-1.71 (dq, 1 H, $J = 14.5, 7.3$ Hz), 1.45 1.37 (m, 2 H), 1.17-1.09 (m, 2 H), 0.93 (t, 3 H, $J = 7.3$ Hz), 0.74 (t, 3 H, $J = 7.3$ Hz); ^{13}C NMR (75MHz, CDCl_3) δ 167.2, 148.3, 140.2, 140.2, 133.7, 133.6, 132.7, 132.6, 132.4, 132.3,

132.2, 131.9, 130.0, 129.3, 128.8, 128.6, 127.8, 59.5, 52.3, 31.4, 30.2, 23.2, 22.3, 14.5, 14.2; MS (EI) 475 (M^{+} , 59), 446 (16), 432 (14), 364 (63), 274 (45), 218 (53), 201 (100), 77 (48); HRMS (EI) calcd for $C_{29}H_{34}NO_3P$ 475.2276, found 475.2283.



59

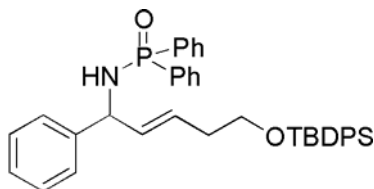
(E)-N-(3-Propinyl-1-phenylhex-2-enyl)-P,P-diphenylphosphinamide (59). According to the general procedure E, Cp_2ZrHCl (0.2 g, 0.8 mmol), 4-octyne (0.1 mL, 0.8 mmol), aldimine **47** (0.2 g, 0.5 mmol) and Me_2Zn (2 M in toluene, 0.4 mL, 0.8 mmol) afforded **59** (130 mg, 62%) as a colorless solid: m.p. 108.1-108.8 °C (EtOAc/hexanes); IR (KBr) 3187, 2956, 2928, 2868, 1436, 1184, 1125, 1107, 748, 699 cm^{-1} ; 1H NMR (300MHz) δ 7.94-7.83 (m, 4H), 7.47-7.38 (m, 6H), 7.37-7.24 (m, 5H), 5.60 (t, 1 H, $J = 7.2$ Hz), 4.72 (t, 1 H, $J = 10.5$ Hz), 3.23 (dd, 1 H, $J = 9.9, 6.0$ Hz), 2.07 (dt, 3 H, $J = 14.4, 7.2$ Hz), 1.69 (dt, 1 H, $J = 9.0, 6.5$ Hz), 1.45 (dt, 2 H, $J = 14.7, 7.4$ Hz), 1.14 – 1.06 (m, 2 H), 0.96 (t, 3 H, $J = 7.3$ Hz), 0.72 (t, 3 H, $J = 7.2$ Hz); ^{13}C NMR (75MHz) 142.7, 140.2, 133.7, 133.6, 132.4, 132.2, 132.0, 128.4, 128.2, 127.5, 127.4, 127.1, 59.4, 55.7, 31.2, 29.9, 23.0, 22.0, 14.2, 14.0; MS (EI) 417(M^{+} , 28), 306 (43), 258 (35), 218 (82), 216 (93), 201 (100); HRMS (EI) calcd for $C_{27}H_{32}NOP$ 417.2222, found 417.2217.



60

(E)-Methyl 4-((1-diphenylphosphinoyl)amino-2-propylhex-2-enyl)benzoate (60).

According to the general procedure E, Cp₂ZrHCl (0.2 g, 0.8 mmol), 4-octyne (0.1 mL, 0.9 mmol), Me₂Zn (2.0 M in toluene, 0.4 mL, 0.8 mmol) and aldimine **54** (0.2 g, 0.5 mmol), afforded **60** (180 mg, 74%) as a colorless solid: m.p. 91.9-92.3 °C (hexanes/EtOAc); IR (KBr) 3181, 2957, 2930, 2869, 1722, 1610, 1436, 1281, 1185, 1107, 1123, 1019 cm⁻¹; ¹H NMR (300MHz) δ 7.97-7.77 (m, 6 H), 7.50-7.35 (m, 8 H), 5.50 (t, J = 7.2 Hz, 1 H), 4.76 (t, J = 10.6 Hz, 1 H), 3.90 (s, 3 H), 3.28 (dd, J = 10.3, 6.3 Hz, 1 H), 2.14-2.02 (m, 3 H), 1.74-1.71 (dq, J = 14.5, 7.3 Hz, 1 H), 1.45-1.37 (m, 2 H), 1.17-1.09 (m, 2 H), 0.93 (t, J = 7.3 Hz, 3 H), 0.74 (t, J = 7.3 Hz, 3 H); ¹³C NMR (75MHz) δ 167.21, 148.28, 140.24, 140.18, 133.71, 133.61, 132.72, 132.59, 132.41, 132.28, 132.16, 131.89, 130.02, 129.29, 128.77, 128.61, 128.78, 59.51, 52.29, 31.40, 30.15, 23.23, 22.34, 14.46, 14.23; MS (EI) 475 (M⁺, 59), 446 (16), 432 (14), 364 (63), 274 (45), 218 (53), 201 (100), 77 (48); HRMS (EI) calculated for C₂₉H₃₄NO₃P 475.2276, found 475.2283.

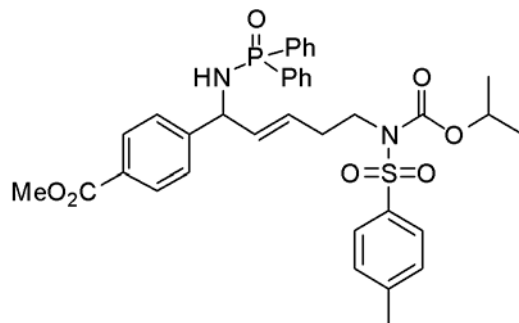


61

(E)-N-(5-((tert-Butyldiphenylsilyl)oxy))-1-phenylpent-2-enyl)-P,P-diphenylphosphinamide

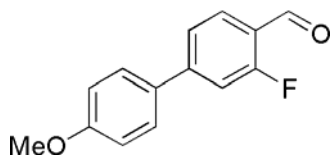
(61).⁵¹ According to the general procedure E, Cp₂ZrHCl (0.1 g, 0.4 mmol), alkyne **49** (0.15 g,

0.8 mmol), aldimine **47** (0.75 g, 0.25 mmol) and Me₂Zn (2 M in toluene, 0.19 mL, 0.38 mmol) afforded **61** (96 mg, 64%) as a colorless solid: ¹H NMR (300MHz, CDCl₃) δ 7.91-7.87 (m, 2 H), 7.84 – 7.79 (m, 2 H), 7.63 (d, 4 H, *J* = 6.4 Hz), 7.45 – 7.23 (m, 17H), 5.73 (dd, 1 H, *J* = 15.4, 6.0), 5.52 (dt, 1 H, *J* = 15.5, 6.5 Hz), 4.80 (td, 1 H, *J* = 9.4, 6.2 Hz), 3.63 (t, 2 H, *J* = 6.5 Hz), 3.23 (t, 1 H, *J* = 6.4 Hz), 1.01 (s, 9 H).



62

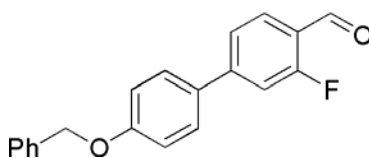
4-((1-Diphenylphosphinoylamino-5-(isopropoxycarbonyltosylamino))-pent-2-enyl)benzoic acid methyl ester (62).⁵¹ According to the general procedure E, Cp₂ZrHCl (0.1 g, 0.4 mmol), alkyne **53** (0.1 g, 0.5 mmol), Me₂Zn (0.2 mL, 0.4 mmol, 2.0M in toluene), and aldimine **54** (0.1 g, 0.3 mmol), afforded **62** (140 mg, 80%) as a colorless solid: m.p. 62.8-64.8 °C (EtOAc/hexanes); IR (KBr) 3167, 3057, 2982, 2952, 1723, 1609, 1437, 1362, 1280, 1186, 1167, 1107, 1122, 1087 cm⁻¹; ¹H NMR (300MHz) δ 7.97-7.89 (m, 4H), 7.83-7.74 (m, 4H), 7.51-7.26 (m, 10H), 5.82 (dd, 1 H, *J* = 15.4, 5.5 Hz), 5.51 (td, 1 H, *J* = 14.2, 6.4 Hz), 4.85-4.79 (m, 2 H), 3.91 (s, 3 H), 3.84 (t, 2 H, *J* = 7.0 Hz), 3.63 (td, 1 H, *J* = 7.1), 2.42 (s, 3 H), 1.27 (s, 1 H), 1.09 (d, 6 H, *J* = 6.2), 0.97-0.86 (m, 1 H); ¹³C NMR (75MHz) δ 167.2, 152.0, 147.9, 147.8, 144.7, 137.4, 135.0, 134.9, 132.6, 132.5, 132.4, 132.2, 132.1, 131.7, 130.1, 129.5, 129.4, 128.9, 128.8, 128.7, 128.6, 128.5, 127.538, 127.540, 72.1, 56.5, 52.7, 46.7, 33.1, 21.9; MS (EI) 674 (M⁺, 45), 473 (48), 416 (28), 404 (52), 216 (87), 201 (100), 155 (40), 91 (65); HRMS (EI) calcd for C₃₆H₃₉N₂O₇PS 674.2216, found 674.2224.



65a

2-Fluoro-4'-methoxybiphenyl-4-carbaldehyde (65a). Suzuki coupling.⁶² General Procedure

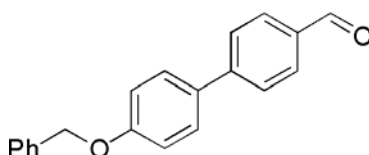
F: A literature procedure⁶¹ was used with some modifications. DAPCy catalyst⁶³ (0.02 g, 0.04 mmol) was dissolved in a round bottom flask (50 mL) in dry dioxane (12 mL), under nitrogen atmosphere at r.t. 4-Bromo-2-fluorobenzaldehyde (0.4 g, 2.0 mmol) was added as solid, followed by 4-methoxybenzeneboronic acid (0.5 g, 3.0 mmol) and Cs₂CO₃ (1.3 g, 4.0 mmol), also added as solids. The reaction mixture was left to stir at r.t. under nitrogen atmosphere for 16 h. The reaction was quenched by pouring into deionized water (20 mL), and diluted with EtOAc (200 mL). The organic layer was dried over Na₂SO₄, filtered and concentrated in vacuo. The residue was purified by flash chromatography (19:1 hexanes/EtOAc) to afford **65a** (320 mg, 70%), after crystallization from CH₂Cl₂ and hexanes as a colorless solid. ¹H NMR CDCl₃ δ 10.36 (s, 1 H), 7.91 (t, 1 H, *J* = 9 Hz), 7.57 (dt, 2 H, *J* = 12, 3 Hz), 7.46 (dd, 2 H, *J* = 9, 0.9 Hz), 7.35 (dd, 1 H, *J* = 12, 1.8 Hz), 7.00 (dt, 2 H, *J* = 12, 1.8 Hz), 3.94 (s, 3 H). The data matched that previously reported.³⁶



65b

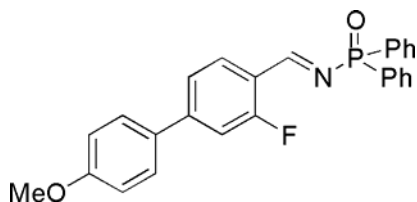
4'-Benzyloxy-2-fluorobiphenyl-4-carbaldehyde (65b). According to the general procedure F, DAPCy (0.04 g, 0.04 mmol), 4-bromo-2-fluorobenzaldehyde (0.41 g, 2.0 mmol), 4-

benzyloxybenzeneboronic acid (0.68 g, 3 mmol) and Cs_2CO_3 (1.3 g, 4.0 mmol) afforded **65b** (330 mg, 88%) as a colorless solid: m.p. 124.0-125.0 °C (EtOAc/hexanes); IR (KBr) 3448, 1689, 1618, 1601, 1580, 1266, 1251, 1183, 1011, 833, 753 cm^{-1} ; ^1H NMR (300MHz, CDCl_3) δ 10.35 (s, 1 H), 7.90 (t, 1 H, $J = 8.4$ Hz), 7.57 (d, 2 H, $J = 8.4$ Hz), 7.47-7.32 (m, 5H), 7.08 (d, 2 H, $J = 9.2$ Hz), 5.13 (s, 2 H); ^{13}C NMR (75MHz, CDCl_3) δ 187.0, 165.3 (d, $J = 192.3$ Hz), 160.0, 149.4 (d, $J = 6.8$ Hz), 136.8, 131.3, 129.4, 128.9, 128.7, 128.4, 127.7, 122.9, 122.4 (d, $J = 5.8$ Hz), 115.7, 114.2 (d, $J = 16.1$ Hz), 70.4; MS (EI) 306 (M^+ , 23), 307 (7), 215 (5), 157 (10), 159 (8), 133 (8), 91 (100); HRMS (EI) calcd for $\text{C}_{20}\text{H}_{15}\text{FO}_2$ 306.1056, found 306.1049.



65c

4'-Benzyloxybiphenyl-4-carbaldehyde (65c)⁸⁰ According to the general procedure F, DAPCy (0.04 g, 0.04 mmol), 4-bromobenzaldehyde (0.4 g, 2.0 mmol), 4-benzyloxybenzeneboronic acid (0.7 g, 3.0 mmol) and Cs_2CO_3 (1.3 g, 4.0 mmol) afforded **65c** (290 mg, 50%) as a colorless solid: ^1H NMR (300MHz, CDCl_3) δ 10.03 (s, 1 H), 7.93 (d, 2 H, $J = 8.4$ Hz), 7.71 (d, 2 H, $J = 8.2$ Hz), 7.58 (d, 2 H, $J = 8.8$ Hz), 7.48-7.34 (m, 5H), 7.08 (d, 2 H, $J = 8.8$ Hz), 5.13 (s, 2 H).

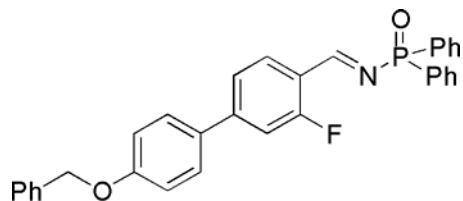


67a

***N*-(4-(4'-Methoxy-2'-fluorobiphenylmethylidene))-*P,P*-diphenylphosphinamide (67a).**

General Procedure G: A literature procedure⁵² was used with some modifications. In brief, TiCl_4 (0.1 mL, 0.8 mmol) was added dropwise into a solution of 4'-benzyloxybiphenyl-4-

carbaldehyde (0.2 g, 1.0 mmol), diphenylphosphinamide (0.2 g, 1.0 mmol) and Et₃N (0.4 mL, 3.0 mmol) in freshly distilled CH₂Cl₂ (50 mL), cooled to 0 °C. Stirring was continued at 0 °C for 10 min. The mixture was warmed to r.t. and stirring was continued for 20 h. The mixture was concentrated. The residue quickly filtered through SiO₂ and eluted with EtOAc. Solvent was removed in vacuo to afford **67a** (50 mg, 47%) as a colorless solid, m.p. 122.2-124.0°C (EtOAc/hexanes); IR (KBr) 3032, 1739, 1604, 1204, 1127, 1108, 843, 807, 698, 564 cm⁻¹; ¹H NMR (300MHz, CDCl₃) δ 9.65 (d, 1 H, *J* = 31.5 Hz), 8.46 (t, 1 H, *J* = 9.0 Hz), 8.13-8.08 (m, 4H), 7.88 (d, 2 H, *J* = 9.0 Hz), 7.80 (d, 2 H, *J* = 9.0 Hz), 7.72 (d, 1 H, *J* = 1.8 Hz), 7.69-7.61 (m, 6H, *J* = 9.0 Hz), 3.98 (s, 3 H); ¹³C NMR (75MHz, CDCl₃) δ 160.4, 133.7, 132.0, 131.8, 131.7, 131.6, 131.5, 131.0, 129.0, 128.5, 128.3, 128.3, 122.5, 114.5, 55.4; MS (EI) 429 (M⁺, 34), 202 (100), 77 (22); HRMS (EI) calcd for C₂₆H₂₁FNO₂P 429.1294, found 429.1282.

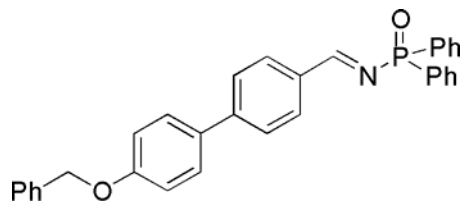


67b

***N*-(4-(4'-Benzyloxy-2'-fluorobiphenyl-methylidene))-*P,P*-diphenylphosphinamide (67b).**

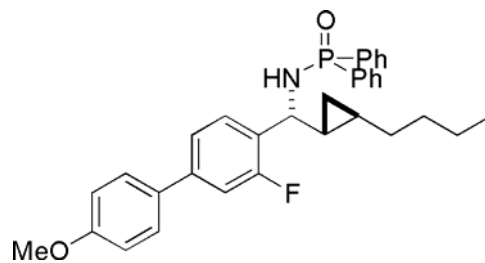
According to the general procedure G, 4'-benzyloxy-3-fluorobiphenyl-4-carbaldehyde (0.5 g, 1.6 mmol), diphenylphosphinamide (0.4 g, 1.6 mmol), TiCl₄ (0.1 mL, 1.3 mmol) and Et₃N (1.3 mL, 8.0 mmol), afforded **67b** (550 mg, 67%) as a colorless solid: m.p. 125-127 °C(EtOAc/hexanes); IR (KBr) 3034, 1604, 1436, 1253, 1202, 1126, 1024, 803, 731, 695 cm⁻¹; ¹H NMR (300MHz, CDCl₃) δ 9.63 (d, 1 H, *J* = 31.8 Hz), 8.25 (t, 1 H, *J* = 7.5 Hz), 7.96 (dd, 2 H, *J* = 10.2, 2.7 Hz), 7.57 (d, 4H, *J* = 8.4 Hz), 7.49-7.41 (m, 12 H), 7.08 (d, 2 H, *J* = 8.4 Hz), 5.13 (s, 2 H); ¹³C NMR (75MHz, CDCl₃) δ 167.0, 164.3 (d, *J* = 256.7 Hz), 159.6, 148.4 (d, *J* = 9.2 Hz), 136.6, 132.1,

131.8, 131.6, 131.5, 131.3, 129.0, 128.6 (d, $J = 6.4$ Hz), 128.4, 128.1, 127.4, 122.5, 115.5, 113.9 (d, $J = 20.1$), 70.1; MS (EI) 505 (M^{+} , 17), 366 (20), 332 (64), 91 (100); HRMS (EI) calcd for $C_{32}H_{25}FNO_2P$ 505.1607, found 505.1589.



67c

***N*-(4-(4'-Benzyloxy-biphenyl-methylidene))-*P,P*-diphenylphosphinamide (67c).** According to the general procedure G, $TiCl_4$ (0.1 mL, 0.8 mmol), 4'-Benzyloxybiphenyl-4-carbaldehyde (0.3 g, 1.0 mmol), diphenylphosphinamide (0.2 g, 1.0 mmol) and Et_3N (0.9 mL, 6.0 mmol) afforded **67c** (383 mg, 79%) as a colorless solid: m.p. 184.0-185.0 °C (EtOAc/hexanes); IR (KBr) 3448, 1621, 1599, 1438, 1202, 1189, 1124, 1107, 832, 819, 727 cm^{-1} ; 1H NMR (300MHz, $CDCl_3$) δ 9.34 (d, 1 H, $J = 32.0$ Hz), 8.05 (d, 1 H, $J = 7.6$ Hz), 7.97 (td, 2 H, $J = 10.3, 2.8$ Hz), 7.57 (d, 4H, $J = 8.4$ Hz), 7.49-7.41 (m, 12 H), 7.08 (d, 2 H, $J = 8.4$ Hz), 5.13 (s, 2 H); ^{13}C NMR (75MHz, $CDCl_3$) δ 159.1, 145.9, 136.6, 133.8, 132.4, 132.1, 131.7, 131.7, 131.6, 131.5, 130.7, 128.6, 128.5, 128.3, 128.0, 127.4, 126.9, 115.3, 70.0; MS (EI) 487 (M^{+} , 13), 202 (41), 91 (100); HRMS (EI) calcd for $C_{32}H_{26}NO_2P$ 487.1701 found 487.1694.



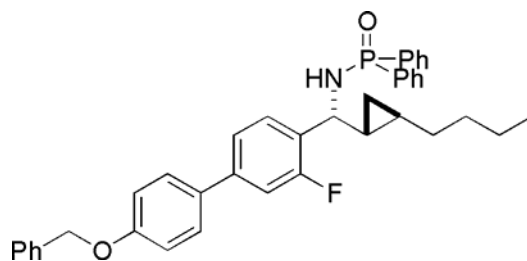
68a

***N*-(*R*^{*})-(((1*R*^{*},2*R*^{*})-2-Butylcyclopropyl)-(4'-methoxy-2-fluoro-4-(phenyl)phenyl)methyl)-**

***P,P*-diphenylphosphinamide (68a). General procedure H:** A literature procedure⁵² was used

with modifications. A suspension of Cp₂ZrHCl (0.2 g, 0.6 mmol) in freshly distilled dichloromethane (2.0 mL) was treated with 1-hexyne (0.1 mL, 0.6 mmol) and the mixture was heated in the Emrys Optimizer (Biotage) microwave (80 °C, 300W) for 1 min. The mixture was cooled to -78 °C, treated with Me₂Zn (2 M in toluene, 0.3 mL, 0.6 mmol), warmed to 0 °C and aldimine **67a** (0.1 g, 0.2 mmol) was added. The mixture was heated in the microwave (100 °C, 300 W) for 10 min. then cooled to r.t. and treated with diiodomethane (0.2 mL, 2.1 mmol) and left to stir at r.t. for 16 h. The mixture was then cooled to 0 °C and quenched by addition of absolute methanol (0.5 mL) with vigorous stirring, and after 5 min. diluted with EtOAc (100 mL). The solution was filtered through a pad of Florisil and concentrated in vacuo. The residue was chromatographed over SiO₂ (EtOAc/hexane 1:1 – 3:1) to afford **68a** (34 mg, 30%) as a colorless solid, m.p. 168.0-170.5 °C (EtOAc/hexanes); IR (KBr) 3201, 2925, 1609, 1492, 1436, 1252, 1186, 816, 697, 540 cm⁻¹; ¹H NMR (300MHz, CDCl₃) δ 7.92 – 7.85 (m, 2 H), 7.77 – 7.70 (m, 2 H), 7.48 (app d, 2 H, *J* = 8.8 Hz), 7.48 – 7.38 (m, 4H), 7.33 – 7.27 (m, 2 H), 7.21 (dd, 1 H, *J* = 7.9, 1.7 Hz), 7.16 (d, 1 H, *J* = 1.8 Hz), (app dd, 1 H, *J* = 7.5, 5.1 Hz), 6.97 (app d, 2 H, *J* = 8.8 Hz), 3.86 (s, 3 H), 3.62 (dd, 1 H, *J* = 9.6, 6.9 Hz), 1.35 – 1.25 (m, 6H), 1.17 – 1.11 (m, 2 H), 0.88 (t, 3 H, *J* = 6.9 Hz), 0.80 – 0.74 (m, 2 H), 0.40 (app dt, 1 H, *J* = 9.1, 4.8 Hz), 0.23 (app dt, 1

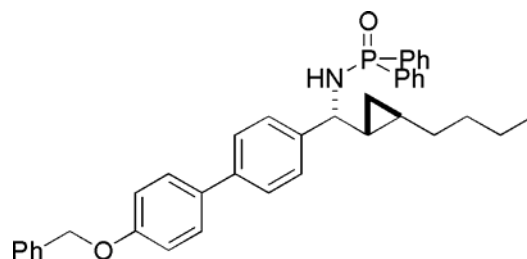
H, $J = 8.3, 5.1$); NMR (75MHz, CDCl_3) ^{13}C δ 162.3, 159.5, 159.0, 132.4, 132.3, 131.9, 131.8, 131.7, 131.5, 128.5, 128.3, 128.1, 127.9, 122.0, 114.3, 113.8, 113.5, 55.3, 55.1, 33.3, 31.7, 26.0, 22.5, 19.1, 14.0, 10.6; HRMS (MALDI) calcd for $\text{C}_{33}\text{H}_{36}\text{FNO}_2\text{P}$ 528.2468 $[\text{M}+\text{H}]^+$, found 528.2267.



68b

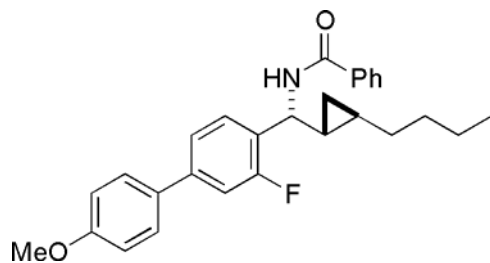
N-(R^*)-((($1R^*$, $2R^*$)-2-Butylcyclopropyl)-(4'-benzyloxy-2-fluoro-4-(phenyl)phenyl)methyl)-*P,P*-diphenylphosphinamide (**68b**). According to the general procedure H, Cp_2ZrHCl (0.4 g, 1.5 mmol), 1-hexyne (0.2 mL, 1.5 mmol), Me_2Zn (2 M in toluene, 0.7 mL, 1.5 mmol), aldimine **67b** (0.3 g, 0.5 mmol) and diiodomethane (0.4 mL, 4.9 mmol), afforded **68b** (200 mg, 68%) as a colorless solid: m.p. 171.8-173.0 °C (EtOAc/hexanes); IR (KBr) 3164, 2955, 2923, 2855, 1609, 1523, 1493, 1249, 1185, 1110, 1071, 822, 724, 695, 538 cm^{-1} ; ^1H NMR (300MHz, CDCl_3) δ 7.91 (d, 1 H, $J = 6.9$ Hz), 7.87 (d, 1 H, $J = 6.9$ Hz), 7.77 (d, 1 H, $J = 7.2$ Hz), 7.73 (d, 1 H, $J = 7.2$ Hz), 7.50 – 7.43 (m, 8H), 7.41 – 7.37 (m, 4H), 7.34 – 7.27 (m, 4H), 7.21 (app d, 1 H, $J = 8.1$ Hz), 7.15 (app d, 1 H, $J = 5,7$ Hz), 7.12 (s, NH), 7.05 (app d, 1 H, $J = 8.7$ Hz), 5.12 (s, 2 H), 3.86 (dd, 1 H, $J = 18.3, 9.4$ Hz), 3.62 (app t, 1 H, $J = 6.9$ Hz), 1.34 – 1.38 (m, 6H), 1.29 – 1.23 (m, 2 H), 1.19 – 1.11 (m, 2 H), 0.88 (t, 3 H, $J = 6.9$ Hz), 0.81 – 0.75 (m, 1 H), 0.41 (app dt, 1 H, $J = 9.0, 4.5$ Hz), 0.24 (app dt, 1 H, $J = 8.4, 5.1$); ^{13}C NMR (75MHz, CDCl_3) δ 162.1, 158.9, 158.6, 141.5, 136.7, 133.9, 132.9, 132.3, 132.2, 131.8, 131.7, 131.5, 131.2, 128.5, 128.3, 127.9, 127.4, 122.0, 115.1, 113.7, 113.4, 70.0, 55.0, 33.2, 26.0, 22.5, 19.1, 14.1, 10.5; MS (EI) 603 (M^+ , 56), 546

(14), 532 (25), 506 (16), 402 (9), 256 (12), 201 (52), 91 (100), 77 (14); HRMS (qTOF) calcd for $C_{39}H_{40}FNO_2P$ 604.2815 $[M+H]^+$, found 604.2815.



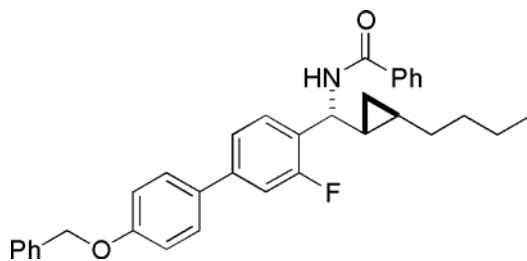
68c

N-(*R*^{*})-(((1*R*^{*},2*R*^{*})-2-Butylcyclopropyl)-(4'-benzyloxy-4-(phenyl)phenyl)methyl)-*P,P*-diphenylphosphinamide (**68c**). According to the general procedure H, Cp_2ZrHCl (0.3 g, 1.2 mmol), 1-hexyne (0.1 mL, 1.2 mmol), Me_2Zn (2 M in toluene, 0.6 mL, 1.2 mmol), aldimine **67c** (0.2 g, 0.4 mmol) and diiodomethane (0.3 mL, 4.0 mmol), afforded **68c** (100 mg, 40%) as a colorless solid: m.p. 154.0-156.0 °C (EtOAc/hexanes); IR (KBr) 3448, 3179, 2953, 2923, 2856, 1608, 1498, 1437, 1248, 1181, 1124, 1109, 817, 724, 695, 538 cm^{-1} ; 1H NMR (300MHz, $CDCl_3$) δ 7.95 – 7.89 (m, 2 H), 7.78 – 7.72 (m, 2 H), 7.51 – 7.34 (m, 12 H), 7.27 (d, 2 H, $J = 7.5$ Hz), 7.14 (d, 2 H, $J = 8.7$ Hz), 5.20 (s, 2 H), 3.90 – 3.87 (m, 1 H), 3.48 – 3.47 (m, 1 H), 1.32 – 1.27 (m, 6H), 1.21 (t, 3 H, $J = 7.1$ Hz), 1.14 – 1.12 (m, 2 H), 0.97 – 0.95 (m, 2 H), 0.84 (m, 1 H), 0.41 (app dt, 1 H, $J = 9.0, 4.7$ Hz), 0.25 (app dt, 1 H, $J = 8.4, 4.9$ Hz); ^{13}C NMR (75MHz, $CDCl_3$) δ 158.2, 139.4, 136.9, 133.6, 132.4, 132.3, 132.0, 131.9, 131.7, 131.6, 128.5, 128.3, 128.1, 128.0, 127.4, 127.2, 126.5, 115.1, 70.0, 33.2, 31.7, 26.8, 22.5, 19.0, 14.1; MS (EI) 585 (M^+ , 15), 514 (13), 501 (42), 384 (36), 201 (79), 91 (100); HRMS (qTOF) calcd for $C_{39}H_{40}NO_2P$ $[M+H]^+$ 586.2797, found 586.2875.



69a

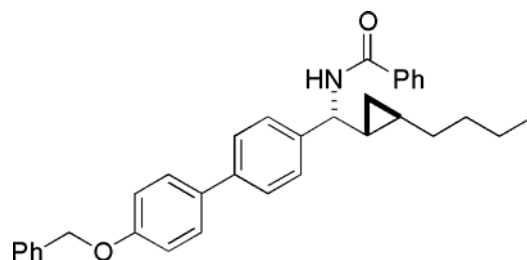
N-(*R*^{*})-(((1*R*^{*},2*R*^{*})-2-Butylcyclopropyl)-(4'-methoxy-2-fluoro-4-(phenyl)phenyl)methyl)-benzamide (**69a**), (30 mg, 61%) was obtained from **68a** following the literature procedure⁵² as a colorless solid: m.p. 158.0-160.5 °C (EtOAc/hexanes); IR (KBr) 3288, 2954, 2921, 2856, 1736, 1635, 1530, 1027, 818, 710, 695 cm⁻¹; ¹H NMR (300MHz, CDCl₃) δ 7.80 (app d, 2 H, *J* = 6.9 Hz), 7.53 – 7.41 (m, 6H), 7.36 (app t, 2 H, *J* = 7.8 Hz), 7.30 (d, 1 H, *J* = 1.8 Hz), 7.27 (app s, 1 H), 7.23 – 7.22 (m, 1 H), 6.97 (d, 2 H, *J* = 8.7 Hz), 6.84 (d, 1 H, *J* = 8.1 Hz), 4.73 (t, 1 H, *J* = 8.4 Hz), 3.85 (s, 3 H), 1.43-1.26 (m, 5 H), 1.24 – 1.09 (m, 1 H), 0.99– 0.90 (m, 1 H), 0.86 (t, 3 H, *J* = 6.9 Hz), 0.59 (app dt, 1 H, *J* = 9.0, 4.8 Hz), 0.36 (app dt, 1 H, *J* = 9.0, 5.1); ¹³C NMR (75MHz, CDCl₃) δ 166.4, 161.2 (d, *J* = 242.8 Hz), 142.0, 134.7, 132.1, 131.3, 129.4 (d, *J* = 6.8 Hz), 128.5, 128.0, 126.9, 122.3, 114.3, 114.0 (d, *J* = 22.4 Hz), 55.3, 54.5, 33.3, 31.8, 24.0, 22.3, 18.5, 14.0, 10.8; HRMS (MALDI) calcd for C₂₈H₃₀FNO₂Na 454.2158 [M+Na]⁺, found 454.1686.



69b

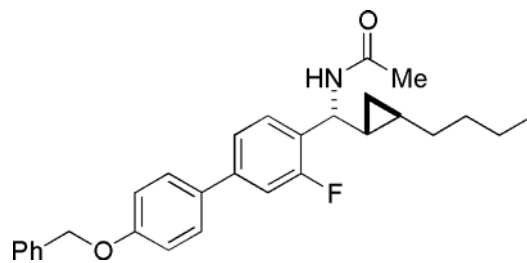
N-(*R*^{*})-(((1*R*^{*},2*R*^{*})-2-Butylcyclopropyl)-(4'-benzyloxy-2-fluoro-4-(phenyl)phenyl)methyl)-benzamide (**69b**), (35 mg, 57%) was obtained from **68b** following the literature procedure⁵² as a colorless solid: m.p. 144.0-146.0 °C (EtOAc/hexanes); IR (KBr) 3295, 2922, 1736, 1634, 1365,

1025, 822, 697 cm^{-1} ; ^1H NMR (400MHz, CDCl_3) δ 7.79 (app d, 2 H, $J = 7.6$ Hz), 7.51 – 7.26 (m, 12 H), 7.03 (app d, 2 H, $J = 8.0$ Hz), 6.80 (d, 2 H, $J = 7.6$ Hz), 5.11 (s, 2 H), 4.73 (app t, 1 H, $J = 8.8$ Hz), 1.36 – 1.32 (m, 6H), 1.18– 1.13 (m, 1 H), 0.93 – 0.91 (m, 2 H), 0.86 (t, 3 H, $J = 6.8$ Hz), 0.59 (app dt, 1 H, $J = 9.6, 4.8$ Hz), 0.36 (app dt, 1 H, $J = 9.2, 5.1$ Hz); ^{13}C NMR (100 MHz, CDCl_3) 166.9, 158.9, 137.0, 134.8, 131.732, 129.7, 129.6, 128.9, 128.8, 128.3, 127.7, 127.1, 122.6, 115.4, 114.2 (d, $J = 24.3$ Hz), 70.3, 54.9, 33.6, 32.1, 29.9, 24.2, 22.7, 18.8, 14.3, 11.2; MS (EI) 507 (M^+ , 21), 423 (17), 332 (16), 105 (100), 91 (84); HRMS (EI) calcd for $\text{C}_{34}\text{H}_{34}\text{FNO}_2$ 507.2574 found 507.2591.



69c

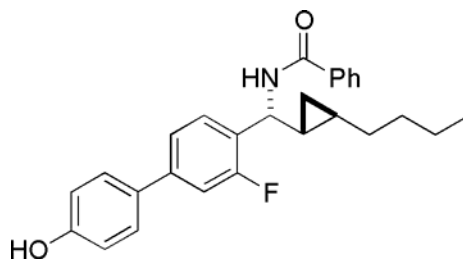
***N*-(*R*^{*})-(((*1R*^{*},*2R*^{*})-2-Butylcyclopropyl)-(4'-benzyloxy-4-(phenyl)phenyl)methyl)benzamide (69c)**, (13 mg, 22%) was obtained from **68c** following the literature procedure⁵² as a colorless solid: m.p. 141.0-143.5 °C (EtOAc/hexanes); IR (KBr) 3293, 2954, 2919, 2855, 1630, 1499.5, 1254, 1169, 1084 cm^{-1} ; ^1H NMR (300MHz, CDCl_3) δ 7.81 (d, 2 H, $J = 7.3$ Hz), 7.51 – 7.45 (m, 8H), 7.41 (d, 2 H, $J = 7.2$ Hz), 7.37 – 7.33 (m, 2 H), 7.04 (d, 2 H, $J = 8.4$ Hz), 6.50 (d, 1 H, $J = 7.5$ Hz), 5.11 (s, 2 H), 4.70 (app t, 1 H, $J = 8.4$ Hz), 1.43-1.31 (m, 8H), 1.03 – 0.95 (m, 2 H), 0.85 (t, 3 H, $J = 6.9$ Hz), 0.64 (app dt, 1 H, $J = 8.7, 5.1$ Hz), 0.49 (app dt, 1 H, $J = 9.3, 4.8$); Insufficient amount of material to obtain ^{13}C NMR; MS (EI) 489 (M^+ , 79), 405 (76), 368 (76), 314 (93), 277 (74), 106 (85), 92 (72), 77 (100); HRMS (EI) calcd for $\text{C}_{34}\text{H}_{35}\text{NO}_2$ 489.2668 found 489.2646.



69d

***N*-(*R*^{*})-(((1*R*^{*},2*R*^{*})-2-Butylcyclopropyl)-(4'-benzyloxy-2-fluoro-4-**

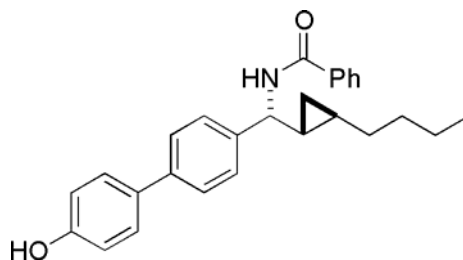
(phenyl)phenyl)methyl)acetamide (69d), (40 mg, 75%) was obtained from **68b** following the literature procedure⁵² as a colorless solid: m.p. 186.0-188.0 °C (EtOAc/hexanes); IR (KBr) 3293, 2923, 1631, 1529, 1254, 1025, 825, 694 cm⁻¹; ¹H NMR (300MHz, CDCl₃) δ 7.81 (app d, 2 H, *J* = 6.9 Hz), 7.54 – 7.44 (m, 10H), 7.41 (app d, 2 H, *J* = 6.9 Hz), 7.37 – 7.33 (m, 2 H), 7.04 (d, 2 H, *J* = 8.7 Hz), 6.52 (d, 1 H, *J* = 7.8 Hz), 5.12 (s, 2 H), 4.71 (app t, 1 H, *J* = 8.4 Hz), 2.17 (s, 3 H), 1.44 – 1.26 (m, 6H), 1.23 – 1.19 (m, 1 H), 1.06 – 0.95 (m, 2 H), 0.86 (t, 3 H, *J* = 6.6 Hz), 0.64 (app dt, 1 H, *J* = 9.6, 4.8 Hz), 0.48 (app dt, 1 H, *J* = 9.2, 5.1 Hz); ¹³C NMR (75MHz, CDCl₃) δ 166.6, 158.4, 140.5, 139.8, 137.0, 134.8, 133.7, 131.4, 128.5, 128.0, 127.9, 127.4, 127.1, 126.9, 126.8, 115.2, 70.1, 57.0, 33.4, 31.8, 30.8, 24.4, 22.4, 17.9, 14.0, 11.4; HRMS (MALDI) calcd for C₂₉H₃₃FNO₂ 446.2489 [M+H]⁺, found 446.2247.



70b

***N*-(*R*^{*})-(((1*R*^{*}, 2*R*^{*})-2-Butylcyclopropyl)-(4'-hydroxy-2-fluoro-4-(phenyl)phenyl)methyl)-benzamide (70b). Benzyl ether deprotection. General procedure I: According to the**

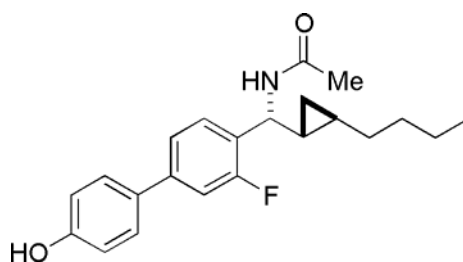
literature procedure⁸¹ with some modifications, biphenyl *C*-cyclopropylalkylamide **69b** (0.04 g, 0.07 mmol) was dissolved, under N₂ atmosphere at r.t. in a round bottom flask (25 mL), in 1:1 mixture of absolute MeOH and freshly distilled THF (5mL). The flask was evacuated three times and fitted with a balloon of H₂ gas (1 atm). Pd(OH)₂ (20% w/w) on carbon (0.03 g) was added as solid. The reaction mixture was left to stir under a continuous H₂ atmosphere at r.t. for 16h. The mixture was concentrated and loaded directly onto a SiO₂ column (1:1 EtOAc/hexanes) to afford **70b** (20 mg, 69%) as a colorless solid: m.p. 184-186 °C (EtOAc/hexanes); IR (KBr) 3398, 2923, 1686, 1611, 1527, 1491, 1279, 1174, 708 cm⁻¹; ¹H NMR (400MHz, CDCl₃) (mixture of diastereomers 6:1, major diastereomer is presented) δ 8.25 (d, 1 H, *J* = 5.1 Hz), 7.97 (d, 2 H, *J* = 5.1 Hz), 7.68 (app t, 1 H, *J* = 5.4 Hz), 7.64 – 7.59 (m, 3 H), 7.40 (app t, 1 H, *J* = 6 Hz), 7.34 (d, 2 H, *J* = 6.3 Hz), 7.24 – 7.23 (m, 1 H), 7.07 (d, 1 H, *J* = 5.7 Hz), 6.77 (d, 2 H, *J* = 6.6 Hz), 4.82 (t, 1 H, *J* = 6.3 Hz), 1.53 – 1.45 (m, 6H), 1.36 – 1.32 (m, 2 H), 1.28 – 1.25 (m, 2 H), 1.02 (t, 3 H, *J* = 5.7 Hz), 0.76 (dt, 1 H, *J* = 6.6, 3.3 Hz), 0.52 (dt, 1 H, *J* = 6.3, 4.2 Hz); ¹³C NMR (100 MHz, CDCl₃) δ 167.4, 161.2 (d, *J* = 244.8 Hz), 142.4 (d, *J* = 8.4 Hz), 134.2, 133.9, 132.1, 131.2, 130.4, 129.2, 128.8, 128.2, 127.2, 126.4 (d, *J* = 12.3 Hz), 122.4, 116.0, 113.9 (d, *J* = 22.1 Hz), 55.3, 33.5, 32.1, 23.9, 22.7, 18.8, 14.3, 11.0; MS (API-ES) 440 ([M+Na]⁺, 53), 418 ([M+H]⁺, 25), 297 (100), 227 (15), 201 (43); HRMS (MALDI) calcd for C₂₇H₂₉FNO₂ 418.2182 [M+H]⁺, found 418.2062.



70c

***N*-(*R*^{*})-(((1*R*^{*},2*R*^{*})-2-Butylcyclopropyl)-(4'-hydroxy-4-(phenyl)phenyl)methyl)-benzamide**

(70c). According to the general procedure I, **70c** (5 mg, 92%) was obtained from **69d** as a colorless solid: m.p. 162.0-164.0 °C (EtOAc/hexanes); IR (KBr) 3269, 2954, 2923, 2853, 1611, 1572, 1527, 1500, 1491, 1274, 1209, 1175, 813, 717 cm⁻¹; ¹H NMR (400MHz, CDCl₃) δ 7.82 (d, 2 H, *J* = 8.0 Hz), 7.52 (app d, 2 H, *J* = 7.6 Hz), 7.48 – 7.41 (m 7H), 7.35 (d, 2 H, *J* = 8.0 Hz), 6.77 (d, 2 H, *J* = 8.0 Hz), 6.59 (app d, 1 H, *J* = 7.6 Hz), 4.65 (t, 1 H, *J* = 8.4 Hz), 1.37 – 1.30 (m, 5H), 1.03 – 0.98 (m, 2 H), 0.86 (t, 3 H, *J* = 7.2 Hz), 0.64 (dt, 1 H, *J* = 9.2, 4.8 Hz), 0.47 (dt, 1 H, *J* = 8.4, 5.2 Hz); ¹³C NMR (100MHz, CDCl₃) 166.9, 155.4, 140.2, 139.9, 134.5, 133.3, 133.2, 131.6, 128.7, 128.2, 127.7, 126.9, 126.8, 115.6, 58.0, 33.4, 31.9, 24.5, 22.5, 18.0, 14.1, 11.3; MS (APCI) 400 ([M+H]⁺, 100); (MALDI) calcd for C₂₇H₂₉NO₂ 400.2271 [M+H]⁺, found 400.1815.



70d

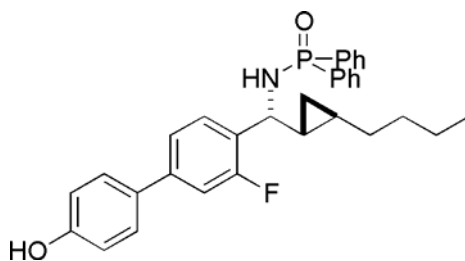
***N*-(*R*^{*})-(((1*R*^{*},2*R*^{*})-2-Butylcyclopropyl)-(4'-hydroxy-2-fluoro-4-(phenyl)phenyl)methyl)-**

acetamide (70d). According to the general procedure I, **70d** (15 mg, 94%) was obtained from

69d as a colorless solid: m.p. 196.0-198.0 °C (EtOAc/hexanes); IR (KBr) 2955, 2927, 2850,

1706, 1679, 1518, 1448, 1205, 1117, 1089, 905, 822, 795 cm⁻¹; ¹H NMR (300MHz, CDCl₃) δ

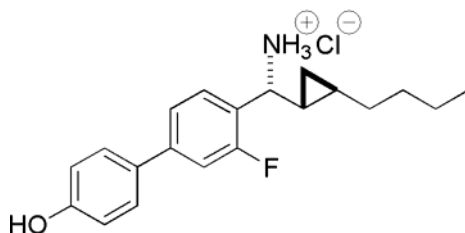
8.59 (s, 1 H), 7.66 (d, 1 H, $J = 8.0$ Hz), 7.50 (dd, 4H, $J = 8.5, 2.8$ Hz), 7.36 (d, 1 H, $J = 8.1$ Hz), 6.91 (d, 1 H, $J = 8.6$ Hz), 4.74 (t, 1 H, $J = 8.4$ Hz), 2.87 (s, 3 H), 1.39 – 1.27 (m, 5H), 1.25-1.15 (m, 2 H), 1.05 – 0.95 (m, 2 H), 0.88 (t, 3 H, $J = 6.8$ Hz), 0.50 (dt, 1 H, $J = 8.8, 4.6$ Hz), 0.25 (dt, 1 H, $J = 8.4, 4.9$ Hz); ^{13}C NMR (75MHz, CDCl_3) δ 170.0, 161.8 (d, $J = 350.3$ Hz), 159.4, 143.7, 132.6, 130.8 (d, $J = 6.2$ Hz), 129.8, 123.7, 117.6, 114.7 (d, $J = 22.4$ Hz), 52.7, 35.1, 33.3, 25.8, 24.0, 23.9, 19.7, 15.4, 11.7; MS (APCI) 356 ($[\text{M}+\text{H}]^+$, 100); HRMS (MALDI) calcd for $\text{C}_{22}\text{H}_{26}\text{FNO}_2\text{Na}$ 378.1845 $[\text{M}+\text{Na}]^+$, found 378.2202.



71

***N*-(*R*^{*})-(((1*R*^{*},2*R*^{*})-2-Butylcyclopropyl)-(4'-hydroxy-2-fluoro-4-(phenyl)phenyl)methyl)-*P,P*-diphenylphosphinamide (71).** According to the general procedure I, **71** (40 mg, 0.08 mmol, 80%) was obtained from *C*-cyclopropylalkyl diphenylphosphinamide **68b** (0.1 g, 0.1 mmol) as a colorless solid: m. p. 134.0-136.0 °C (EtOAc/hexanes); ^1H NMR (300MHz, CDCl_3) δ 8.00 – 7.89 (m, 4H), 7.57 – 7.46 (m, 6H), (d, 2 H, $J = 8.6$ Hz), 7.10 (app dd, 1 H, $J = 7.8, 1.8$ Hz), 7.06 (d, 1 H, $J = 1.5$ Hz), 6.98 (app dd, 1 H, $J = 7.8, 1.5$ Hz), 6.67 (app d, 2 H, $J = 8.7$ Hz), 3.87 (dd, 1 H, $J = 10.5, 6.9$ Hz), 3.63 (dd, 1 H, $J = 18.2, 8.5$ Hz), 1.47-1.30 (m, 5H), 1.27 – 1.18 (m, 1 H), 1.16 – 1.08 (m, 2 H), 0.95 (t, 3 H, $J = 6.9$ Hz), 0.62 – 0.56 (m, 1 H), 0.33 (app dt, 1 H, $J = 9.6, 6.6$ Hz), 0.23 (app dt, 1 H, $J = 8.4, 5.1$); ^{13}C NMR (75MHz, CDCl_3) δ 160.6 (d, $J = 242.9$ Hz), 162.2, 158.9, 157.7, 142.1, 133.4, 132.7 (d, $J = 9.3$ Hz), 132.1, 131.9, 131.8, 130.1 (d, $J = 19.0$ Hz), 128.7, 128.5, 127.8, 127.6, 121.9, 115.9, 113.2 (d, $J = 22.6$ Hz), 55.9, 33.4, 32.0, 26.1, 22.6,

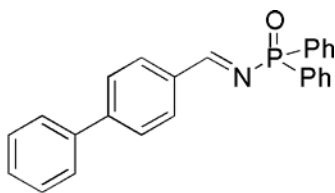
19.2, 14.1, 10.4; MS (EI) 513 (M^+ , 40), 470 (10), 456 (18), 442 (32), 429 (26), 416 (59), 312 (21), 256 (25), 201 (100); HRMS (EI) calcd for $C_{32}H_{33}FNO_2P$ 513.2233 found 513.2219.



72

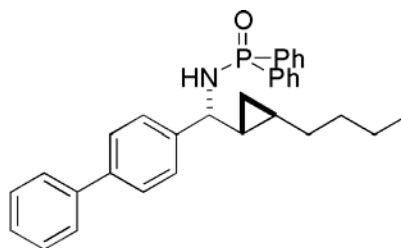
***N*-(*R*^{*})-(((1*R*^{*},2*R*^{*})-2-Butylcyclopropyl)-(4'-hydroxy-2-fluoro-4-**

(phenyl)phenyl)methyl)amine hydrochloride (72), (8 mg, 43%) was obtained following the literature procedure⁵² for removal of diphenylphosphine protecting group and recrystallization as chloride salt from EtOH/ether, as a colorless solid: m.p. 147.5-149.0 °C (EtOH/diethyl ether); IR (KBr) 3432, 2927, 2365, 2346, 1499, 1265, 1208, 1036, 824, 731, 562 cm^{-1} ; 1H NMR (300MHz, CD_3OD) δ 7.49 – 7.44 (m, 3 H), 7.42 (app s, 1 H), 7.37 (app s, 1 H), 7.33 (app s, 1 H), 6.81 (d, 2 H, $J = 8.7$ Hz), 3.84 (app d, 1 H, $J = 9.9$ Hz), 1.51 – 1.33 (m, 6H), 1.28 – 1.20 (m, 2 H), 1.17 – 1.11 (m, 2 H), 0.88 (t, 3 H, $J = 6.9$ Hz), 0.52 (dt, 1 H, $J = 9.3, 4.8$ Hz), 0.41 (dt, 1 H, $J = 9.3, 5.1$ Hz); ^{13}C NMR (75MHz, CD_3OD) δ 161.8 (d, $J = 244.1$ Hz), 159.0, 145.7 (d, $J = 7.4$ Hz), 133.7, 131.1, 129.8, 129.0, 123.7, 122.5 (d, $J = 14.6$ Hz), 116.8, 114.4 (d, $J = 22.7$), 55.2, 34.0, 32.4, 23.5, 22.3, 20.4, 14.2, 11.3; (MALDI) calcd for $C_{20}H_{25}FNO$ 314.1914 $[M+H]^+$, found 314.1841.



74

***N*-[4-(Phenyl)phenylmethylidene]-*P,P*-diphenylphosphinamide (74).**⁵² According to the general procedure H, TiCl_4 (0.2 mL, 1.6 mmol), biphenyl-4-carbaldehyde (0.4 g, 2.0 mmol), diphenylphosphinamide (0.4 g, 2.0 mmol) and Et_3N (1.7 mL, 12 mmol) afforded **74** (430 mg, 56%) as a colorless solid: $^1\text{H NMR}$ (300MHz) δ 9.37 (d, 1 H, $J = 31.9$ Hz), 8.10 (d, 2 H, $J = 8.3$ Hz), 8.01-7.93 (m, 4H), 7.74 (d, 2 H, $J = 8.3$ Hz), 7.68-7.63 (m, 2 H), 7.69-7.61 (m, 9H).



75

***N*-(*R**)-(((1*R**,2*R**)-2-Butylcyclopropyl)-(4-(phenyl)phenyl)methyl)-*P,P*-diphenylphosphinamide (75).**⁵² According to the general procedure H, Cp_2ZrHCl (0.3 g, 1.2 mmol), 1-hexyne (0.1 mL, 1.2 mmol), Me_2Zn (2 M in toluene, 0.6 mL, 1.2 mmol), aldimine **74** (0.2 g, 0.4 mmol) and diiodomethane (0.3 mL, 4.0 mmol), afforded **75** (70 mg, 36%) as a colorless solid: $^1\text{H NMR}$ (300MHz) δ 7.94 – 7.88 (m, 2 H), 7.78 – 7.72 (m, 2 H), 7.57 (d, 2 H, $J = 7.8$ Hz), 7.50 – 7.41 (m, 8H), 7.37 (app d, 2 H, $J = 6\text{Hz}$), 7.31 (d, 2 H, $J = 8.1$ Hz), 3.62 (dd, 1 H, $J = 18.0, 9.9$ Hz), 3.39 – 3.35 (m, 1 H), 1.31 – 1.26 (m, 4 H), 1.21 (t, 3 H, $J = 6.9$ Hz), 1.11 – 0.97 (m, 2 H), 0.88 – 0.81 (m, 2 H), 0.77 – 0.71 (m, 1 H), 0.41 (app dt, 1 H, $J = 8.4, 4.8$ Hz), 0.25 (app dt, 1 H, $J = 9.6, 5.1$).

5.2. Biology

5.2.1. Plasmids and Transient Transfection Assays

The CMV-ER α , ERE-tk-Luc, and CMV- β -gal plasmids were provided by Dr. Ron Evans at the Salk Institute. HEK293 cells were plated in 48-well plates with DMEM medium containing 10% FBS and allowed to attach and grow for 48h. They were then transfected with the plasmids entrained in *N*-[1-(2,3-dioleoyloxy)propyl]-*N,N,N*-trimethylammonium methylsulfate (DOTAP) (Roche) at a density of 10,000 cells per well.^{15,23} The liposomes contained 1.0 μ g of reporter plasmid (ERE-tk-Luc), 0.5 μ g of CMV-ER α , and 0.5 μ g of the transfection control (CMV- β -gal) per well. Plasmids were premixed in PBS and mixed with DOTAP. Cells were treated with transfection mixture in serum- and phenol red-free DMEM. After 4h, the medium was replaced with DMEM containing 10% FBS. Twenty-four hours later, the medium was changed to DMEM containing 10% dextran-coated charcoal-stripped FBS and test chemicals were added. After 24h in the presence of test agent, cells were lysed and assayed for luciferase and β -galactosidase activities. Transfections were performed in triplicate, and each experiment was repeated at least twice.

5.2.2. Luciferase Assay

The medium was removed and cell monolayers were frozen at -80°C . After 30 min, 150 μ L of cell culture lysis reagent was added to each well and incubated at 4 oC for an additional 30 min.

Luciferase assay reagents were prepared as described previously.^{53,54} Cell extracts were clarified by centrifugation for 3 min at 3000 rpm at room temperature and supernatants were transferred to 96-well assay plates. For each assay, 50µL of supernatant was mixed with 50µL of luciferase assay buffer. Luminescence was read using a Victor luminometer. Luciferase activity was normalized to β-galactosidase activity and data was calculated as fold of induction as compared to vehicle control (DMSO, 0.1% final volume).

5.2.3. Antagonism

Antagonism in the luciferase assay was calculated using the following formula

$$\% \text{ Inhibition} = [100 - ((L + E2) / (E2))] \times 100$$

where L+E2 represents normalized luciferase activity (using β-Gal as the internal control) in cells treated simultaneously with E2 and the test compounds, and E2 the normalized luciferase activity in cells treated with E2 alone. GraphPad Prism 4 software was used for constructing dose-response curves and calculating IC₅₀s. IC₅₀s were estimated from dose-dependence curves that best fit the data obtained as an average from at least two transfections performed in triplicate.

5.2.4. Antiproliferative Assays

MCF-7 ERα positive breast cancer cells were plated in 96-well plates at 4000 cells/well in phenol red-free RPMI-1640 containing 10% dextran-coated charcoal-stripped FBS and 1nM E2, and allowed to attach for 24h. The cells were incubated in the presence of test compounds (at

concentrations ranging from 25pM to 50 μ M) and 1nM E2 for 6 days. Cell density was determined by the 3-(4,5-dimethylthiazol-2-yl)-5-(3-carboxymethoxyphenyl)-2-(4-sulfophenyl)-2H-tetrazolium (MTS) dye reduction assay using phenazine methanesulfonate as the electron acceptor as described previously. Absorbance was measured at 490nm minus that at 630nm 2h after incubation with the reagents. Data represents the average of at least two independent experiments done in quadruplicate. E2-stimulated growth of MCF-7 cells at day 6 was set to 100% growth.

MDA-MB231 ER α negative cells were plated in 96-well plates at 1000 cells/well and allowed to attach to the plastic for 72 h in phenol red-free RPMI-1640 containing 10% FBS. Test agents and control compounds (colchicine and TAM) were added over the range of 3.2nM–50 μ M and cells were incubated for 72h. Cell density was determined with the MTS assay. GraphPad Prism 4 software was used for constructing dose-response curves and calculating GI50 values. GI50 values were estimated from dose-dependence curves that best fit the data.

5.2.5. ER Competitor Assays

The ER α and ER β competitor assays were performed according to manufacturer's recommendations (PanveraTM) with some modifications. The assay was performed in 384-well, nonbinding, square, black-bottom black plates (Costar) in a total volume of 40 μ L per well. Fluorescence polarization was measured using an AnalystTM AD & HT Assay Detection Systems (Molecular Devices) fluorescence plate reader. The instrumental set up was validated using serial dilutions (100nM to 1pM) of methylfluorescein (Sigma) in the assay buffer. The G value, a

correction factor that accounts for differences in the instrument optical system geometry and plate well size and geometry, was calcd and found to be 1 for the 384-well plates and fluorescence polarization used. The "Z" height for detection was empirically determined to be optimally 1.25 mm for 40 μ L total volume per well in 384-well plates. Fluorescence was measured in the perpendicular and horizontal dimensions with 485 nm excitation and 530 nm emission interference filters with the appropriate FL505 dichroic mirror. Recombinant human estrogen receptor (ER) was used at the recommended concentration of 15 nM, and Fluormone™ ES2 was used at 1 nM in the final mixture. The needed volume of 2X concentration of ER α complexed with Fluormone™ ES2 (ER/ES2) was prepared on ice and distributed in 20 μ L/well. The 70 library members and controls (raloxifene and tamoxifen) were prepared at three concentrations (10, 2 and 0.4 μ M) in the assay buffer. The dilutions of test compounds were added to the plate in 20 μ L/well. Final concentrations of the test compounds were 5, 1 and 0.2 μ M. Each compound concentration was tested in duplicate. 17 β -Estradiol at 1 μ M served as a positive control. Fluorescence polarization was calcd after background subtraction from perpendicular and horizontal fluorescence measurements with the Analyst™ AD & HT Assay Detection Systems integrated software. Fluorescence polarization is described in dimensionless mP values that are calcd using the following formula: $mP = 1000 \times (S - G \times P) / (S + G \times P)$, where S = fluorescence counts after background subtraction measured in the parallel plane, P = fluorescence counts after background subtraction measured perpendicular plane, G = calibrated correction value. Average mP values for duplicate measurements were used to calculate percent competition for test compounds as compared to mP value of 1 μ M 17 β -estradiol. The percent competition was calcd by the following formula: $\% I = [(mP_0 - mP) / (mP_0 - mP_{100})] \times 100$, where mP₀ is mP value for 0% competition as referred to high polarization of fluorescently

labeled estradiol complexed to ER α (ER/ES2 complex); mP100 is mP value for 100% competition, as referred to low polarization in presence of 1 μ M E2; and mP is fluorescence polarization in the presence of test compound. Percent competition was calcd for each compound in three concentrations. Compounds that showed 50% or higher competition at 0.2 μ M and also showed concentration dependence in their effects were identified as competitors and were considered positive hits in the screening of the library.

5.2.6. Docking in CAChe

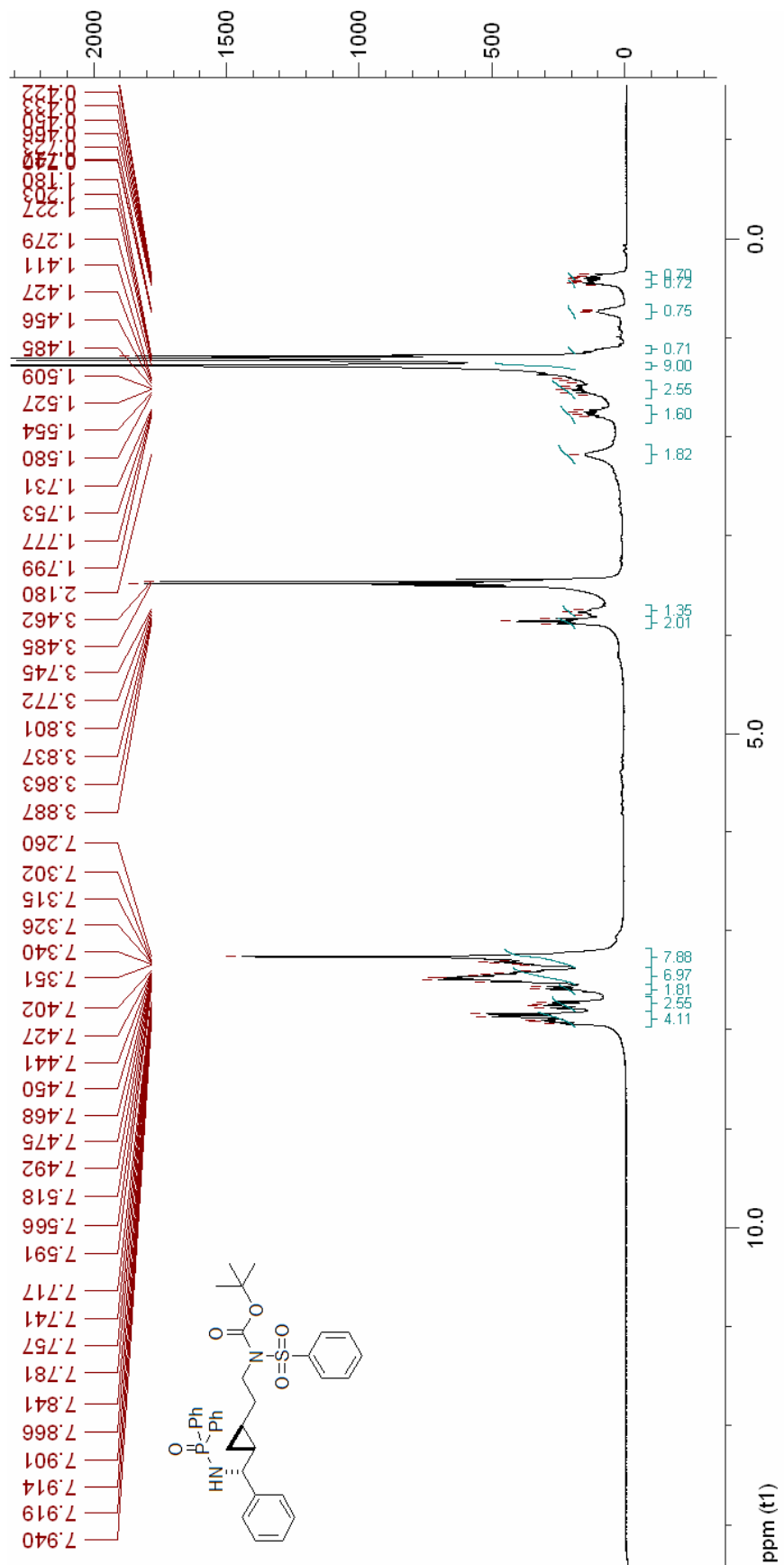
When the protein-ligand crystal structure of interest is downloaded from the PDB Databank it needs to be processed before any docking studies. The detailed protocol for this process follows the guidance of the software manufacturer with some details highlighted in the example of the GEN-ER β -LBD crystal structure. The 1QKM crystal structure GEN-ER β -LBD was uploaded using BioMedCACHe and atoms were locked at their crystallographic positions in space. The bonding in the HET groups was checked and corrected by displaying the protein chain, ER β -LBD, and the ligand in different colors. Genistein (GEN) was selected and bonding and charge were examined to check the accuracy of the genistein structure. The tool “beautify valence” was used to assign adequate hydrogen atoms, electrons and the atom hybridization. The next step is to balance the charge in the protein. Depending upon its environment in a protein crystal, the histidine residue can be neutral or protonated. When CACHe reads a PDB file, the histidine is assumed to be neutral unless a charge has been specified in the PDB file. Therefore, the histidines need to be protonated.⁸² ND1 (nitrogen atoms) atoms are found and changed to the +1 charge. After the entire protein molecule is selected and the “beautify valence” tool is applied,

hydrogen atoms, electrons and hybridization are added to the protein and water molecules. The total number of atoms changes. After this step, the H-bonds are subjected to “beautify H-bonds”. Hydrogen atoms in hydroxyl groups and water molecules are rotated to maximize hydrogen bonding. Only the geometry of the hydrogen atoms are changed with these “beautify” commands. When the “analyze sequence” tool is used, the ligand can be selected, and then, by using the “select neighbor” tool, the pocket around the ligand is defined. Usually the selection is 5Å. The following amino acid residues in 1QKM were selected by this tool: M295, L298, T299, L301, A302, E305, W335, M336, L339, M340, L343, R346, F356, I373, I376, F377, L380, G472, H475, L476, L477, M479, V484, V487. Once the pocket was defined and noted, the ligand GEN was selected and deleted from this structure, and the ER β -LBD was saved. Docking in BioMedCACHe used the “FastDock” algorithm. In the present work the ligand was allowed to be flexible and protein was kept rigid. The scoring function was PMF and the genetic algorithm parameters used for each run were as follows: population size = 1000 and maximal generations between 10000 and 25000. Docking scores of compared ligands were obtained under identical conditions. It is worth noting that these numbers can serve only for comparison between ligands docked under same conditions into the same binding site and should be taken as relative measure. Before newly synthesized or otherwise interesting compounds were docked, as a standard the original ligand from the crystal structure, like GEN in the presented case above, was minimized by MM3 and then re-docked back into the pocket. The same orientation and hydrogen bonding to key residues were reproduced as compared to the crystal structure. Usually this procedure was repeated multiple times to assure reproducibility. Then the test ligand was superimposed to GEN and this was the starting point for docking. GEN was removed and the test ligand docked into GEN pocket.

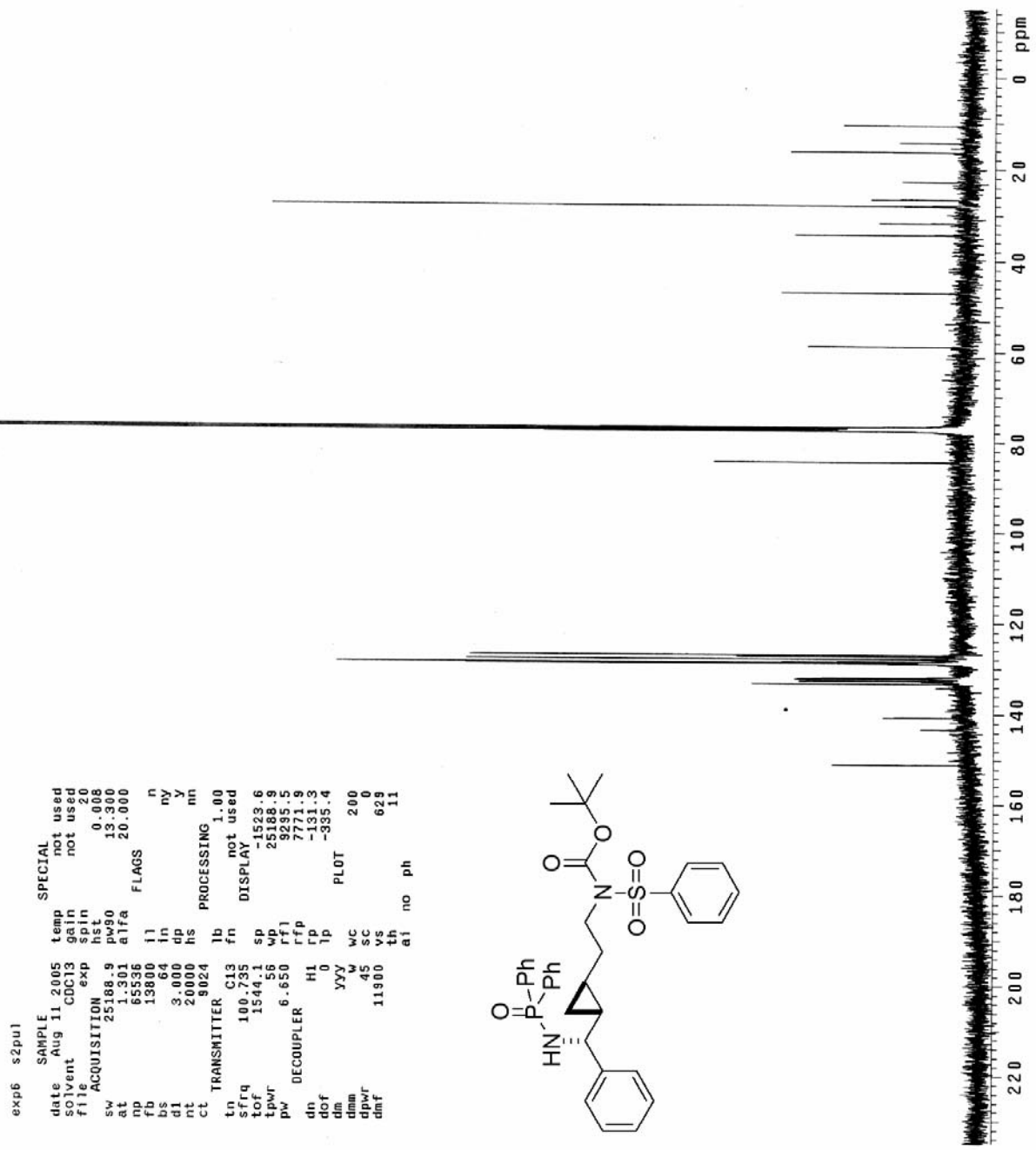
6. Appendix

^1H and ^{13}C NMR data for the key intermediates and biologically active final compounds.

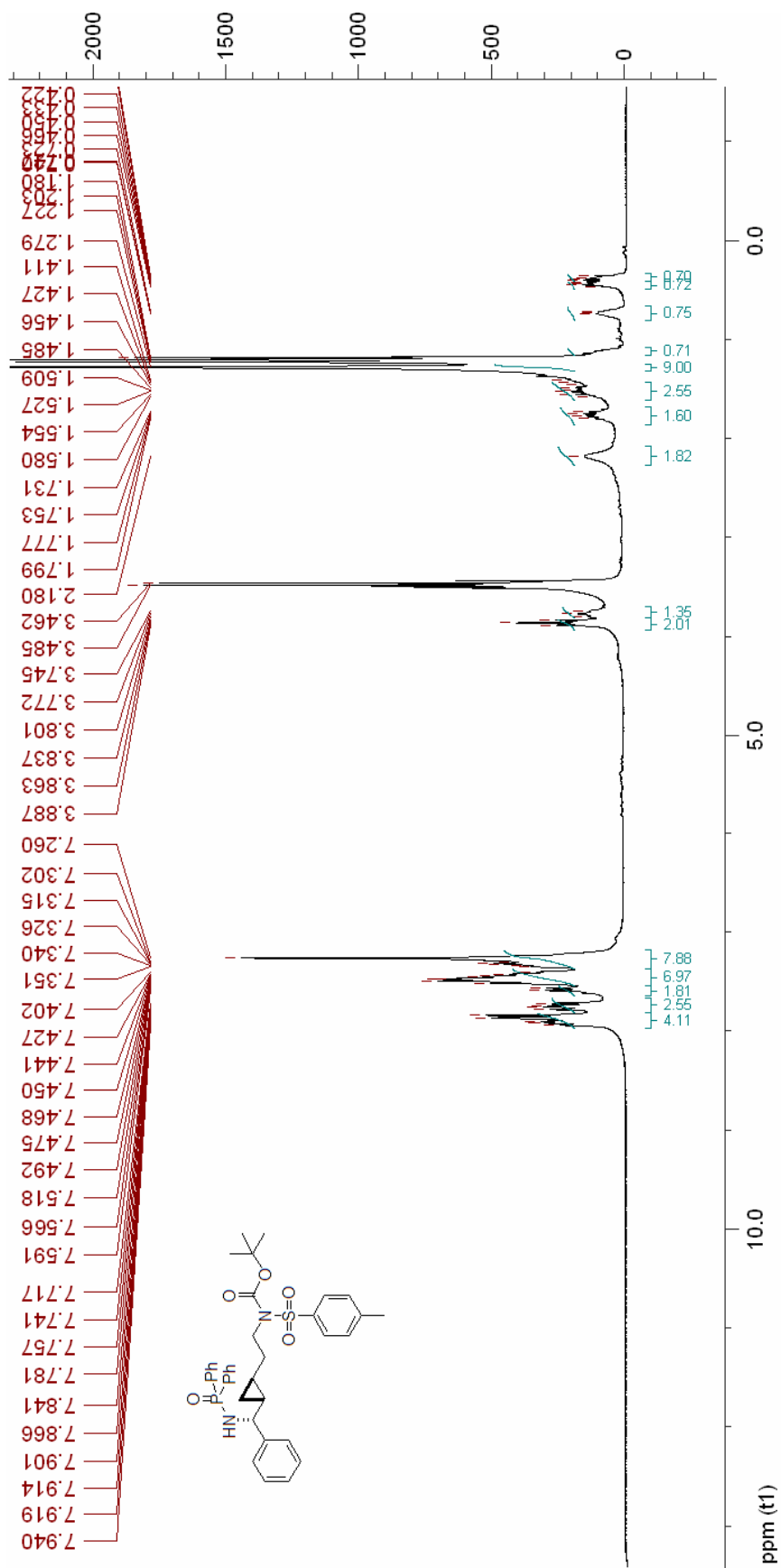
48a ¹H NMR, 300MHz, Bruker, CDCl₃



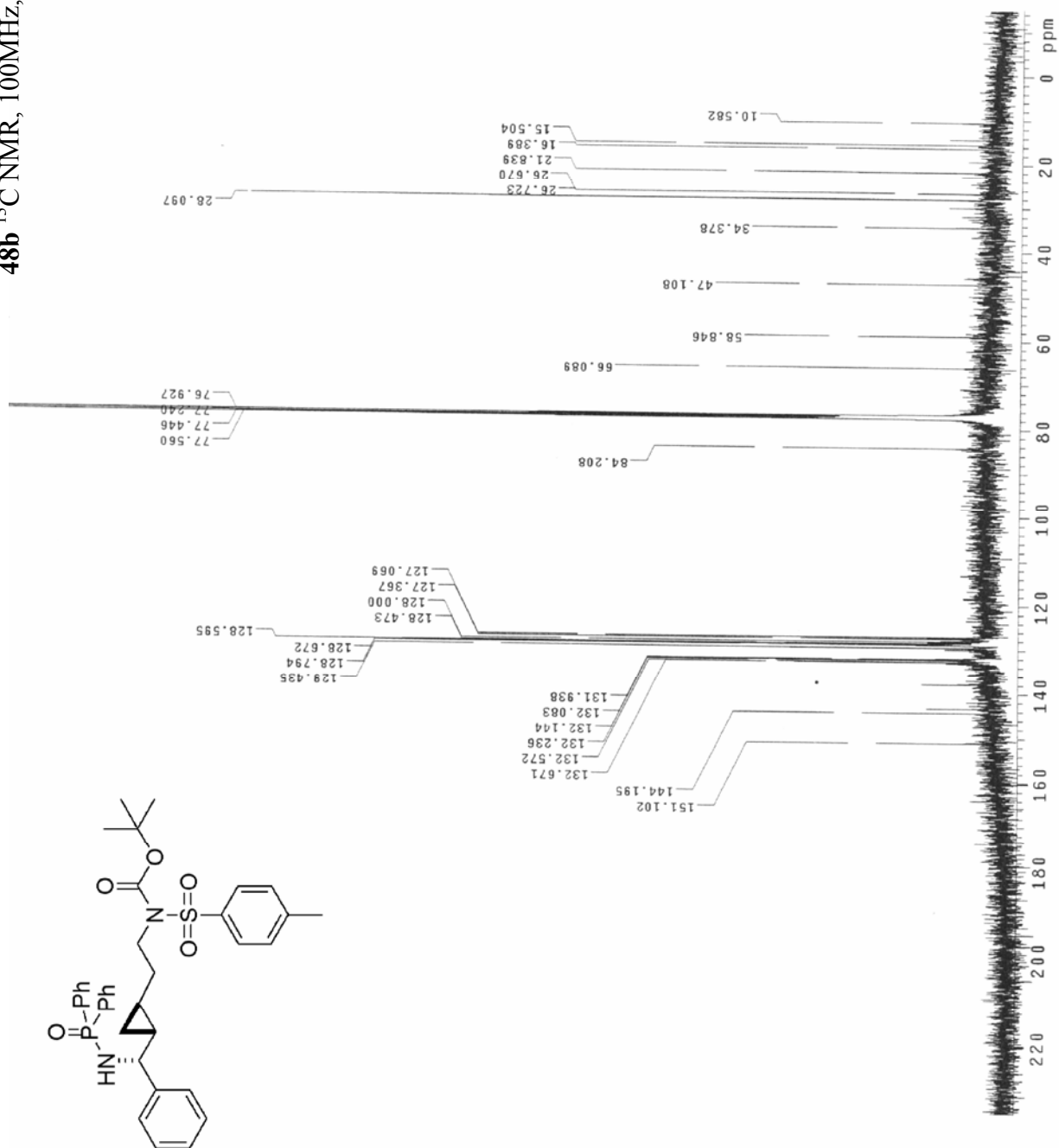
48a ¹³C NMR, 100MHz, Varian, CDCl₃



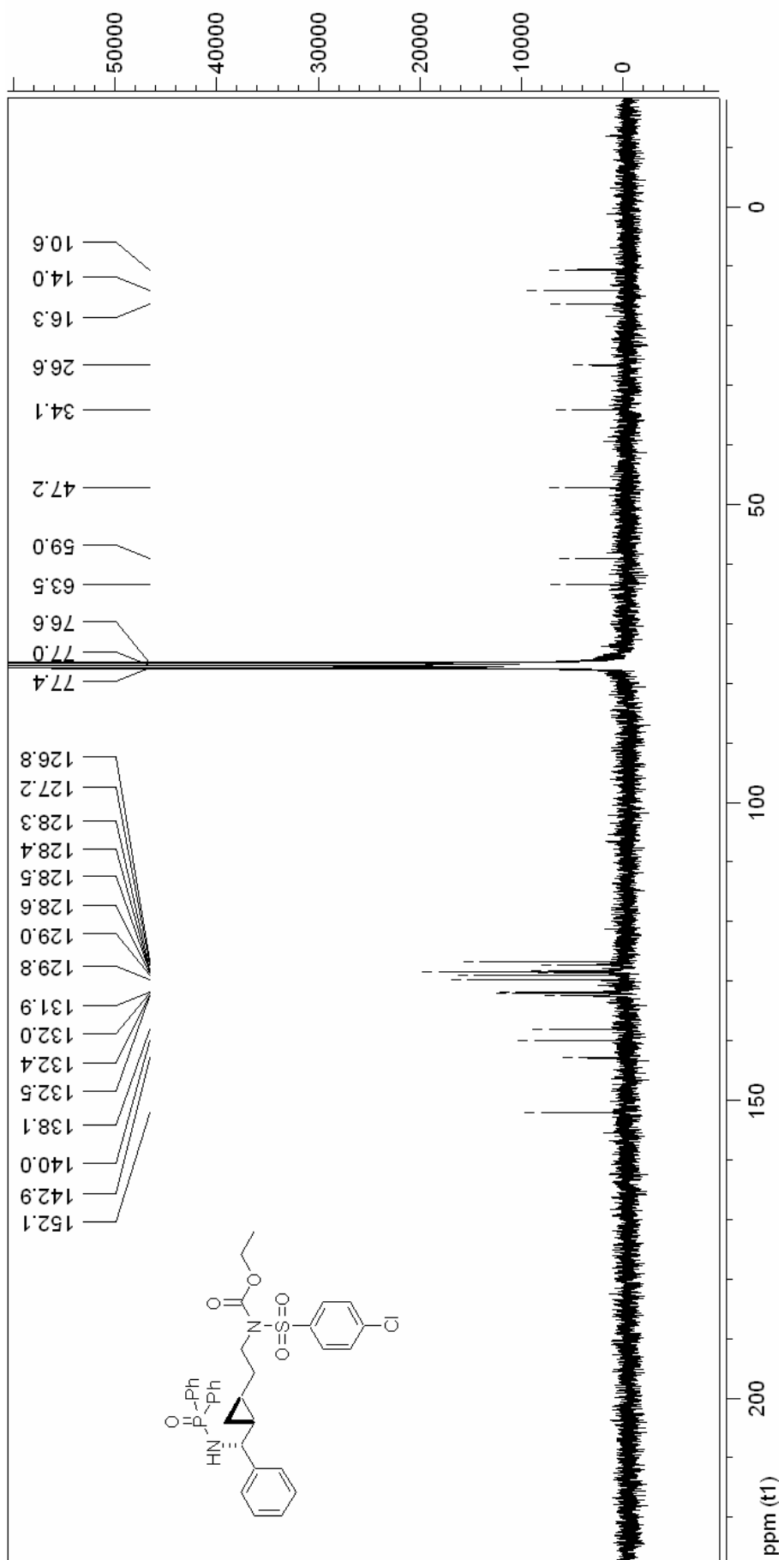
48b ¹H NMR, 300MHz, Bruker, CDCl₃



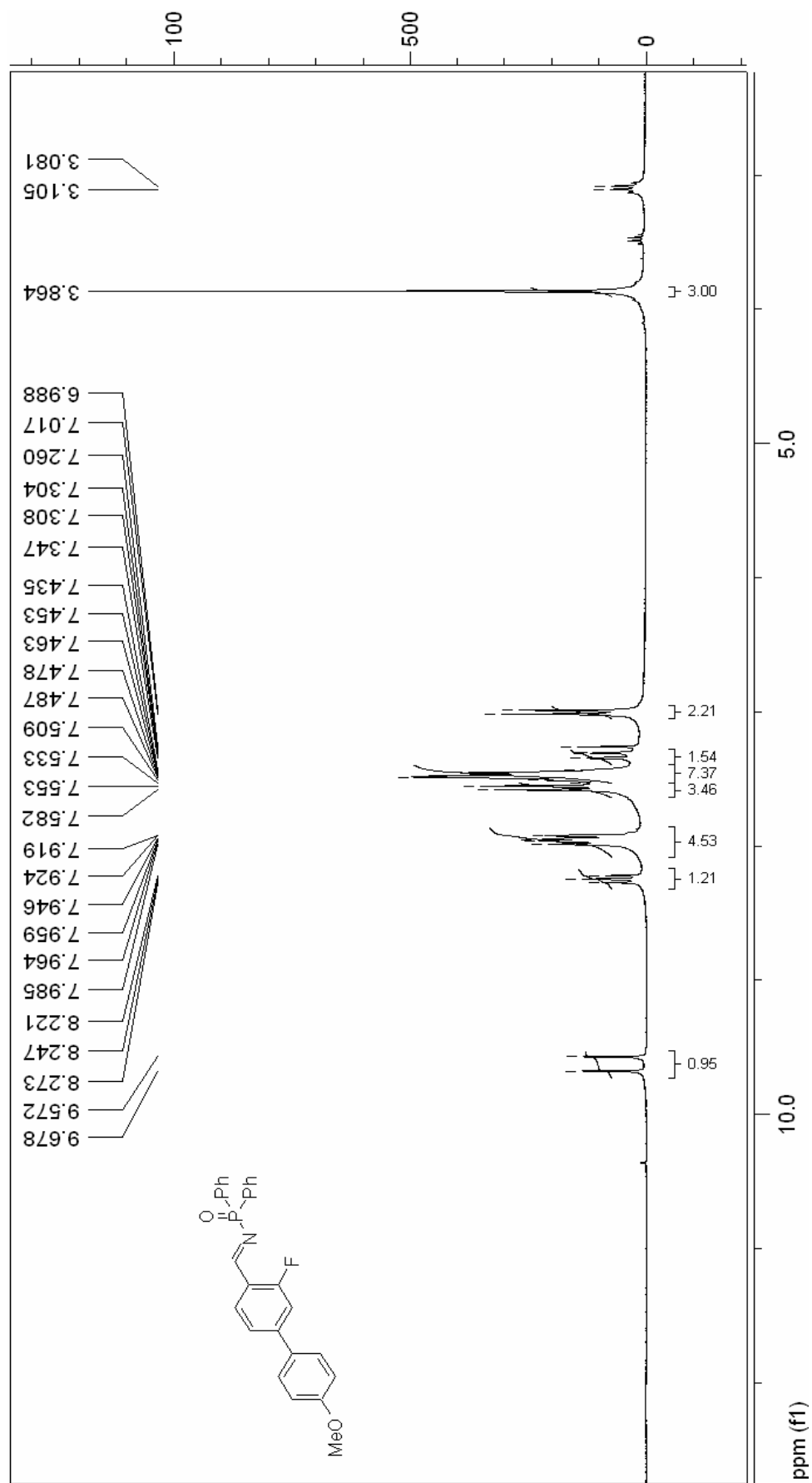
48b ¹³C NMR, 100MHz, Varian, CDCl₃



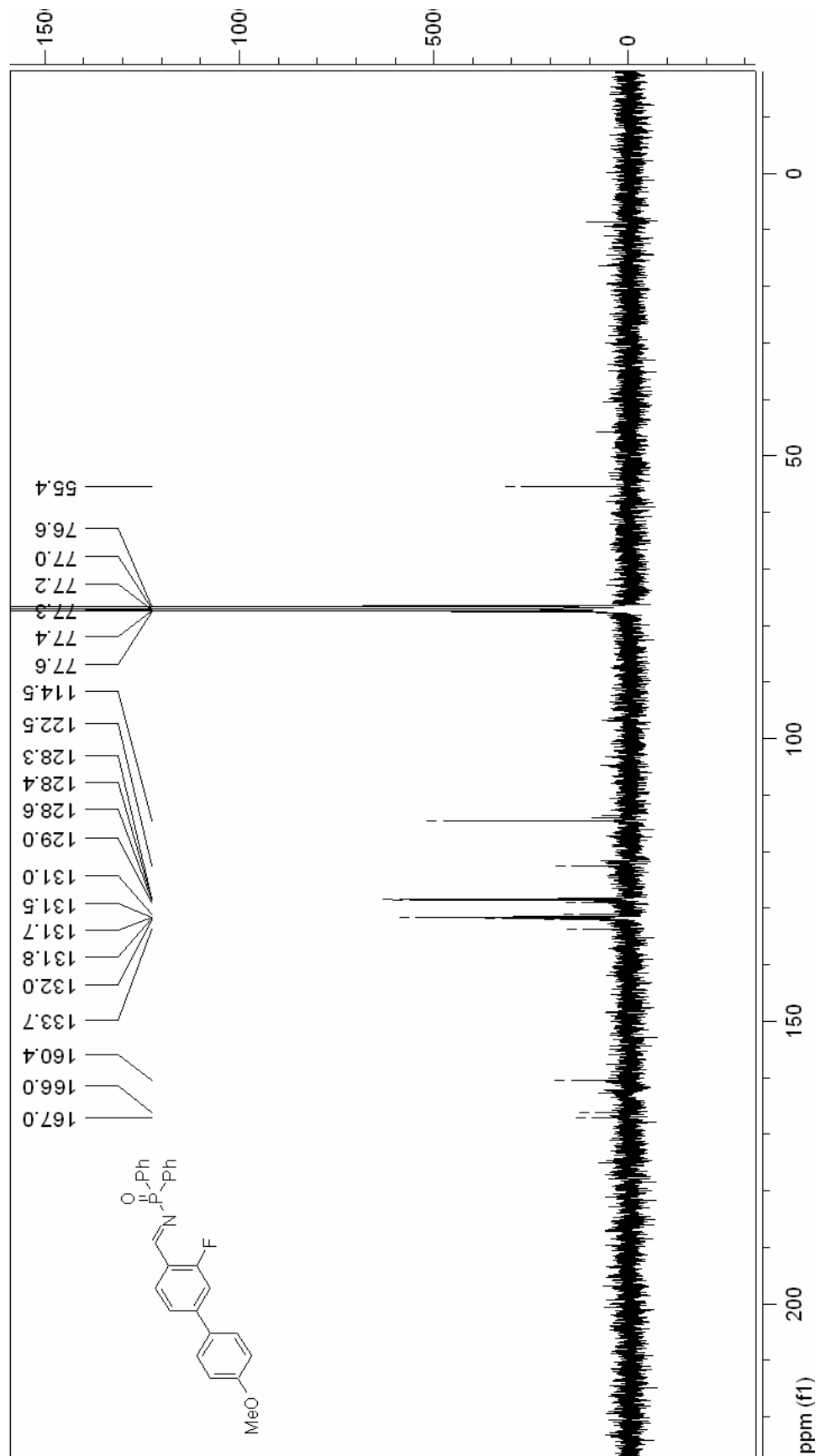
48c ¹³C NMR, 75MHz, Bruker, CDCl₃



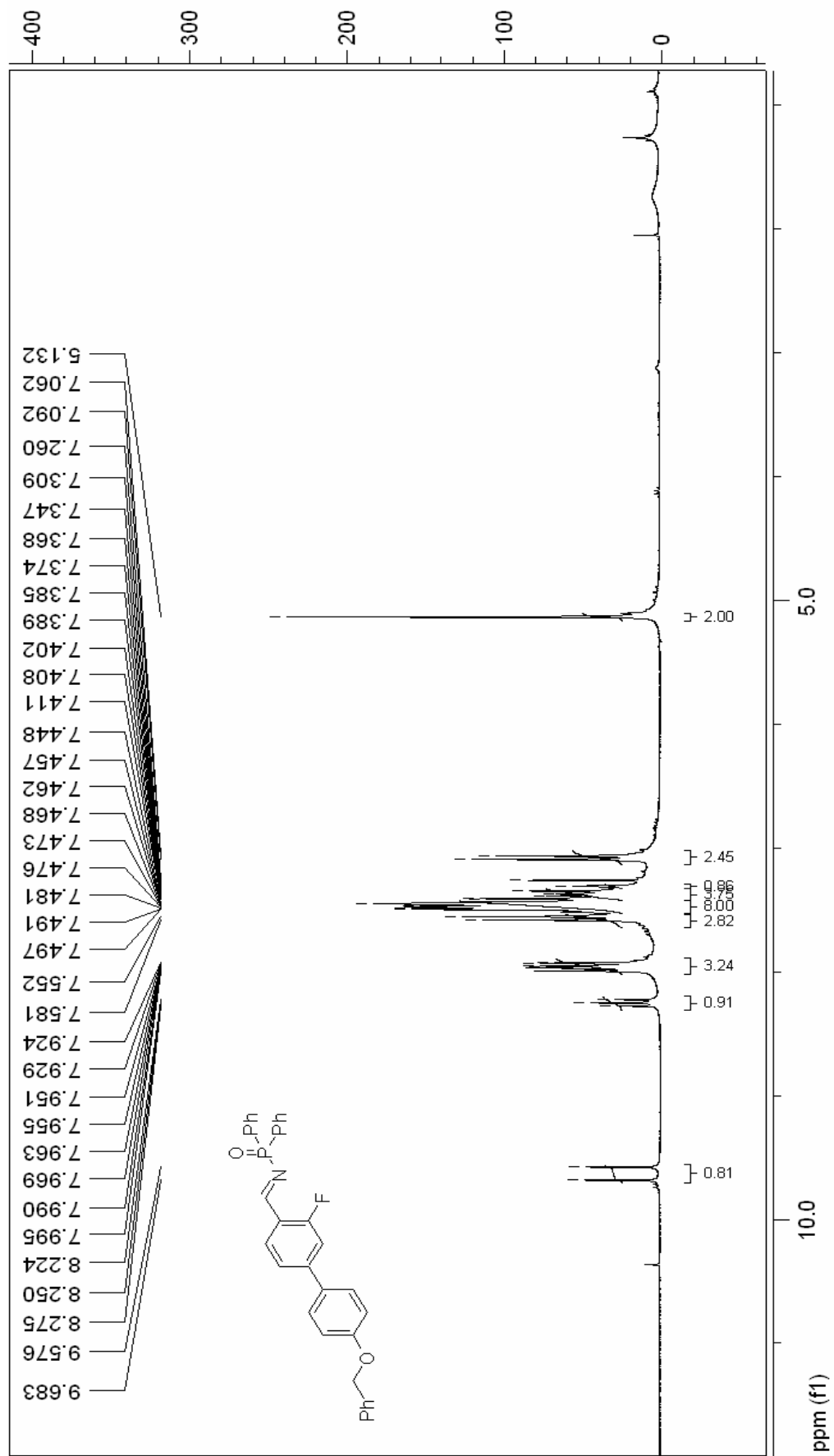
67a ¹H NMR, 300MHz, Bruker, CDCl₃



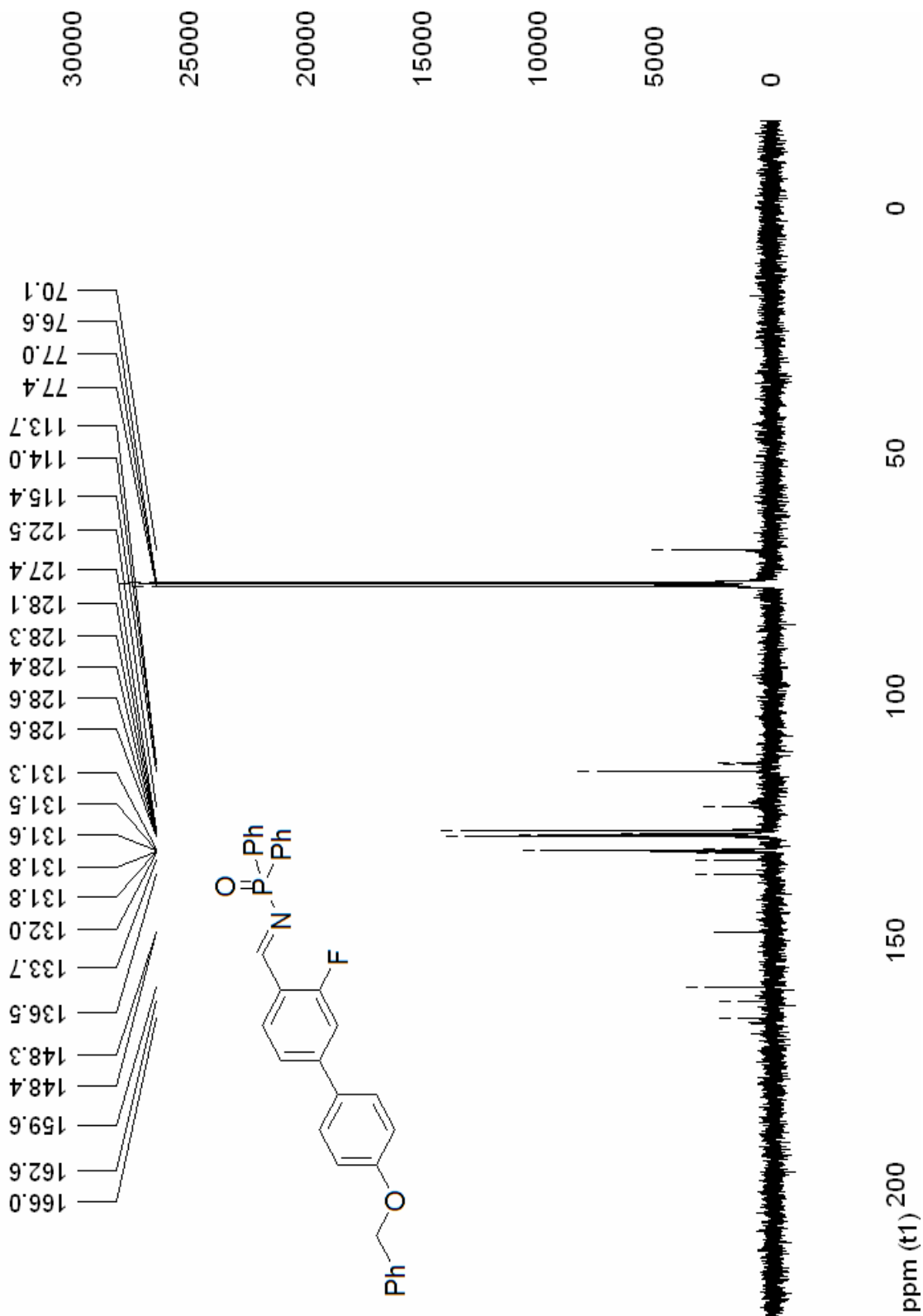
67a ¹³C NMR, 75MHz, Bruker, CDCl₃



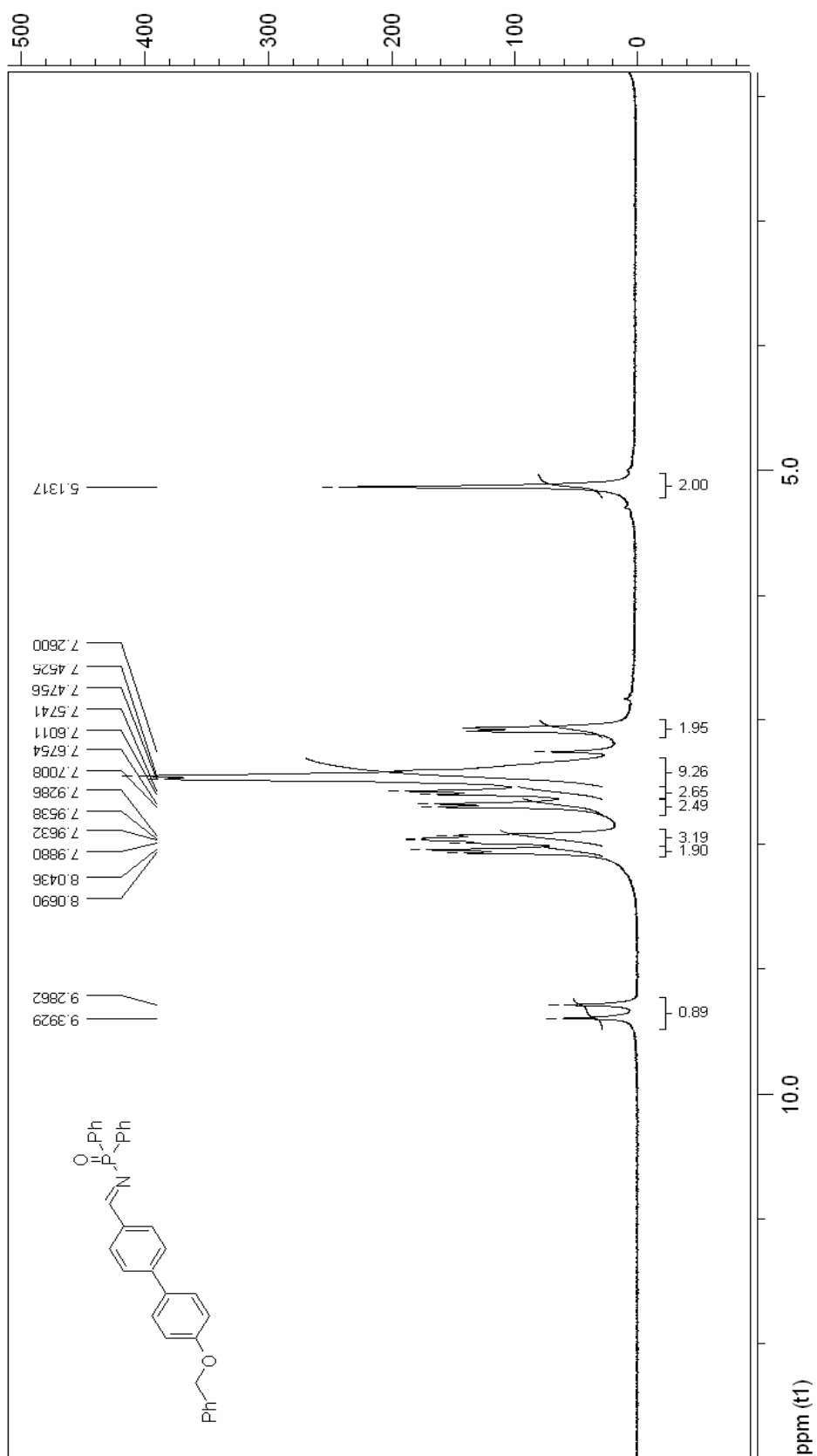
67b ¹H NMR, 300MHz, Bruker, CDCl₃



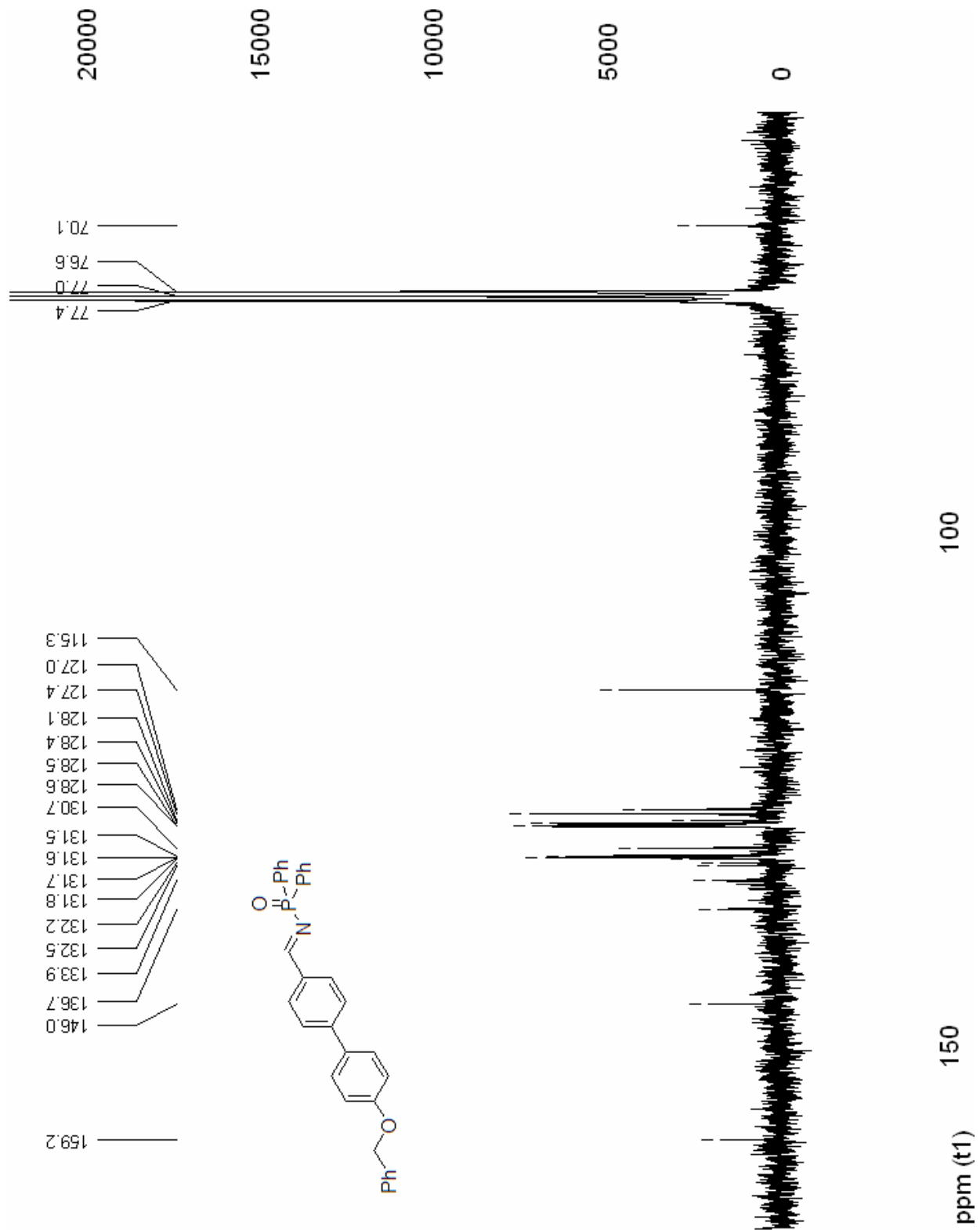
67b ¹³C NMR, 75MHz, Bruker, CDCl₃



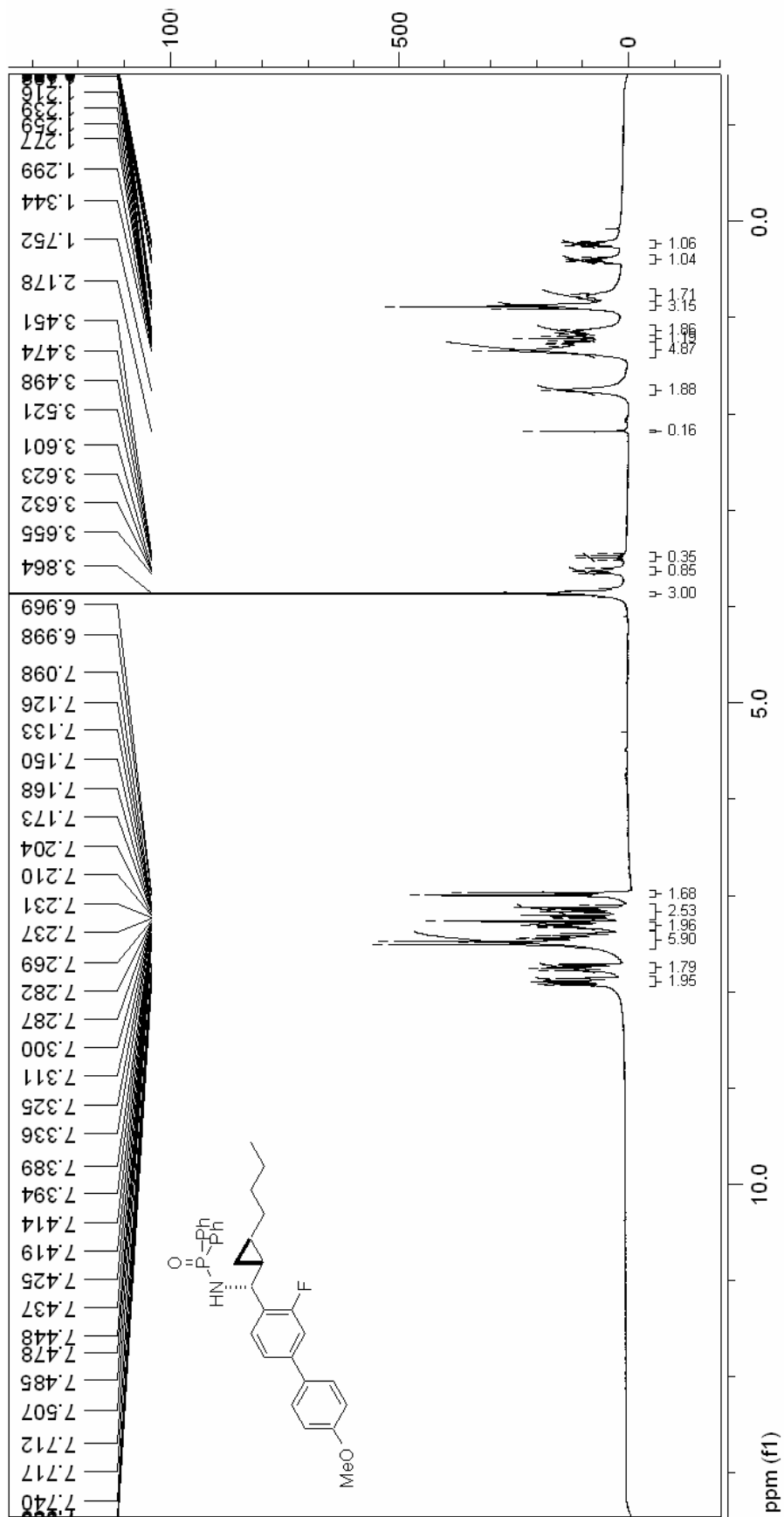
67c ¹H NMR, 300Hz, Bruker, CDCl₃



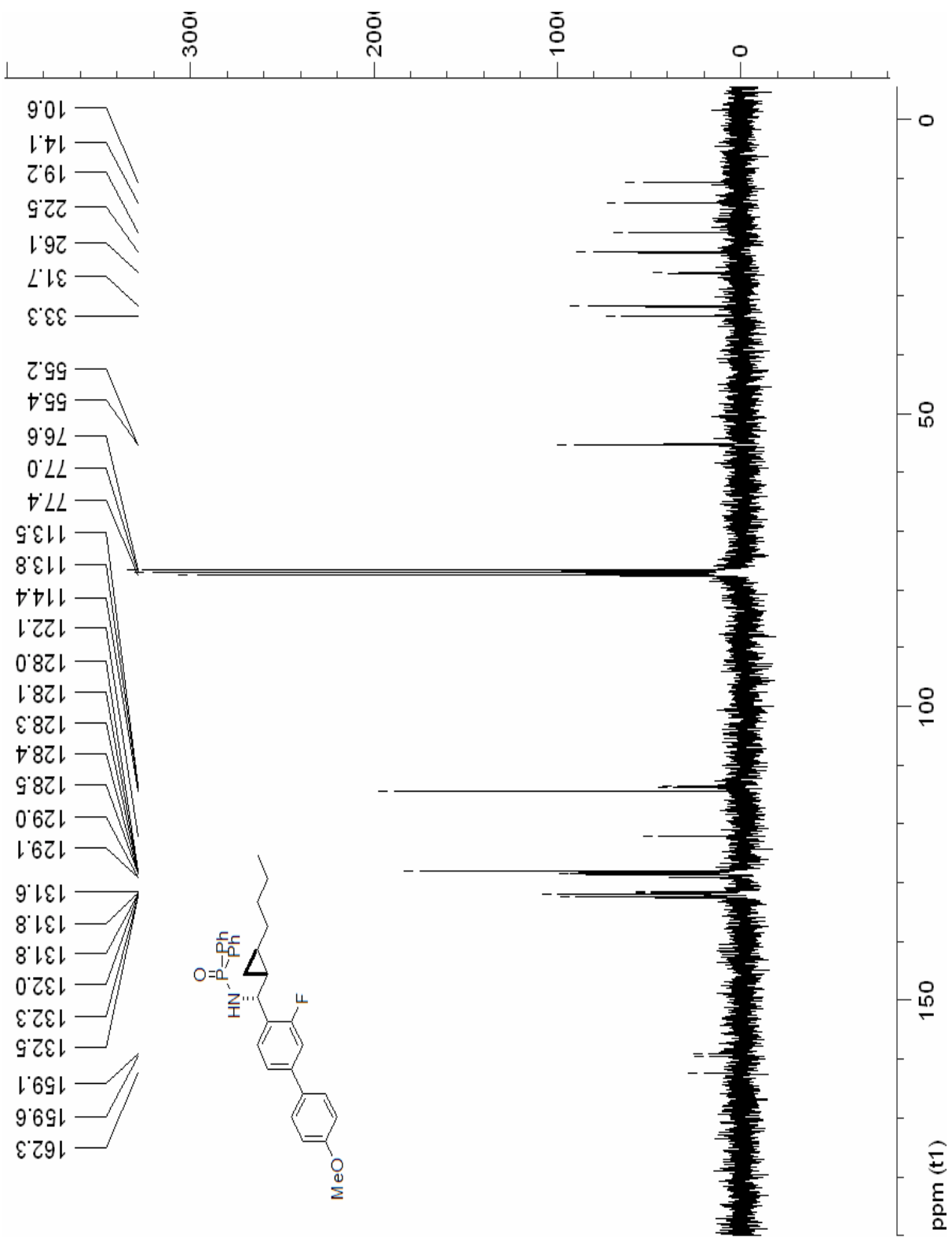
67c ¹³C NMR, 75MHz, Bruker, CDCl₃



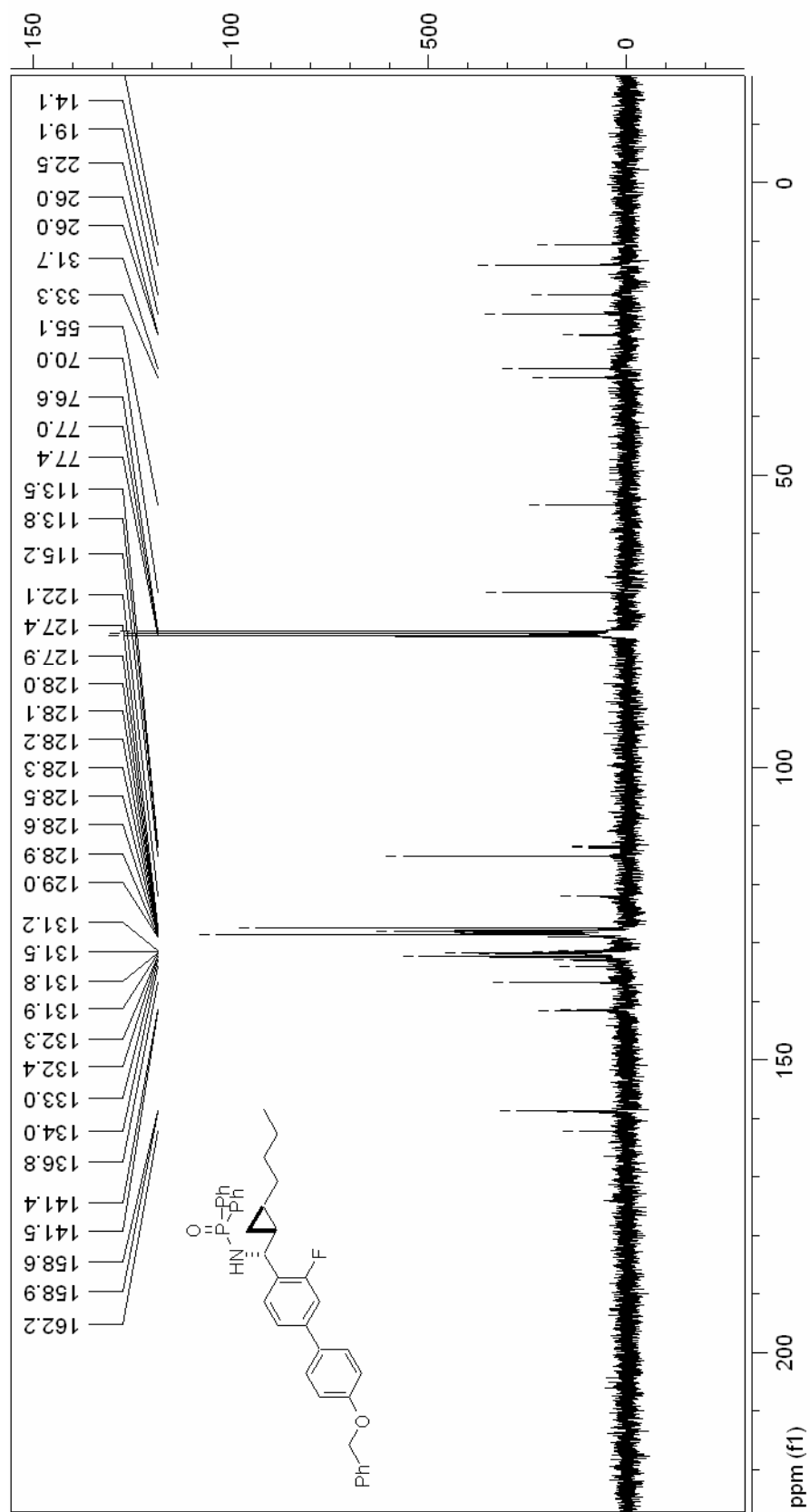
68a ¹H NMR, 300Hz, Bruker, CDCl₃



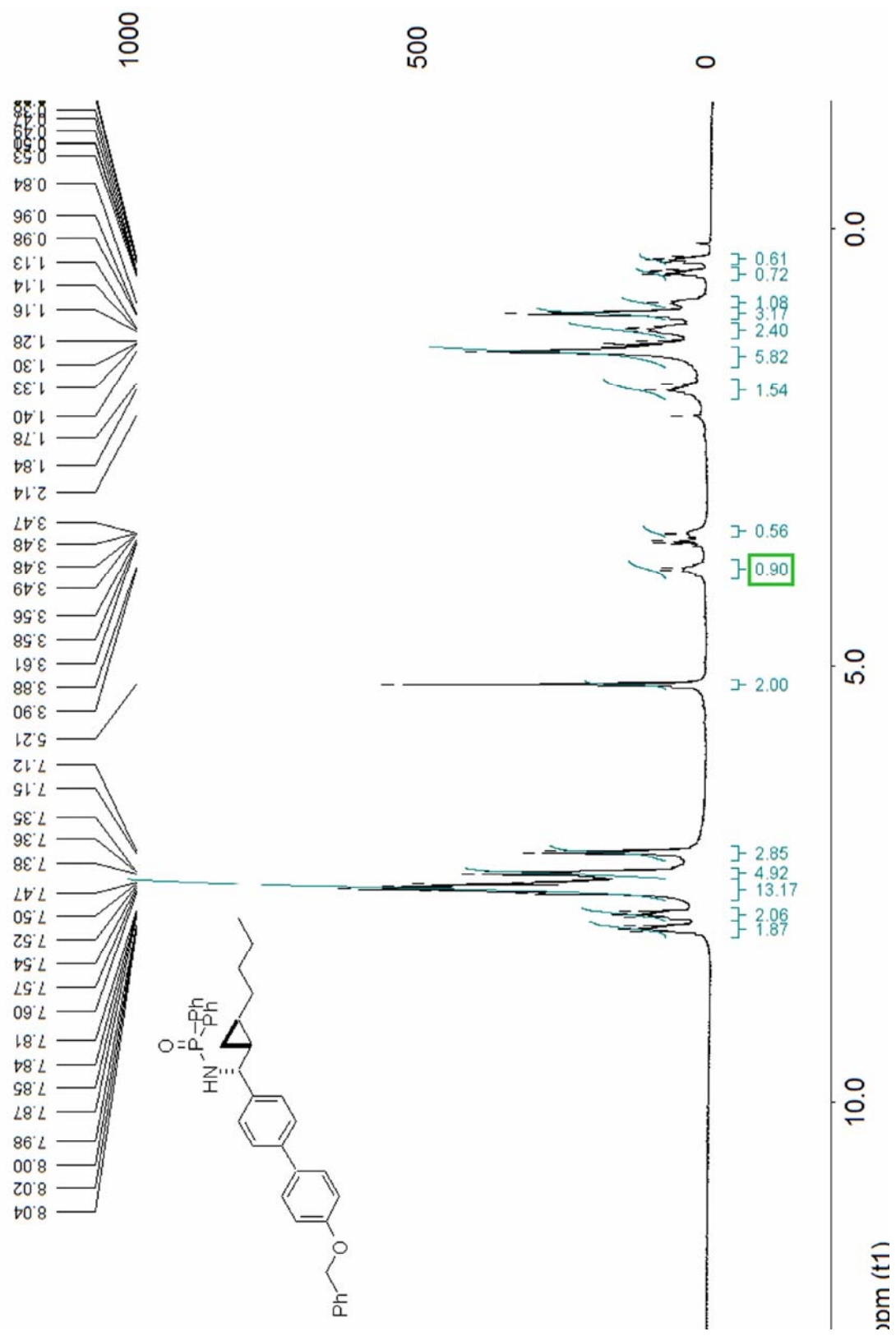
68a ¹³C NMR, 75MHz, Bruker, CDCl₃



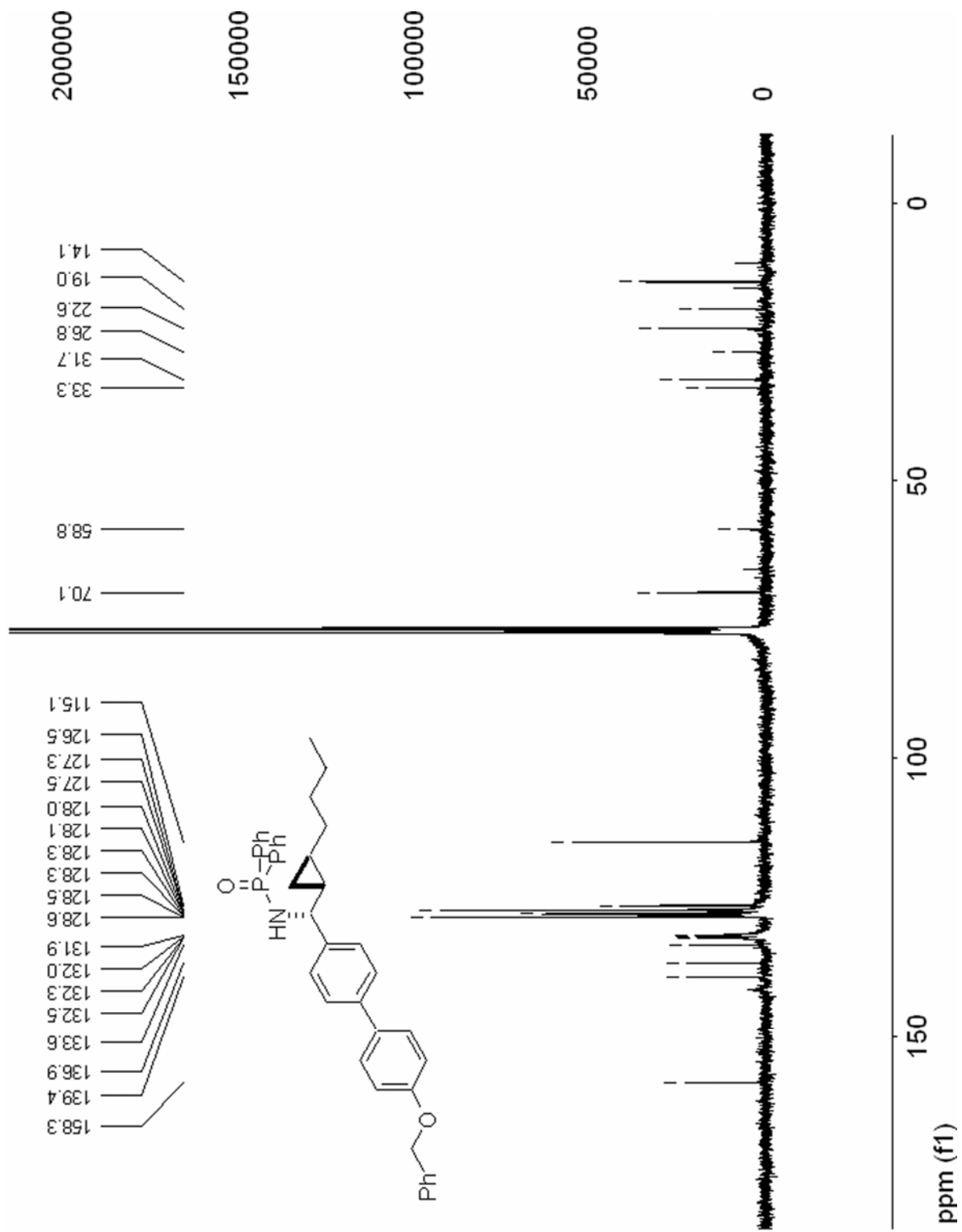
68b ^{13}C NMR, 75MHz, Bruker, CDCl_3



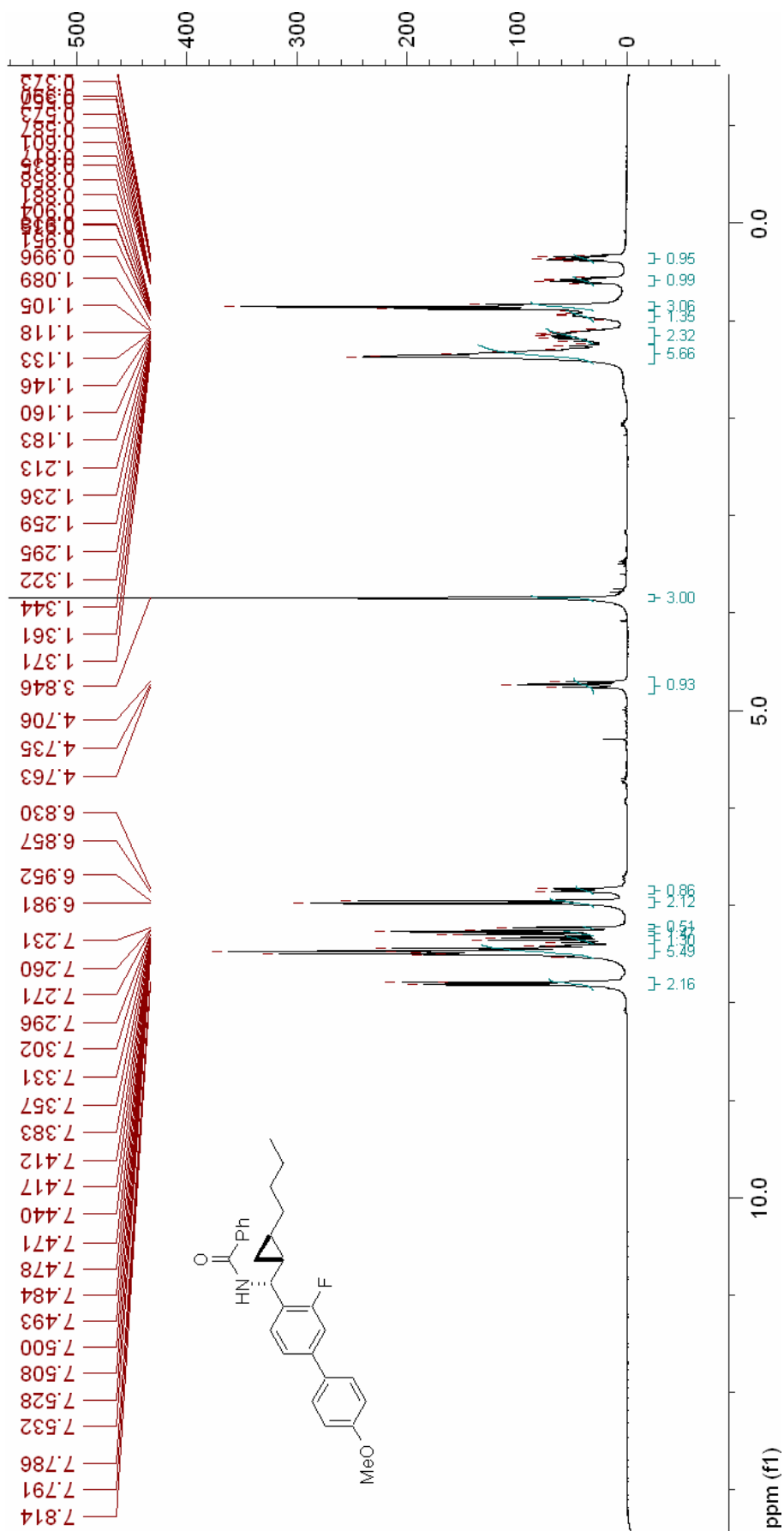
68c ^1H NMR, 300MHz, Bruker, CDCl_3



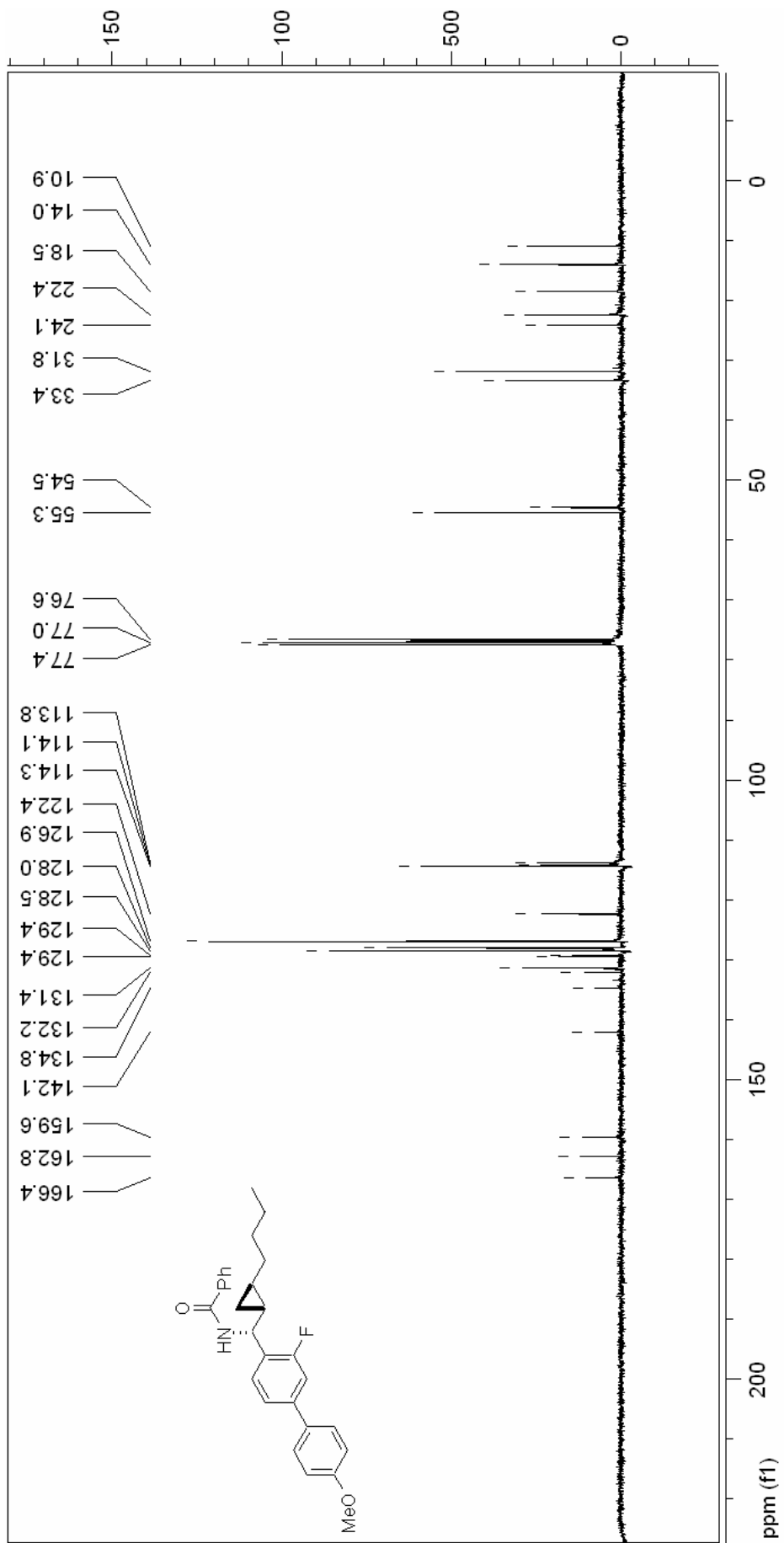
68c ¹³C NMR, 75MHz, Bruker, CDCl₃



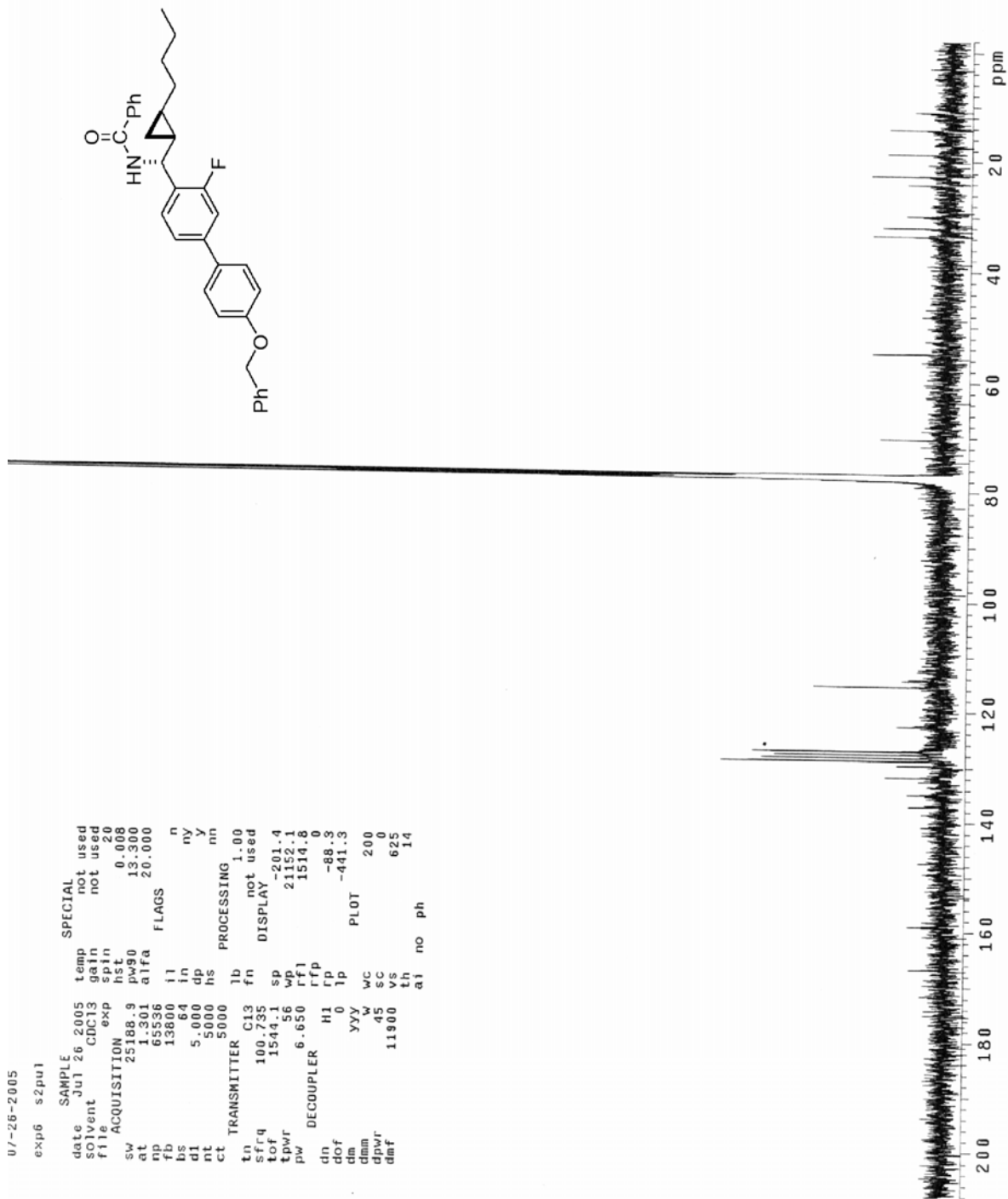
69a ¹H NMR, 300MHz, Bruker, CDCl₃



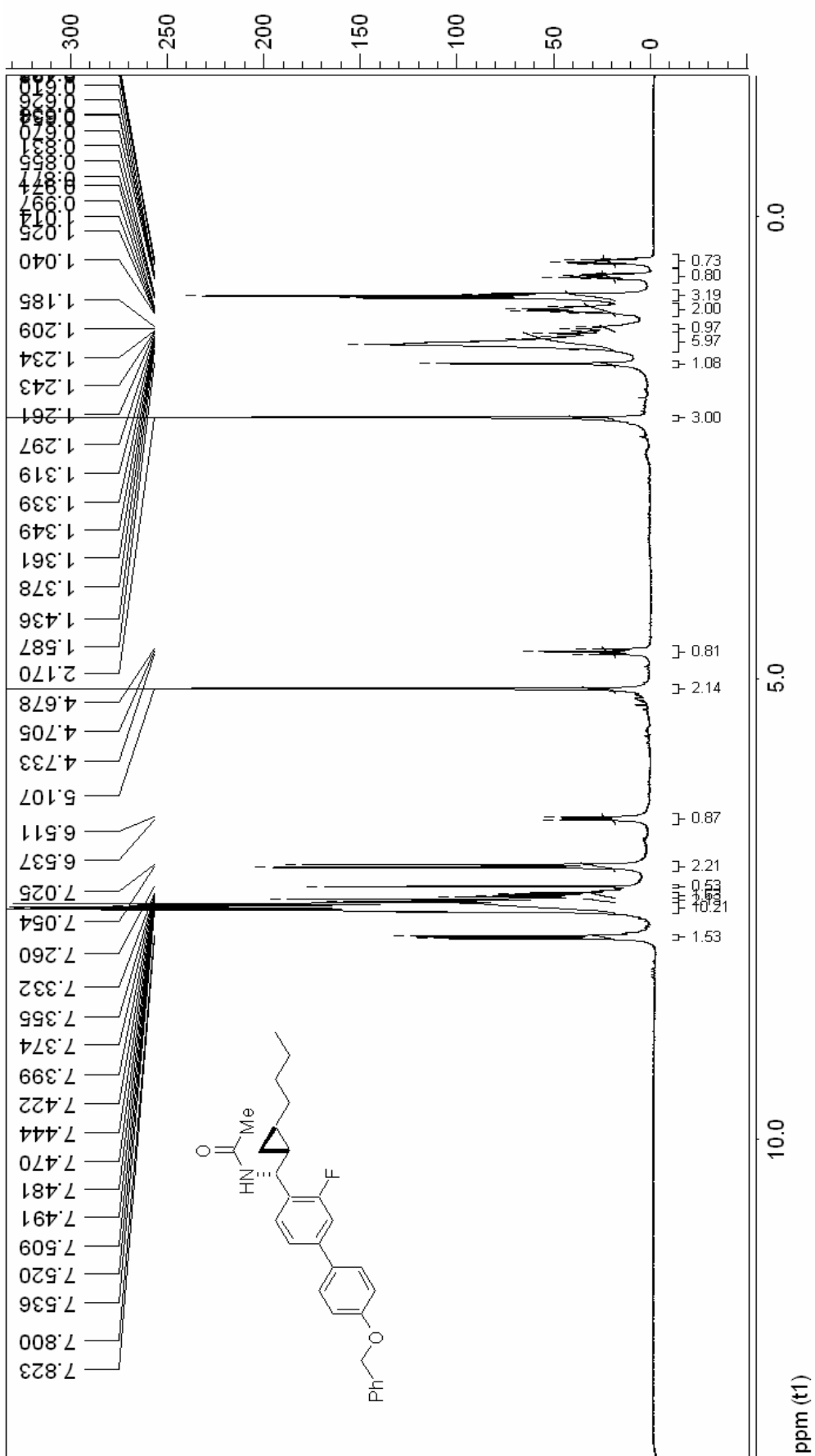
69a ¹³C NMR, 75MHz, Bruker, CDCl₃



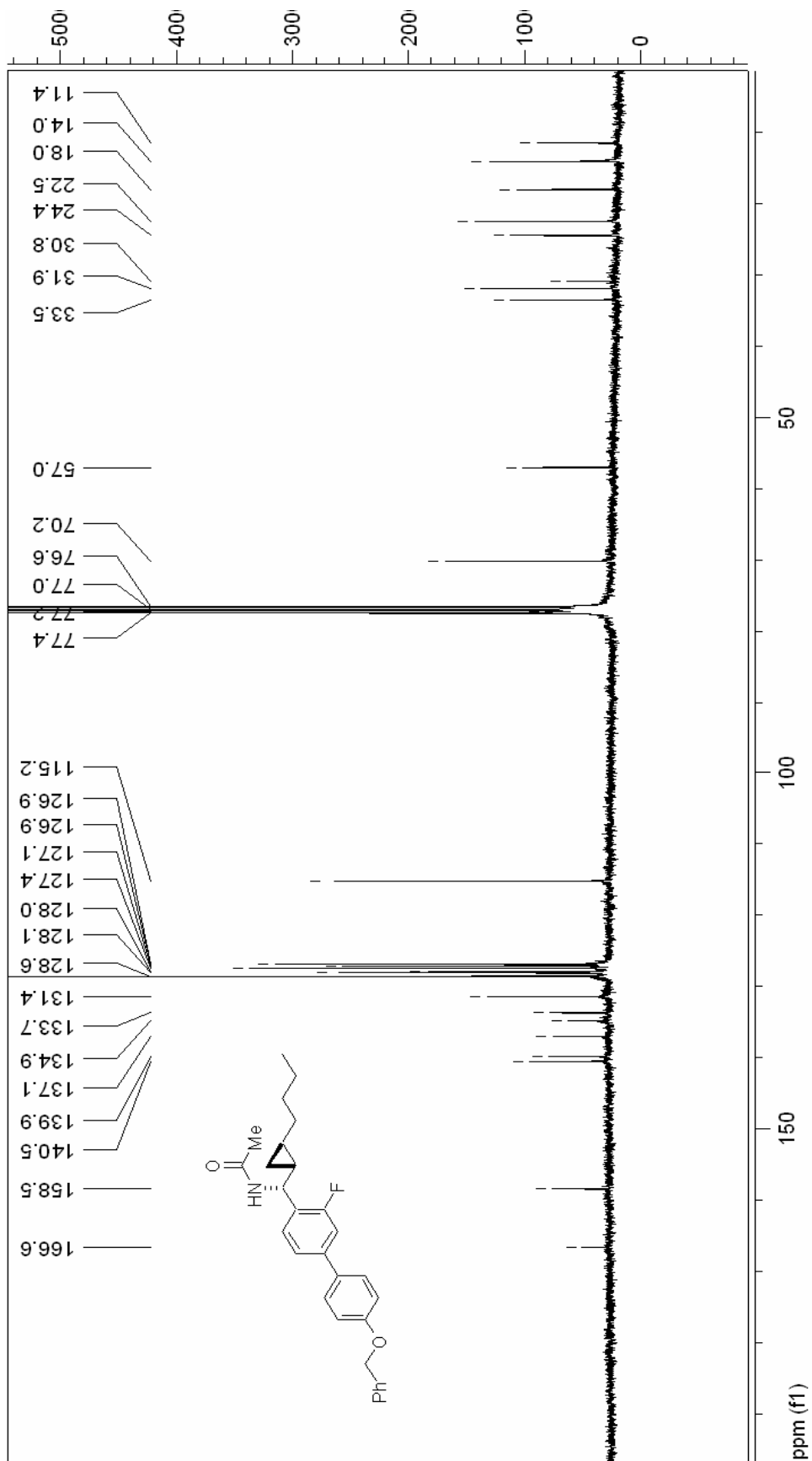
69b ¹³C NMR, 75MHz, Bruker, CDCl₃



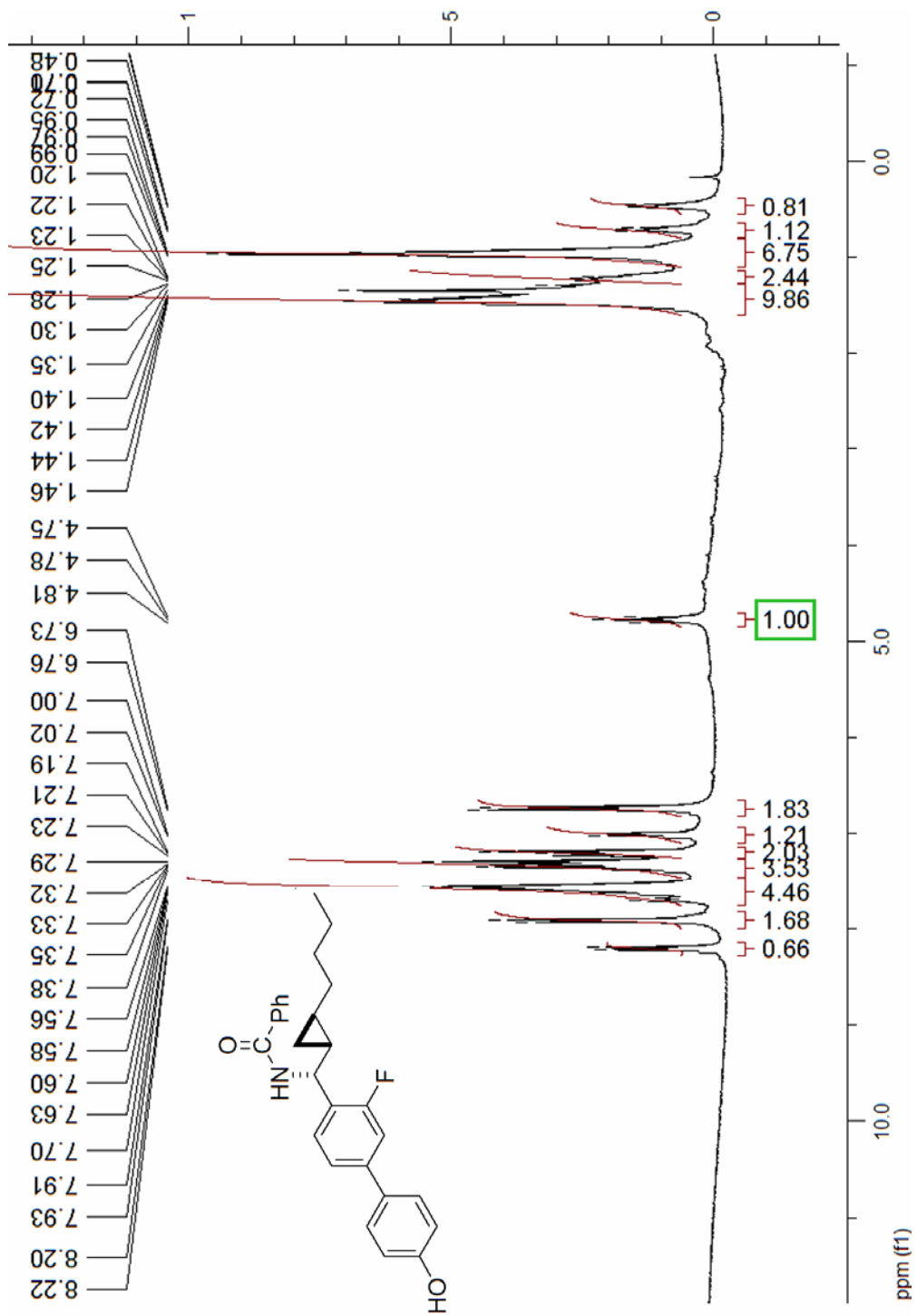
69d ¹H NMR, 300MHz, Bruker, CDCl₃



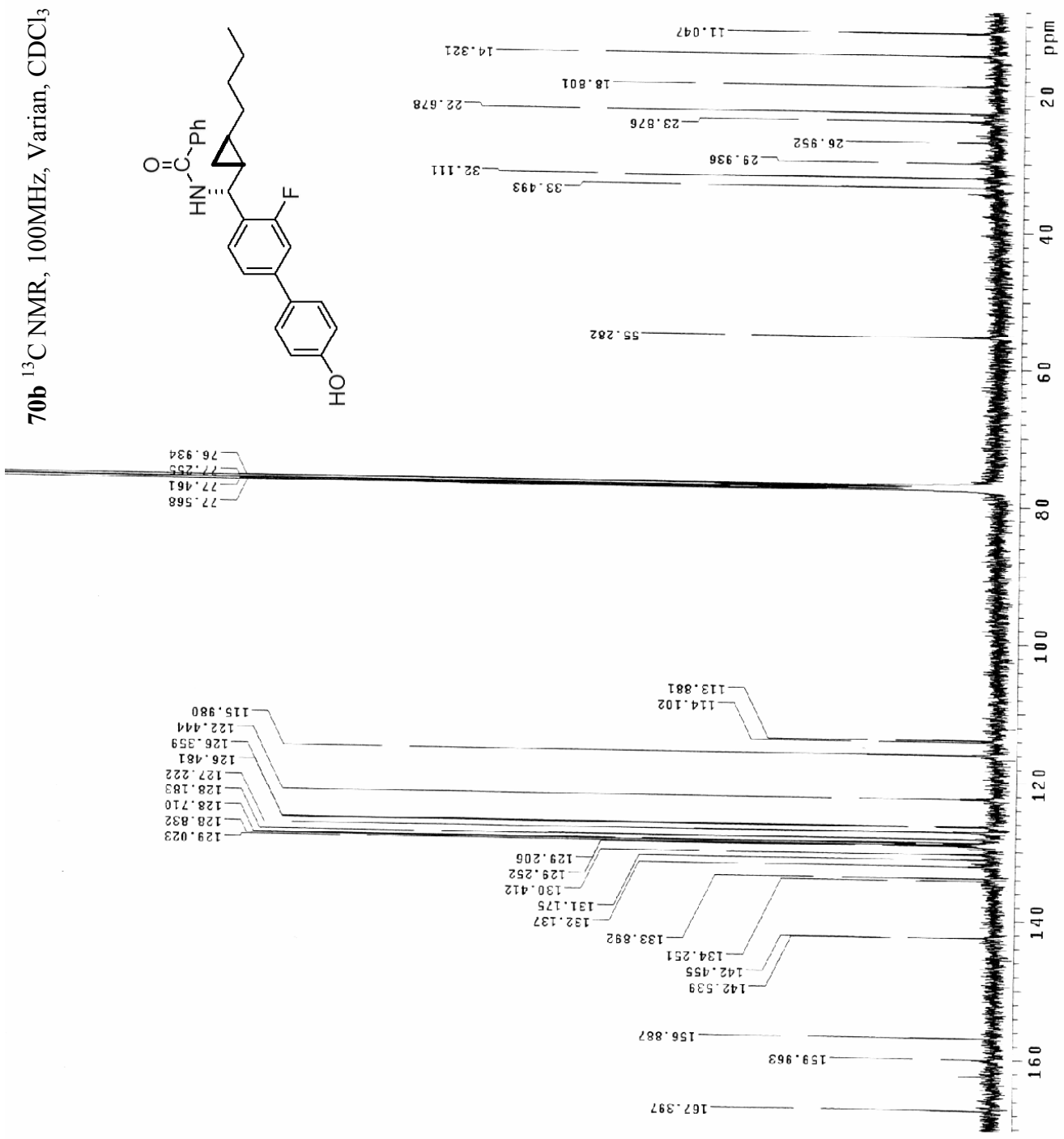
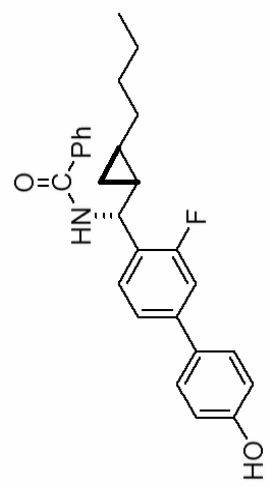
69d ¹³C NMR, 75MHz, Bruker, CDCl₃



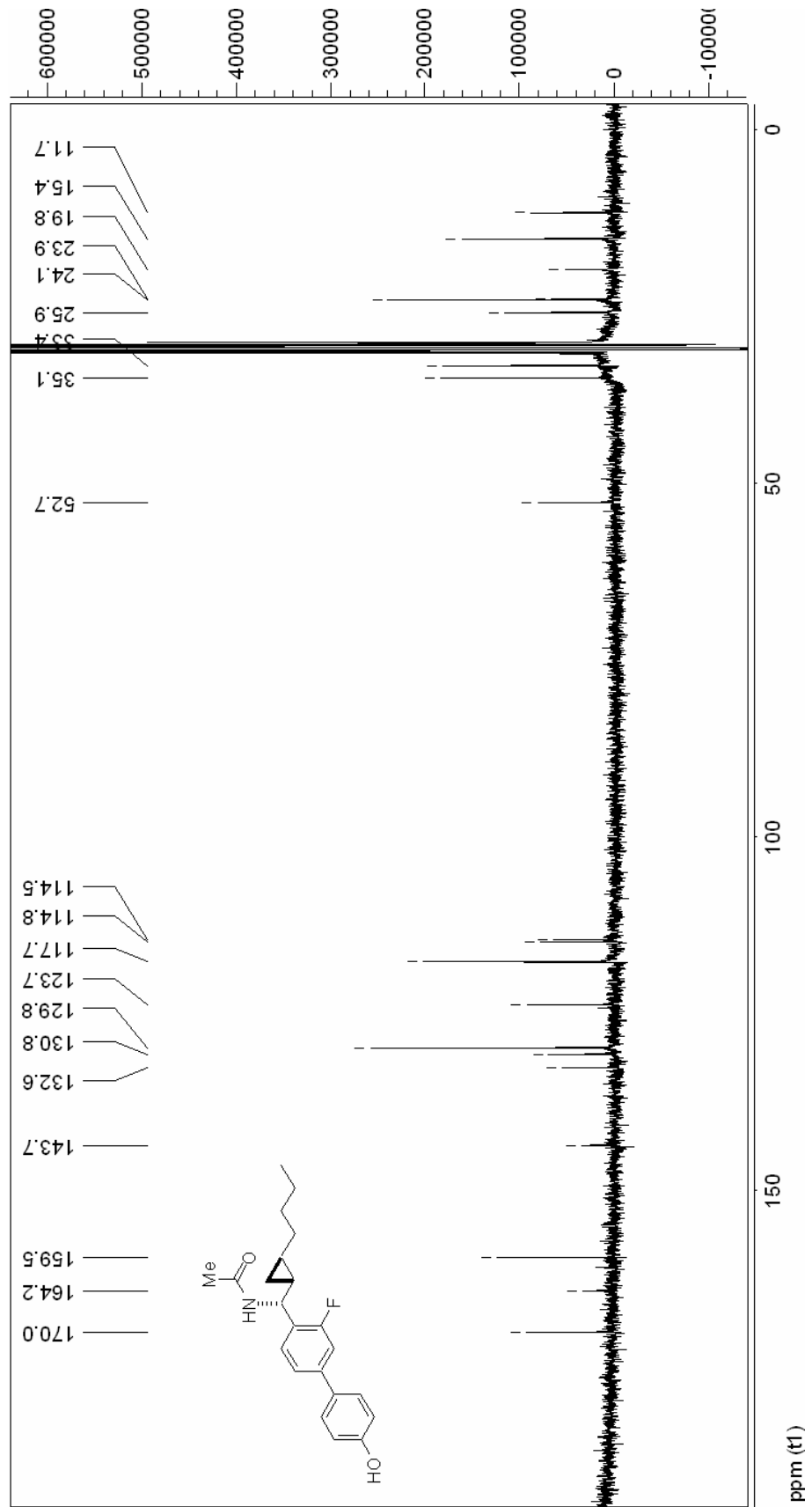
70b ¹H NMR, 300MHz, Bruker, CDCl₃



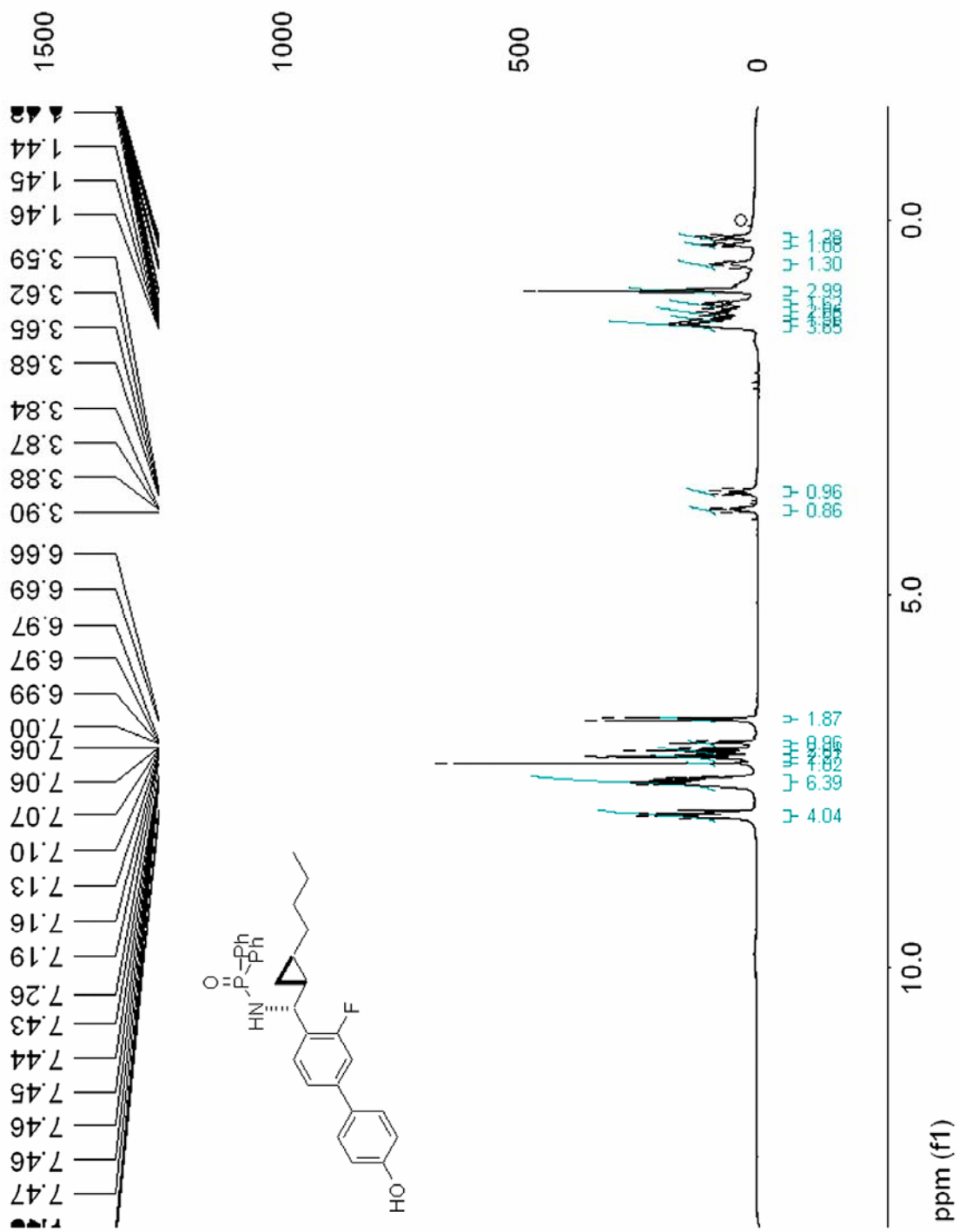
70b ¹³C NMR, 100MHz, Varian, CDCl₃



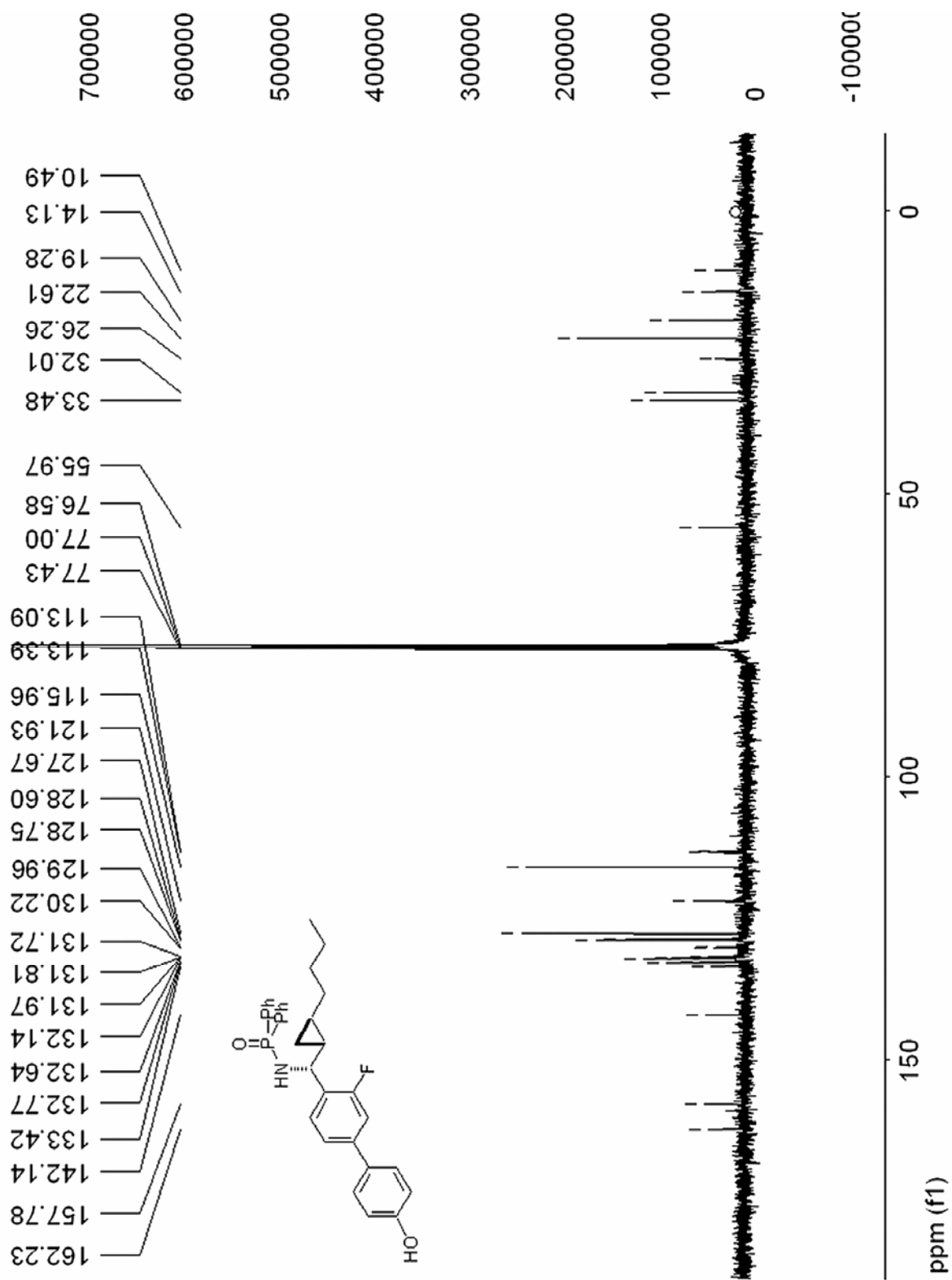
70d ¹³C NMR, 75MHz, Bruker, CO(CD₃)₂



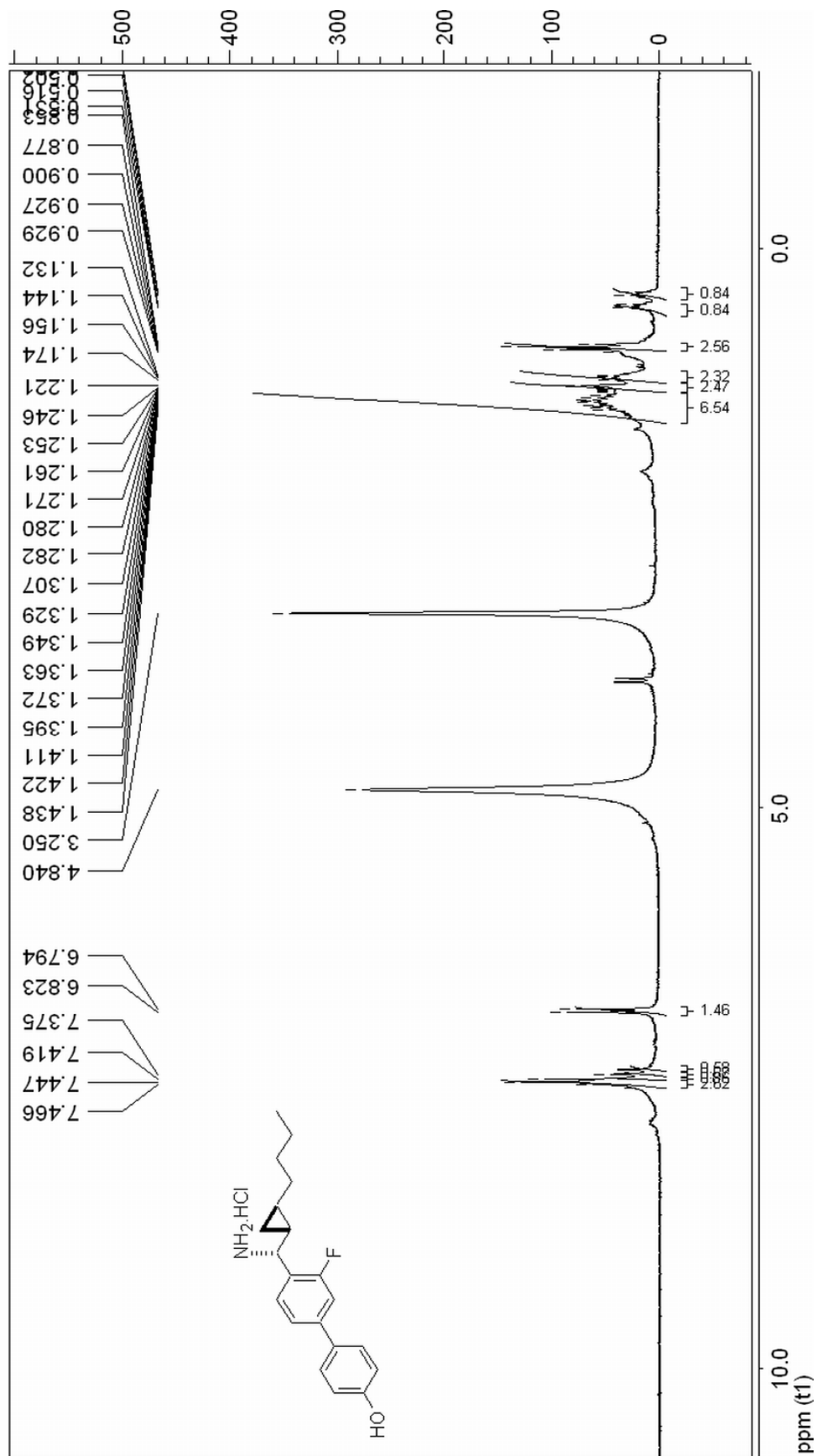
71 ¹H NMR, 300MHz, Bruker, CDCl₃



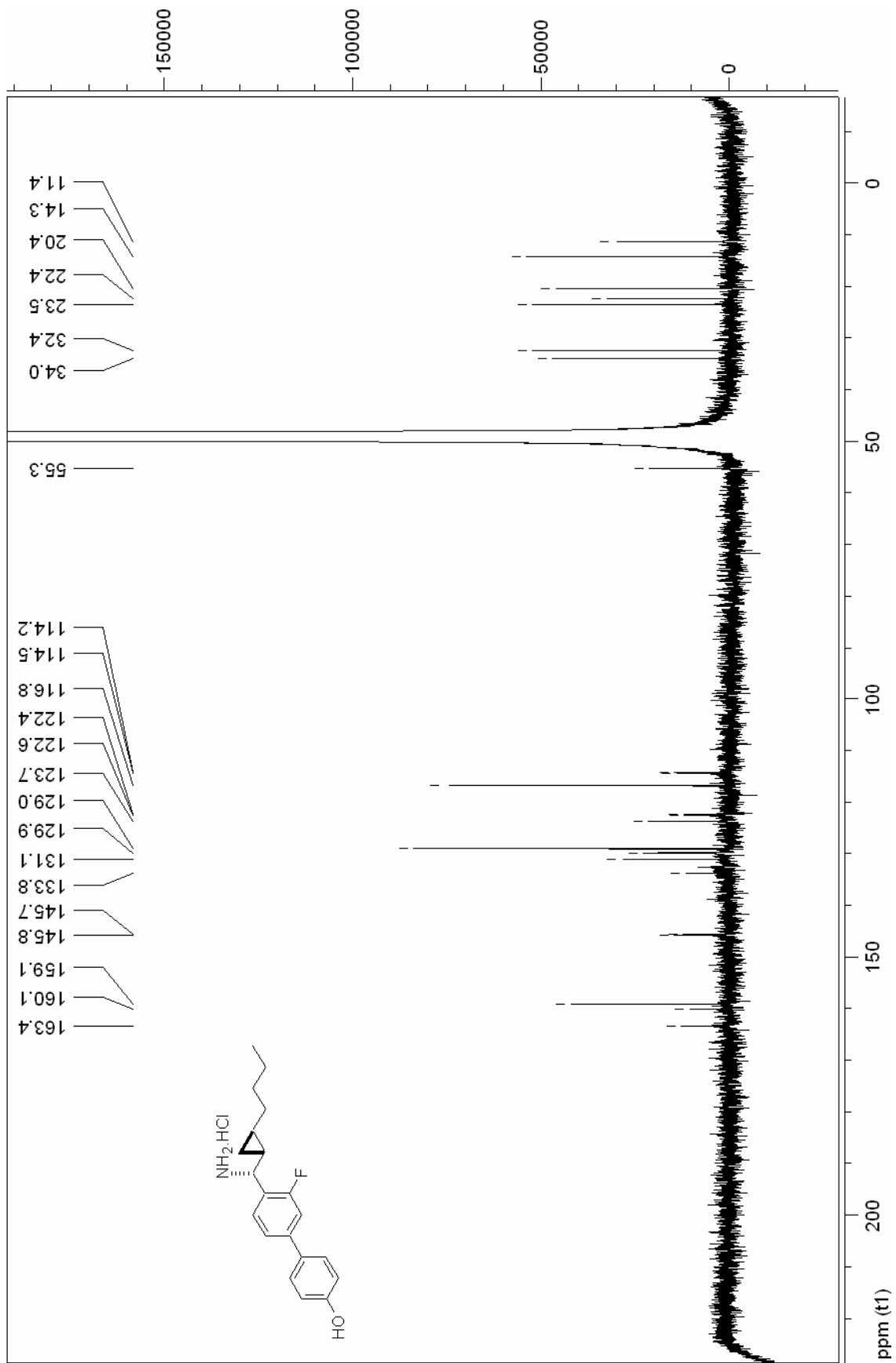
71 ¹³H NMR, 75MHz, Bruker, CDCl₃



72 ¹H NMR, 300MHz, Bruker, CD₃OD



72 ¹³C NMR, 75MHz, Bruker, CD₃OD



7. References

-
1. Clarke, R.; Liu, M. C.; Bouker, K.B.; Gu, Z.; Lee, R. Y.; Zhu, Y.; Skaar, T. C.; Gomez, B.; O'Brien, K.; Wang, Y.; Hilakivi-Clarke, L. A. Antiestrogen resistance in breast cancer and the role of estrogen receptor signaling. *Oncogene* **2003**, *22*, 7316-7339.
 2. Manni, A.; Verderame, M. F.; "Selective Estrogen Receptor Modulators: Research and Clinical Applications", Humana Press **2002**
 3. MacGregor Schafer, J.; Bentrem, D. J.; Takei, H.; Gajdos, C.; Badve, S.; Jordan, V. C. A mechanism of drug resistance to tamoxifen in breast cancer. *J. Steroid Biochem. Mol. Biol.* **2002**, *83*, 75-83
 4. Fisher, B.; Costantino, J. P.; Wickerham, D. L.; Redmond, C. K.; Kavanah, M.; Cronin, W. M.; Vogel, V.; Robidoux, A.; Dimitrov, N.; Atkins, J.; Daly, M.; Wieand, S.; Tan-Chiu, E.; Ford, L.; Wolmark, N. Tamoxifen for prevention of breast cancer: Report of the National Surgical Adjuvant breast and bowel project P-1 study. *J. Natl. Can. Inst.* **1998**, *90*, 1371-1388.
 5. Herynk, M.H.; Fuqua, S. A. W. Estrogen receptor mutations in human disease. *Endocr. Rev.* **2004**, *25*, 869-898.
 6. Nettles, K. W.; Greene, G. L. Ligand control of coregulaator recruitment to nuclear receptors. *Ann. Rev. Phys.* **2005**, *67*, 309-333.
 7. Nilsson, S.; Makela, S.; Treuter, E.; Tujague, M.; Thomsen, J.; Andersson, G.; Enmark, E.; Pettersson, K.; Warner, M.; Gustafsson, J-Å. Mechanisms of estrogen action. *Physiol. Rev.* **2001**, *81*, 1535-1565.
 8. Koehler, K. F.; Helguero, L. A.; Haldosén, L.A.; Warner, M.; Gustafsson, J. Å. Reflections on the discovery and significance of estrogen receptor β . *Endocr. Rev.* **2005**, *26*, 465-478.

-
9. Clarke, R.; Leonessa, F.; Welch, J.N.; Skaar, T. C. Cellular and molecular pharmacology of antiestrogen action and resistance. *Pharmacol. Rev.* **2001**, *53*, 25-71.
 10. Platet, N.; Cathiard, A. M.; Gleizes, M.; Garcia, M. Estrogens and their receptors in breast cancer progression: a dual role in cancer proliferation and invasion. *Crit. Rev. Oncol. Hematol.* **2004**, *51*, 55-67.
 11. Hall, J. M.; Couse, J. F.; Korach, K. S. The multifaceted mechanisms of estradiol and estrogen receptor signaling. *J. Biol. Chem.* **2001**, *276*, 36869-36872.
 12. Dobrzycka, K.M.; Townson, S.M.; Jiang, S.; Oesterreich, S. Estrogen receptor corepressors - a role in human breast cancer? *Endocr. Relat. Cancer*, **2003**, *10*, 517-536.
 13. Kuiper, G. G.; Enmark, E.; Peltö-Huikko, M.; Nilsson, S.; Gustafsson, J. Å. Cloning of a novel estrogen receptor expressed in rat prostate and ovary. *Proc. Natl. Acad. Sci.* **1996**, *93*, 5925-5930.
 14. Ström, A.; Hartman, J.; Foster, J.S.; Kietz, S.; Wimalasena, J.; Gustafsson, J. Å. Estrogen receptor β inhibits 17β -estradiol-stimulated proliferation of the breast cancer cell line T47D. *Proc. Natl. Acad. Sci.* **2003**, *101*, 1566-1571.
 15. Nakopoulou, L.; Lazaris, A.C.; Panayotopoulou, E. G.; Giannopoulou, I.; Givalos, N.; Markaki, S.; Keramopoulos, A. The favourable prognostic value of oestrogen receptor β immunohistochemical expression in breast cancer. *J. Clin. Pathol.* **2004**, *57*, 523-528.
 16. Myers, E.; Fleming, F. J.; Crotty, T. B.; Kelly, G.; McDermott, E. W.; O'Higgins, N. J.; Hill, A. D.; Young, L. S. Inverse relationship between ER- β and SRC-1 predicts outcome in endocrine-resistant breast cancer. *Br. J. Cancer* **2004**, *89*, 1-7.

-
17. Sun, J.; Baudry, J.; Katzenellenbogen, J. A.; Katzenellenbogen, B. S. Molecular basis for the subtype discrimination of the estrogen receptor- β -selective ligand, diarylpropionitrile. *Mol. Endocrinol.* **2003**, *17*, 247-258.
18. Brzozowski, A. M.; Pike, A. C. Molecular basis of agonism and antagonism in the oestrogen receptor. Dauter, Z.; Hubbard, R. E.; Bonn, T.; Engstrom, O.; Ohman, L.; Greene, G. L.; Gustafsson, J. Å.; Carlquist, M. *Nature* **1997**, *389*, 753-758.
19. Katzenellenbogen, B. S.; Katzenellenbogen, J. A. Defining the “S” in SERMs. *Science* **2002**, *295*, 2380-2381.
20. Hall, J. M.; McDonnell, D. P.; Korach, K. S. Allosteric regulation of estrogen receptor structure, function, and coactivator recruitment by different estrogen response elements. *Mol. Endocrinol.* **2002**, *16*, 469-486.
21. Tamrazi, A.; Carlson, K. E.; Rodriguez, A. L.; Katzenellenbogen, J. A. Coactivator proteins as determinants of estrogen receptor structure and function: spectroscopic evidence for a novel coactivator-stabilized receptor conformation. *Mol. Endocrinol.* **2005**, *19*, 1516-1528.
22. Veeneman, G. H. Non-Steroidal Subtype Selective Estrogens. *Curr. Med. Chem.* **2005**, *12*, 1077-1136.
23. Kraichely, D. M.; Sun, J.; Katzenellenbogen, J. A.; Katzenellenbogen, B. S. Conformational changes and coactivator recruitment by novel ligands for estrogen receptor- α and Estrogen Receptor- β : correlations with biological character and distinct differences among SRC coactivator family members. *Endocrinology* **2000**, *141*, 3534–3545.
24. Meyers, M. J.; Sun, J.; Carlson, K. E.; Marriner, G. A.; Katzenellenbogen, B. S.; Katzenellenbogen, J. A. Estrogen receptor- β potency-selective ligands: structure-activity

relationship studies of diarylpropionitriles and their acetylene and polar analogues. *J. Med. Chem.* **2001**, *44*, 4230-4251.

25. Manas, E. S.; Xu, Z. B.; Unwalla, R. J.; Somers, W. S. Understanding the selectivity of genistein for human estrogen receptor- β using X-ray crystallography and computational methods. *Structure* **2004**, *12*, 2197-2207.

26. Harris, H. A.; Albert, L. M.; Leathurby, Y.; Malamas, M. S.; Mewshaw, R. E.; Miller, C. P.; Kharode, Y. P.; Marzolf, J.; Komm, B. S.; Winneker, R. C.; Frail, D. E.; Henderson, R. A.; Zhu, Y.; Keith, J. C. Jr. Evaluation of an estrogen receptor- β agonist in animal models of human disease. *Endocrinology* **2003**, *144*, 4241-4249.

27. Fink, B. E.; Mortensen, D. S.; Stauffer, S. R.; Aron, Z. D.; Katzenellenbogen, J. A. Novel structural templates for estrogen-receptor ligands and prospects for combinatorial synthesis of estrogens. *Chem. Biol.* **1999**, *6*, 205-219.

28. Edsall, R. J. Jr.; Harris, H. A.; Manas, E. S.; Mewshaw, R. E. ER β ligands. Part 1: The discovery of ER β selective ligands which embrace the 4-hydroxy-biphenyl template. *Bioorg. Med. Chem.* **2003**, *11*, 3457-3474.

29. Collini, M. D.; Kaufman, D. H.; Manas, E. S.; Harris, H. A.; Henderson, R. A.; Xu, Z. B.; Unwalla, R. J.; Miller, C. P. 7-Substituted 2-phenyl-benzofurans as ER β selective ligands. *Bioorg. Med. Chem. Lett.* **2004**, *14*, 4925-4929.

30. McDevitt, R. E.; Malamas, M. S.; Manas, E. S.; Unwalla, R. J.; Xu, Z. B.; Miller, C. P.; Harris, H. A. Estrogen receptor ligands: design and synthesis of new 2-arylidene-1-ones. *Bioorg. Med. Chem. Lett.* **2005**, *15*, 3137-3142.

-
31. De Angelis, M.; Stossi, F.; Waibel, M.; Katzenellenbogen, B. S.; Katzenellenbogen, J. A. Estrogen receptor ligands: design and synthesis of new 2-arylidene-1-ones. *Bioorg. Med. Chem.* **2005**, *13*, 6529-6542.
32. De Angelis, M.; Stossi, F.; Carlson, K. A.; Katzenellenbogen, B. S.; Katzenellenbogen, J. A. Indazole estrogens: highly selective ligands for the estrogen receptor. *J. Med. Chem.* **2005**, *48*, 1132-1144.
33. Malamas, M. S.; Manas, E. S.; McDevitt, R. E.; Gunawan, I.; Xu, Z. B.; Collini, M. D.; Miller, C. P.; Dinh, T.; Henderson, R. A.; Keith, J. C. Jr.; Harris, H. A. Design and synthesis of aryl diphenolic azoles as potent and selective estrogen receptor- β ligands. *J. Med. Chem.* **2004**, *47*, 5021-5040.
34. Compton, D. R.; Sheng, S.; Carlson, K. E.; Rebacz, N. A.; Lee, I. Y.; Katzenellenbogen, B. S.; Katzenellenbogen, J. A. Pyrazolo[1,5-a]pyrimidines: estrogen receptor ligands possessing estrogen receptor antagonist activity. *J. Med. Chem.* **2004**, *47*, 5872-5893.
35. Miller, C. P.; Collini, M. D.; Harris, H. A. Constrained phytoestrogens and analogues as ER β selective ligands. *Bioorg. Med. Chem. Lett.* **2003**, *13*, 2399-2403.
36. Yang, C.; Edsall, R. Jr.; Harris, H. A.; Zhang, X.; Manas, E. S.; Mewshaw, R. E. ER β Ligands. Part 2: Synthesis and structure-activity relationships of a series of 4-hydroxy-biphenyl-carbaldehyde oxime derivatives. *Bioorg. Med. Chem.* **2004**, *12*, 2553-2570.
37. Zhao, L.; Brinton, R. D. Structure-based virtual screening for plant-based ER β -selective ligands as potential preventative therapy against age-related neurodegenerative diseases. *J. Med. Chem.* **2005**, *48*, 3463-3466.
38. Pike, A. C.; Brzozowski, A. M.; Hubbard, R. E.; Bonn, T.; Thorsell, A. G.; Engström, O.; Ljunggren, J.; Gustafsson, J. Å.; Carlquist, M. Structure of the ligand-binding domain of

oestrogen receptor beta in the presence of a partial agonist and a full antagonist. *EMBO J.* **1999**, *18*, 4608-4618.

39. Manas, E. S.; Xu, Z. B.; Unwalla, R. J.; Somers, W. S. Understanding the selectivity of genistein for human estrogen receptor- β using X-ray crystallography and computational methods. *Structure* **2004**, *12*, 2197-2207.

40. Distance measurements were performed in CAChe after MM3 minimization of each presented ligand by the author J. Janjic, **2005**, unpublished.

41. Wipf, P.; Kendall, C.; Stephenson, C. R. J. Three-component aldimine addition-cyclopropanation. An efficient new methodology for amino cyclopropane synthesis. *J. Am. Chem. Soc.* **2001**, *123*, 5122-5123.

42. Wipf, P.; Kendall, C.; Stephenson, C.R. J. Dimethylzinc-mediated additions of alkenylzirconocenes to aldimines. New methodologies for allylic amine and C-cyclopropylalkylamine syntheses. *J. Am. Chem. Soc.* **2003**, *125*, 761-768.

43. Wipf, P.; Kendall, C. Tandem zirconocene homologation-aldimine allylation. *Org. Lett.* **2001**, *3*, 2773-2776.

44. Wipf, P.; Jahn, H. Synthetic applications of organochlorozirconocene complexes. *Tetrahedron* **1996**, *52*, 12853-12913.

45. Wipf, P.; Kendall, C. Novel applications of alkenyl zirconocenes. *Chem. Eur. J.* **2002**, *8*, 1778-1784.

46. Wipf, P.; Xu, W.; Smitrovich, J. H.; Lehmann, R.; Venanzi, L. M. Copper-catalyzed conjugate additions of organozirconocenes. Synthetic and mechanistic studies. *Tetrahedron* **1991**, *50*, 1935-1954

-
47. Wipf, P.; Wang, X. A new ligand scaffold for catalytic asymmetric alkylzinc additions to aldehydes. *Org. Lett.* **2002**, *4*, 1197-1200.
48. Janjic J. M.; Mu, Y.; Kendall, C.; Stephenson, C. R. J.; Balachandran, R.; Raccor, B. S.; Lu, Y.; Zhu, G.; Xie, W.; Wipf, P.; Day, B. W. New antiestrogens from a library screen of homoallylic amides, allylic amides, and C-cyclopropylalkylamides. *Bioorg. Med. Chem.* **2005**, *13*, 157-164.
49. Leadbeater, N.E. Fast, easy, clean chemistry by using water as a solvent and microwave heating: the Suzuki coupling as an illustration. *Chem. Comm.* **2005**, *23*, 2881-2902.
50. Kappe, C.O. *Angew. Chem. Int. Ed.* **2004**, *43*, 6250-6284.
51. Wipf, P.; Janjic, J. M.; Stephenson, C. R. J. Microwave-assisted synthesis of allylic amines: considerable rate acceleration in the hydrozirconation-transmetalation-alimine addition sequence. *Org. Biomol. Chem.* **2004**, *2*, 443-445.
52. Wipf, P.; Coleman, C. M.; Janjic, J. M.; Iyer, P. S.; Fodor, M. D.; Shafer, Y. A.; Stephenson, C. R. J.; Kendall, C.; Day, B. W. Microwave-assisted “libraries from libraries” approach toward the synthesis of allyl- and C-cyclopropylalkylamides. *J. Comb. Chem.* **2005**, *7*, 322-330.
53. Xie, W.; Yeuh, M. F.; Radominska-Pandya, A.; Saini, S. P. S.; Negishi, Y.; Bottroff, B. S.; Cabrera, G. Y.; Tukey, R. H.; Evans, R. M. Control of steroid, heme, and carcinogen metabolism by nuclear pregnane X receptor and constitutive androstane receptor. *Proc. Natl. Acad. Sci.* **2003**, *100*, 4150-4155.
54. Xie, W.; Barwick, J. L.; Simon, C. M.; Pierce, A. M.; Safe, S.; Blumberg, B.; Guzelian, P.S.; Evans, R. M. Reciprocal activation of xenobiotic response genes by nuclear receptors SXR/PXR and CAR. *Genes Dev.* **2000**, *14*, 3014-3023.

-
55. Day, B. W.; Magarian, R. A.; Pento, J. T.; Jain, P. T.; Mousissian, G. K.; Meyer, K. L. Synthesis and biological evaluation of a series of 1,1-dichloro-2,2,3-triarylcyclopropanes as pure antiestrogens. *J. Med. Chem.* **1991**, *34*, 842-851.
56. Mitsunobu, O. The use of diethyl azodicarboxylate and triphenylphosphine in synthesis and transformation of natural products. *Synthesis* **1981**, 1-28.
57. Markowicz, M. W.; Dembinski, R. Fluorous, chromatography-free Mitsunobu reaction. *Org. Lett.* **2002**, *4*, 3785-3787.
58. O'Keefe, C. K.; Chesworth, R. Amide and sulfonamide ligands for the estrogen receptor. PCT Int. Appl. **2004**, WO 2004026823
59. Lipinski, C. A.; Lombardo, F.; Dominy, B. W.; Feeney, P. J. Experimental and computational approaches to estimate solubility and permeability in drug discovery and development settings. *Adv. Drug Deliv. Rev.* **1997**, *23*, 3-25.
60. Parker, G. J.; Law, T. L.; Lench, F. J.; Bolger, R. E. Development of high throughput screening assays using fluorescence polarization: nuclear receptor-ligand-binding and kinase/phosphatase assays. *J. Biomol. Screen.* **2000**, *5*, 77-88.
61. Tao, B.; Boykin, D. W. Simple amine/Pd(OAc)₂-catalyzed Suzuki coupling reactions of aryl bromides under mild aerobic conditions. *J. Org. Chem.* **2004**, *69*, 4330-4335.
62. Suzuki, A. J. Recent advances in the cross-coupling reactions of organoboron derivatives with organic electrophiles, 1995–1998. *Organomet. Chem.* **1999**, *576*, 147-168.
63. Tao, B.; Boykin, D.W. *trans*-Pd(OAc)₂(Cy₂NH)₂ catalyzed Suzuki coupling reactions and its temperature-dependent activities toward aryl bromides. *Tetrahedron Lett.* **2003**, *44*, 7993-7996.
64. Personal communication with Dr. Christopher Kendall

-
65. Brzozowski, A. M.; Pike, A. C.; Dauter, Z.; Hubbard, R. E.; Bonn, T.; Engstrom, O.; Ohman, L.; Greene, G. L.; Gustafsson, J. A.; Carlquist, M. Molecular basis of agonism and antagonism in the oestrogen receptor. *Nature* **1997** *389*, 753-758.
66. The MCF-7 cell-based test of biphenyl C-cyclopropylalkylamides was performed by Miranda Sarachine, Dept. of Pharmacology, Univ. of Pittsburgh.
67. Hanson, R. N.; McCaskill, E.; Dilis, R.; Ho, S. M.; Era of Hope **2005**, poster presentation, Philadelphia, PA, June 2005
68. Speirs, V.; Malone, C.; Walton, D. S.; Kerin, M. J.; Atkin S. L. Increased expression of estrogen receptor β mRNA in tamoxifen-resistant breast cancer patients. *Cancer Res.* **1999**, *59*, 5421-5424.
69. Esslimani-Sahla, M.; Simony-Lafontaine, J.; Kramar, A.; Lavaiil, R.; Mollevi, C.; Warner, M.; Gustafsson, J. A.; Rochefort, H. Estrogen receptor β (ER β) level but not its ER β cx variant helps to predict tamoxifen resistance in breast cancer. *Clin. Cancer Res.* **2004**, *10*, 5769-5776.
70. Graham, J. D.; Bain, D. L.; Richer, J. K.; Jackson, T. A.; Tung, L.; Horwitz, K. B. Thoughts on tamoxifen resistant breast cancer. Are coregulators the answer or just a red herring? *J. Steroid Biochem. Mol. Biol.* **2000**, *74*, 255-259.
71. Levenson, A. S.; Jordan, V. C. MCF-7: the first hormone-responsive breast cancer cell line. *Cancer Res.* **1997**, *57*, 3071-3078.
72. Michalides, R.; Griekspoor, A.; Balkenende, A.; Verwoerd, D.; Janssen, L.; Jalink, K.; Floore, A.; Velds, A.; Van 't Veer, L.; Neeffjes, J. Tamoxifen resistance by a conformational arrest of the estrogen receptor α after PKA activation in breast cancer. *Cancer Cell* **2004**, *5*, 597-605.

-
73. Osborne, C. K.; Bardou, V.; Hopp, T. A.; Chamness, G. C.; Hilsenbeck, S. G.; Fuqua, S. A. W.; Wong, J.; Allred, D. C.; Clark, G. M.; Schiff, R. Role of the estrogen receptor coactivator AIB1 (SRC-3) and HER-2/neu in tamoxifen resistance in breast cancer. *J. Natl. Cancer Inst.* **2003**, *95*, 353-361.
74. Hsu, T. M.; Law, S. M.; Duan, S.; Neri, B. P.; Kwok, P. Y. Genotyping single-nucleotide polymorphisms by the invader assay with dual-color fluorescence polarization detection. *Clin. Chem.* **2001**, *47*, 1373-1377.
75. Geistlinger, T. R.; McReynolds, A. C.; Guy, R. K. Ligand-selective inhibition of the interaction of steroid receptor coactivators and estrogen receptor isoforms. *Chem. Biol.* **2003**, *11*, 273-281.
76. Gottlieb, H. E.; Kotlyar, V.; Nudelman, A. NMR chemical shifts of common laboratory solvents as trace impurities. *J. Org. Chem.* **1997**, *62*, 7512-7515.
77. Wipf, P.; Stephenson, C. R. J. Three-component synthesis of α,β -cyclopropyl- γ -amino acids. *Org. Lett.* **2005**, *7*, 1137-1140.
78. Arylsulfonyl isocyanates. *Ger. Offen.* **1983**, 8 pp. DE 3132944 A1 19830303
79. Jennings, W. B.; Lovely, C. J. The titanium tetrachloride induced synthesis of N-phosphinoylimines and N-sulphonylimines directly from aromatic aldehydes. *Tetrahedron* **1991**, *47*, 5561-5568.
80. Barr, K. J.; Cunningham, B. C.; Flanagan, W. M.; Lu, W.; Raimundo, B. C.; Waal, N. D.; Wilkinson, J.; Zhu, J.; Yang, W. Salicylate analogs as interleukin-4 antagonists. *PCT Int. Appl.* **2002**, 34 pp. WO 2002044128.

81. Maloney, D. J.; Deng, J.-Z.; Starck, S. R.; Gao, Z.; Hecht, S. M. (+)-Myristinin A, a naturally occurring DNA polymerase inhibitor and potent DNA-damaging agent. *J. Am. Chem. Soc.* **2005**, *127*, 4140-4141.

82. BioMedCACHe software user manual, **2003**.